3D-Microstructured Protein Chip for Cancer Diagnosis

Zhugen Yang

ÉCOLE CENTRALE LYON

N° d'ordre: 2012-18

Thèse de l'Université de Lyon
délivrée par l'Ecole Centrale de Lyon

Soutenue publiquement le 20/07/2012

Par

M. Zhugen YANG

Préparée à l'Institut des Nanotechnologies de Lyon

3D-Microsturctured Protein Chip for Cancer Diagnosis

Ecole Doctorale Electronique, Electrotechnique, Automatique

Spécialité: Micro et Nanotechnologies

Composition du jury:

M. Michel SEVE	Prof. CHU Grenoble, Grenoble	Président
Mme Claire-Marie PRADIER	DR CNRS- Paris VI, Paris	Rapporteur
M. Pierre-Jean LAMY	Chef de LBSO, Montpellier	Rapporteur
M. Claude LAMBERT	HDR CHU, Saint-Etienne	Examinateur
Mme Yasemin ATAMAN-ONAL	PHD, bioMérieux, Lyon	Examinateur
Mme Eliane SOUTEYAND	DR CNRS- ECL, Lyon	Directeur de thèse
Mme Emmanuelle LAURENCEAU	MCF INL- ECL, Lyon	Co-directeur de thèse

UNIVERSITÉ DE LYON

Acknowledgements

It is a great pleasure to sincerely thank Dr Guy Hollinger, Director of the Lyon Institute of Nanotechnology (INL) for welcoming in the laboratory, UMR 5270 CNRS at the Ecole Centrale de Lyon.

First of all, I would like to thank my supervisor Dr Eliane Souteyrand and my co-supervisor Dr Emmanuelle Laurenceau who brought me into the fantastic world of biosensor, and gave me continuous guidance, support, encouragement, and invaluable advices during the past three years. They not only helped me with structure and defining the end of the projects, but also allowed me a lot of autonomy in such interdisciplinary project.

Secondly, I am so grateful for the PhD fellowship from China Scholarship Council (CSC) which gave me financial aids to carry out my thesis work in France.

Thanks the members of my dissertation committee, Dr Claire-Marie Pradier and Dr Pierre-Jean Lamy who agreed to review the manuscript of the thesis. I am grateful to Dr Michel Sève, Dr Claude Lambert and Dr Yasemin Ataman-Önal, who kindly accepted to be member of my PhD jury. The thesis would not have been completed without their cooperation and constructive suggestions.

I would like to express my great appreciation to cooperated institutes and personals, and this thesis would not be possible without their help and support. Dr Yasemin Ataman-Önal and Dr Geneviève Choquet-Kastylevsky were kindly acknowledged for provision us protein products for research activities. Thanks for Dr Jérôme Solassol, from CHU Montpellier, Laboratoire de biologie cellulaire et hormonale, Hôpital Arnaud de Villeneuve, providing us breast cancer sera sample for test. I'd like to express my acknowledgement to Dr Claude Lambert for the colorectal cancer sera samples contributions. Thanks Prof. Thierry Delair for giving us chitosan for surface modification, from Polymer Materials and Biomaterials Laboratory (LMPB), Université Claude Bernard Lyon 1.

I would like to express my appreciation to Dr Nicolas Xanthopoulos and Dr Vincent Laporte, Ecole Polytechnique Fédérale de Lausanne (EPFL), who helped us to finish XPS characterization. Dr Vincent Dugas, Université de Lyon, Laboratoire des Sciences Analytiques (LSA) – UMR CNRS 5180, was acknowledged for the help on determination of surface grafting density. Technical supports of NanoLyon are also appreciated for all the infrastructures.

I would like to thank the all group members of Chemistry and Nanobiotechnology. Dr Yann Chevolot has continuously supported me in my work over the last three years. He

showed me a lot of crucial technologies and experimental skills, and acted as a discussion partner in the project. I much appreciate Dr Jean-Pierre Cloarec, who designed the effective analysis method for plenty of data extracted from microarray and also a nice academic discussion partner for the project. Besides, I appreciate very much to Dr Thomas Gehin for the favour of spotting. Dr Magali Phaner-Goutorbe, a nice and easy-going professor in our group, thank you very much for the favours of finishing my required courses of doctoral school. Thanks Dr Virginie Monnier, who helped me with the first administration issues when I entered the lab with difficulties in speaking French. Isabel Nabeth and Maryline Diserio help a lot for the chance of conversations during the coffee time of our group.

In my daily work, I have been extremely lucky and blessed with many cheerful and friendly colleagues and friends who are working or once worked in the group: Ning Sui, Alice Goudot, Delphine Sicard, Francisco Palazon, Amandine Cornillon, Rémy Beland, Vanessa Chenel, Richard Villey, Dr Dimitri Charrier, Dr Marie Trevisan and Dr Maksym Iazykov etc. Here, I would like to express my special thanks to Dr Jing Zhang for her selfless help both on the scientific and daily life at the moment when I joined the group.

I would like to thank all the Chinese PhD students for the great times we have spent together in the past three years at ECL: Gang Niu, Xianqing Meng, Shi Yin, Taiping Zhang, Nanhao Zhu, Zheng Li, Huibin Li, Jun Yuan, Ningning Liu, Yun Zhou, Tao Xu, Yu Zhang, Tanli Huang, Biao Zhou etc. Specific thanks Boyang Gao for the help with program to process data.

Finally, I would like to thank my parents, who are without-a-doubt the best parents I could imagine, for their encouragement through all the difficult times. I appreciate supports and encouragements from my sisters and brothers-in-law very much. Thanks my girlfriend Juanxi, to be my wife soon, who is always around me. I haven’t thanked you nearly enough for what you have done and continue to do for me. We will continuously welcome our wonderful future together.

Abstract

Protein microarrays are becoming powerful tools to screen and identify tumor markers for cancer diagnosis, because of the multiplex detection and minute volume of sample requirement. Due to the diversity and variation in different cancers, no single tumor marker is sensitive and specific enough to meet strict diagnostic criteria. Therefore, a combination of tumor markers is required to increase sensitivity and to establish distinct patterns to increase specificity. To obtain reliable tests, the development of reproducible surface chemistry and immobilization procedure are crucial steps in the elaboration of efficient protein microarrays. In this thesis, 3D micro-structured glass slides were functionalized with various surface chemistries like silane monolayer (amino, epoxy and carboxy), and polymer layers of Jeffamine, chitosan, carboxymethyl dextran (CMD), maleic anhydride-alt-methyl vinyl ether copolymer (MAMVE) for physical adsorption or covalent binding with proteins. Surface characterizations, such as X-ray photoelectron spectroscopy (XPS) and Attenuated total reflectance Fourier transform infrared spectroscopy (ATR-FTIR), confirmed the monolayer/polymer grafting on the glass slides. Colorimetric assay for determining amine density of three aminated surfaces demonstrated that APDMES had more grafting density than Jeffamine and chitosan. Contact angle measurements show that polymer surfaces were more hydrophilic than monolayer surfaces due to the increasing dosages of polar functional groups. Moreover, the parameters such as additives and pH of spotting buffer, probe concentration, blocking procedures etc, were optimized for tumor marker detection. Under the optimized conditions, antibody microarrays were validated with purified tumor antigens. The best analytical performances obtained for each tumor antigen tested were strongly dependent on functionalized surfaces, e.g. MAMVE exhibited best analytical performances for CEA and Hsp60 while NHS leads to best results for PDI and CA19-9. Besides, the implemented antibody microarrays were applied to tumor marker detection from colorectal cancer sera. This evaluation shows the interest to combine several tumor markers on the same surface and the combination of tumor markers on their specific surface lead to remarkably increase the positive responses of tested cancer sera (even up to 100 %). A second type of microarrays (tumor-associated antigens - TAA microarrays) was designed to discriminate breast cancer patients from healthy donors through the detection of tumor autoantibodies. This study included a cohort of 29 breast cancer patients' and 28 healthy donors' sera. A panel of five TAAs (Hsp60, p53, Her2, NY-ESO-1 and Hsp70) immobilized on their respective optimized surface chemistry allowed to specifically detect over 82% of breast cancer patients.

Keywords: protein microarray; surface chemistry; immobilization; tumor marker; cancer diagnosis.

Table of contents

Abbreviations

Ac	Sodium acetate buffer, pH 4.5
AC	Atomic concentration
AFM	Atomic force microscopy
AFP	Alpha-fetoprotein
APDIPES	(3-aminopropyl) diisopropylethoxysilane
APDMES	(3-aminopropyl) dimethylethoxysilane
APTES	(3-aminopropyl)triethoxysilane
ATR FTIR	Attenuated total reflectance Fourier transform infrared
BAA	Bromoacetic acid
BE	Binding energy
BOE	Buffered oxide etchant
BSA	Bovine serum albumin
CA	Carbonhydrate antigen
Car	Sodium carbonate buffer
CBB	Coomassie brilliant blue
CEA	Carcinoembryonic antigen
CMD	Carboxylmethyl dextran
COOH	Carboxylic acid surface
CRC	Colorectal cancer
CT	Computed tomography
CTC	Circulating tumor cell
CVD	Chemical vapor deposition
Cy3	Cyanine 3
Cy5	Cyanine 5
DD	Degree of deacetylation
DDI	DNA-directed immobilisation
DI water	Deionized water
DIC	N, N'-diisopropylcarbodiimide
DMSO	Dimethyl sulfoxide
DS	Degree of substitution
EBV-NA	Ebstein bar virus nuclear antigen 1
ELISA	Enzyme-linked immunosorbent assay

FCM	Flow cytometry
FOBT	Faecal occult blood test
GPDMES	(3-glycidoxypropyl) dimethylethoxysilane
GPTS	(3-glycidoxypropyl) trimethoxysilane
GSTP1	Glutathione S-transferase P1
Her2	Human epidermal growth factor receptor 2
HIV	Human immunodeficiency virus
Hsp 60	Heat shock proteins 60
Hsp 70	Heat shock proteins 70
MAMVE	Maleic anhydride-alt-methyl vinyl ether
MEMS	Micro-electromechanical systems
MeOH	Methanol
MES	2-(N-morpholino) ethanesulfonic acid
MHP	Measle hemagglutinin protein
MRI	Magnetic resonance imaging
MS	Mass spectrometry
NHS	N-hydroxysuccinimide
NMR	Nuclear magnetic resonance
NSE	Neuron-specific enolase
p53	Protein / Tumor protein 53
PBS	Phosphate-buffered saline
PCR	Polymerase chain reaction
PET	Positron emission tomography
PET-CT	Positron emission tomography fused with computed tomography
pI	Isoelectric point
PMT	Photomultiplier tube
PSA	Prostate-specific antigen
PVA	Poly vinylalcohol
QCM	Quartz-crystal microbalance
RMS	Root mean square values
SAM	Self-assembling monolayers
SD	Standard deviation
SDS	Sodium dodecyl sulfate
SNR	Signal-to-noise ratio
SPR	Surface plasmon resonance
TAA	Tumor-associated antigen

TBS	Tris-buffered saline
TDSUM	Tert-butyl-11-(dimethylamino)silylundecanoate
THF	Tetrahydrofuran
ToF-SIMS	Time-of-flight secondary ion mass spectrometry
XPS	X-ray photoelectron spectroscopy

General Introduction

The global burden of cancer has more than doubled in the past 30 years and it has become leading cause of death in the world. Cancer diagnosis is of great interest due to the widespread occurrence of the disease and high death rate. Effective screening will allow cancer patients to be accurately diagnosed in early stage and successfully treated. Conventional techniques for cancer diagnosis include imaging techniques as well as cytology and biochemical assays. With the recent development of proteomic technologies, varieties of tumour markers were identified and employed for cancer diagnosis and prognosis in clinical oncology with immunoassay methods. However, the low abundance of many tumor markers in patient sera is a challenge for diagnostic techniques especially due to lacking detection sensitivity and specificity. Furthermore, thanks to the diversity and variation in different cancers, no single tumor marker is sensitive and specific enough to meet strict diagnostic criteria. Therefore, a combination of tumor markers is required to increase sensitivity and to establish distinct patterns related to one cancer in order to increase specificity of the diagnosis.

Protein microarray approaches have many advantages for the identification of tumor biomarkers associated with the humoral response, in particular due to their capacity for high throughput analysis and minute sample requirement. Since tumor markers are often present in the sample at low level (below nM), there is an urgent need to implement protein microarray for ultrasensitive detection of tumor markers. One of the crucial parameters for the development of sensitive protein microarray is surface chemistry which determines the way of protein immobilization and influences biological activity. Detection conditions are also important in the elaboration of efficient protein microarrays. The specificity of protein microarray for diagnosis or prognosis is related to the choice of protein to be targeted, and so to the choice of protein to be immobilized. Many studies suggest that a single biomarker is not sufficiently sensitive and specific for implementation of a global screening strategy, thus panels of biomarkers are required to improve sensitivity and specificity.

In this context, the objective of this thesis was to develop original protein microarrays functionalized with various surface chemistries, for the sensitive and specific detection of cancer biomarkers. Two different kinds of protein microarrays were implemented for different application goals. One was antibody microarray for the detection of cancer biomarkers involved in colorectal cancer. The other was antigen microarray for the identification of autoimmune profiles in breast cancer.

In the first chapter, the state of art about cancer diagnosis and protein microarrays is documented, as well as the key points of the study. Conventional techniques of cancer diagnosis and follow-up were introduced as well as some methods in developments, in particular on colorectal and breast cancers. Then the parameters of protein microarray elaboration such as substrates, surface chemistry, immobilization procedures, detection methods, were presented and special focus on protein microarray for cancer diagnosis was described.

Chapter 2 presents the original parts of protein microarrays developed in this thesis: microstructuration of the solid support (glass slides) and functionalization with various surface chemistries. Microstructured glass slides give the opportunity to test multiple experimental conditions in one assay with the advantage of small volume consumption. Developed surface chemistries are based on silane monolayers with amino terminal function ((3-aminopropyl) dimethylethoxysilane: APDMES), epoxy terminal function ((3-glycidoxypropyl) dimethylethoxysilane: GPDMES), or carboxy terminal function (tert-butyl-11-(dimethylamino) silylundecanoate: TDSUM). Then various polymers were grafted on these silane monolayers: chitosan, carboxymethyl dextran (CMD), maleic anhydride-alt-methyl vinyl ether (MAMVE) and Jeffamine. All these functionnalized surfaces were characterized to evaluate their physico-chemical properties before protein immobilization. Both physical adsorption and covalent binding of proteins were targeted in the choice of surface chemistries developed.

In Chapter 3, four model proteins (bovine serum albumin, myoglobin, streptavidin, immunoglobulin G) with different characteristics (molecular weight, isoelectric point, structure) were immobilized onto the various surface chemistries. Parameters such as composition and pH of spotting buffer, blocking procedures, protein concentration were evaluated versus surface properties, in order to define optimal conditions for the implementation of our protein microarrays.

Then chapter 4 describes the implementation of antibody microarray for the sensitive detection of colorectal cancer biomarkers (CEA, Hsp60, PDI, DEFA6 and p53). Optimal surface chemistries were selected for serologic immunoassay according to best performances obtained in purified conditions.

At last, chapter 5 is dedicated to antigen microarray for the evaluation of autoimmune response in breast cancer. 10 tumor-associated antigens (TAAs) related to breast cancer were immobilized onto microstructured glass slides functionalized with various surface chemistries.

The presence of autoantibodies directed against these TAAs was evaluated in 29 sera from breast cancer patients and 28 healthy donors. A panel of 5 TAAs and 2 surfaces chemistries were selected to improve sensitivity and specificity of the detection of cancer patients to 82%.

This work was performed within the framework of the program “Groups of Five Ecoles Centrales” between China Scholarship Council (CSC) and Institut des Nanotechnologies de Lyon (INL), CNRS UMR 5270, site Ecole Centrale de Lyon. The project has been supported by the INL technology platform NANOLYON and collaboration with bioMérieux (France) and two French hospitals (CHU Montpellier and CHU Saint-Etienne).

Chapter 1 State of Art

1.1. Cancer diagnosis

1.1.1. Key data related to cancers

Cancer is a common term for neoplasms or tumors that are malignant. These malignancies are composed of undifferentiated, unspecialized cells with atypical cell structures which work differently from the normal cells in the body organ where they originate.

The global burden of cancer has more than doubled during the past 30 years. It was reported by World Health Organization that there were around 12.4 million incident cases of cancer (6 672 000 in men and 5 779 000 in women) and 7.6 million deaths from cancer (4 293 000 in men and 3 300 000 in women) all over the world in 2008 [1]. The continued growth and aging of the world's population will greatly affect the cancer burden. By 2030, it was estimated that there would be 27 million incident cases of cancer, 17 million cancer deaths annually and 75 million persons alive with cancer within five years of diagnosis. Globally, lung and breast cancer was the commonest incident cancer and cause of cancer-related mortality for men and women, respectively.

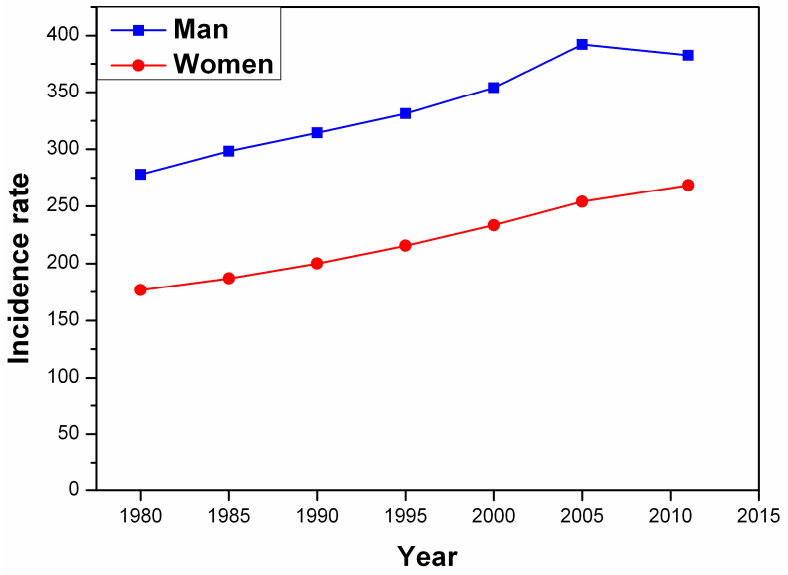

Figure 1-1 The incidence rate of cancer for man and women between 1980 and 2005 as well as the year of 2011 with the world standardized mode, date from INCA (collection rapports & syntheses – 2011, www.e-cancer.fr)

In France, key data reported by The French National Cancer Institute (INCA) (collection rapports & syntheses – 2011, www.e-cancer.fr) gives an estimation of 365 000 new cases in

2011 (207 000 men and 158 500 women) and a (world standardized) incidence rate of 382.7 for 100 000 men and 268.5 for 100 000 women (Figure 1-1). The average age at diagnosis in 2005 was 67 years old for men and 64 years old for women. The number of deaths is estimated at 147 000 people for 2011 (84 500 men and 63 000 women), the (world standardized) mortality rate would be 138.6 for 100 000 men and 77.6 for 100 000 women. During the period of 2004-2008, the median age for death was 72 years for men and 76 years for women. The survival for 5 years of patients diagnosed between 1989 and 1997 was 44 % for men and 63 % for women, respecitively. Among different type of cancer, the most frequent are prostate (71 000 new cases), lung (27 500) and colorectal (21 500) for men and breast (53 000) colorectal (19 000) and lung (12 000) for women.

Facing this scourge, policy of screening programs have been developed especially for breast cancer with a free mammography every 2 years for women older than 50 years and for colorectal cancer with hemoccult test. It was noticed that beyond the aging population, risk factors related to lifestyle have been clearly identified. Thus, tobacco smoking is the best-understood major human carcinogen. Other modifiable risk factors for cancer include alcohol consumption, excessive exposure to sunlight, lack of physical activity, overweight and obesity, dietary factors, occupational exposures and chronic infection [1].

1.1.2. Tumorigenesis

Tumor cell is part of a tissue growing abnormally, which may be either malignant or benign in nature. Benign tumor cells do not invade neighboring tissues, but may grow to grand size and cause other problems: breathing, mobility, circulatory. Malignant tumor cells are generally referred to as cancer cells, able to metastasize or spread to neighboring tissues and grow tumors. Cancer cells, originating from normal cells but mutating insensitively to normal growth control and immortal, can invade surrounding tissue and form metastases at a distant place.

The progression of cell cycle is complex and a multistep process, tightly regulated by “checkpoints”, which enables a speed regulation of proliferation and maintaining the integrity of the cellular genome. Thus, normal cells “self” control their own growth and will destroy themselves if they become unhealthy. On the contrary, these “checkpoints” are altered in many tumors. As a consequence, cancer occurs when gene alterations of a cell prevent these controls from functioning properly. The problems may come from damage to the gene or may be inherited, which is probably caused by various sources inside or outside of the cell. Three types of genes have been associated to the dysfunction of cell growth leading to the cancer development:

- **oncogenes** (c-onc) resulting from mutation of protooncogenes, which drive the cell proliferation. With gene alteration, the cell proliferation becomes uncontrolled. The most known oncogenes are Ha-ras, myc and abl.

- **tumor suppressor genes** which are negative regulators in the cell growth process. In cancer, the two copies of these genes are inactivated. For instance, the silencing of tumor suppressor genes through aberrant DNA methylation of a CpG island(s) in the promoters in these genes is a common epigenetic change [2]. Tumor suppressor genes as BRCA1, p16INK4a, p15INK4b, p14ARF, p53 and APC are among those that are silenced by hypermethylation. The frequency of aberrant methylation is somewhat tumor type specific [3].

- **care taker genes** encoding products that stabilize the genome, able to detect and repair DNA lesions.

Table 1-1 Common tumor markers currently used in cancer detection

Tumor markers	Characteristics	Related cancers	Typical samples
CEA	Subtle posttranslational modifications might create differences between tumor CEA and normal CEA	Colorectal, lung, breast, pancreatic, bladder	Serum [4, 5]
CA19-9	Evaluated also in inflammatory bowel disease	Colorectal, pancreatic	Serum [4, 6]
Hsp60, 70, 90	Evaluated in environmental stress conditions like infection, inflammation	Colorectal, breast, bladder	Serum [7, 8]
p53	Mutated or changed in more than 50 % tumors	Colorectal, breast etc	Serum [9, 10]
EGFR (Her01)	Binding of proteins to a ligand induces receptor dimerization, tyrosine autophosphorylation, cell proliferation	Colorectal, pancreatic, breast, lung	Tissue [4]
CA15-3, 27, 29	Elevated in benign breast conditions	Breast	Blood [4]
CA125	High sensitivity in advance stage	Epithelial ovarian	Blood [4]
Her-2 /neu	20-30% patients are positive to Her-2 oncogene present in multiple copies	Breast	Tissue [11]
NSE	Better sensitivity towards specific types of lung cancer	Lung	Blood [13]
AFP	Elevated during pregnancy and liver cancer	Germ cell cancer of ovaries	Blood [4]

Biomarker is a biological molecule found in blood, other body fluids, or tissues that is a sign of a normal or abnormal process, or of a condition or disease. A biomarker may be used to see how well the body responds to a treatment for a disease or condition [14, 15]. Tumor

markers are substances produced by tumor cells or by other cells of the body in response to cancer or certain benign (non cancer) conditions. Thus, mutation of protooncogenes into oncogenes or alterations of tumor suppressor genes lead to abnormal protein production called tumor-specific antigens, like prostate-specific antigen (PSA) [15]. Other examples of tumor-specific antigens concern the abnormal products of ras and p53 genes [16, 17]. On the contrary, mutation of other genes unrelated to the tumor formation may also lead to synthesis of abnormal proteins which are called tumor-associated antigens (TAAs). Besides, cancer cells accumulate mutations that are possibly recognized as "non-self" by the immune system, which can produce autoantibodies against tumor antigen, referred to anti-tumor antigen autoantibodies [18]. There is a very wide panel of biomarkers relative to cancer. Table 1-1 summarized some common tumor markers currently used in cancer detections, such as carcinoembryonic antigen (CEA), carbohydrate antigen (CA) 19-9, Heat-shock proteins (Hsp) 60, protein/tumor protein 53 (p53), epidermal growth factor receptor (EGFR), cancer antigen (CA)15-3, 27, 29, CA125, human epidermal growth factor Receptor 2 (Her2), PSA, Neuron-specific enolase (NSE) and alpha-fetoprotein (AFP).

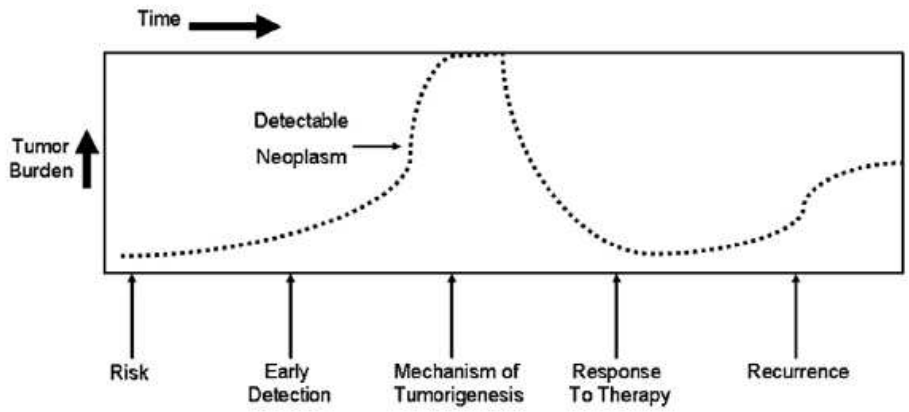

Figure 1-2 Application of various biomarkers for different stage of cancer progression, adapted from [19]

As is shown in Figure 1-2, Tainsky et al [19] suggested that cancer biomarkers can be employed as a specific purpose in mind such as the early detection of cancer, diagnosis, prognosis, response to anticancer therapies or cancer recurrence. Cancer cells provide the biomarker material leading to their own detection, their non-invasive detection in body fluids and tissues, and thus reveal the presence of tumors or the level of tumor burden. Therefore, the ideal marker would be useful not only in diagnosis, but staging and prognosis of cancer, provide an estimation of tumor burden, and serve for monitoring effects of therapy, detecting recurrence, localization of tumors, and screening in general populations [19, 20].

Most tumor markers do not suit the ideal profile for diagnosis which usually exists at nM range or below in the physiological sample, due to lack of sensitivity and specificity of the available tests. Besides, any protein or chemical has the potential to become a tumor marker. As tumor cells grow and multiply, some of their substances increase in tumor tissues and/or leak into the bloodstream or other fluids. The tumor marker can be measured in blood, urine, stool or tissue depending on its generation place. Screening tests for cancer are a way of detecting cancer early, before there are any symptoms [21]. Since an abnormal tumor marker level may suggest cancer, measurements of tumor markers are employed to diagnose cancer, usually with combination of other tests like a biopsy. Tumor associated antigens (TAAs), tumor-specific antigens as well as their autoantibodies could be regarded as tumor markers, which are possibly exploited as serological tools for the early diagnosis and management of cancer [18].

1.1.3. Conventional techniques for cancer detection

The key point of ultimate success for cancer treatment is the accurate diagnosis at the early stage, so it is necessary for oncology researchers to develop sensitive and specific techniques to detect cancer. The current conventional techniques for cancer diagnosis include [22]: endoscopy, biopsy, cytology specimen tests as well as imaging/radiology tests such as X-rays, computed tomography (CT) scans, magnetic resonance imaging (MRI), positron emission tomography fused with computed tomography (PET-CT) and ultrasounds [23, 24]. Additionally, some special classical methods were only employed to detect certain kinds of cancers [14], e.g. the Papanicolau test for women to detect cervical cancer and mammography to detect breast cancer, prostate-specific antigen (PSA) level detection in blood sample for men to detect prostate cancer [4], occult blood detection for colon cancer.

However, both strengths and limitations exist on each detection technique. For example, during a biopsy, a small tissue sample which is suspected to contain cancer is removed from the part of patients' body and sent to a laboratory for analysis. If cancer cells are found, a doctor will have enough information to make a positive diagnosis. Depending on the part of the body in question, a biopsy was performed either through an injection that extracts tissue or fluid from the body, or via a small surgery. For certain cancers such as colorectal cancer or esophageal cancer, tissue bits are removed during screening tests. It was suggested that these biopsies are very invasive and require exactly knowing the localization of the tumor, depending on sophisticated infrastructures. Furthermore, others like lung and liver cancer may require more invasive techniques to acquire a tissue sample. Alternatively, imaging techniques vary in the level of detail they show and the risks they present to patients. Moreover, the choice of the used imaging method strongly depends on what type of cancer

was suspected. Generally, MRIs are used to help diagnose brain cancer and lymphoma, mammogram X-rays are used for breast cancer and CT scans are used for lung cancer. Unlike imaging with X-rays or MRI, PET provides functional information by using 18Fdeoxyglucose (FDG), a glucose analogue labelled with positron emitting fluorine [23, 24]. Most malignant tumors have a higher glucose metabolism than normal tissue, take up more FDG than the surrounding tissue and emit more positrons, therefore the areas of malignancy show up as areas of increased activity on the scan. When PET is combined with CT functional, information can be located anatomically and detected accurately. But imaging/radiology techniques are usually costly and thus not available for many people in developing countries.

With the recent development of proteomic technologies, varieties of tumor markers such as reported in Table 1-1 were identified and employed for cancer detection with immunoassay methods [4, 5]. In particular, enzyme-linked immunosorbent assay (ELISA), first reported by Engvall and Perlmann in 1971 [25], has been widely employed to detect tumor markers for cancer diagnosis [4]. The main procedures of a traditional ELISA are described as following:

- firstly, an unknown amount of antigen (or antibody) is fixed to the surface of a solid support;
- secondly, a specific antibody (or antigen) linked with an enzyme is added to bind to the fixed antigen (or antibody);
- finally, the enzyme is permitted to react with its substance and then the quantitative determination can be obtained according to the substance.

There are a large number of categories of ELISA, such as direct assay, indirect assay and sandwich ELISA (Figure 1-3).

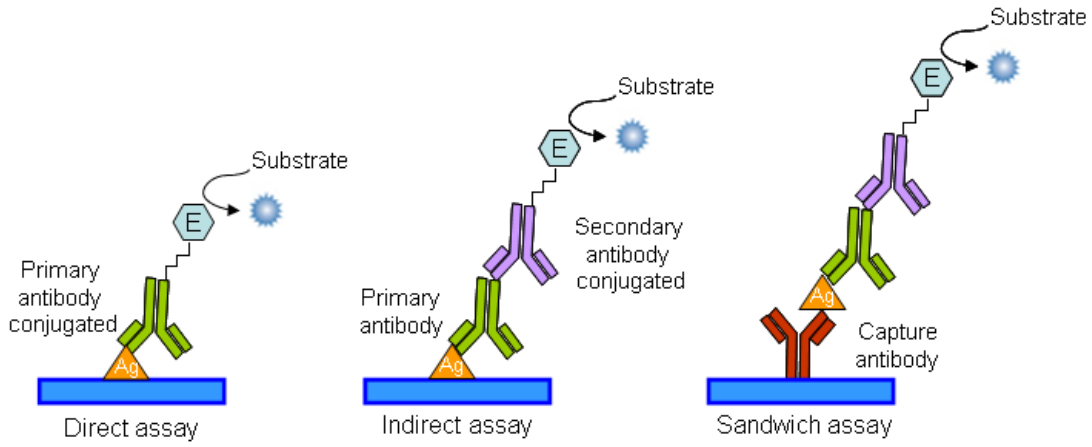

Figure 1-3 Schematic illustration of common ELISA formats, in the assay, the antigen of interest is immobilized by direct adsorption to the assay plate or by first attaching a capture antibody to the plate surface. Detection of the antigen can then be performed using an enzyme-conjugated primary antibody (direct detection) or a matched set of unlabeled primary and conjugated secondary antibodies (indirect detection).

Table 1-2 Examples of immunoassay for tumor markers analysis

Tumor markers	Assay principle	Detection method	Limit of detection	Refs
CEA	ELISA, Catalog # EA-0104, Signosis Inc. CA, USA	Colorimetry	1 ng/ml	-
CA19-9	ELISA, Catalog # EA-0102, Signosis Inc. CA, USA	Colorimetry	15 U/ml	-
Hsp60	ELISA, Catalog # ADI-EKS-600, ENZO Life Sci INT'L, INC., USA	Colorimetry	3.1 ng/ml	-
CA125	ELISA, Catalog # BC1013, Panomics, Inc. USA	Colorimetry	5 U/ml	-
CEA	Enzyme-labelled gold nanoparticles probles	Colorimetry	0.012 ng/ml	[26]
CEA	Flow-through multianalytesystem with substrate zone-resolved technique	Chemilu-minescence	0.6 ng/ml	[27]
CEA	Layer-by-layer assembly of gold nannoparticles-multi-walled carbon naotubes-thinonine multilayer films	Electro-chemistry	0.01 ng/ml	[28]
AFP	Fluorescence quenching signal of gold nanoparticles	Fluorescence	0.17 nM	[29]
PSA	Fluorophore-based bio-barcode amplification method	Fluorescence	30 nM	[30]

Currently, ELISA has been commonly employed in the fields of medical laboratories, manufacturers of *in vitro* diagnostic products, regulatory bodies, and external quality assessment and proficiency-testing organizations, as an easy-to-use for quick and accurate results. However, conventional ELISA may confront sensitive problems, and the large requirement of samples also burdens its wide application, in particular for tumor markers measurement due to the quite low concentration at the early stage of cancer. Therefore, research efforts were dedicated on developments of novel immunoassays [31, 32] and new signal amplification system to improve specificity and sensitivity for traditional assays. For instance, Lee and co-workers [33] incorporated an enzyme-cascading system into ELISA, with a trypsinogen-enterokinase combination as the cascading enzyme system, to detect AFP and PSA markers. With colorimetric for read-out, the implemented ELISA allows a limit of detection to 0.1-10 pM for AFP and PSA in whole human serum under the optimal assay conditions. Table 1-2 summarized some commercial ELISA kits and examples of immunoassays which have been developed for tumor markers analysis. It was suggested that the new technologies could improve the limit of detection for tumor markers, however, the low frequency and heterogeneity of tumor markers in patients' sera still brings challenges to

classical ELISA for detection of cancer, especially due to the lack of sensitivity and specificity of individual markers.

1.1.4. Techniques in development

Since cancer is the most leading cause of death in the world, plenty of researchers were dedicated on detection and screening techniques. Besides conventional techniques, other methods were also developed such as circulating cancer cells, flow cytometry, etc.

Circulating tumor cells (CTCs) are isolated tumor cells disseminated from the site of disease in metastatic and/or primary cancers, which possess antigenic and/or genetic characteristics of a specific tumor type and can be identified and measured in the peripheral blood of cancer patients [34]. Monoclonal antibodies directed against histogenic proteins and polymerase chain reaction (PCR) based molecular assays amplifying tissue-specific transcripts are the two main approaches used for the detection of CTCs [35]. The molecular assays have generally been considered more sensitive, while immunocytochemistry has the advantage of allowing the morphological assessment of stained cells. On the basis of expression on epithelial cells (epithelial-specific markers) or their specific expression on certain tissues (tissue-specific markers), different markers have been used for the detection of CTCs separately or in combination, such as CK19, CK18, mucin-1, CEA and mammaglobin for breast cancer [35, 36]. A recent report shows that CTC evaluation can confirm tumor diagnosis and identify patients with advanced bladder cancer. However, due to the low overall sensitivity, CTC detection assays should not be used as initial screening tests [37].

When CTCs are present in patients with presumably localized disease, they are regarded as relativity to disease relapse and therefore are obvious targets for adjuvant treatment strategies. In patients with metastatic disease, CTC enumeration and monitoring is thought to correlate with tumor load and may predict response to therapy. Moreover, the genetic and phenotypic profiling of CTCs often differs from that of the primary tumor and could be used to select the most effective targeted therapy [35]. Consequently, the study of CTCs, apart from the impact on refining prognosis, has the exciting potential of individualizing treatment strategies for cancer patients. The research into CTCs may provide new insight into the biology of cancer and the process of metastasis. It was expected that CTC detection may become a valuable tool to refine prognosis in cancer patients. Besides, CTC phenotyping and profiling may serve as a real-time tumor biopsy for individualized targeted therapies.

The quantification and assessment of circulating tumor cells (CTCs) has been proposed as one strategy to monitor treatment effectiveness and disease prognosis. However, CTCs have been an elusive population of cells to study due to their small number and difficulties associated with isolation protocols. *In vivo* flow cytometry can overcome these limitations

and provide insights in the role which these cells play during primary and metastatic tumor growth [38]. Flow cytometry (FCM) is a technique for counting and examining microscopic particles, such as cells and chromosomes, by suspending them in a stream of fluid and passing them by an electronic detection apparatus [39]. It allows simultaneous multiparametric analysis of the physical and/or chemical characteristics of up to thousands of particles per second, recently becoming an integral tool in immune monitoring.

In FCM, cells in a fluid medium are streamed in a single file through a capillary tube, and light from several lasers is directed at each individual cell as it passes through. Typically, each cell is labelled with different fluorescent dyes conjugated to monoclonal antibodies recognizing specific cellular markers, which may be cell surface or intracellular proteins. Each cell hit by laser light leads to scatter and activation of the fluorescent dyes bound to the cell. The light from forward and side scatter are detected electronically in separate channels, as is the light emitted by each fluorescent dye molecule when it relaxes from its activated state. Since each monoclonal antibody of a given specificity is bound to a different fluorescent dye, the amount of light in each wavelength detected will be directly proportional to the number of bound antibodies of that specificity, and a measure of the density of the cellular marker targeted by that monoclonal antibody on each cell [39, 40]. Therefore, FCM assays offer the ability to measure cellular marker levels for individual cells. With flow rates of thousands of cells per second, FCM can also capture cellular population statistics in a single assay. Compared to assays like microarrays and proteomics that measure aggregate features of the entire mixture of cells, FCM can test both the phenotype and function of specific cell subtypes in a sample including many different cell subtypes. However, the ability of FCM to identify and characterize rare cell subsets is particularly critical in monitoring the immune response following cancer immunotherapy and detection of minimal residual disease (MRD), where the cells of interest typically constitute much less than 1% of the total immune cells in the peripheral blood [39].

1.1.5. Breast cancer

Breast cancer is the most common cancer among women worldwide. It was estimated that 636 000 and 514 000 incident cases occurred in developed and developing countries during 2002, respectively. Besides, it is also the most important cause of neoplastic deaths among women (around 410 000 worldwide in 2002) [1]. In France, INCA estimated with world standardized model (collection rapports & syntheses – 2011, www.e-cancer.fr) that in the year of 2011, 53 000 new cases of breast cancer occurred, an incidence rate of 99.7 for 100 000 women, a death number of 11 500, a death rate of 16.0 for 100 000 women. The mean ages of diagnostic in 2005 are 60 years old, and the average ages of death between 2004

and 2008 are 71 years old. The global survival rate for 5 years diagnosed between 1989 and 1997 is 85 %, and 97 % diagnosed patients can survive for 1 year. Common tools for diagnosis of breast cancer include mammography, ultrasonography, magnetic resonance imaging (MRI), and positron emission tomography (PET).

1.1.5.1. Current screening methods

Mammography was the main and suitable approach for breast cancer control and screening which has been shown to reduce breast cancer mortality by around 25 % in the screened population [41]. However, the sensitivity of mammography depends on the age of women due to dense breast reducing the ability of mammograms to detect early lesions. For women of above 60 years old with breast tissue that is not dense, the sensitivity is 95 %. There is some evidence for a reduction in risk of dying from breast cancer in women aged 40-49 years who undergo annual mammography, but the sensitivity reduces to less than 50% in those 40 years old or less [1]. Specificity of mammograms in symptomatic patients is generally high with reports ranging from 87.7% to 98.6% [42, 43]. As is the case for sensitivity, the specificity of mammography also reduces in the younger patients with dense breast tissue [43]. To sum up, mammography can identify suspicious microcalcifications, but cannot distinguish between certain lobular invasive carcinomas, Paget's disease of the nipple, inflammatory carcinoma, and small carcinomas [41]. In comparison, ultrasonography is more effective to diagnose small tumors in women with dense breast and to differentiate solid lesions from cystic lesions. Ultrasound is better than mammography for detecting invasive breast cancer (92% patients). The combination of ultrasound and mammography is significantly better than either modality used alone, together resulting in 9 % more breast cancers detected [44].

The women at-risk include genetic susceptibility, histological risk and patients previously exposed to mantle radiotherapy for lymphoma. Magnetic resonance imaging (MRI) is highly sensitive and mainly used for screening the high-risk group, which is in particular effective for persons younger than 40 years old. Combination of MRI and mammograms in the group of at-risk population increases the sensitivity from 25-59 % for mammogram alone to 93-100 % for MRI and mammogram [45]. Sardanelli et al [46] evaluated the various modalities in surveillance of at-risk women in a multicenter trial and suggested that routine MRI screening was the most sensitive, compared to other forms of radiological screening. Moreover, it is effective to identify primary foci in non-palpable lesions and auxillary metastases with no evidence of a primary focus, as well as for assessment of response to neoadjuvant chemotherapy. In dynamic contrast-enhanced MRI, images are recorded before and after given a contrast substance to patients. Malignant lesions are generally highly

permeable, with rapid uptake and elimination of contrast substance, whereas benign lesions have slow rising, persistent enhancement kinetics [41]. Although MRI has good diagnosis accuracy, the rate of false-positive cases is still high and MRI findings cannot be the sole indication for breast surgery[47]. Besides, the high cost, lower specificity compared to other modalities [48], and the difficulty of performing real-time MRI guided biopsies [49] may prevent its general acceptance.

Alternatively, positron emission tomography (PET) is used to discover undetected metastatic foci in any distant organ and can evaluate the status of auxillary nodes in the preoperative staging process [50]. A research group reported that tumor marker guided PET scan in the follow-up of breast cancer patients has a sensitivity of 92 %, specificity of 75 % and a positive predictive value of 89 % in the detection of occult tumor recurrence [51]. However, PET could not identify low-grade lesions and tumours less than 5 mm in size.

To sum up, in many randomised studies and population studies, mammography has been shown as the only screening test which could reduce mortality rates of breast cancer if a large proportion of the population used the procedure [52]. However, ultrasonography seems promising for women with dense breasts [53] such as those before menopause, and MRI has been valuable in the screening of women at high risk of breast cancer, especially for those who are younger than 50 years [41].

1.1.5.2. Tumor markers detections

As mentioned in section 1.1.2, tumor markers were produced when normal cells transforms to neoplastic cells, which could potentially be employed for early cancer diagnosis. Compared to image techniques, tumor markers detection are cost-effective and not invasive. A large number of tumour markers are relative to breast cancer, and the following types of Mucins (CA15-3, CA27-29), oncofoetal proteins (CEA), oncoproteins (Her2, c-myc, p53), cytokeratins (TPA, ESR) are among the many proposed as a tumour marker for breast cancer. Besides, mammaglobin, survivin, livin, NY-ESO-1, Annexin XI-A, Endostatin, Hsp90, Hsp70, Hsp60 and p62 are also described [54, 55].

Depending on the breast tumor markers, the detection methods include solid matrix-blotting, immunohistochemistry (IHC), fluorescence in-situ hybridisation (FISH), enzyme immunoassay (EIA) and ELISA. The different approaches can be employed to test various targets relative to tumour markers, such as DNA or gene copy number (FISH, Southern blot), mRNA (Northern blot), cell surface protein (Western blot, cell surface ELISA and IHC) and circulating protein (serum ELISA and EIA). Besides, different tissues samples can be utilized depending on the method of assay: fresh frozen tissue for Southern, Northern and Western blots and IHC; formalin-fixed, paraffin-embedded tissue for IHC and FISH; and serum or

tissue extracts for ELISA and EIA. In particular, ELISA is widely used to test breast tumour markers in either fresh tumour cytosolic fractions or in circulating serum for detection of antigens or the immune response (antibodies) to such antigens [4]. Compared to tissue samples usually obtained following biopsy or surgery, the serum sample can be collected more easily, non-invasively, and on repeated occasions. However, the histological information cannot be obtained by ELISA and an ELISA blood test may measure a different marker endpoint to IHC.

Table 1-3 Cut-off values and sensitivities of measurements in blood tumor marker for breast cancer

Tumors	Cut-off	Sensitivity	Refs
CEA	6 ng/ml	53 %	[56]
CA15-3	40 U/ml	56 %	[56]
CEA and CA15-3	-	94 %	[57]
CEA and CA15-3 and ESR	-	100 %	[58]

Since breast cancer is a heterogeneous disease, these tumours express many aberrant proteins and single tumor markers detection of either antigens or antibodies usually lack sensitivity and specificity in most reported studies. From early study [59] CA15-3 has a higher sensitivity than CEA but with a similar specificity. High sensitivity up to 87 % with high specificity reaching 96 % was reported when using CA 15-3 alone. However, combining several tumor markers demonstrates to be better than any single markers in the diagnosis and monitoring of breast cancer. Table 1-3 summarized the comparison of sensitivities from single markers and combination of them for breast cancer tested in blood samples. As is shown in Table 1-3, the sensitivity could reach beyond 90 % when the two markers (CEA and CA15-3) are used together [57]. It has been know that ESR, frequently tested in clinical medicine, is prone to increase in patients with cancer, particularly as the disease progresses. Elevation of ESR has been reported in patients with breast cancer and a sensitivity of even 100 % could be reached when a panel of three markers are employed for detection [58]. Using a combination of CA15-3, CEA and ESR, 100% of patients are detected [60], which provides the only validated method of assessing the response to systemic therapy for a disease and not by others criteria [59]. In a study performed by the European Group for Serum Tumour Markers in Breast Cancer, 83 patients with metastatic breast cancer assessable for CA15-3 and CEA (with 67 patients assessable for ESR as well) were recruited and prospectively evaluated in 11 centres from six European countries. Among the 67 patients who had all three markers assessed in the form of the biochemical index score, 84 % of patients had elevation

of one or more of these three markers while during therapy the number rose to 96 %. The other 4 % remained in remission throughout the study with all markers below the cut-off levels [60]. Additionally, blood tumor markers measurement is also proposed as valuable tool in monitoring therapy. Compared to conventional assessment by clinical/radiological criteria which often require expensive imaging techniques such as CT or MRI scans, biochemical assessment may bring about at least 50 % cost-savings [59].

1.1.6. Colorectal cancer

Colon and rectal cancers account for approximately 9.4 % of total worldwide cancer cases, equivalent to about 1 million new cases, with a similar number of cases in men and women for colon cancer and a male predominance for rectal cancer from World Cancer Report 2008 [1]. Incidence of colorectal cancer (CRC) ranks fourth in men after lung, prostate and stomach; and third in women after breast and cervix uteri. Currently, colorectal cancer is one of the most common malignancies, with one of the highest cancer mortality rates in the world.

In France, it was estimated by INCA with world standardized model (collection rapports & syntheses – 2011, www.e-cancer.fr), that in the year of 2011 there are 40 500 (21 500 men and 19 000 women) new cases of CRC, an incidence rate of 36.3 for 100 000 men and 24.7 for 100 000 women, a death number of 7 500 (9 200 men and 8 300 women), a death rate of 13.8 for 100 000 men and 8.2 for 100 000 women. The mean ages of diagnostic in 2005 are 70 for men and 73 for women, and the average ages of death between 2004 and 2008 are 75 for men and 80 for women. The global survival rate for 5 years diagnosed between 1989 and 1997 is 56 % (55 % for men and 57 % for women). Patients could have excellent prognosis following surgical resection if their tumor is still localized at diagnosis.

1.1.6.1. Current screening methods

Currently, the screening methods of CRC include colonoscopy, flexible sigmoidoscopy (FS), the faecal occult blood test (FOBT), DNA stool testing, virtual CT scanning, proteomic stool testing, biomarker detection and blood profiling (e.g. surface enhanced laser desorption and ionization time-of-flight mass spectrometry SELDI). Table 1-4 shows the reported sensitivity and specificity for each technology with both advantages and disadvantages. Moreover the detected regions of colorectum also depend on each screening method (Figure 1-4). Colonoscopy is the gold standard for early detection of CRC with a high sensitivity and specificity. However, it is expensive, requires highly trained staff, is invasive and requires uncomfortable bowel preparation [61]. Alternatively, flexible sigmoidoscopy is a rapid

procedure for CRC screening, with low complication rate and no need of sedation or overnight hospital stay. However, it only allows screening of the distal colon (Figure 1-4) and hence misses tumors located in the transverse and ascending colon and the caecum [62].

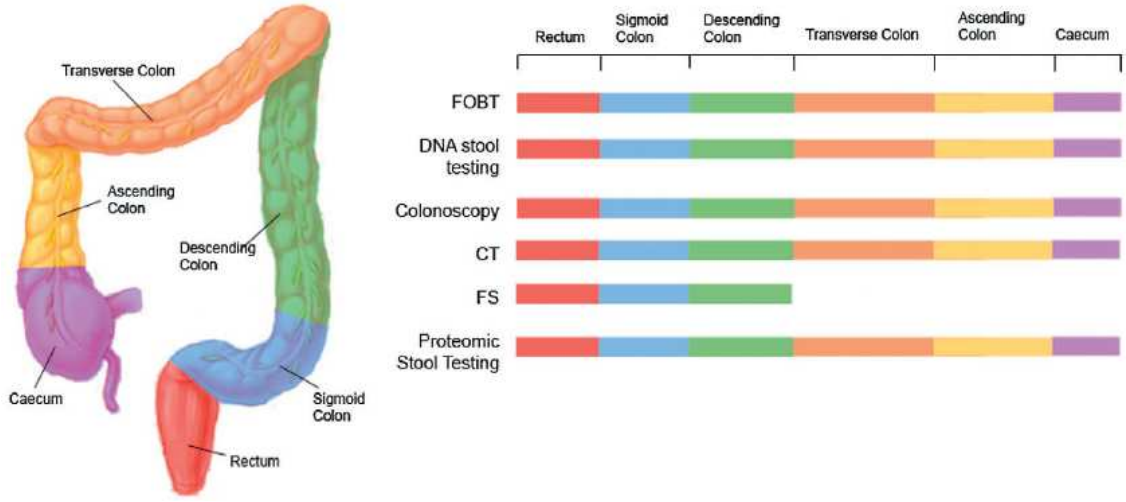

Figure 1-4 Regions of the colorectum screened by different CRC diagnostic tests: FOBT, DNA stool testing, colonoscopy, CT, FS and proteomic stool testing [63]

Table 1-4 Comparison of sensitivity and specificity of each detection method for CRC

Methods	Sensitivity	Specificity	Refs
Colonoscopy	97 %	98 %	[61]
Flexible sigmoidoscopy (FS)	69 %	95 %	[62]
CT	90 %	94 %	[64]
FOBT	52.6 %	87.2 %	[63]
Faecal DNA testing	92 %	93 %	[65]
Faecal protein biomarkers (CEA)	86 %	> 90 %	[66]
Faecal protein biomarkers (M2-PK)	78 %	93 %	[67]
Combination of markers(haemonglobin-haptoglobin, S1000A12)	98 %	79 %	[68]
Blood profiling (SELDI)	95 %	91 %	[69]
Cell line profiling (Secretome analysis) Growth/differentiation factor 15 (GDF 15)	77.8 %	99.4 %	[70]

Computed tomographic (CT) colonography uses radiation-based imaging and various methods of image manipulation (multiplanar reconstructions, three-dimensional constructions) to visualize the endolumen of the colon for polyps. High sensitivity and specificity (90 % and 94%) was reported for detection of large polyps (>10 mm) in populations with a higher

prevalence of polyps (Table 1-4), but depends on the detected population [64]. Sensitivity ranged from 55 to 94% with a specificity of ~95% if CT colonography is used in populations with average risk of CRC development and low-prevalence of polyps (i.e. the general population). Besides, CT colongraphy has difficulty in detecting flat or depressed polyps and the procedure still requires prior bowel preparation, with the risks associated with the ionizing radiation doses for producing the images.

1.1.6.2. Biomarkers for CRC

Compared to other screening methods for CRC, biomarkers detection are non invasive, cost-effective and convenient. Tanaka et al. [71] summarized the common biomarkers for detection CRC, including subjects of plasma, serum and stool (Table 1-5).

Table 1-5 Molecular biomarkers for the detection of CRC [71]

Tumor makers	Types	Subjects	Clinical use
Fecal hemoglobin	Protein	Stool	
CEA	Protein	Serum	In use
CA19-9	Carbohydrate	Serum	
K-ras, APC, L-DNA, p53	DNA	Stool	Clinical
TIMP-1	Protein	Serum	validation
Spondin-2, DcR3, Trail-R2,			
Reg IV, MIC1	Protein	Serum	
PSME3, NNMT, CRMP-2	Protein	Serum	
SELDI (apolipoprotein C1, C3a-des Arg, α1-			Preclinical
antitrypsin, transfeering)	Protein	Serum	development
HNP1-3, MIF, M-CSF, M2-PK, Prolactin	Protein	Serum	
CCSA-2, -3, -4; MMP-9, -7; Laminin	Protein	Serum	
Septin 9	DNA	Plasma	

Carcinoembryonic antigen (CEA) is a high molecular weight glycoprotein, one common oncofetal antigen belonging to the immunoglobulin superfamily. The carboxy-terminal of CEA contains a hydrophobic region which is modified to provide a glycosyl phosphatidylinositol link to the cell membrane [71]. It has been used for many years as a biomarker of CRC as well as cancers developing in other tissues. CEA is usually identified in serum, but can also be determined in biopsy samples. High CEA levels are specifically associated with CRC progression, and increased levels of the marker are expected to fall

following CRC surgery [72]. However, even in the absence of cancer, high CEA levels may also occur in response to inflammatory conditions, such as hepatitis, inflammatory bowel disease (IBD), pancreatitis, and obstructive pulmonary disease. Moreover CEA may not be elevated when CRC is at advanced stage. Therefore, CEA does not provide sufficient sensitivity and reliability for the early detection of CRC. The potential value of the CEA test lies in its use to measure the course of the progression of cancer as a prognostic marker. Locker et al. [10] described CEA as a marker for colorectal cancer but not as a screening test for colorectal cancer. CEA may be ordered preoperatively in patients with colorectal carcinoma if it would assist in staging and surgical treatment planning. Although elevated preoperative CEA (>5 mg/mL) may correlate with poorer prognosis, data are insufficient to support the use of CEA to determine whether to treat a patient with adjuvant therapy.

Carbohydrate antigen (CA) 19-9 is a tumor-associated antigen (first described by Koprowski and co-workers [73]) defined by a monoclonal antibody (1116 NS 19-9) produced by a hybridoma prepared from mouse spleen, immunized with a human colorectal carcinoma cell line. CA19-9, which is the second most investigated gastrointestinal tumor marker, is known to be a sialylated Lewis-a antigen. Although CA 19-9 is the best marker available for pancreatic adenocarcinoma, CA 19-9 is less sensitive than CEA for CRC and also gives less information than CEA. Other carbohydrate antigens, such as CA 50, CA 195, CA 242, CA M26, CA M25, CA M43 and CA 72-4, have also been evaluated extensively [74]. However, these antigens are not useful markers for the detection of CRC due to their sensitivity, stage dependency and specificity.

One of the crucial parameters for biomarkers tests is to improve sensitivity and specificity. Recently, four serum biomarkers, spondin-2, tumor necrosis factor receptor superfamily member 6B (DcR3), TRAIL receptor 2 (TRAIL-R2) and Reg IV were evaluated in 600 serum samples [71]. All four markers, as well as a fifth marker, macrophage inhibitory cytokine 1 (MIC1), were elevated in patients with CRC when compared to normal controls and patients with benign diseases. Besides, this five-serum biomarker panel may have better sensitivity and specificity than CEA to improve the detection rate of early stage CRC. These results keeps in agreement with the tumor marked diction for breast cancer diagnosis.

The FOBT is the most widely prescribed primary screening tool, which tests for the presence of blood or blood products in stool samples. It is a cheap and non-invasive test, but with a high rate of both false-positive and false-negative results [61]. The antibody-based iFOBT is more specific for human blood with sensitivity of 52.6% and a specificity of 87.2% (Table 1-4), which is also probably specific for blood originating from the colorectum as blood from the gut degrades as it travels down the digestive tract [75]. All positive FOBTs should be followed up with colonoscopy. The poor selectivity and sensitivity of the test puts an excessive burden on current colonoscopy services and subjects a large number of patients

to unnecessary colonoscopy. Hence, there is an urgent need to develop more sensitive, reliable and specific screening tests for early stage colon cancer when therapy is most likely to be effective [63]. Currently, antibody-based methods are the most widely used for quantitative biomarkers measurement, with techniques such as ELISA, IHC or microarrays. Recent studies using protein arrays [76] demonstrated that antibody specificity is often lacking, and the validation of the signals observed must be taken into consideration.

1.2. Protein microarray

1.2.1. Introduction

Protein chips (microarrays) are of increasing importance in biomedical diagnosis, drug delivery, food testing etc, due to the advantages of high throughput, miniaturized sample requirement and multiplex detection. Initially, thousands of different expression bacteria clones were arrayed on large protein binding membranes in order to screen cDNA libraries for clones expressing recombinant proteins in Escherichia coli [77]. Then the miniaturization technology was developed to protein microarray. Typically, protein microarrays consist of immobilized proteins spatially addressed on solid supports (such as silicon, glass slides, etc). Proteins immobilized onto surface (referred as probes) usually include peptides, purified recombinant proteins, antibodies or fragments thereof, antigens, or other proteins. Ideally, probes should keep activity, remain stable and do not be destroyed during the experimental procedures. After washing and blocking unreacted sites on the surface to avoid too high background signal, the collection of proteins arranged (in arrays) on the substrate is then incubated with analyte containing targeted molecules to be detected. Analyte could be serum, salivia or other samples chasing for molecules recognition events. The binding is detected by using a label, either covalently bound to the putative interaction partner or a secondary antibody, or by novel label-free methods. The signal could be determined by various techniques if an interaction occurs on the surface. Moreover, a large number of binding events are detected in parallel by scanning the entire array. Figure 1-5 illustrates a general scheme of a typical protein microarray experiment.

Currently, protein microarrays come in a variety of formats, depending on the proteins to be immobilized and their functions [78, 79]. Typically, it includes three categories:

- (1) Function arrays, aiming at discovering protein function in fundamental research. In this protein microarrays, a large set of purified proteins or peptides or even an entire proteome are immobilized on the substrate to screen in parallel a range of biochemical interactions; such as effects of substrates or inhibitors on enzyme activities [80, 81] protein-drug or hormone effector interactions [82, 83].

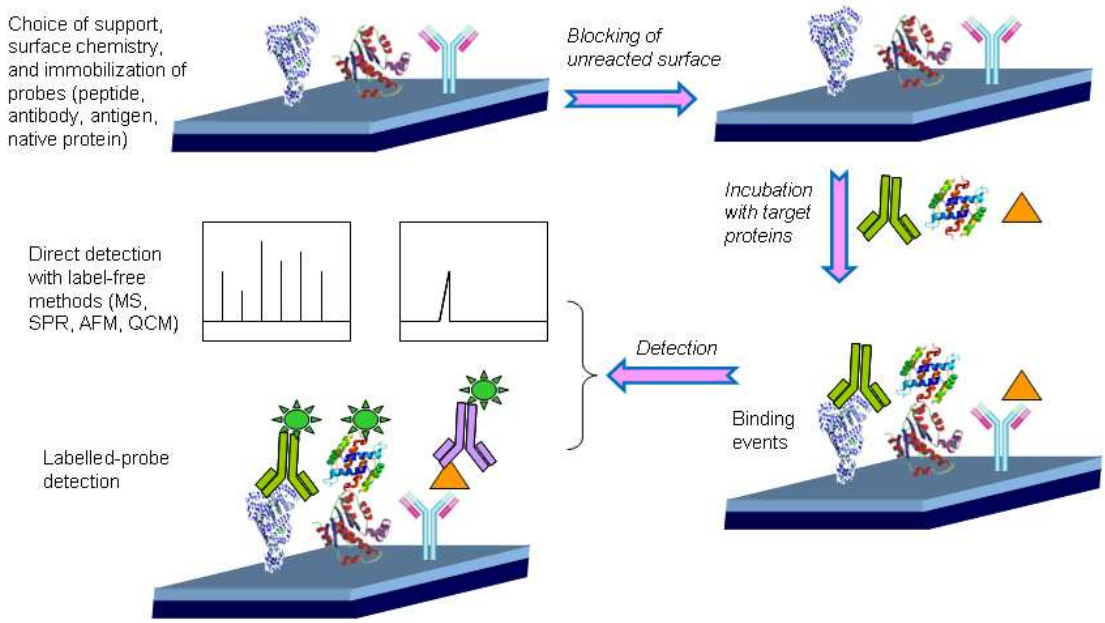

Figure 1-5 General scheme of a typical protein microarray experiment, MS: mass spectrometry, SPR: surface plasmon resonance, AFM: atomic force microscopy, QCM: quartz crystal microbalance.

- (2) Detection arrays (or analytical arrays): In protein detection microarrays, the probes are affinity reagents (antigens or antibodies) rather than the native proteins themselves, to determine protein abundances in a complex matrix such as serum [84, 85]. Analytical arrays can be employed to assay antibodies for diagnosis of rheumatoid arthritis [86] or autoimmunity diseases [87]. The emphasis is that antibody microarrays have been widely applied in biomarker screening and diagnosis of cancer. More details will be summarized in the following part of this chapter.

- (3) Reverse phase arrays (usually referred as reverse phase microarrays): In this category of protein microarrays, the probes include tissues [88], cell lysates [89] or serum samples [90], which are spotted on the surface and recognized with one antibody per analyte for a multiplex readout. A major advantage of the reverse phase arrays is the requirement of tiny volume of protein extracts for the generation of tens of microarrays, which can be analyzed in a highly automated fashion compared to gel electrophoresis.

Generally, protein microarray has played a key role for detecting interactions between proteins and recognition of antibody/antigen, which has been proved a powerful tool applied in diagnosis of cancer. Herein, more details of protein microarray will be summarized in the following, such as solid support, surface chemistry, detection techniques etc.

1.2.2. Substrates of protein microarray

1.2.2.1. The choice for solid substrates of protein microarray

One of the most important factors that determine the performance of protein microarrays is the solid substrate on which the proteins are immobilized. The selected materials used as the solid support of protein microarray should not only efficiently immobilize proteins on its surface but also keep their best biological activities. Generally, the solid support for the protein microarray should meet the requirements as following:

Firstly, the solid support should provide optimal binding conditions with high binding capacities of proteins and keep the stability of the resulting biosensor layer. Because protein has no specific uniform adhesion due to its complex structure, the immobilization on the support depends on the properties of each protein.

Secondly, materials must be adapted to the detection methods used. For instance, a label free detection as SPR (Surface Plasmon Resonnance) requires a dielectric/metal interface with two different reflexion indices. In this case, a thin metal layer (gold or silver) must be deposited on the surface of glass slide. For electrochemical detection, solid support must be conducting (metal or semiconductor materials as Si/SiO2 are required for potentiometric measurement). Besides, the physical properties of supports should have no great effects on the detection information of biosensor layer and low intrinsic signals. For example, auto-fluorescence or background of the support is avoided if using fluorescence scanning as the detection system.

At last, the solid support must be suitable for high-throughput manufacturing and screening procedures. This includes rapid and inexpensive production in high quantities, ease of handling during storage and preparation procedures as well as high reproducibility. The material should also be compatible with all fabrication steps including harsh washing conditions or micro-technological steps. Thus, it is required to provide a non-denaturing environment to avoid the loss of activity and binding sites during the process of immobilization, because the objective of protein microarray technology is the investigation of interactions between proteins with their biological activities.

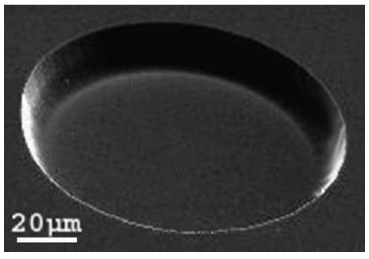

Figure 1-6 SEM image of the 3D microreactor with diameter of 100 µm and depth of 14.8 µm [91]

From the viewpoint of physical structure, the solid substrate includes 2-dimension (2D, flat) or 3-dimension (3D, with microstructure such as microwell on the surface). The flat 2-dimension (2D) slides are commonly used as the solid support for manufacturing protein microarray due to the low cost and easy treatment. However, protein microarray based on 2D supports normally can just be put in contact with only one solution. In order to perform multiplex analysis of a set of sample analyte, Mazurczyk et al [91] developed one process to elaborate 3-dimension (3D). By photolithography onto glass slides, they groove microwells with depths exceeding 100 μm and surface roughness below 10 nm (Figure 1-6). These microstructured slides not only retain surface properties of the original glass substrate, but also do not increase the fluorescence background level. This makes it possible to use the existing methods of glass surface functionalisation for protein immobilization and the classical fluorescence scanner for detection.

1.2.2.2. Typical substrates

Previously, filterable membranes, such as polyvinylidene fluoride (PVDF) and cellulose nitrate membranes were chosen as the support for high-density protein microarrays, due to their low-price, easy-preparation, and direct immobilization of large amount of protein without surface modification [92]. The interaction between the surface and proteins is physical adsorption, which represents the simplest process of protein binding, although it is rather uncontrollable. Close proximity between the adsorptive surface and the reactive site of protein could have unfavourable effects on the biological activity towards its ligands. Besides, the surface of the solid may also be susceptible to exchanging adsorbed protein due to the surrounding solution and non-specific adsorption could be also a problem. Therefore, they have been gradually replaced by other solid supports due to their too many uncontrolled parameters. However, some groups now arrayed proteins on polymer support primarily for optical and economical reasons [93, 94]. Cyclic polyolefin slides, like Zeonor representing a class of new polymeric materials with excellent optical and mechanical properties, were employed to immobilize antibody [93]. Glycidyl methacrylate (GMA)-modified polyethylene terephthalate (PET) plastic, which can introduce high density of epoxy groups to PET surface by grafting GMA photopolymer, was described as good solid support to manufacture high performance protein microarrays [94].

Glass is a popular material as solid support for protein microarray, primarily due to its low fluorescence, transparency, low cost, and resistance to high temperature [95]. Glass surfaces can be modified by silane chemistry introducing specific functional group such as amino groups, epoxide, carboxylic acid and aldehyde, which can directly react with protein

by physisorption/chemisorption or further covalent bind with other biocompatible chemistries (*e.g.* chitosan) to generate novel surfaces. In addition, glass offers a number of practical advantages over porous membranes and gel pads, which is easy to handle and adaptable to automatic readers. Currently, two major categories of microarray slides exist: gel-coated surfaces, such as polyacrylamide [96] or agarose [97] and non-gel-coated modified glass surfaces, such as aldehyde [32], poly-L-lysine [98], or nickel-coated slides [99]. In addition, gold film deposited on the solid support is commonly employed as the protein microarray substrate with the SPR detection [100].

1.2.3. Surface modification of substrates

The crucial parameter in the elaboration of protein microarrays is the design of stable and reproducible surfaces which enable to retain biological activity of immobilized proteins. In the past decades, a lot of surface chemistries have been reported to meet the requirements of protein microarrays, and can be typically divided into three groups as following [101]: two dimension (2D), three dimension (3D) and other concept surfaces (Table 1-6).

The surface chemistry of protein microarray used either in an interaction or capture mode has to provide several key functions. It is essential to keep high binding capacity for any proteins without changing their biological active (three-dimensional structure, functionality and binding sites) conformation, as well as low auto-fluorescence in order to generate a high signal to noise ratio. Such a task is not only important for immobilization of the relatively stable antibodies, but becomes crucial for the detection of protein-protein interactions on protein microarrays [101]. With most of solid support (glass slide/silicon) of protein microarrays, it is not easy to graft proteins directly on the surface and keep stable attachments. In consequence, it is necessary to introduce new chemical reactive groups on the surface of solid support by biofunctional cross-linker, which possesses one reacting group towards the substrate and a second reacting group for the subsequent surface biofuctionalization. For constructing protein microarray or biosensors, silanes are often used to functionalize glass slide/silicon for covalent protein immobilization or further coupling with other chemistries to attach proteins.

Table 1-6 Surface chemistries for protein microarray

	Surface chemistry	Surface coating	References
2D surfaces	Amine slides	Amine groups	[102-104]
	Aldehyde slides	Aldehyde groups	[104, 105]
	Epoxy slides	Epoxy groups	[103, 104]
	MaxiSorb slides	Polystyrene-based modified surface	[104]
	Mercapto slides	Mercaptopropyltrimethoxy-silane groups	[105]
3D surfaces	Hydrogel slides	Modified polyacrylamide gel	[106]
	Agarose slides	Agarose gel	[97]
	Polyacrylamide gel	Polyacrylamide gel	[96, 107]
	FAST slides	Nitrocelluose-based matrix	[102, 103, 107]
Others	PEG-epoxy slides	Polyethylene glycol layer with reactive epoxy groups	[103, 107]
	Dendrimer slides	Dendrimer layer with reactive epoxy groups or carbonyl-diimidazole	[103]
	BSA-NHS slides	Bovine serum albumin activated with N-hydroxysuccinimide	[32]
	Ni-NTA slides	Nickel-nitrilotriacetic acid complex	[99]
	DMA-NAS-MAPS slides	N,N-dimethylacrylamide, N,N-acryloyloxysuccinimide, [3-(methacryloyl-oxy) propyl]-trimethoxysilyl copolymer	[108]
	Streptavidin slides	Streptavidin	[109, 110]
	Avidin slides	Avidin	[111]

1.2.3.1. Organosilane for protein microarray

Organosilanes (silanes) are widely used and often serve as the foundation layer in the fields of biosensors and biochip technology and it can react with a wide range of materials (bearing surface with hydroxyl groups). Furthermore, commercial silanes bearing various chemical functional groups are readily available for different requirements. The silanes are normally composed of two distinct reactive moieties (Figure 1-7): the silyl head group and the organic reactive group classically carried at the end of an aliphatic chain. The silyl head group undergoes reaction with surface hydroxyl groups leading to a robust tethering of the silane molecules to the substrate. Then, organic functions (carboxyl, amino, epoxy etc reported commonly), permit the immobilization of biological probes via covalent or electrostatic interaction [112-114].

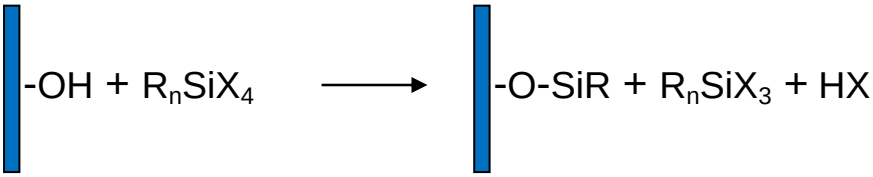

Figure 1-7 General equation of silanization on solid surface

The two grafting mechanisms are included in the reaction between organosilane (chloro or alkoxysilane) and the silanol on the surface of glass/silicon: (1) At elevated temperature (more than 150 ^{o}C) and under anhydrous conditions, silane (chlorosilanes) molecules react readily with the surface silanols to form siloxane bridges [115, 116]. (2) At low temperature, the weak reactivity of alkoxysilanes is offset by the presence of stoichiometric excess of amine. A pentavalent transition-state adduct was generated during the base catalysed reaction with surface silanol groups. The comparisons of two reaction mechanisms were reported for aminosilanes (e.g. dimethyaminosilane) in solution [117].

Generally, silanes includes mono- and multifunctional (tri or di-chloro or -alkoxysilane), with respect to the number of reactive group of silanol. Previously, the majority work focused more on multifunctional silanes due to their higher reactivity than monofunctional silanes [118, 119]. The compact self-assembling monolayers (SAMs) of the silane molecules could be formed on the interface between the liquid and solid substrate. Under appropriate conditions (solvent composition, alkyl chain length, and temperature), the long aliphatic chains of some alkylsilane molecules are able to establish dispersive interactions leading to highly ordered SAMs [117, 120, 121]. The stability of the layer mainly depends on the temperature and the length of the alkyl chain [121]. Because thermal agitation is intended to disrupt dispersive interactions, SAMs are prepared at low temperatures (<40 °C). Once assembled, the film of silane molecules has to be frozen: multifunctional silane molecules (di or trifunctional) form a 2-dimensional polymeric network of silane molecules connected by intermolecular siloxane bonds (further cross-linking). Water is essential to hydrolyze the alkoxy or chlorosilane, but the excess of water may reduce polymerization in solution and consequently the formation of thick and nonhomogeneous organosilane layers. Thus, the reaction conditions should be well-controlled (solvent, silane concentration, water content, temperature, surface preparation, etc.) in order to obtain homogeneous and reproducible SAMs on the surface of substrate [118].

Compared to multifunctional silanes, although monofunctional silanes generally lead to less dense layers on the surface [120, 122], they are more reproducible because of simple and reliable reaction routes. Besides, it is easy to remove the dimers from the surface, which may be formed due to the presence of water during the process. Each silane forms one siloxane

bond with the surface. Silane grafting density, with respect to fully hydroxylated substrate, is thus limited by the size of the head group (0.32 nm–0.38 nm) [120]. The covalent attachment of each monofunctional silane could ensure a good stability of the layer towards harsh conditions (washing or subsequent chemical treatments on the surface) [114, 123]. Owing to these advantages, monosilanes recently are of more special interests in the fields of biosensors and biochips.

Dugas et al. [114, 116] developed a monofunctional silanization protocol called "Impregnation Protocol" (IP) where the tert-butyl-11-(dimethylamino) silylundecanoate (TDSUM) was dissolved in dry pentane in the presence of the substrate. The pentane was evaporated leading to the impregnation of the surface by the silane molecules (also called thin condensed film process [112]). Under these conditions, it was demonstrated by using infrared spectroscopy on high surface area silica, that all accessible surface silanol groups reacted with silane molecules to form a dense and continuous layer [116]. This protocol was compatible with the surface modification of glass slides [114, 124], porous silicon [124] and silica [125]. The resulting organosilane layers were robust and reproducible with regards to the covalent immobilization of amino-modified oligonucleotides. This robustness was well established by performing 25 successive cycles of hybridization/denaturation onto the same surface without observing any degradation [124]. These surfaces can also withstand the deprotection/oxidation steps during the oligonucleotide synthesis directly performed on the chip by using the phosphoramidite chemistry [126, 127]. The silanization by impregnation protocol is well adapted at research laboratory level, but not industrially viable and environmental with regards to reagents consumption, solvent waste management, cost and security.

Table 1-7 Comparaison of the two silanization methods: peak to valley height (Δz) and root mean square values (RMS) measured by AFM [113]

Substrates processes	Silica			Glass slide		
	Bare	IP	GP	Bare	IP	GP
Δ*z* (nm)	0.4±0.1	0.5±0.1	1.5±0.2	1.5±0.2	1.5±0.3	3.5±0.5
RMS	0.24±0.05	0.24±0.05	0.45±0.05	0.8±0.1	0.8±0.1	1.5±0.2

On the basis of IP protocol, Dugas and colleagues [113] developed a gas phase (GP) silanization protocol with the purpose of cost efficiency, facility and mass production for the industrial process. The comparative study indicates that IP leads to smooth surfaces whereas GP induces the formation of islands features suggesting a non-continuous silane layer (Table 1-7) but the density of the immobilized probes remained similar.

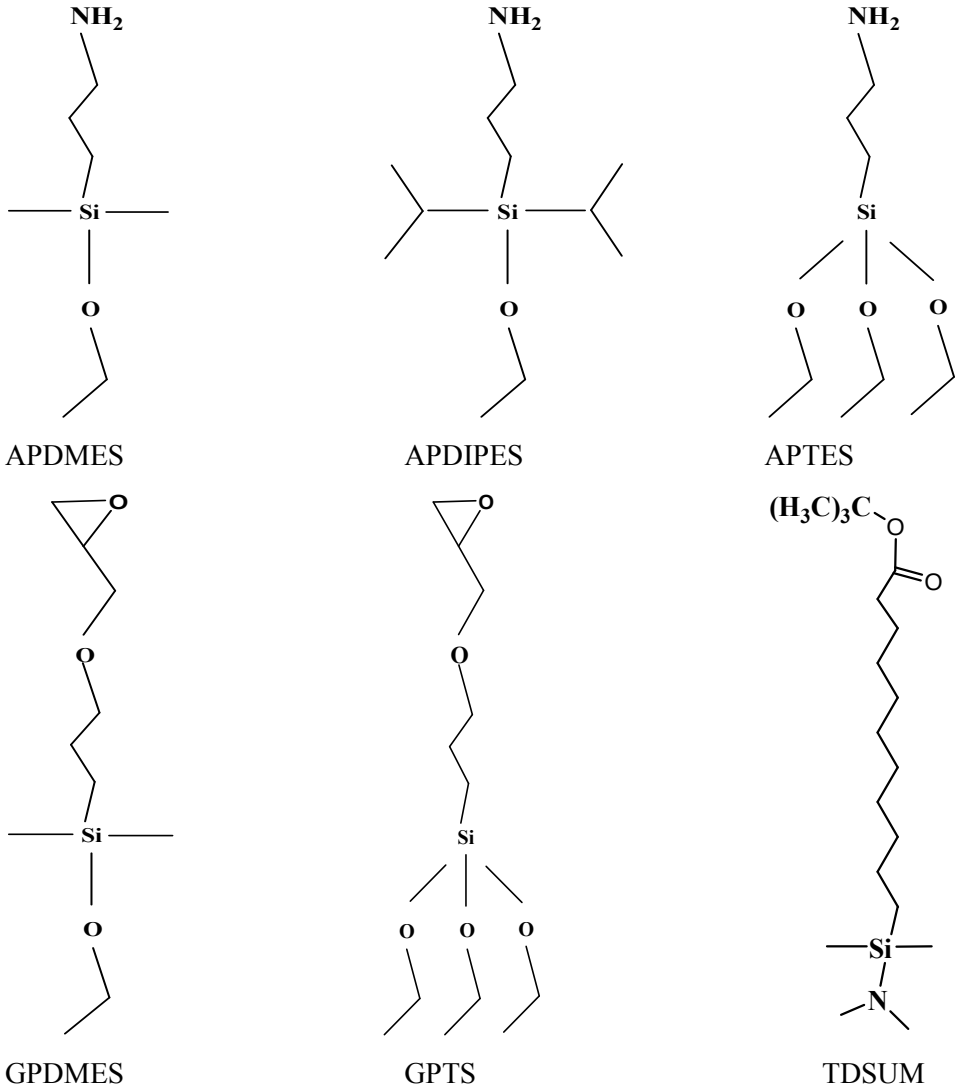

Figure 1-8 Schemes of amino, expoxysilane with mono- and multifunctionality

In addition, chemical vapor deposition (CVD) was also employed for silanization with two monofunctional aminosilanes (3-amino-propyl-dimethyl-ethoxysilane APDMES, and 3-aminopropyldiisopropylethoxysilane, APDIPES) and one trifunctional aminosilane (3-aminopropyltriethoxysilane, APTES) [123]. The robust films formed on the surface showed good stability against storage in the laboratory, but APDIPES films retain most of their integrity at pH = 10 for several hours and are more stable than APTES or APDMES layers. It is important that the controllable film did not depend on the any volume of three aminosilanes, which could lower the cost of processes and make them more environmentally friendly. Alternatively, silane with the functionality of epoxy group were also reported, such as 3-glycidoxypropyltrimethoxysilane (GPTS) [128] and 3-glycidoxy-propyl-dimethyl-ethoxysilane (GPDMES) [129, 130]. After silanization on the surface of glass slide, it can

directly immobilize proteins to manufacture protein microarray or biosensors. Figure 1-8 presents the chemical structure of several common silanes with various functionality groups.

1.2.3.2. Functionalization with cross linkers

High molecular weight polymers such as various derivatives of collagen, dextran, or cellulose have been commonly employed as surface chemistry for protein immobilization [131-133]. Chemical adsorption occurring between the polymer surface and proteins allow robust protein immobilization with good reproducibility. They can be applied to a wide range of proteins and versatile linkage processes. However, chemical modification of proteins causes loss of activity and low immobilization efficiency. It also requires multiple functional surfaces [134]. Alternatively, chemically activated surfaces like active esters with biopolymer will facilitate the sample preparation but also with excellent protein immobilization capacity. Carboxymethyl dextran (CMD) was an efficient surface chemistry for manufacturing biosensor/biochip and it has been reported to be excellent immobilization of both monoclonal and polyclonal antibodies [135, 136]. The activation of carboxyl groups generates reactive succinimide esters on CMD surface (Figure 1-9), which could react spontaneously with amine and other nucleophilic groups, allowing direct immobilization of molecules containing such groups.

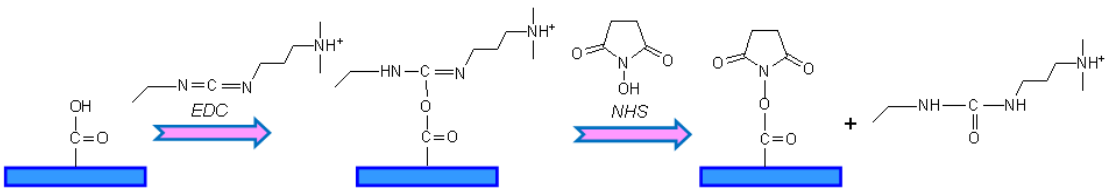

Figure 1-9 Schematic illustration of activation of carboxymethyl dextran with 1-Ethyl-3-(3-dimethylaminopropyl) carbodiimide hydrochloride (EDC) / N-Hydroxysuccinimide (NHS) [137]

There is a commonly commercial product of biosensor, sensor chip CM5 (Biacore, GE healthcare), with carboxymethyl dextran (CMD) covalent attached on a gold surface specially designed for SPR measurement. The ligand is covalently bound to the sensor chip surface by carboxyl moieties on the dextran. Functional groups on the ligand that can be used for coupling include amine, thiol, aldehyde or carboxyl groups. Sensor chip CM5 with a high binding capacity gives a high response, advantageous for capture assays and for interactions involving small molecules, proteins, nucleic acids and carbohydrates. High surface stability provides accuracy and precision and allows repeated analysis on the same surface. The surface matrix on Sensor Chip CM5 extends about 100 nm from the gold surface under physiologic buffer conditions (Figure 1-10). Recently, Sensor Chip CM7 was developed by

Biacore, which has chemical properties similar to Sensor Chip CM5, but with a three times higher immobilization capacity to achieve the required immobilization levels needed to give higher analyte responses.

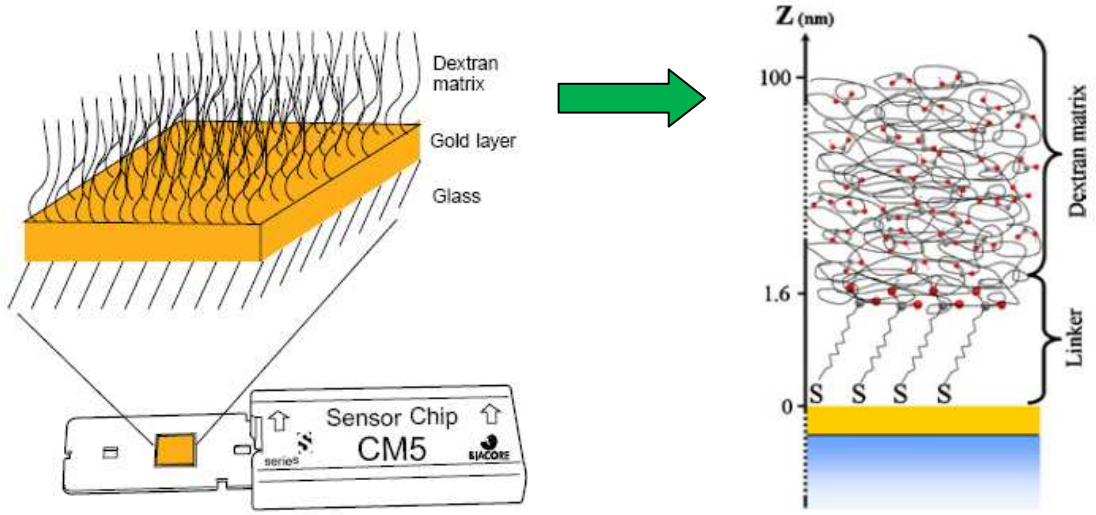

Figure 1-10 Schematic illustration of the structure of the sensor chip surface CM-series chips [138, 139] CM5 sensor chip

Perrin and co-workers [140] immobilized the recombinant protein derived from the viral capsid p24 of the human immunodeficiency virus (HIV) on maleic anhydride and methyl vinyl ether copolymer (MAMVE) coated surface to elaborate array detecting infected human sera. The conjugated copolymer largely improved detection sensitivity of anti-p24 antibodies in infected human sera. In a previous work [141], our group developed silanized glass slides functionalized with N-hydroxysuccinimide (NHS) ester and with MAMVE copolymer for immunofluorescent assays. Analytical performances of these microarrays were evaluated for the detection of anti-histone autoantibodies present in the sera of patients suffering from an autoimmune disease, systemic lupus erythematosus. The detection limit of our MAMVE copolymer microarrays was 50-fold lower than that of the classical ELISA, indicating that MAMVE functionalization is an efficient surface chemistry for protein. Lee et al [134] developed a highly sensitive protein microarray, ProteoChip, coated with ProLinker, novel calixcrown derivative with a bifunctional coupling property. This derivative permits efficient immobilization of capture proteins on solid matrixes and makes high throughput analysis of protein-protein interactions possible. The detection sensitivity of ProteoChip was as low as 1–10 femtogram/mL of analyte protein, useful for detection of tumor markers. It is a powerful tool for development of chip-based screening microarrays to monitor protein-protein interactions (*e.g.* drug target) as well as for biomarker assays which require high detection sensitivity.

Lee et al [142] evaluated various surface modification methods for reducing nonspecific interactions of proteins on the surface of small-molecule microarrays during proteomic screening. A significantly enhanced signal-to-noise ratio and stronger fluorescence signal were obtained on Jeffamine-modified glass surfaces. They successfully immobilized small-molecule to identify a novel inhibitor of tyrosinase, a major target of melanin biosynthesis for the development of novel whitening agents in the cosmetics industry and biomedical research. Kim and co-workers [143] modified the glass surfaces with monolayers produced by silanisation and polymer layers for fabricating protein microarray. Covalent binding and non-specific antibody adsorption were examined by quantifying IgG-peroxidase conjugates immobilized to the polymer-grafted glass substrates. Polymer-grafted glass substrates showed that non-specific adsorption was reduced by 10-60% as compared with 3-aminopropyltriethoxysilane (APTS)-treated substrate. In particular, chitosan-grafted substrates exhibited very low non-specific protein adsorption, which suggests that grafting the surface with chitosan is one of the best surface modification methods for the fabrication of protein microarrays. It demonstrates that cross-linker coated surface with sufficient steric space could maintain the native conformation of proteins and prevent the loss of biological activities.

Consequently, the 2D surfaces bind proteins and antibodies either by weak interactions (electrostatic, Van der Waals and hydrogen bond,) or through the formation of covalent bonds, with advantages of strong attachment combined with low experimental variation. However, 2D surfaces suffer from fast evaporation of the liquid environment and the close protein surface contact, which may influence the three dimensional structure of proteins. For example, antibodies immobilized on aldehyde-surfaced solid support had lower binding affinities or reduced specificities of antibody-antigen interactions [92]. Therefore, three-dimensional (3D) gel or membrane-modified surfaces, such as polyacrylamide [96, 106], agarose [97] and nitrocellulose [102] were increasingly attracted more attentions due to the advantages of preservation of the native protein conformation, like CMD gel (Figure 1-11). On the other hand, there is also the combination of disadvantages for 3D surfaces such as large variations in signal intensity [105]. Besides, the third group includes surface coatings (Table 1-6), such as dendrimer or avidin slides, which contains characteristics of both 2D and 3D surfaces mentioned above. They do not have a visible 3D structure, and cannot be considered as two-dimensional because they display a supramolecular structure on their surface [101].

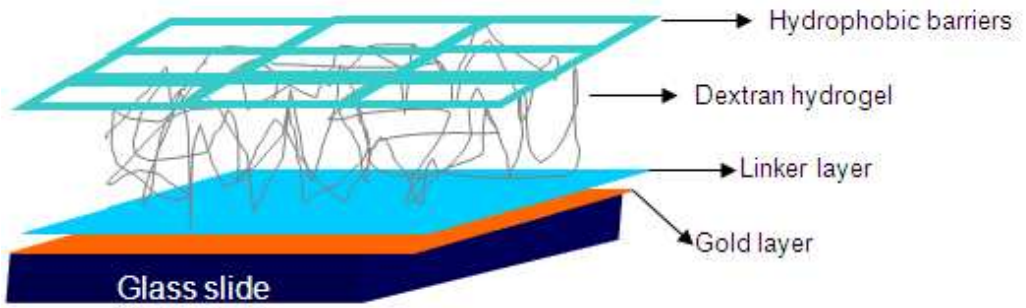

Figure 1-11 Schematic illustration of a CMD hydrogel on top of which hydrophobic barriers have been introduced by microcontact printing of tetraoctadecylammonium bromide (TOAB) molecules [144]

1.2.4. Surface characterization techniques

To monitor the surface modification, a lot of surface characterization tools have been used as reported in many publications. Challenge consists in obtaining a fine surface characterization at both macro and nano scale of successive thin layers coating on solid substrate. Thus, combination of various techniques is required.

1.2.4.1. ATR- FTIR

Application of FTIR spectroscopy has been shown to be a useful tool in monitoring structural changing on the surface of the solid support, which has been considered one of simple, directly, flexible and sensitive in situ infrared technique. For attenuated total reflection Fourier transform infra red (ATR-FTIR), the infrared beam samples a surface by internal reflection of the light. The molecule of interest is placed on the surface, and the infra red light penetrates the surface via the evanescent field. The analysis of the special band in the spectrum can indicate the chemical component on the surface, such as monolayer or polymer layer on substrates. White et al. [145] observed the gas-phase reaction of (3-aminopropyl)dimethylethoxysilane (APDMES) with silica using infrared spectroscopy. It was found that on APDMES surface the N–H stretching mode at 3346 cm^{-1} and bending mode at 1622 cm^{-1} for the gaseous molecule shift to 3370 and 1596 cm^{-1}, respectively. These frequency shifts are consistent with an increase in N–H bond strength and this is expected for H-bonding of the N atom of the amine with the surface SiOH groups.

1.2.4.2. X-ray Photoelectron Spectroscopy (XPS)

X-ray Photoelectron Spectroscopy (XPS) was developed in the mid 1960s by K. Siegbahn and his research group, who was awarded the Nobel Prize for Physics in 1981 for his work in XPS. The phenomenon is based on the photoelectric effect outlined by Einstein in 1905 where the concept of the photon was used to describe the ejection of electrons from a surface when photons impinge upon it. XPS involves directing a beam of X-rays onto a sample, penetrating to a distance of a few micrometres. This causes the ejection of electrons from core energy levels in atoms on or near the surface, but only if the energy of the X-rays is great enough to overcome the energy holding the electrons to the nucleus (known as the binding energy). Only a small amount of these electrons emerge from the sample surface without suffering any energy loss through collisions on the path through the sample bulk. The chance of an electron reaching the surface without any energy loss decreases greatly as the distance from the surface increases. The binding energy of an electron can then be calculated if the kinetic energy of the electrons is known [51]. The following equation (Eq.1-1) is used to describe the relationship between the binding energy of an electron and its kinetic energy when ejected from its orbital:

$$E_{kin} = hv - E_{bind} - \Phi \tag{1-1}$$

where E_{kin} is the electrons kinetic energy, E_{bind} is its binding energy, hv is the energy of the X-rays used and Φ is the work function of the spectrometer. Al Kalpha (1486.6eV) or Mg Kalpha (1253.6eV) are often employed as the photon energies for XPS, sometimes with the choice of Ti Kalpha (2040 eV) X-ray lines.

The XPS technique is highly surface specific due to the short range of the photoelectrons that are excited from the solid [146]. The energy of the photoelectrons leaving the sample is determined by means of a concentric hemispherical analyser (CHA) and this gives a spectrum with a series of photoelectron peaks. The binding energy of the peaks are characteristic of each element and the peak areas can be used (with appropriate sensitivity factors) to determine the composition of the materials surface. Besides, the shape of each peak and the binding energy can be slightly altered by the chemical state of the emitting atom. Therefore, XPS provides quantitative chemical bonding information about all elements except Hydrogen and Helium.

1.2.4.3. Contact angel measurement

One of the important characteristics of a liquid penetrant material is its ability to freely wet on the surface of the object being inspected. At the liquid-solid surface interface, if the molecules of the liquid have a stronger attraction to the molecules of the solid surface than to each other (the adhesive forces are stronger than the cohesive forces), wetting of the surface occurs. Alternately, if the liquid molecules are more strongly attracted to each other than the molecules of the solid surface (the cohesive forces are stronger than the adhesive forces), the liquid beads-up and does not wet the surface of the part. One way to quantify a liquid's surface wetting characteristics is to measure the contact angle of a drop of liquid placed on the surface. The contact angle is the angle formed by the solid/liquid interface and the liquid/vapor interface measured from the side of the liquid (Figure 1-12).

The contact angle results were determined from the sessile drop measurements by means of the geometric mean method of Owens, Wendt, and Rabel. They applied the Young's Equation: [147]

$$\gamma_{sl} = \gamma_{sv} - \gamma_{lv}\cos\theta \tag{1-2}$$

Where γ represents surface tension or surface energy, the subscripts *sl*, *sv*, and *lv* refers to the solid-vapor, solid-liquid, and liquid-vapor interfaces, respectively, and θ is the contact angle formed between a pure liquid and the surface of the solid as shown schematically in Figure 1-12.

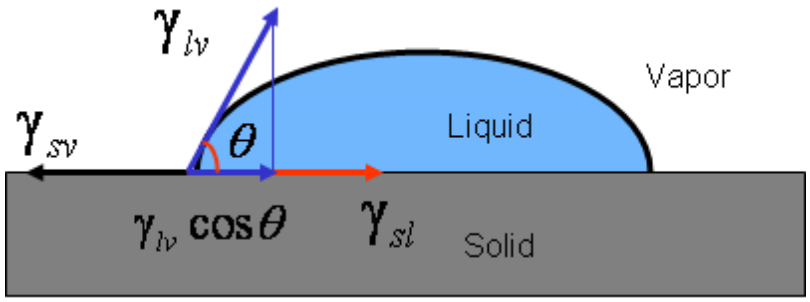

Figure 1-12 Schematic illustration of the Young's Equation at the three phase boundary of a sessile drop on a solid surface

The surface energies, viz., the total energy (γ_{sv}), the dispersive energy (γ_{sv}^{D}) and the polar energy (γ_{sv}^{P}) are calculated from the wetting angle (θ) according to the Owens-Wendt equations [148]. The Owens-Wendt two-parameter model presents that the surface tensions of the solid-vapor and liquid-vapor inter-phases consist of two components: a dispersive one accounting for van der Waals and other non-site-specific interactions and a polar one

accounting for dipole-dipole, dipole-induced dipole, hydrogen bonding and other site-specific interactions [147].

$$\gamma_{sv} = \gamma_{sv}^{D} + \gamma_{sv}^{P} \tag{1-3}$$

$$\gamma_{lv} = \gamma_{lv}^{D} + \gamma_{lv}^{P} \tag{1-4}$$

Where *D* and *P* refers to the dispersive and polar parts of the surface tension, respectively. The γ_{sl} value was defined with geometric mean method by Good [149] in Eq. 6.

$$\gamma_{sl} = \gamma_{lv} + \gamma_{sv} - 2\sqrt{\gamma_{lv}^{D} + \gamma_{sv}^{D}} - 2\sqrt{\gamma_{lv}^{P} + \gamma_{sv}^{P}} \tag{1-5}$$

By combining the Young's Equation Eq. 1-2 and Eq.1-5 leads to Eq.1-6

$$\frac{(\cos\theta + 1)\gamma_{lv}}{2\sqrt{\gamma_{lv}^{D}}} = \sqrt{\gamma_{sv}^{P}}\sqrt{\frac{\gamma_{lv}^{P}}{\gamma_{lv}^{D}}} + \sqrt{\gamma_{sv}^{D}} \tag{1-6}$$

The two unknown components of the surface energy γ_{sv}^{P} and γ_{sv}^{D} in Eq. 1-6 can be determined from the previously measured contact angles against the test fluids with known values of surface tension components. The plots for different liquids and the same surface are situated on a straight line. A plot of $\frac{(\cos\theta + 1)\gamma_{lv}}{2\sqrt{\gamma_{lv}^{D}}}$ versus $\sqrt{\frac{\gamma_{lv}^{P}}{\gamma_{lv}^{D}}}$ for different liquids calculates the dispersive component γ_{sv}^{D} (square of the *y*-intercept), the polar component (square of the slope) and consequently the surface energy of the solid-vapor interface γ_{sv} from Eq. 1-3.

In our study, this technics will be useful to be sure that chemical surface modification is effective through the measure of the change of hydrophobic/hydrophilic character of the new surface state. Notice that this technics gives macroscopic informations.

1.2.5. Interaction between surface chemistry and proteins

Currently, several strategies of interaction between the surface of solid substrate and proteins are available for protein immobilization, such as physical adsorption, covalent cross-linking and specific affinity (Figure 1-13) [31, 150]. Physical adsorption normally offers the

simplest process of immobilization. Aminosilane and poly-L-lysine coatings on the surface are convenient and popular methods of attaching proteins to glass by adsorption. These coatings do not require modification of proteins and are widely used. However, they are relatively uncontrollable and can lead to destroy protein activity by protein denaturation and steric hindrance [31, 151]. Besides, it tends to be suitable only for probes with larger molecules. Presumably, larger molecules bear a sufficient negative charge so as to be electrostatically attracted to the positively charged, protonated amine. Small peptides do not attach well to these positively charged surfaces.

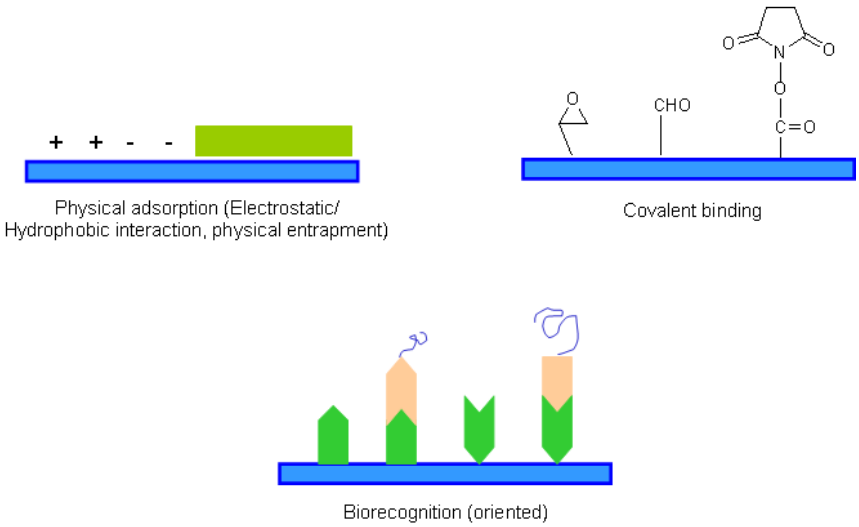

Figure 1-13 Comparison of different method for protein attachment on the surface of solid substrate with electrostatic/hydrophobic interaction, adsorption/absorption, covalent cross-linking and affinity attachment

Due to the limitations associated with non-covalent glass attachment chemistries, more attentions are focused on the available covalent glass immobilization methods, which provide the strongest attachment of probe proteins onto activated substrate. These include epoxide, isothiocyanate, N-hydroxysuccinimide (NHS) ester, amine, semicarbazide, and aldehyde-derivatized surfaces, often introduced by silianization on the solid support [31, 99, 152, 153]. Compare to physical adsorption, covalent binding gives a more durable and stable linkage to the solid substrate, capable of withstanding high temperatures or organic solvents. Besides, pre-activated surface can attach with the terminal group of proteins, for example, epoxides or succinimide esters, can couple with a terminal amine group of proteins to form a stable linkage. On the other hand, some pre-treatment for the protein is necessary, for example, semicarbazide-coated glass requires that the moiety be derivatized with a benzaldehyde group. The emphasis is that the steric hindrance between protein and surface from the short spacer provided by silanes may reduce the affinity of probe and the accessibility of analytes. These

requirements for pre-modification of the sample burdens the sample preparation step and can limit the types of materials that can be attached. In addition, many of the covalent immobilization methods are not optimal for small molecules, such as peptides, which do not avidly cross-link to aldehyde coated slides. More reactive groups such as epoxides or NHS esters are better for immobilization of small molecules, but they are less stable.

Alternatively, specific affinity, such as protein A or G with Fc part of an antibody [154] and biotin–avidin/streptavidin interaction [155], are employed for site specific protein immobilization. When the proteins are attached to the surface via their affinity tags, it is very likely that every protein molecule uniformly attaches to the surface and, therefore, proteins are more likely to remain in their native conformation, while the analytes have easier access to the active sites of protein [31]. Both nickel- [99] or avidin-coated [152, 156] glass slides are reported to provide a strong, specific attachment with a low level of background fluorescence. Although the affinity attachment is easy to retain the native conformation and to control the orientation of immobilized protein, it requires conjugation of the probe protein to be immobilized with affinity tag (polyhistidine, biotin, etc) and specifically modified substrate [157]. The requirement burdens the sample preparation step and limits the range of analytes that can be bound to glass.

Wacker et al. [109] evaluated the different immobilisation strategies by comparison of the immobilisation of antibodies by DNA-directed immobilisation (DDI), direct spotting, and streptavidin-biotin attachment. The study suggested that DDI and direct spotting led to the highest signal intensities, with DDI displaying the best spot homogeneity and reproducibility as well as the lowest consumption of antibody. Nevertheless, DDI is disadvantaged by the additional efforts arising from the separate preparation of DNA-protein conjugates for each antibody. The effects of the orientation of antibodies and Fab were also observed by Peluso and colleagues [110], indicating that an up to 10-fold increase could be detected in analyte-binding capacity of slide surfaces that promoted oriented immobilisation.

1.2.6. Detection techniques for protein microarrays

Current detection techniques for protein microarray can be typically divided into two groups [79]: (1) Label-free methods, such as mass spectrometry (MS), surface plasmon resonance (SPR) and grating-coupled surface plasmon resonance (GC-SPR), atomic force microscopy (AFM), micro-electromechanical systems (MEMS) cantilevers and quartz-crystal microbalance analysis (QCM). (2) Labelled probe methods, like fluorescence, chemiluminescence, electrochemiluminescence and radioactivity detection.

The label-free detection methods are promising tools to characterize binding events on surface of solid substrates, no needing for labeling of molecules that may affect protein

activity. However, they are generally based on sophisticated equipment not easily available in all clinical laboratories. Besides, coupling protein microarrays to real-time and label-free detection systems compatible with high-throughput methods would strongly enhance the ability to understand protein function on a proteome scale.

Labeled probe methods have directly evolved from clinical immunoassays, radioimmunoassay or ELISA protocols where they are widely used. The labeled methods typically include three groups derived from ELISA as previously illustrated (Figure 1-3):

(a) Direct approach when a mixture of proteins is immobilized and the detection is performed using labeled binding molecules such as antibodies. Usually referred as reverse phase protein microarray [158], each spot of the array includes an individual test sample. Therefore, an array may consist of several sera of different patients or cellular lysates containing a complex mixture of proteins. Then the spot is incubated with one detection protein (typically an antibody) allowing the comparison of a single analyte in different samples

(b) Indirect approach when immobilized antibodies are employed as capture ligands and probed by labeled proteins. A known capture ligand is immobilized on the surface and probed by a labeled complex mixture of proteins. The test sample can be a cellular lysate or a serum in which multiple analytes are measured simultaneously. In a two colour approach, pharmacological treatments or protein expression profiles can be compared [159].

(c) Sandwich approach when a first immobilized antibody serve as a capture agent for the assayed protein which is revealed by a recognition with a secondary labeled antibody) [79]. The sandwich assay format relies on immobilized antibodies for capturing the protein of interest while a second labeled antibody directed against the captured protein is used for detection. In this method, two distinct antibodies, each with affinity to separate epitopes on the protein of interest are required.

The bottlenecks of labeled-probe methods are the production of antibodies and the quantitative labeling of antibodies/antigens. Existing collections of analyte specific antibodies cover a limited fraction of the proteome. Labeled probe detection methods mainly use fluorescence, chromogenic, chemiluminescence, electro-chemiluminescence or radioactive labeling strategies. It is necessary to provide high sensitivity (with high signal to noise ratio (SNR)) and high throughput for detection methods developed for protein microarray due to the miniaturized format. The use of fluorescent probes and signal amplification techniques with chromogenic or fluorescent probes usually leads to performances that meet such requirements. The advantages and disadvantages of three kinds of labeled methods were summarized in Table 1-8 [79, 101].

Table 1-8 Comparison of three labeled methods for protein microarrays detections

	Direct	Indirect	Sandwich
Commonly used agents	Fluorophore-NHS ester	Fluorophore-secondary antibody conjugates, Fluorophore-protein A or L conjugates, Specific-tag specific antibody conjugates, Fluorophore-streptavidin conjugates TSA: horseradish peroxidase-secondary antibody conjugate, Fluorophore-tyramide conjugate	RCA: antibody-primer conjugate, DNA circle, polymerase, fluorescent oligonucleotide probes
Method	Direct attachment of dye to the analyte	Incubation with labeled generic binders that are often species or tag-specific, TSA: enzymatic formation of tyramide radicals that attach to the phenol moiety of tyrosine residues	RCA: extension of primer and labeled oligonucleotide probes hybridization
Advantages	No additional incubation steps necessary	Labeled generic binders can be obtained commercially; No labeling step necessary; Enzyme-antibody fusions are available commercially	Enzyme can be attached directly or indirectly to the analyte
Disadvantages	Difficulty of reproducible labeling of complex protein solutions. Labeling can alter structure of the molecule. Need to remove unbound dye	Requires additional incubation step All analytes require a common tag or motif to which the generic binder can bind Stringent washing steps are required	Higher variations can arise owing to different incubation times

Abbreviations: NHS, N-hydroxysuccinimide; RCA, rolling circle amplification; TSA, tyramide signal amplification.

1.3. Protein microarray for cancer diagnosis

Although cancer is one of the main causes of death in the world, advanced screening and diagnosis methods would help reduc cancer fatalities. Sensitive detections of cancer biomarkers are critical components in clinical diagnostics of cancer. As already reported, sera of cancer patients contain tumor-associated antigens (TAAs), which can be detected before clinical symptoms [18, 160-162]. Besides, cancer-associated autoantibodies (AAbs) are often driven by intracellular proteins that are mutated, modified, or aberrantly expressed in tumor cells and hence could be regarded as immunological reporters that could help uncover molecular events underlying tumorigenesis. Emerging evidence suggests that each type of cancer might trigger an unique autoantibody signature that reflect the nature of the malignant

process in the affected organ [163]. Consequently, both TAAs and AAbs could be used as tumor markers for detection; however, the variability and lacking specificity of tumor markers bring challenges to effective analysis. Recently, the advent of novel genomic, proteomic, and high throughput approaches like protein microarray have accelerated interests in tumor markers for cancer detection. In particular, protein microarray has demonstrated to be powerful tools for multiplex screening and identifying tumor markers (TAAs and AAbs) from minute samples [18, 164].

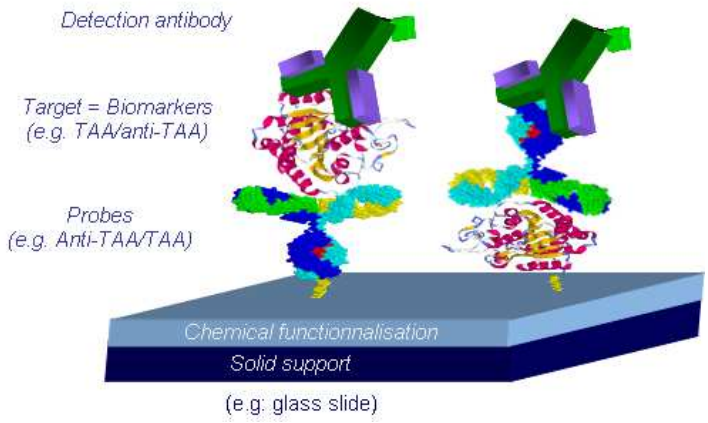

Figure 1-14 Schematic illustration of forward-phase and reverse-phase microarrays [165]

The two common types of microarrays for exploring the immunoproteome are defined as forward-phase and reverse-phase microarray (Figure 1-14) depending on the nature of the capture/target molecule [165, 166]. Reverse-phase microarrays employ the antigenic nature of proteins as probes to capture antibodies, which can be used to identify novel TAAs or validate known TAAs by screening the sera from patients. The probes such as TAAs, commercial recombinant proteins or lysates from cancer tissue or cell lines were immobilized onto microarray, and then be probed with patient and/or control sera in a multiplexed approach followed by incubation with secondary labeled antibody for detection. Alternatively, forward-phase microarrays utilize immobilized antibodies as probes to capture TAAs in sera of cancer patients and validate diagnosis. Immunoreactive fractions from both of microarrays can be subsequently detected and data analysed. In a word, one system is to detect tumor antigens and another is to detect autoantibodies.

1.3.1. Detection of tumor antigens

Antibody microarray technology has begun to play a significant role for detection and quantification of proteins in complex biological samples. The ability of antibodies to perform

highly specific protein capture makes this approach particularly well suited for detecting rare analytes in highly heterogeneous mixtures, like biomarkers in serum. Hence, antibody microarray could offer the ability to identify new panels of TAAs produce in cancer [167]. Haab and co-workers [98] tested multiple antibody-antigen interactions by localizing specific components of the complex mixtures on the antibody microarray to defined cognate spots. The analytical performance demonstrates that 20 % of the arrayed antibodies provided specific and accurate measurements of their cognate ligands at or below concentrations of 1.6µg/ml. In particular, some pairs of antibody-antigen allowed detection of the cognate ligands at absolute concentrations below 1 ng/ml, indicating that the sensitivities are sufficient for measurement of many clinically important proteins in patient blood samples.

Recent works have been looked into the use of antibody microarrays to identify tumour-related antigens and serum protein profiling [168, 169]. Multiple antigen expression patterns would be more specifically dysregulated in the different human neoplasms than individual protein profiles, because of the inherent complexity and heterogeneity of the mechanisms involved in neoplastic cell development [170]. Therefore, it would be more informative for characterisation of cancer biomarkers to design wide panels of antigens. Antibody microarrays provide sufficient density and high throughput for parallel screening of many biological samples to discover antigens across large patient populations. Orchekowski et al [171] used antibody microarrays to probe the associations of multiple serum proteins with pancreatic cancer and to explore the use of combined measurements for sample classification. A logistic-regression algorithm distinguished cancer samples from healthy donors with a 90 % and 93 % sensitivity and a 90 % and 94 % specificity in duplicate experiment sets. Cancer samples were distinguished from benign disease samples with 95 % and 92 % sensitivity, and 88 % and 74 % specificity in duplicate experiment sets. The classification accuracies were significantly improved over those achieved using individual antibodies, which demonstrates an effective strategy with antibody microarrays to profile proteins and identify candidate biomarkers.

In another report [172], protein markers of colorectal carcinogenesis and progression were identified with protein microarrays and validated on tissue microarrays. Using cancer and adjacent normal samples from 10 patients with early and 6 with advanced colorectal cancer, 67 differentially expressed genes were identified between normal and cancer samples. A marker set containing 6 proteins (CCNA1, AR, TOP1, TGFB, HSP60, ERK1) was developed which could differentiate normal specimen, early and late stage of colorectal cancer with high sensitivity and specificity. The results shows that mRNA and protein expression of 143 genes showed strong positive correlations ($R(2) > 0.8$), while a negative correlation ($R(2) > 0.9$) was found in case of 95 genes. Therefore, a correlation could be established between transcriptome and antibody microarray results. Thus, the former may be

used as a high-capacity screening method before applying antibody microarrays containing already planned targets. It was suggested that antibody microarrays may have a fundamental importance in screening marker combinations and in future applications in diagnostics of cancer.

Boehm et al. [173] immobilized 23 antibodies on nitrocellulose slides to determine the levels of acute phase proteins, interleukins and complement factors in 101 participants sera (49 women with primary breast cancer and 52 healthy age-matched controls). Statistical analysis of reaction intensities identified six proteins (interleukine (IL)-6, Hsp60, Hsp70, C3/3b, glial fibrillary acid proteins (GFAP) and ionized calcium binding adaptor molecule (IBA) 1) that showed significantly ($p < 0.05$) different levels in breast cancer patients vs. healthy donors. The neural network distinguished cancer patients from controls with a sensitivity of 69 % and a specificity of 76 %. Sanchez-Carbayo et al [84] selected antibodies against targets differentially expressed in bladder tumors and designed antibody microarrays for detection of bladder cancer. Serum protein profiles measured by an antibody microarray containing 254 antibodies discriminated bladder cancer patients from controls ($n = 95$) with a correct classification rate of 93.7 %. A second independent antibody microarray containing 144 antibodies revealed that protein profiles provide predictive information by stratifying patients with bladder tumors ($n = 37$) based on their overall survival ($P = 0.0479$). Besides, serum proteins were associated with pathological stage, tumor grade and survival, which also be validated by immunohistochemistry of tissue microarrays, demonstrating to contain bladder tumors ($n = 173$). The results provide experimental evidence for the use of several integrated technologies strengthening the process of biomarker discovery. Serum protein profiles obtained by antibody microarrays proved to be comprehensive means for bladder cancer diagnosis and clinical outcome stratification. This could potentially assist in screening of cancer patients who would benefit from early, individualized therapeutic intervention.

Consequently, antibody microarray analysis could be used as a powerful tool for the development of improved diagnostics and biomarker discovery for cancer patients. However, a plethora of parameters such as surface chemistry, composition and pH of the spotting buffer, blocking reagents, antibody concentration, storage procedures etc, have effects on analytical performances (sensitivity, specificity, limit of detections) of antibody microarray [101, 110]. These parameters should also be taken into account for detection and identification of cancer biomarkers. Since early diagnosis of cancer implies biomarkers have to be detected at low concentration, high sensitivity assay is desirable for cancer biomarker discovery and validation from clinical samples like serum. Miller and co-workers [174] developed a practical strategy for profiling prostate cancer sera by identifying differential fluorescently labeled protein expression patterns. Protein abundances from 33 prostate cancer and 20 control serum samples were compared to abundances from a common reference pool.

Compared to the traditional chemically derivatised silica surface, the detection limit of antigens were improved by 6-fold, down to 200 ng/ml, by using a three-dimensional acrylamide gel surface. Moreover, most abundant antigens (such as PSA, C-reactive proteins, serum amyloid A and α-1-anti-trypsin, among others) have been detected in serum samples using this approach. In a recent report, Luo et al [175] optimized parameters of antibody microarray with Taguchi design for detection of five breast cancer biomarkers: CA15-3, CEA, HER2, MMP9, and uPA. Two successive optimization rounds with each 16 experimental trials were performed, in which three factors (capture antibody, detection antibody, and analyte) at four different levels (concentrations) in the first round and seven factors (including buffer solution, streptavidin-Cy5 dye conjugate concentration, and incubation times for five assay steps) with two levels each in the second round, as well as five two-factor interactions between selected pairs of factors were tested. The concentration of capture antibody, streptavidin-Cy5, and buffer composition were identified as the most significant factors for all assays; analyte incubation time and detection antibody concentration were significant only for MMP9 and CA15-3, respectively. Interactions between pairs of factors were less influential compared with single factor effects. Under the Taguchi optimal conditions, the assay sensitivity was improved between 7 and 68 times but depending on the analyte, reaching 640 fg/mL for uPA.

In conclusion, antibody microarrays have been successfully used for protein profiling of biological samples for screening tumor-associated antigens [168]. Highly parallel protein profiling using antibody microarrays does not only facilitate more rapid biomarker discovery, but also enable the direct observation of relationships between proteins. Furthermore, one could examine combinations of multiple markers that might increase the statistical significance of a diagnosis from single data sets [174]. However, validation test are required to rule out cross-reactivity or lack of specificity of antibodies and well established antibody pairs for most antigens have not yet been developed. Accordingly, there is a noteworthy lack of highly specific antibodies or alternative high-affinity capture reagents that can be functional in a protein microarray format.

1.3.2. Detection of autoantibodies

Novel biomarkers are urgently required to detect early cancer and reduce the current mortality rate. Autoantibodies have not only been used to identify TAAs as diagnostic/prognostic markers and potential therapeutic targets, but they also represent excellent biomarkers for the early detection of tumors and potential markers for monitoring the efficacy of treatment [165]. The presence of autoantibodies during early stages of malignancy and their inherent stability in sera would enable the detection of cancer at a stage

when treatments are most effective. On the other hands, an early report [98] demonstrates that sometimes antigen may works better than antibody on an array format, probably due to the loss of antibody activity by degradation or denaturation on storage or during the printing process, or due to inappropriate antibody orientation onto the array surface. In the study, 115 pairs of antibody-antigen interactions on protein microarrays were tested and only 60 % of printed antibodies could detect each specific antigen in a pool of 115 antigens and only around 20 % of the antibodies could quantitatively detect differences in the antigen concentrations. Moreover, it may also reflect the fact that many antibodies target denatured proteins and therefore recognise linear epitopes that remain inaccessible in the native form. On the contrary, when this experiment was inverted, that is, when antigen arrays were probed with a pool of antibodies, a much larger number of antibody-antigen pairs could be detected and quantified. It is pointed out that certain antigens sometimes may be more labile or sensitive tools for detection. Furthermore, validation of autoantibody biomarkers is a vital step towards clinical implementation; therefore the detection of autoantibodies with antigen microarrays might supply a clinically useful non invasive approach to cancer detection and diagnosis.

Scanlan et al [176] firstly attempt to establish the reactivity of a cancer-associated antigen array in patients with colorectal cancer and examined humoral immune responses to 77 candidate antigens identified by serological expression cloning (SEREX). A panel of 13 antigens (p53, MAGEA3, SSX2, NY-ESO-1, HDAC5, MBD2, TRIP4, NY-CO-45, KNSL6, HIP1R, Seb4D, KIAA1416, and LMNA) was selected for further assays. Analysis of autoantibodies, reactive to at least one of these antigens, made it possible to discriminate between patients with colon cancer and healthy donors with 46 % sensitivity and 100 % specificity ($p < 10^{-10}$). The reactivity of each individual antigen (excluding highly immunogenic p53) varied from 3 to 8 %. Only five individually tested antigens (p53, MAGEA3, NY-ESO-1, TRIP4, and HIP1R) displayed significant difference in seroreactivity between patients with large intestinal cancer and healthy donors. These results demonstrates that the use of an array of 13 cancer-associated antigens allowed 6-9-fold increase in sensitivity of cancer detection with preservation of 100 % specificity of each individual antigen [177]

Zhang and co-workers [178, 179] demonstrated a stepwise increase in the sensitivity of diagnostics for different types of cancer (64 cases of breast cancer, 46 cases of colorectal cancer, 91 cases of stomach cancer, 56 cases of lung cancer, 206 cases of prostate cancer, and 65 cases of hepatocellular carcinoma) by increasing the number of antigens included into the array from 5-20 % for individual antigens (c-MYC, p53, CCNB1, p62, KOC, IMP1, and BIRC5) to 44-68% when using ELISA detection on arrays. Besides, along with the drastic increase in sensitivity, the specificity of cancer detection with antigen array is comprised

between 89-95% (compared to different control groups), i.e. decreased by only 5-10 % in comparison with individual antigen specificity. On the basis of the characteristic sero-reactivity patterns of different cancer types, [179] a statistical algorithm of recursive partitioning for the analysis of the same seven antigens were employed in the same cohorts of patients, with adding additional control groups and in some cases lowered the reactivity threshold level from +3 to +2 standard deviation of absorption in control group. This strategy can achieve sensitivity of 77-92 % and specificity of 85-91 % depending upon type of cancer, and the patients were classified into three cohorts according to the cancer type. In each of these cohorts, the desired levels of sensitivity and specificity could be achieved by analysis of reactivity to only three (of seven) antigens included in the array.

Additionally, the same group recently detected antibodies against eight selected tumor-associated antigens (TAAs) in 30 sera from chronic hepatitis by means of Enzyme-linked immunosorbent assay (ELISA), 30 from liver cirrhosis, and 142 from HCC, which were also confirmed by slot blot, Western blotting and immunoprecipitation assay [162]. The results demonstrate that a mini-array of eight TAAs enhanced antibody detection for diagnosis of hepatocellular Carcinoma (HCC). More studies in patients with HCC and precursor conditions such as chronic hepatitis, alcoholic hepatitis and liver cirrhosis using enlarged TAA mini-array panels might further improve the sensitivity and specificity of this mode of cancer immunodiagnosis, which may also be benefit for the early detection of cancer in some patients with predisposing conditions. Furthermore, they concluded that no single antigen is likely to demonstrate an autoantibody response in all patients, especially for heterogeneous disease like breast cancer [161, 180]. The combination of greater numbers of tumour-associated antigens within a panel will enhance the detection of the specific cancer using autoantibody assays and different cancers may require different panel of markers [161].

Some common TAAs combinations were reported to detect autoantibodies from breast cancer such as p53 and c-myc with addition of MUC1 and Her2 [59], Her2, NY-ESO1, BRCA1, BRCA2, and MUC1 [181], cyclin B1, survivin, p62, koc and IMP1 [178] and survivin [182]. Megliorino et al. [182] demonstrated that survivin was noted in only 8.4 % of all cancers with breast, lung, lymphoma and hepatocellular cancers showing higher prevalence compared to normal human serum. However, the detection rate increased to over 26.6% in breast cancer if combining p53 and c-myc to survivin within a panel [182], which may play potential role for clinical diagnosis. Another combination panel was evaluate with koc, p62 [183], survivin and livin [184]. The analytical sensitivities to breast cancer for the panels range from 16% (Koc and p62) [183] to 82% (MUC1, p53, c-myc and Her2) [59]. Moreover, the difference in sensitivities depends upon individual markers within the panel and cut-off value used. Recently, Desmet et al [164] immobilized a panel of 12 TAAs (Cyclin B1, Cyclin D1, Complement factor H, c-myc, IMP1, p53, p62, survivin, Her2/neu, Koc, NY-

ESO-1 and PSA) onto the nitrocellulose/cellulose acetate membrane of a 96-well filtering microtiter plate bottom, in order to directly detect auto-antibodies in patient sera with a staining approach based on alkaline phosphatase labeling. The results show that TAA microarrays can capture specific purified anti-TAA antibodies. 9 proteins from the 12 TAAs panel were shown to generate specific signal and 5 antigens (p53, NY-ESO-1, IMP1, cyclin B1 and c-myc) can interact with more than 10 % of the positive sera from cancer patients. This protein subpanel was proven to be able to detect 72.2% of the cancer patients tested (within a 34 panel of 18 patients and 16 healthy donors).

Consequently, antigen microarray could be well applied to the identification of autoantibody signatures in cancer. The identification of TAAs recognised by the patient's immune response represents an exciting approach to identify novel diagnostic cancer biomarkers and may contribute towards a better understanding of the molecular mechanisms involved [167]. It also could be employed to identify complex autoantibody signatures that may represent disease subgroups, early diagnostics and facilitated the analysis of vaccine trials. The detection of AAbs within a panel of tumor antigens can greatly enhance the sensitivity of the markers to detect breast and other cancers as mentioned above. Different cancers may require different combination panels of tumor markers.

To sum up, protein microarrays allow multiplex identification of antibodies and their TAAs, which offer a powerful tool to identify potential cancer biomarkers and foretell a promising future for the implementation of sensitive and specific tests. However, the clinical impact of these potential biomarkers remains to be evaluated using complementary analysis. Indeed, published results demonstrate that most antibodies and antigens that have been identified demonstrate weak frequency (20% - 30% of patients) and are weakly or not correlated with classical clinical parameters (histological type, tumor stage, survival, etc.) [166]. Therefore, it is necessary to clinically validate the reported results using a broader independent patient population in order to determine the value of potential biomarkers in terms of sensitivity, specificity and predictive value. The combination of several antibodies or antigens seems to be a very promising way for the detection of tumors with higher efficiency than isolated biomarkers [167, 181]. These results predict many upcoming developments in the field of cancer diagnostics. It is suggested that molecular signatures, associated with clinical and anatomopathological data, will facilitate improvement of diagnosis and prognosis in cancer.

1.4. Aims of the thesis

The main objective of this work was to provide a powerful analysis tool to identify serological profiles for cancer diagnosis and prognosis. To this aim we propose to investigate

molecular diagnosis through elaboration of customized protein microarray for the detection of reliable cancer biomarkers in patients'sera. Indeed, microarrays allow high throughput and multiplex detection of biomolecules. However, with standard format only one biological sample is analyzed. Thus, for the analysis of multiple biological samples in the same assay, we manufactured microstructured microarray containing microwells allowing the physical separation of the samples.

Another limitation of standard protein microarray is their low sensitivity due to partial loss of biological activity following protein immobilization on the surface.Thus, one major aim of this thesis was to increase the sensitivity of protein microarray optimizing immobilization parameters for each protein. We developed various surface chemistries (monolayers versus polymer layers; adsorption versus covalent grafting) and evaluated their ability to retain maximal biological activity of the immobilized protein.

To achieve reproducible surface chemistries, these functionalized surfaces were characterized with standard surface analytical techniques (attenuated total reflection Fourier transform infra red (ATR-FTIR), X-ray photoelectron spectroscopy (XPS), contact angle measurement). The immobilization capacity of each surface was evaluated with fluorescent labeled proteins (BSA, myoglobin, IgG and streptavidin) displaying various physico-chemical characteristics. Thus, another aim of the thesis was to define the best surface chemistry to choose depending on protein properties. Of course other parameters such as the concentration of probe proteins, the spotting buffer (various pH and additives), capping buffer, incubation conditions (temperature) as well as the detection antibody concentration, were optimized for each protein on each surface.

Then, the last aim of the thesis was to validate these optimized protein microarrays to identify specific biomarker profiles of two type of cancers (colorectal cancer and breast cancer). Two kind of protein microarrays were designed: an antibody microarray to detect tumor markers in sera from colorectal cancer, a tumor-associated antigen microarray to evaluate autoantibodies level in sera from breast cancer (see Figure 1-14).

The sketch of the thesis was illustrated in Figure 1-15.

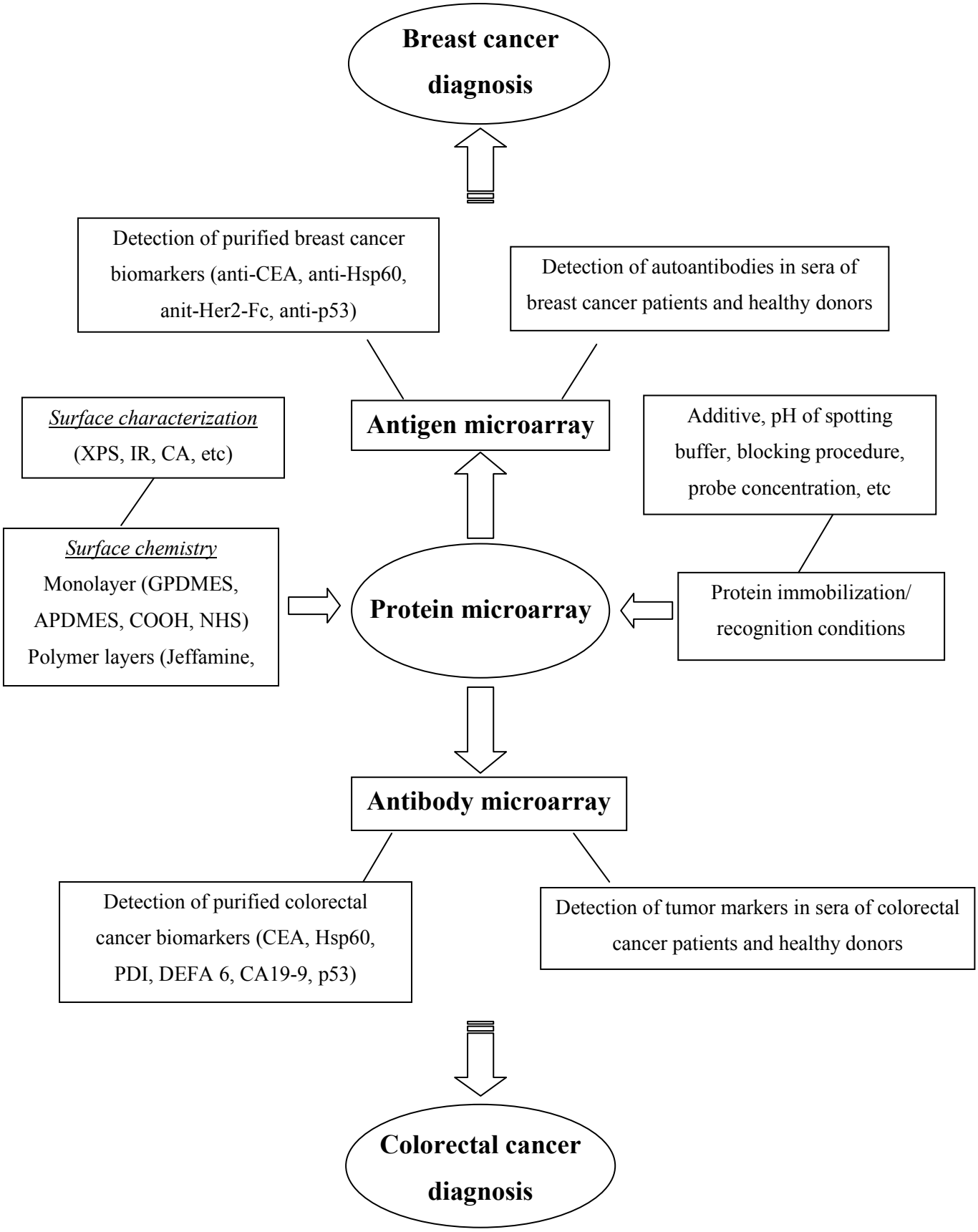

Figure 1-15 Sketch of the thesis work

References

[1] P. Boyle, B. Levin, World Cancer Report, in, Lyon, 2008.

[2] S.B. Baylin, J.G. Herman, DNA hypermethylation in tumorigenesis: epigenetics joins genetics, Trends Genet., 16 (2000) 168-174.

[3] M. Esteller, P.G. Corn, S.B. Baylin, J.G. Herman, A gene hypermethylation profile of human cancer, Cancer Res., 61 (2001) 3225-3229.

[4] J.A. Ludwig, J.N. Weinstein, Biomarkers in cancer staging, prognosis and treatment selection, Nat. Rev. Cancer, 5 (2005) 845-856.

[5] D. Sidransky, Emerging molecular markers of cancer, Nat. Rev. Cancer, 2 (2002) 210-219.

[6] C.C. Chen, S.H. Yang, J.K. Lin, T.C. Lin, W.S. Chen, J.K. Jiang, H.S. Wang, S.C. Chang, Is it reasonable to add preoperative serum level of CEA and CA19-9 to staging for colorectal cancer?, J. Surg. Res., 124 (2005) 169-174.

[7] T. Lebret, R.W.G. Watson, V. Molinie, A. O'Neill, C. Gabriel, J.M. Fitzpatrick, H. Botto, Heat shock proteins HSP27, HSP60, HSP70, and HSP90, Cancer, 98 (2003) 970-977.

[8] K.J. Fuller, R.D. Issels, D.O. Slosman, J.G. Guillet, T. Soussi, B.S. Polla, Cancer and the Heat-Shock Response, Eur. J. Cancer, 30A (1994) 1884-1891.

[9] D.L. Wickerham, Breast cancer chemoprevention: progress and controversy, Surg. Oncol. Clin. N. Am., 19 (2010) 463-473.

[10] G.Y. Locker, S. Hamilton, J. Harris, J.M. Jessup, N. Kemeny, J.S. Macdonald, M.R. Somerfield, D.F. Hayes, R.C. Bast, Jr., ASCO 2006 update of recommendations for the use of tumor markers in gastrointestinal cancer, J. Clin. Oncol., 24 (2006) 5313-5327.

[11] I.C. Henderson, A.J. Patek, The relationship between prognostic and predictive factors in the management of breast cancer, Breast Cancer Res. Treat., 52 (1998) 261-288.

[12] W.J. Catalona, Clinical utility of measurements of free and total prostate-specific antigen (PSA): A review, Prostate, (1996) 64-69.

[13] R. Molina, J.M. Auge, J.M. Escudero, R. Marrades, N. Vinolas, E. Carcereny, J. Ramirez, X. Filella, Mucins CA 125, CA 19.9, CA 15.3 and TAG-72.3 as Tumor Markers in Patients with Lung Cancer: Comparison with CYFRA 21-1, CEA, SCC and NSE, Tumor Biol., 29 (2008) 371-380.

[14] Y.E. Choi, J.W. Kwak, J.W. Park, Nanotechnology for Early Cancer Detection, Sensors, 10 (2010) 428-455.

[15] S.M. Dhanasekaran, T.R. Barrette, D. Ghosh, R. Shah, S. Varambally, K. Kurachi, K.J. Pienta, M.A. Rubin, A.M. Chinnaiyan, Delineation of prognostic biomarkers in prostate cancer, Nature, 412 (2001) 822-826.

[16] J.L. Schultze, R.H. Vonderheide, From cancer genomics to cancer immunotherapy: toward second-generation tumor antigens, Trends Immunol., 22 (2001) 516-523.

[17] P.G. Coulie, T. Hanagiri, M. Takenoyama, From tumor antigens to immunotherapy, Int. J. Clin. Oncol., 6 (2001) 163-170.

[18] C.A. Casiano, M. Mediavilla-Varela, E.M. Tan, Tumor-associated antigen arrays for the serological diagnosis of cancer, Mol. Cell. Proteomics, 5 (2006) 1745-1759.

[19] M.A. Tainsky, Genomic and proteomic biomarkers for cancer: a multitude of opportunities, Biochim. Biophys. Acta, 1796 (2009) 176-193.

[20] R.J. Pamies, D.R. Crawford, Tumor markers. An update, Med. Clin. North Am., 80 (1996) 185-199.

[21] R.C. Bast, S. Bates, A.B. Bredt, C.E. Desch, H. Fritsche, L. Fues, D.F. Hayes, N.E. Kemeny, M. Kragen, J. Jessup, G.Y. Locker, J.S. Macdonald, R.G. Mennel, L. Norton, P. Ravdin, T.J. Smith, S. Taube, R.J. Winn, Clinical practice guidelines for the use of tumor markers in breast and colorectal cancer, J. Clin. Oncol., 14 (1996) 2843-2877.

[22] Y.M. Yin, Y. Cao, Y.Y. Xu, G.X. Li, Colorimetric Immunoassay for Detection of Tumor Markers, Int. J. Mol. Sci., 11 (2010) 5078-5095.

[23] T. Beyer, D.W. Townsend, T. Brun, P.E. Kinahan, M. Charron, R. Roddy, J. Jerin, J. Young, L. Byars, R. Nutt, A combined PET/CT scanner for clinical oncology, J. Nucl. Med., 41 (2000) 1369-1379.

[24] M.F. Kircher, U. Mahmood, R.S. King, R. Weissleder, L. Josephson, A multimodal nanoparticle for preoperative magnetic resonance imaging and intraoperative optical brain tumor delineation, Cancer Res., 63 (2003) 8122-8125.

[25] E. Engvall, P. Perlmann, Enzyme-linked immunosorbent assay (ELISA). Quantitative assay of immunoglobulin G, Immunochemistry, 8 (1971) 871-874.

[26] M.Y. Liu, C.P. Jia, Y.Y. Huang, X.H. Lou, S.H. Yao, Q.H. Jin, J.L. Zhao, J.Q. Xiang, Highly sensitive protein detection using enzyme-labeled gold nanoparticle probes, Analyst, 135 (2010) 327-331.

[27] Z.F. Fu, H. Liu, H.X. Ju, Flow-through multianalyte chemiluminescent immunosensing system with designed substrate zone-resolved technique for sequential detection of tumor markers, Anal. Chem., 78 (2006) 6999-7005.

[28] C.F. Ou, R. Yuan, Y.Q. Chai, M.Y. Tang, R. Chai, X.L. He, A novel amperometric immunosensor based on layer-by-layer assembly of gold nanoparticles-multi-walled carbon nanotubes-thionine multilayer films on polyelectrolyte surface, Anal. Chim. Acta, 603 (2007) 205-213.

[29] L.M. Ao, F. Gao, B.F. Pan, R. He, D.X. Cui, Fluoroimmunoassay for antigen based on fluorescence quenching signal of gold nanoparticles, Anal. Chem., 78 (2006) 1104-1106.

[30] B.K. Oh, J.M. Nam, S.W. Lee, C.A. Mirkin, A fluorophore-based bio-barcode amplification assay for proteins, Small, 2 (2006) 103-108.
[31] H. Zhu, M. Snyder, Protein chip technology, Curr. Opin. Chem. Biol., 7 (2003) 55-63.
[32] G. MacBeath, S.L. Schreiber, Printing proteins as microarrays for high-throughput function determination, Science, 289 (2000) 1760-1763.
[33] Y.M. Lee, Y. Jeong, H.J. Kang, S.J. Chung, B.H. Chung, Cascade enzyme-linked immunosorbent assay (CELISA), Biosens. Bioelectron., 25 (2009) 332-337.
[34] R.F. Swaby, M. Cristofanilli, Circulating tumor cells in breast cancer: A tool whose time has come of age, BMC Med., 9 (2011).
[35] D. Mavroudis, Circulating cancer cells, Annals of oncology : official journal of the European Society for Medical Oncology / ESMO, 21 Suppl 7 (2010) vii95-100.
[36] A. Stathopoulou, D. Mavroudis, M. Perraki, S. Apostolaki, I. Vlachonikolis, E. Lianidou, V. Georgoulias, Molecular detection of cancer cells in the peripheral blood of patients with breast cancer: Comparison of CK-19, CEA and maspin as detection markers, Anticancer Res., 23 (2003) 1883-1890.
[37] P. Msaouel, M. Koutsilieris, Diagnostic value of circulating tumor cell detection in bladder and urothelial cancer: systematic review and meta-analysis, BMC Cancer, 11 (2011).
[38] D. Hwu, S. Boutrus, C. Greiner, T. DiMeo, C. Kuperwasser, I. Georgakoudi, Assessment of the role of circulating breast cancer cells in tumor formation and metastatic potential using in vivo flow cytometry, J. Biomed. Opt., 16 (2011).
[39] J. Frelinger, J. Ottinger, C. Gouttefangeas, C. Chan, Modeling flow cytometry data for cancer vaccine immune monitoring, Cancer Immunol. Immunother., 59 (2010) 1435-1441.
[40] L.A. Herzenberg, J. Tung, W.A. Moore, L.A. Herzenberg, D.R. Parks, Interpreting flow cytometry data: a guide for the perplexed, Nat. Immunol., 7 (2006) 681-685.
[41] U. Veronesi, P. Boyle, A. Goldhirsch, R. Orecchia, G. Viale, Breast cancer, Lancet, 365 (2005) 1727-1741.
[42] Sidharth, B. Thapa, Y. Singh, P. Sayami, U. Khanal, Mammographic Diagnosis of Breast Carcinoma: An Institutional Experience, Journal of Nepal Medical Association, 47 (2008) 62-65.
[43] W.E. Barlow, C.D. Lehman, Y.Y. Zheng, R. Ballard-Barbash, B.C. Yankaskas, G.R. Cutter, P.A. Carney, B.M. Geller, R. Rosenberg, K. Kerlikowske, D.L. Weaver, S.H. Taplin, Performance of diagnostic mammography for women with signs or symptoms of breast cancer, J. Natl. Cancer Inst., 94 (2002) 1151-1159.
[44] S.R.C. Benson, J. Blue, K. Judd, J.E. Harman, Ultrasound is now better than mammography for the detection of invasive breast cancer, Am. J. Surg., 188 (2004) 381-385.
[45] S.J. Lord, W. Lei, P. Craft, J.N. Cawson, I. Morris, S. Walleser, A. Griffiths, S. Parker, N. Houssami, A systematic review of the effectiveness of magnetic resonance imaging (MRI) as

an addition to mammography and ultrasound in screening young women at high risk of breast cancer, Eur. J. Cancer, 43 (2007) 1905-1917.

[46] F. Sardanelli, F. Podo, G. D'Agnolo, A. Verdecchia, M. Santaquilani, R. Musumeci, G. Trecate, S. Manoukian, S. Morassut, C. de Giacomi, M. Federico, L. Cortesi, S. Corcione, S. Cirillo, V. Marra, Multicenter comparative multimodality surveillance of women at genetic-familial high risk for breast cancer (HIBCRIT study): Interim results, Radiology, 242 (2007) 698-715.

[47] B.K. Szabo, P. Aspelin, M.K. Wiberg, B. Bone, Dynamic MR imaging of the breast - Analysis of kinetic and morphologic diagnostic criteria, Acta Radiol., 44 (2003) 379-386.

[48] C.C. Riedl, L. Ponhold, D. Flory, M. Weber, R. Kroiss, T. Wagner, M. Fuchsjager, T.H. Helbich, Magnetic resonance imaging of the breast improves detection of invasive cancer, preinvasive cancer, and premalignant lesions during surveillance of women at high risk for breast cancer, Clin. Cancer Res., 13 (2007) 6144-6152.

[49] J.G. Elmore, K. Armstrong, C.D. Lehman, S.W. Fletcher, Screening for breast cancer, Jama-Journal of the American Medical Association, 293 (2005) 1245-1256.

[50] R.L. Wahl, B.A. Siegel, R.E. Coleman, C.G. Gatsonis, Prospective multicenter study of axillary nodal staging by positron emission tomography in breast cancer: A report of the staging breast cancer with PET study group, J. Clin. Oncol., 22 (2004) 277-285.

[51] M. Suarez, M.J. Perez-Castejon, A. Jimenez, M. Domper, G. Ruiz, R. Montz, J.L. Carreras, Early diagnosis of recurrent breast cancer with FDG-PET in patients with progressive elevation of serum tumor markers, Q. J. Nucl. Med., 46 (2002) 113-121.

[52] L. Tabar, M.F. Yen, B. Vitak, H.H.T. Chen, R.A. Smith, S.W. Duffy, Mammography service screening and mortality in breast cancer patients: 20-year follow-up before and after introduction of screening, Lancet, 361 (2003) 1405-1410.

[53] P. Crystal, S.D. Strano, S. Shcharynski, M.J. Koretz, Using sonography to screen women with mammographically dense breasts, Am. J. Roentgenol., 181 (2003) 177-182.

[54] M.J. Duffy, Serum tumor markers in breast cancer: Are they of clinical value?, Clin. Chem., 52 (2006) 345-351.

[55] R. Molina, V. Barak, A. van Dalen, M.J. Duffy, R. Einarsson, M. Gion, H. Goike, R. Lamerz, M. Nap, G. Soletormos, P. Stieber, Tumor markers in breast cancer - European Group on Tumor Markers recommendations, Tumor Biol., 26 (2005) 281-293.

[56] W. Jager, S. Kramer, V. Palapelas, L. Norbert, Breast-Cancer and Clinical Utility of Ca-15-3 and Cea, Scand. J. Clin. Lab. Invest., 55 (1995) 87-92.

[57] E.C. Coveney, J.G. Geraghty, F. Sherry, E.W. McDermott, J.J. Fennelly, N.J. O'Higgins, M.J. Duffy, The clinical value of CEA and CA 15-3 in breast cancer management, Int. J. Biol. Markers, 10 (1995) 35-41.

[58] A.R. Dixon, I. Jonrup, L. Jackson, S.Y. Chan, R.A. Badley, R.W. Blamey, Serological Monitoring of Advanced Breast-Cancer Treated by Systemic Cytotoxic Using a Combination of Esr, Cea, and Ca15.3 - Fact or Fiction, Dis. Markers, 9 (1991) 167-174.

[59] K.L. Cheung, C.R.L. Graves, J.F.R. Robertson, Tumour marker measurements in the diagnosis and monitoring of breast cancer, Cancer Treat. Rev., 26 (2000) 91-102.

[60] J.F.R. Robertson, D. Pearson, M.R. Price, C. Selby, R.W. Blamey, A. Howell, Objective Measurement of Therapeutic Response in Breast-Cancer Using Tumor-Markers, Br. J. Cancer, 64 (1991) 757-763.

[61] R.J. Davies, R. Miller, N. Coleman, Colorectal cancer screening: Prospects for molecular stool analysis, Nat. Rev. Cancer, 5 (2005) 199-209.

[62] S.A. Goodbrand, R.J.C. Steele, An Overview of Colorectal Cancer Screening, Scott. Med. J., 53 (2008) 31-37.

[63] C.S. Ang, J. Phung, E.C. Nice, The discovery and validation of colorectal cancer biomarkers, Biomed. Chromatogr., 25 (2011) 82-99.

[64] P.J. Pickhardt, J.R. Choi, I. Hwang, J.A. Butler, M.L. Puckett, H.A. Hildebrandt, R.K. Wong, P.A. Nugent, P.A. Mysliwiec, W.R. Schindler, Computed tomographic virtual colonoscopy to screen for colorectal neoplasia in asymptomatic adults, N. Engl. J. Med., 349 (2003) 2191-2200.

[65] D.A. Ahlquist, Next-Generation Stool DNA Testing: Expanding the Scope, Gastroenterology, 136 (2009) 2068-2073.

[66] Y. Kim, S. Lee, S. Park, H. Jeon, W. Lee, J.K. Kim, M. Cho, M. Kim, J. Lim, C.S. Kang, K. Han, Gastrointestinal tract cancer screening using fecal carcinoembryonic antigen, Ann. Clin. Lab. Sci., 33 (2003) 32-38.

[67] C. Tonus, G. Neupert, M. Sellinger, Colorectal cancer screening by non-invasive metabolic biomarker fecal tumor M2-PK, World J. Gastroenterol., 12 (2006) 7007-7011.

[68] J. Karl, N. Wild, M. Tacke, H. Andres, U. Garczarek, W. Rollinger, W. Zolg, Improved Diagnosis of Colorectal Cancer Using a Combination of Fecal Occult Blood and Novel Fecal Protein Markers, Clin. Gastroenterol. Hepatol., 6 (2008) 1122-1128.

[69] D.G. Ward, N. Suggett, Y. Cheng, W. Wei, H. Johnson, L.J. Billingham, T. Ismail, M.J.O. Wakelam, P.J. Johnson, A. Martin, Identification of serum biomarkers for colon cancer by proteomic analysis, Br. J. Cancer, 94 (2006) 1898-1905.

[70] H. Xue, B.J. Li, J. Zhang, M.L. Wu, Q. Huang, Q. Wu, H.Q. Sheng, D.D. Wu, J.W. Hu, M.D. Lai, Identification of Serum Biomarkers for Colorectal Cancer Metastasis Using a Differential Secretome Approach, J. Proteome Res., 9 (2010) 545-555.

[71] T. Tanaka, M. Tanaka, T. Tanaka, R. Ishigamori, Biomarkers for Colorectal Cancer, Int. J. Mol. Sci., 11 (2010) 3209-3225.

[72] M.J. Duffy, Carcinoembryonic antigen as a marker for colorectal cancer: Is it clinically useful?, Clin. Chem., 47 (2001) 624-630.

[73] H. Koprowski, M. Herlyn, Z. Steplewski, H.F. Sears, Specific antigen in serum of patients with colon carcinoma, Science, 212 (1981) 53-55.

[74] S. Hundt, U. Haug, H. Brenner, Blood markers for early detection of colorectal cancer: A systematic review, Cancer Epidemiol. Biomark. Prev., 16 (2007) 1935-1953.

[75] J. Potack, S.H. Itzkowitz, Practical Advances in Stool Screening for Colorectal Cancer, J. Natl. Compr. Canc. Netw., 8 (2010) 81-92.

[76] B.B. Haab, H. Zhou, Multiplexed protein analysis using spotted antibody microarrays, Methods in molecular biology (Clifton, N.J.), 264 (2004) 33-45.

[77] K. Bussow, D. Cahill, W. Nietfeld, D. Bancroft, E. Scherzinger, H. Lehrach, G. Walter, A method for global protein expression and antibody screening on high-density filters of an arrayed cDNA library, Nucleic Acids Res., 26 (1998) 5007-5008.

[78] C. Hultschig, J. Kreutzberger, H. Seitz, Z. Konthur, K. Bussow, H. Lehrach, Recent advances of protein microarrays, Curr. Opin. Chem. Biol., 10 (2006) 4-10.

[79] M. Cretich, F. Damin, G. Pirri, M. Chiari, Protein and peptide arrays: Recent trends and new directions, Biomol. Eng., 23 (2006) 77-88.

[80] Q. Zhu, M. Uttamchandani, D.B. Li, M.L. Lesaicherre, S.Q. Yao, Enzymatic profiling system in a small-molecule microarray, Org. Lett., 5 (2003) 1257-1260.

[81] H.R.C. Dietrich, J. Knoll, L.R. van den Doel, G.W.K. van Dedem, P.A.S. Daran-Lapujade, L.J. van Vliet, R. Moerman, J.T. Pronk, I.T. Young, Nanoarrays: A method for performing enzymatic assays, Anal. Chem., 76 (2004) 4112-4117.

[82] Y. Lee, D.K. Kang, S.I. Chang, M.H. Han, I.C. Kang, High-throughput screening of novel peptide inhibitors of an integrin receptor from the hexapeptide library by using a protein microarray chip, J. Biomol. Screen., 9 (2004) 687-694.

[83] S.H. Kim, A. Tamrazi, K.E. Carlson, J.A. Katzenellenbogen, A proteomic microarray approach for exploring ligand-initiated nuclear hormone receptor pharmacology, receptor selectivity, and heterodimer functionality, Mol. Cell. Proteomics, 4 (2005) 267-277.

[84] M. Sanchez-Carbayo, N.D. Socci, J.J. Lozano, B.B. Haab, C. Cordon-Cardo, Profiling bladder cancer using targeted antibody arrays, Am. J. Pathol., 168 (2006) 93-103.

[85] V. Combaret, C. Bergeron, S. Brejon, I. Iacono, D. Perol, S. Negrier, A. Puisieux, Protein chip array profiling analysis of sera from neuroblastoma patients, Cancer Lett., 228 (2005) 91-96.

[86] W. Hueber, B.A. Kidd, B.H. Tomooka, B.J. Lee, B. Bruce, J.F. Fries, G. Sonderstrup, P. Monach, J.W. Drijfhout, W.J. van Venrooij, P.J. Utz, M.C. Genovese, W.H. Robinson, Antigen microarray profiling of autoantibodies in rheumatoid arthritis, Arthritis Rheum., 52 (2005) 2645-2655.

[87] W.H. Robinson, C. DiGennaro, W. Hueber, B.B. Haab, M. Kamachi, E.J. Dean, S. Fournel, D. Fong, M.C. Genovese, H.E.N. de Vegvar, K. Skriner, D.L. Hirschberg, R.I. Morris, S. Muller, G.J. Pruijn, W.J. van Venrooij, J.S. Smolen, P.O. Brown, L. Steinman, P.J. Utz, Autoantigen microarrays for multiplex characterization of autoantibody responses, Nat. Med., 8 (2002) 295-301.

[88] R. Speer, J.D. Wulfkuhle, L.A. Liotta, E.F. Petricoin, Reverse-phase protein microarrays for tissue-based analysis, Curr. Opin. Mol. Ther., 7 (2005) 240-245.

[89] D. Geho, N. Lahar, P. Gurnani, M. Huebschman, P. Herrmann, V. Espina, A. Shi, J. Wulfkuhle, H. Garner, E. Petricoin, L.A. Liotta, K.P. Rosenblatt, Pegylated, steptavidin-conjugated quantum dots are effective detection elements for reverse-phase protein microarrays, Bioconjug. Chem., 16 (2005) 559-566.

[90] M. Janzi, J. Odling, Q. Pan-Hammarstrom, M. Sundberg, J. Lundeberg, M. Uhlen, L. Hammarstrom, P. Nilsson, Serum microarrays for large scale screening of protein levels, Mol. Cell. Proteomics, 4 (2005) 1942-1947.

[91] R. Mazurczyk, G. El Khoury, V. Dugas, B. Hannes, E. Laurenceau, M. Cabrera, S. Krawczyk, E. Souteyrand, J.P. Cloarec, Y. Chevolot, Low-cost, fast prototyping method of fabrication of the microreactor devices in soda-lime glass, Sensor Actuat B-Chem, 128 (2008) 552-559.

[92] A. Lueking, M. Horn, H. Eickhoff, K. Bussow, H. Lehrach, G. Walter, Protein microarrays for gene expression and antibody screening, Anal. Biochem., 270 (1999) 103-111.

[93] S. Laib, B.D. MacCraith, Immobilization of biomolecules on cycloolefin polymer supports, Anal. Chem., 79 (2007) 6264-6270.

[94] Y.S. Liu, C.M. Li, W.H. Hu, Z.S. Lu, High performance protein microarrays based on glycidyl methacrylate-modified polyethylene terephthalate plastic substrate, Talanta, 77 (2009) 1165-1171.

[95] M. Beyer, T. Felgenhauer, F. Ralf Bischoff, F. Breitling, V. Stadler, A novel glass slide-based peptide array support with high functionality resisting non-specific protein adsorption, Biomaterials, 27 (2006) 3505-3514.

[96] P. Arenkov, A. Kukhtin, A. Gemmell, S. Voloshchuk, V. Chupeeva, A. Mirzabekov, Protein microchips: Use for immunoassay and enzymatic reactions, Anal. Biochem., 278 (2000) 123-131.

[97] V. Afanassiev, V. Hanemann, S. Wolfl, Preparation of DNA and protein micro arrays on glass slides coated with an agarose film, Nucleic Acids Res., 28 (2000) E66.

[98] B.B. Haab, M.J. Dunham, P.O. Brown, Protein microarrays for highly parallel detection and quantitation of specific proteins and antibodies in complex solutions, Genome Biol., 2 (2001) RESEARCH0004.

[99] H. Zhu, M. Bilgin, R. Bangham, D. Hall, A. Casamayor, P. Bertone, N. Lan, R. Jansen, S. Bidlingmaier, T. Houfek, T. Mitchell, P. Miller, R.A. Dean, M. Gerstein, M. Snyder, Global analysis of protein activities using proteome chips, Science, 293 (2001) 2101-2105.

[100] E.P.C. Lai, W.M. Mullett, J.M. Yeung, Surface plasmon resonance-based immunoassays, Methods-a Companion to Methods in Enzymology, 22 (2000) 77-91.

[101] P. Angenendt, Progress in protein and antibody microarray technology, Drug Discov. Today, 10 (2005) 503-511.

[102] B. Kersten, A. Possling, F. Blaesing, E. Mirgorodskaya, J. Gobom, H. Seitz, Protein microarray technology and ultraviolet crosslinking combined with mass spectrometry for the analysis of protein-DNA interactions, Anal. Biochem., 331 (2004) 303-313.

[103] P. Angenendt, J. Glokler, J. Sobek, H. Lehrach, D.J. Cahill, Next generation of protein microarray support materials: Evaluation for protein and antibody microarray applications, J. Chromatogr. A, 1009 (2003) 97-104.

[104] W. Kusnezow, A. Jacob, A. Walijew, F. Diehl, J.D. Hoheisel, Antibody microarrays: An evaluation of production parameters, Proteomics, 3 (2003) 254-264.

[105] P. Angenendt, J. Glokler, D. Murphy, H. Lehrach, D.J. Cahill, Toward optimized antibody microarrays: a comparison of current microarray support materials, Anal. Biochem., 309 (2002) 253-260.

[106] A.Y. Rubina, E.I. Dementieva, A.A. Stomakhin, E.L. Darii, S.V. Pan'kov, V.E. Barsky, S.M. Ivanov, E.V. Konovalova, A.D. Mirzabekov, Hydrogel-based protein microchips: Manufacturing, properties, and applications, BioTechniques, 34 (2003) 1008-+.

[107] B. Kersten, T. Feilner, A. Kramer, S. Wehrmeyer, A. Possling, I. Witt, M.I. Zanor, R. Stracke, A. Lueking, J. Kreutzberger, H. Lehrach, D.J. Cahill, Generation of Arabidopsis protein chips for antibody and serum screening, Plant Mol. Biol., 52 (2003) 999-1010.

[108] M. Cretich, G. Pirri, F. Damin, I. Solinas, M. Chiari, A new polymeric coating for protein microarrays, Anal. Biochem., 332 (2004) 67-74.

[109] R. Wacker, H. Schroder, C.M. Niemeyer, Performance of antibody microarrays fabricated by either DNA-directed immobilization, direct spotting, or streptavidin-biotin attachment: a comparative study, Anal. Biochem., 330 (2004) 281-287.

[110] P. Peluso, D.S. Wilson, D. Do, H. Tran, M. Venkatasubbaiah, D. Quincy, B. Heidecker, K. Poindexter, N. Tolani, M. Phelan, K. Witte, L.S. Jung, P. Wagner, S. Nock, Optimizing antibody immobilization strategies for the construction of protein microarrays, Anal. Biochem., 312 (2003) 113-124.

[111] J.B. Delehanty, F.S. Ligler, A microarray immunoassay for simultaneous detection of proteins and bacteria, Anal. Chem., 74 (2002) 5681-5687.

[112] V. Dugas, C. Demesmay, Y. Chevolot, E. Souteyard, Use of organosilanes in biosensors, Nova Science Publishers, Inc, New Youk, 2010.

[113] M. Phaner-Goutorbe, V. Dugas, Y. Chevolot, E. Souteyrand, Silanization of silica and glass slides for DNA microarrays by impregnation and gas phase protocols: A comparative study, Materials Science and Engineering: C, 31 (2011) 384-390.

[114] V. Dugas, G. Depret, B. Chevalier, X. Nesme, E. Souteyrand, Immobilization of single-stranded DNA fragments to solid surfaces and their repeatable specific hybridization: covalent binding or adsorption?, Sensor Actuat B-Chem, 101 (2004) 112-121.

[115] S. Ek, E.I. Iiskola, L. Niinisto, Gas-phase deposition of aminopropylalkoxysilanes on porous silica, Langmuir, 19 (2003) 3461-3471.

[116] V. Dugas, Y. Chevalier, Surface hydroxylation and silane grafting on fumed and thermal silica, J. Colloid Interface Sci., 264 (2003) 354-361.

[117] C.P. Tripp, M.L. Hair, Chemical Attachment of Chlorosilanes to Silica - a 2-Step Amine-Promoted Reaction, J. Phys. Chem., 97 (1993) 5693-5698.

[118] C.M. Halliwell, A.E.G. Cass, A factorial analysis of silanization conditions for the immobilization of oligonucleotides on glass surfaces, Anal. Chem., 73 (2001) 2476-2483.

[119] C.J. Cai, Z.G. Shen, Y.S. Xing, S.L. Ma, Surface topography and character of gamma-aminopropyltriethoxysilane and dodecyltrimethoxysilane films adsorbed on the silicon dioxide substrate via vapour phase deposition, J Phys D Appl Phys, 39 (2006) 4829-4837.

[120] A.Y. Fadeev, T.J. McCarthy, Self-assembly is not the only reaction possible between alkyltrichlorosilanes and surfaces: Monomolecular and oligomeric covalently attached layers of dichloro- and trichloroalkylsilanes on silicon, Langmuir, 16 (2000) 7268-7274.

[121] J.B. Brzoska, I. Benazouz, F. Rondelez, Silanization of Solid Substrates - a Step toward Reproducibility, Langmuir, 10 (1994) 4367-4373.

[122] M.J. Stevens, Thoughts on the Structure of alkylsilane monolayers, Langmuir, 15 (1999) 2773-2778.

[123] F. Zhang, K. Sautter, A.M. Larsen, D.A. Findley, R.C. Davis, H. Samha, M.R. Linford, Chemical Vapor Deposition of Three Aminosilancs on Silicon Dioxide: Surface Characterization, Stability, Effects of Silane Concentration, and Cyanine Dye Adsorption, Langmuir, 26 (2010) 14648-14654.

[124] F. Bessueille, V. Dugas, V. Vikulov, J.P. Cloarec, E. Souteyrand, J.R. Martin, Assessment of porous silicon substrate for well-characterised sensitive DNA chip implement, Biosens. Bioelectron., 21 (2005) 908-916.

[125] M. Bras, V. Dugas, F. Bessueille, J.P. Cloarec, J.R. Martin, M. Cabrera, J.P. Chauvet, E. Souteyard, M. Garrigues, Optimisation of a silicon/silicon dioxide substrate for a fluorescence DNA microarray, Biosens. Bioelectron., 20 (2004) 797-806.

[126] J.P. Cloarec, Y. Chevolot, E. Laurenceau, M. Phaner-Goutorbe, E. Souteyrand, A multidisciplinary approach for molecular diagnostics based on biosensors and microarrays, Irbm, 29 (2008) 105-127.

[127] M. Cabrera, M. Jaber, V. Dugas, J. Broutin, E. Vnuk, J.P. Cloarec, E. Souteyrand, J.R. Martin, Implementation of DNA chips obtained by microprojection for diagnostic and personalized medicine, Cell. Mol. Biol., 50 (2004) 225-232.

[128] P. Innocenzi, C. Figus, T. Kidchob, M. Valentini, B. Alonso, M. Takahashi, Sol-gel reactions of 3-glycidoxypropyltrimethoxysilane in a highly basic aqueous solution, Dalton Trans., (2009) 9146-9152.

[129] C. Fan, G.P. Lopinski, STM and HREELS investigation of gas phase silanization on hydroxylated Si(100), Surf. Sci., 604 (2010) 996-1001.

[130] S. Demirci, T. Caykara, Formation of dicarboxylic acid-terminated monolayers on silicon wafer surface, Surf. Sci., 604 (2010) 649-653.

[131] J.C. Howard, C. Heinemann, B.J. Thatcher, B. Martin, B.S. Gan, G. Reid, Identification of collagen-binding proteins in Lactobacillus spp. with surface-enhanced laser desorption/ionization-time of flight ProteinChip technology, Appl. Environ. Microbiol., 66 (2000) 4396-4400.

[132] A.D. Delgado, M. Leonard, E. Dellacherie, Surface properties of polystyrene nanoparticles coated with dextrans and dextran-PEO copolymers. Effect of polymer architecture on protein adsorption, Langmuir, 17 (2001) 4386-4391.

[133] L. Muchova, M. Jirsa, M. Kuroki, L. Dudkova, M.J. Benes, Z. Marecek, F. Smid, Immunoaffinity isolation of CEACAM1 on hydrazide-derivatized cellulose with immobilized monoclonal anti-CEA antibody, Biomed. Chromatogr., 15 (2001) 418-422.

[134] Y. Lee, E.K. Lee, Y.W. Cho, T. Matsui, I.C. Kang, T.S. Kim, M.H. Han, ProteoChip: A highly sensitive protein microarray prepared by a novel method of protein, immobilization for application of protein-protein interaction studies, Proteomics, 3 (2003) 2289-2304.

[135] I.E. Tothill, F. Salam, Detection of Salmonella typhimurium using an electrochemical immunosensor, Biosens. Bioelectron., 24 (2009) 2630-2636.

[136] A.N. McCormick, M.E. Leach, G. Savidge, A. Alhaq, Validation of a quantitative SPR assay for recombinant FVIII, Clin. Lab. Haematol., 26 (2004) 57-64.

[137] S. Sam, L. Touahir, J.S. Andresa, P. Allongue, J.N. Chazalviel, A.C. Gouget-Laemmel, C.H. de Villeneuve, A. Moraillon, F. Ozanam, N. Gabouze, S. Djebbar, Semiquantitative Study of the EDC/NHS Activation of Acid Terminal Groups at Modified Porous Silicon Surfaces, Langmuir, 26 (2010) 809-814.

[138] Biacore, Sensor Surface Handbook, in, 2003.

[139] L. Roussille, G. Brotons, L. Ballut, G. Louarn, D. Ausserre, S. Ricard-Blum, Surface characterization and efficiency of a matrix-free and flat carboxylated gold sensor chip for surface plasmon resonance (SPR), Anal. Bioanal. Chem., 401 (2011) 1605-1621.

[140] A. Perrin, D. Duracher, L. Allard, P. Cleuziat, A. Theretz, B. Mandrand, Improved performance of a protein array using conjugated polymers as capture phase for HIV serodiagnosis, Polym. Int., 53 (2004) 586-590.

[141] G. El Khoury, E. Laurenceau, Y. Chevolot, Y. Merieux, A. Desbos, N. Fabien, D. Rigal, E. Souteyrand, J.P. Cloarec, Development of miniaturized immunoassay: influence of surface chemistry and comparison with enzyme-linked immunosorbent assay and Western blot, Anal. Biochem., 400 (2010) 10-18.

[142] H.Y. Lee, S.B. Park, Surface modification for small-molecule microarrays and its application to the discovery of a tyrosinase inhibitor, Mol. BioSyst., 7 (2011) 304-310.

[143] J.K. Kim, D.S. Shin, W.J. Chung, K.H. Jang, K.N. Lee, Y.K. Kim, Y.S. Lee, Effects of polymer grafting on a glass surface for protein chip applications, Colloids and Surfaces B-Biointerfaces, 33 (2004) 67-75.

[144] Y. Zhou, O. Andersson, P. Lindberg, B. Liedberg, Protein microarrays on carboxymethylated dextran hydrogels: Immobilization, characterization and application, Microchim. Acta, 147 (2004) 21-30.

[145] L.D. White, C.P. Tripp, Reaction of (3-Aminopropyl)dimethylethoxysilane with Amine Catalysts on Silica Surfaces, J. Colloid Interface Sci., 232 (2000) 400-407.

[146] M.F. Sunding, I.T. Jensen, P.M. Stenstad, S. Diplas, ARXPS and high energy XPS characterisation of titanium surfaces for medical implants, Surf. Interface Anal., 40 (2008) 751-753.

[147] A.W. Adamson, A.P. GASt, Physical Chemistry of Surfaces 6ed., Wiley, New York, 1997.

[148] D.K. Owens, R.C. Wendt, Estimation of the surface free energy of polymers, J. Appl. Polym. Sci., 13 (1969) 1741-1747.

[149] R.J. Good, L.A. Girifalco, A theory for estimation of surface and interfacial energies. III. Estimation of surface energies of solids from contact angle data, J. Phys. Chem., 64 (1960) 561-565.

[150] S.L. Seurynck-Servoss, C.L. Baird, K.D. Rodland, R.C. Zangar, Surface chemistries for antibody microarrays, Frontiers in Bioscience-Landmark, 12 (2007) 3956-3964.

[151] W. Kusnezow, J.D. Hoheisel, Solid supports for microarray immunoassays, J. Mol. Recognit., 16 (2003) 165-176.

[152] M.L. Lesaicherre, M. Uttamchandani, G.Y. Chen, S.Q. Yao, Developing site-specific immobilization strategies of peptides in a microarray, Bioorg. Med. Chem. Lett., 12 (2002) 2079-2083.

[153] W. Kusnezow, J.D. Hoheisel, Antibody microarrays: promises and problems, BioTechniques, Suppl (2002) 14-23.

[154] E.W. Olle, J. Messamore, M.P. Deogracias, S.D. McClintock, T.D. Anderson, K.J. Johnson, Comparison of antibody array substrates and the use of glycerol to normalize spot morphology, Exp. Mol. Pathol., 79 (2005) 206-209.

[155] P. Pavlickova, N.M. Lensen, H. Paul, M. Schaeferling, C. Giammasi, M. Kruschina, W.D. Du, M. Theisen, M. Ibba, F. Ortigao, D. Kambhampati, Antibody detection in human serum using a versatile protein chip platform constructed by applying nanoscale self-assembled architectures on gold, J. Proteome Res., 1 (2002) 227-231.

[156] C.A. Rowe, L.M. Tender, M.J. Feldstein, J.P. Golden, S.B. Scruggs, B.D. MacCraith, J.J. Cras, F.S. Ligler, Array biosensor for simultaneous identification of bacterial, viral, and protein analytes, Anal. Chem., 71 (1999) 3846-3852.

[157] X.C. Zhou, J.Z. Zhou, Protein microarrays on hybrid polymeric thin films prepared by self-assembly of polyelectrolytes for multiple-protein immunoassays, Proteomics, 6 (2006) 1415-1426.

[158] L.A. Liotta, V. Espina, A.I. Mehta, V. Calvert, K. Rosenblatt, D. Geho, P.J. Munson, L. Young, J. Wulfkuhle, E.F. Petricoin, Protein microarrays: Meeting analytical challenges for clinical applications, Cancer Cell, 3 (2003) 317-325.

[159] E. Kopf, D. Shnitzer, D. Zharhary, Panorama (TM) Ab microarray cell signaling kit: A unique tool for protein expression analysis, Proteomics, 5 (2005) 2412-2416.

[160] F.F. Madrid, N.M. Tang, H. Alansari, R.L. Karvonen, J.E. Tomkiel, Improved approach to identify cancer-associated autoantigens, Autoimmun. Rev., 4 (2005) 230-235.

[161] J.Y. Zhang, Mini-array of multiple tumor-associated antigens to enhance autoantibody detection for immunodiagnosis of hepatocellular carcinoma, Autoimmun. Rev., 6 (2007) 143-148.

[162] J.Y. Zhang, R. Megliorino, X.X. Peng, E.M. Tan, Y. Chen, E.K.L. Chan, Antibody detection using tumor-associated antigen mini-array in immunodiagnosing human hepatocellular carcinoma, J. Hepatol., 46 (2007) 107-114.

[163] C. Desmetz, T. Maudelonde, A. Mange, J. Solassol, Identifying autoantibody signatures in cancer: a promising challenge, Expert Rev. Proteomics, 6 (2009) 377-386.

[164] C. Desmet, G.C. Le Goff, J.C. Bres, D. Rigal, L.J. Blum, C.A. Marquette, Multiplexed immunoassay for the rapid detection of anti-tumor-associated antigens antibodies, Analyst, 136 (2011) 2918-2924.

[165] K. Martin, C. Ricciardelli, P. Hoffmann, M.K. Oehler, Exploring the Immunoproteome for Ovarian Cancer Biomarker Discovery, Int. J. Mol. Sci., 12 (2011) 410-428.

[166] C. Desmetz, C. Cortijo, A. Mange, J. Solassol, Humoral response to cancer as a tool for biomarker discovery, Journal of Proteomics, 72 (2009) 982-988.

[167] G. Kijanka, D. Murphy, Protein arrays as tools for serum autoantibody marker discovery in cancer, Journal of Proteomics, 72 (2009) 936-944.

[168] S. Matarraz, M. Gonzalez-Gonzalez, M. Jara, A. Orfao, M. Fuentes, New technologies in cancer. Protein microarrays for biomarker discovery, Clin. Transl. Oncol., 13 (2011) 156-161.

[169] J. Ingvarsson, A. Larsson, A.G. Sjoholm, L. Truedsson, B. Jansson, C.A.K. Borrebaeck, C. Wingren, Design of recombinant antibody microarrays for serum protein profiling: Targeting of complement proteins, J. Proteome Res., 6 (2007) 3527-3536.

[170] K.S. Anderson, J. LaBaer, The sentinel within: Exploiting the immune system for cancer biomarkers, J. Proteome Res., 4 (2005) 1123-1133.

[171] R. Orchekowski, D. Hamelinck, L. Li, E. Gliwa, M. VanBrocklin, J.A. Marrero, G.F.V. Woude, Z.D. Feng, R. Brand, B.B. Haab, Antibody microarray profiling reveals individual and combined serum proteins associated with pancreatic cancer, Cancer Res., 65 (2005) 11193-11202.

[172] S. Spisak, B. Galamb, F. Sipos, O. Galamb, B. Wichmann, N. Solymosi, B. Nemes, J. Molnar, Z. Tulassay, B. Molnar, Applicability of antibody and mRNA expression microarrays for identifying diagnostic and progression markers of early and late stage colorectal cancer, Dis. Markers, 28 (2010) 1-14.

[173] D. Boehm, K. Keller, N. Boehm, A. Lebrecht, M. Schmidt, H. Koelbl, F.-H. Grus, Antibody microarray analysis of the serum proteome in primary breast cancer patients, Cancer Biol. Ther., 12 (2011) 772-779.

[174] J.C. Miller, H.P. Zhou, J. Kwekel, R. Cavallo, J. Burke, E.B. Butler, B.S. Teh, B.B. Haab, Antibody microarray profiling of human prostate cancer sera: Antibody screening and identification of potential biomarkers, Proteomics, 3 (2003) 56-63.

[175] W. Luo, M. Pla-Roca, D. Juncker, Taguchi design-based optimization of sandwich immunoassay microarrays for detecting breast cancer biomarkers, Anal. Chem., 83 (2011) 5767-5774.

[176] M.J. Scanlan, S. Welt, C.M. Gordon, Y.T. Chen, A.O. Gure, E. Stockert, A.A. Jungbluth, G. Ritter, D. Jager, E. Jager, A. Knuth, L.J. Old, Cancer-related serological recognition of human colon cancer: Identification of potential diagnostic and immunotherapeutic targets, Cancer Res., 62 (2002) 4041-4047.

[177] P.V. Belousov, D.V. Kuprash, A.Y. Sazykin, S.V. Khlgatian, D.N. Penkov, Y.V. Shebzukhov, S.A. Nedospasov, Cancer-associated antigens and antigen arrays in serological diagnostics of malignant tumors, Biochemistry (Mosc.), 73 (2008) 562-572.

[178] J.Y. Zhang, C.A. Casiano, X.X. Peng, J.A. Koziol, E.K.L. Chan, E.M. Tan, Enhancement ot antibody detection in cancer using panel of recombinant tumor-associated antigens, Cancer Epidemiol. Biomark. Prev., 12 (2003) 136-143.

[179] J.A. Koziol, J.Y. Zhang, C.A. Casiano, X.X. Peng, F.D. Shi, A.C. Feng, E.K.L. Chan, E.M. Tan, Recursive partitioning as an approach to selection of immune markers for tumor diagnosis, Clin. Cancer Res., 9 (2003) 5120-5126.

[180] J.Y. Zhang, Tumor-associated antigen arrays to enhance antibody detection for cancer diagnosis, Cancer Detect. Prev., 28 (2004) 114-118.

[181] C. Chapman, A. Murray, J. Chakrabarti, A. Thorpe, C. Woolston, U. Sahin, A. Barnes, J. Robertson, Autoantibodies in breast cancer: their use as an aid to early diagnosis, Ann. Oncol., 18 (2007) 868-873.

[182] R. Megliorino, F.D. Shi, X.X. Peng, X. Wang, E.K.L. Chan, E.M. Tan, J.Y. Zhang, Autoimmune response to anti-apoptotic protein survivin and its association with antibodies to p53 and c-myc in cancer detection, Cancer Detect. Prev., 29 (2005) 241-248.

[183] J.Y. Zhang, E.K.L. Chan, X.X. Peng, M.L. Lu, X. Wang, F. Mueller, E.M. Tan, Autoimmune responses to mRNA binding proteins p62 and Koc in diverse malignancies, Clin. Immunol., 100 (2001) 149-156.

[184] A. Yagihashi, T. Ohmura, K. Asanuma, D. Kobayashi, N. Tsuji, T. Torigoe, N. Sato, K. Hirata, N. Watanabe, Detection of autoantibodies to survivin and livin in sera from patients with breast cancer, Clin. Chim. Acta, 362 (2005) 125-130.

Chapter 2 Elaboration of Protein Microarrays: Chemical Functionalizations and Characterizations*

* This chapter is based on the following contributions:

- Z. G. Yang, E. Laurenceau, Y. Chevolot, Y.A. Önal, G. Choquet-Kastylevsky, E. Souteyrand, Cancer Biomarkers Detection using Microstructured Protein Chip: Implementation of ustomized Multiplex Immunoassay, Procedia Engineering, 25 (2011) 952-955.
- E. Laurenceau, Z.G. Yang, Y. Chevolot, Y. Attaman, G. Choquet-Kastylevsky, E. Souteyrand, Tumor antigens titration on novel miniaturized immunoassay: 3D-Protein chip performance evaluation, Bull. Canc (Paris), 98 (2011) S70-S70.
- Z.G. Yang, Y. Chevolot, V. Dugas, N. Xanthopoulos, V. Laporte, T. Delair, Y. Ataman-Önal, G. Choquet-Kastylevsky, E. Souteyrand, E. Laurenceau. Antibody microarray based on different chain-length amino surfaces for the detection of tumor markers involved in colorectal cancer. Submitted to Biomaterials 2012

2.1. Introduction

Immobilization of biomolecules on solid supports was extensively studied but remains a great challenge in the field of protein microarray. Unlike nucleic acids or peptides, the tertiary structure and reactivity of a given protein is different from another one leading to complexify the immobilization process. Preserving the tertiary structure of proteins is essential for their biological activity. Thus, the interface between the solid support and the protein, e.g. surface chemistry, is a key point to efficiently immobilize proteins and to retain their biological activities [1-5]. Therefore, one major goal of this study aims the elaboration of stable and reproducible surface chemistries, which could provide a homogeneous environment for probes, preventing loss of biological activity and unspecific adsorption.

First, to manufacture, a solid support is required. We choose glass slide because it is cheap and its microstructuration using etching is well controlled in the lab. Second, based on the knowledge of our research group, silane chemistry was performed to introduce homogeneous monolayer on the solid support Different silane molecules were substituted in order to obtain different functional groups on the surface: (3-aminopropyl) dimethylethoxysilane (APDMES) leads to amino groups on the surface, (3-glycidoxypropyl) dimethylethoxysilane (GPDMES) brings epoxy groups, and deprotected tert-butyl-11-(dimethylamin) silylundecanoate (TDSUM) gives carboxylic groups on the surface.

As presented in the literature part (Chapter 1), physical adsorption offers the simplest process of immobilization and is widely used for protein microarray because no protein modifications are needed. Alternatively, covalent binding gives a durable and stable linkage to the solid support. Thus, both physical adsorption and covalent binding of proteins on the functionalized surfaces were targeted in this work. Moreover, in order to reduce non-specific adsorption and to increase the specific area available for protein immobilization, different polymers were grafted on silanized glass slides. Jeffamine and chitosan were covalently grafted on NHS-activated TDSUM surface, whereas NHS-activated carboxymethyl dextran (CMD) and maleic anhydride-*alt*-methyl vinyl ether (MAMVE) were grafted on APDMES surface. Chitosan and CMD are two polysaccharide biopolymers known to limit non-specific adsorption of proteins. In previous studies, MAMVE copolymer was demonstrated to be efficient for protein immobilization and immunoassay [36]. Therefore, immobilization of proteins couls be performed through physical adsorption both on silane monolayers (TDSUM-COOH, APDMES) and on polymer surfaces (Jeffamine, Chitosan), and through covalent linking both on silane monolayers (NHS-activated TDSUM, GPDMES) and on polymer surfaces (CMD, MAMVE). All these surface modifications were illustrated in Figure 2-1.

The physico-chemical properties of these surfaces were characterized by means of standard techniques such as attenuated total reflectance Fourier transform infrared (ATR-FTIR), X-ray photoelectron spectra (XPS), and contact angle measurement. Evaluation of amino density on aminated surfaces was performed by colorimetric assay.

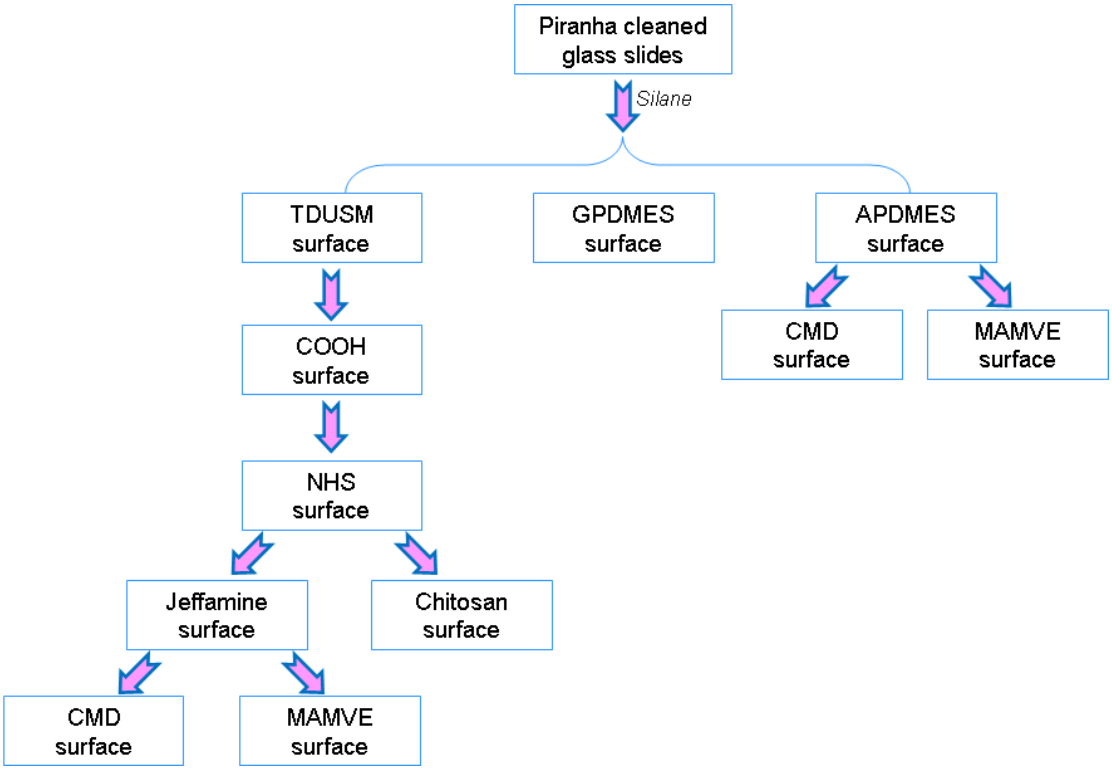

Figure 2-1 Schematic illustration of all the surface modification procedure on glass slides, in the following text of in this thesis, CMD and MAMVE surfaces were both grafted from APDMES surface unless specifically stated.

2.2. Experimental

2.2.1. Materials

Borosilicate flat glass slides (76 x 26 x 1 mm) were purchased from Schott GMBH (Mainz, Germany), silicon (10 x 10 mm) substrates with polished silica wafer (SiO_2 90 ± 10 % nm) was obtained from Siltronics. 96 % Sulphuric acid (H_2SO_4) and 37 % hydrochloric (HCl) acid were supplied by Riedel de Haen, Puriss, Seelze, Germany. All chemicals were of reagent grade or highest available commercial-grade quality and used as received unless otherwise stated. (3-aminopropyl) dimethylethoxysilane (APDMES), (3-glycidoxypropyl) dimethylethoxysilane (GPDMES), dimethyl sulfoxide (DMSO, anhydrous, 99.9%), 0.01 M phosphate-buffered saline (PBS 1x, pH 7.4) at 25 ^{o}C (0.0027 M potassium chloride and 0.138

M sodium chloride), 35 % hydrogen peroxide (H_2O_2) sodium dodecyl sulfate (SDS), sodium bicarbonate $NaHCO_3$, sodium carbonate Na_2CO_3, N-Hydroxysuccinimide (NHS), Jeffamine D-230 (polyoxypropylenediamine), N, N'-diisopropylcarbodiimide (DIC), tetrahydrofuran (THF) (purum grade), Bromoacetic acid (BAA), coomassie brilliant blue (CBB) ($C_{47}H_{48}N_3NaO_7S_2$, >95% purified dye), Dextran T10 (M_w =100 000 - 200 000 g/mol) and maleic anhydride-*alt*-methyl vinyl ether (MAMVE, M_w = 216 000 g/mol) were all obtained from Sigma (St. Quentin Fallavier, France). Dextran T40 (M_w = 40 000 g/mol) was purchased from Pharmacosmos. Tween 20 was purchased from Roth-Sochiel (Lauterbourg, France). Tert-butyl-11-(dimethylamino)silylundecanoate (TDSUM) was home-made silane [8]. Chitosan (M_w=470 000 g/mol, degree of deacetylation (DD) 94 %) was kindly provided by Prof. T. Delair (Polymer Materials and Biomaterials Laboratory (LMPB), Université Claude Bernard Lyon 1). MAMVE copolymer (Mr = 67 000 g/mol) was provided by Biomérieux-CNRS–UMR 2714 (Ecole Normale Supérieure, Lyon, France).

TDF4 detergent for washing glass slides was supplied by Franklab SA, Billancourt, France. Fresh piranha was composed with a mixture of H_2SO_4/H_2O_2 (7/3, v/v). Etching solution was composed of buffered oxide etchant (BOE, Hydrofluoridric acid/ammonium fluoride, v/v, 7/1), HCl and DI water, 1/2/2, v/v/v).

0.02 M sodium carbonate buffers at pH 10.7 were prepared from 0.1 M $NaHCO_3$ and 0.1 M Na_2CO_3 solutions in ultrapure water. 0.01 M 2-(N-morpholino) ethanesulfonic acid (MES) (pH=6.2) was prepared by dissolving the content of one pouch into 1 L ultrapure water and adjust pH up to 6.2. 0.01 M Phosphate buffered saline (PBS) or PBS 1X (pH 7.4) was prepared by dissolving the content of one pouch of dried powder in 1 L of ultrapure water. Deionised (DI) water (18.2 MΩ) was delivered by an Elga water system. Washing buffer contained PBS 1X and 0.1 % Tween 20 (PBS-T) at pH 7.4.

2.2.2. Microstructuration of glass slide

Arrays of 4 x 10 wells microwells were generated on the surface of flat glass slides by means of photolithography and wet etching process on the basis of previous work in our group [9-11] . The scheme of protocol was described in Figure 2-.

Glass slides were washed with TDF4 detergent solution, a fresh Piranha for 10 min, then rinsed with DI water and dried by centrifugation at 1300 rpm for 3 min. A 150 nm chromium layer was deposited on the surface of glass slides with magnetron sputtering (MRC822 system), in order to promote the adhesion of photoresist film with the slide and offer an additional protection against harsh etching solutions. The system was operated at a RF power of 5 kW, reflected power was 2 W, and turret voltages 2.6 kV. The argon flux was set to 50 sccm and the working pressure was 2.6 10^{-3} Torr.

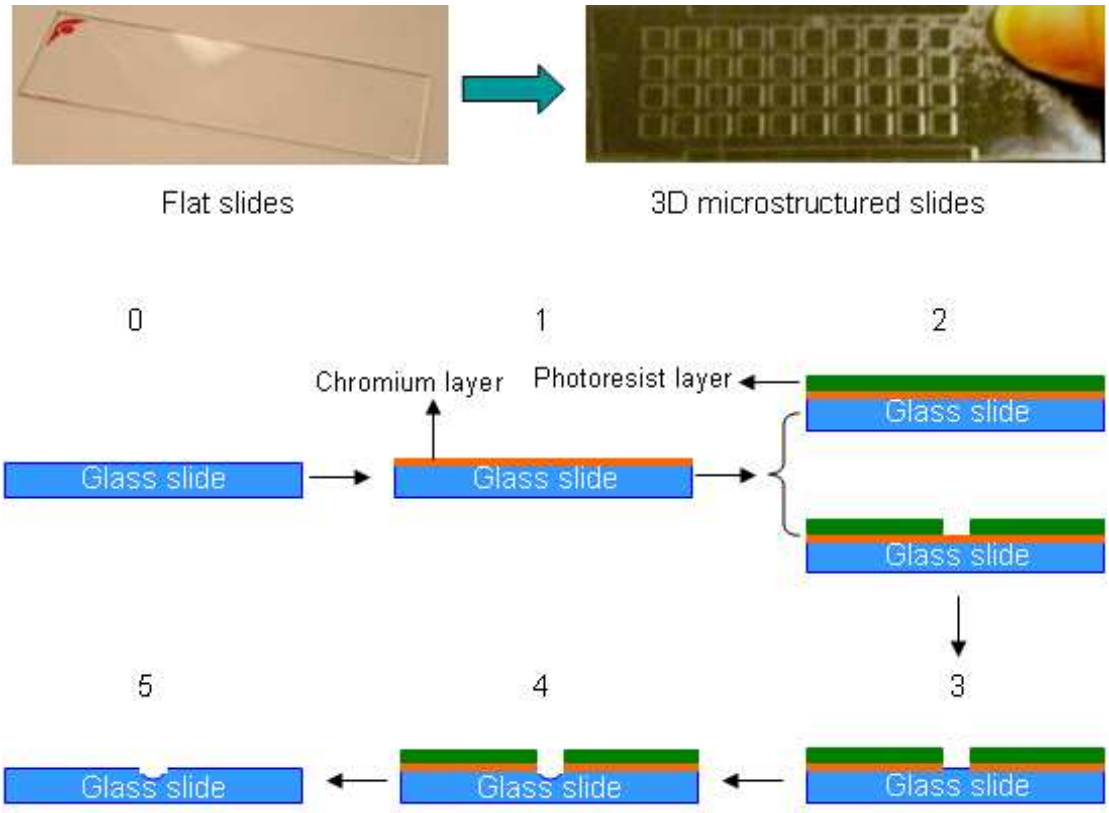

Figure 2-2 Schematic illustration microstructured glass slides and fabrication of microreactors on glass slide: 0, the original glass slide; 1, the deposition of a chromium layer; 2, a photolithographic step; 3, opening of the chromium; 4, glass etching; 5, removing of the protective layers.

SPR 220 4.5 photoresist (Rohm Haas electronic materials, Lucerne, CH) was spin-casted at 4 000 rpm for 30s resulting in a 4 µm thick layer, followed by baking at 115 °C on a hot plate for 90 seconds. Photolithography was performed on a Karl Suss MJB3 Mask Aligner with illumination for 22 seconds. The slides were immersed in MF26 A developer for 1 minute, rinsed in running DI water for 5 min, dried under a dry nitrogen flux and post-baked at 115°C for 2 minutes.

The chromium windows on the glass slides were opened using chromium etchant (Merck, Darmstadt, Germany). The slides were then rinsed in running DI water for 15 minutes and immersed in a freshly prepared wet etching solution at room temperature for 75 min. The slides were rinsed in running DI water for 15 minutes, followed by acetone, ethanol and water to absolutely remove the photoresist. At last, the chromium layer was removed with chromium etchant (Merck, Darmstadt, Germany).

Depth of the microwells was monitored with a mechanical profiler (Alfa-step 500 from KLA Tencor) [9]. The featured 40 square microreactors are homogenous with 3 mm side length, 60 ± 1 µm depth, as well as 4.5 mm spacing between each microreactor in order to be compatible with the spotting robot and multi-channel micropipettes.

2.2.3. Silanization of substrates

The silanization were performed on the basis of previous reports [12, 13]. Tert-butyl-11-(dimethylamino)silylundecanoate (TDSUM), (3-aminopropyl) dimethyl-ethoxysilane (APDMES), and (3-glycidoxypropyl) dimethylethoxysilane (GPDMES) were employed to generate carboxylic acid (COOH), amino and epoxy monolayer, respectively. Functionalization with these silanes was performed either on glass slide or on silica substrate to achieve surface characterizations. Prior to silanization, all the substrates were rinsed with TDF4 detergent and DI water, followed by fresh piranha for 30 min in ultrasonic bath and DI water.

2.2.3.1. Silanization with TDSUM

Prior to the reaction, the reaction chamber was flushed with dry nitrogen. Substrates were heated under reduced pressure for 2 hrs at 150°C and 1 ml of TDSUM was introduced. TDSUM was vaporized by heating at 150°C under reduced pressure ($8 \cdot 10^{-2}$ mbar) and allowed to react for 12 hrs (150°C, $8 \cdot 10^{-2}$ mbar). Samples were then washed sequentially with ultrasonic bath of THF, dichloromethane and DI water.

Tert-butyl esters of TDSUM were hydrolyzed with formic acid for 7 hrs at room temperature to obtain carboxylic groups (COOH surface). Activation of these carboxylic groups was carried out with a mixture of NHS/DIC (molar ratio 1:1, 0.1 M) in THF overnight at room temperature to obtain NHS-activated surface, followed by washing under ultrasonic bath of THF and dichloromethane for 10 min. The detail of the procedure was illustrated in Figure 2-.

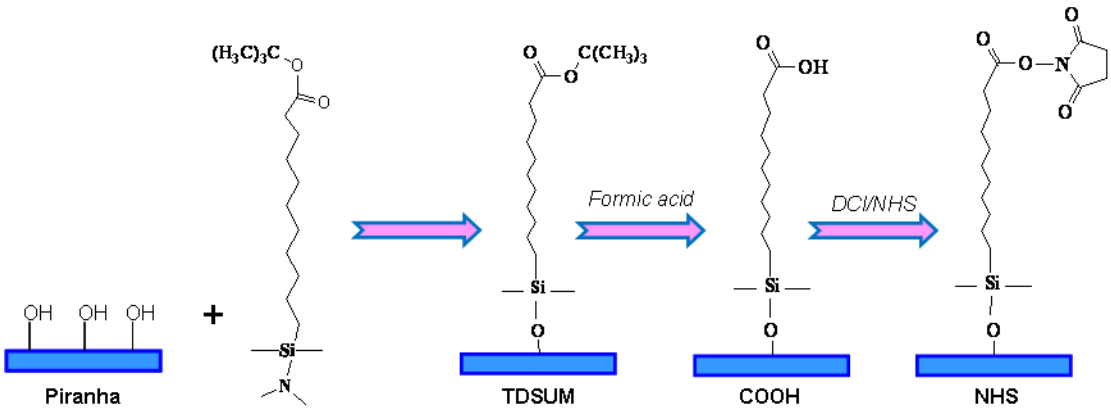

Figure 2-3 Schematic illustration of protocols for silane with TDSUM to obtain COOH and NHS surfaces

2.2.3.2. Silanization with APDMES

The substrates were deposited in the reactor under a nitrogen stream for 2hrs at 150°C. Then the system was left to cool down to room temperature and various volumes (from 0.06 % to 0.6 %, v/v) of APDMES in dry pentane was introduced. The reaction was carried out at room temperature for 1 hr under stirring. After evaporating the pentane, the incubation was allowed overnight at 150°C under nitrogen stream. Finally, the silanized substrates (glass slides, silica) were washed thoroughly with pentane, THF and DI water in ultrasonic bath.

2.2.3.3. Silanization with GPDMES

The substrates were deposited in the reactor under nitrogen stream for 2hrs at 150°C. After the system cools down to room temperature, 0.25 ml of GPDMES in dry pentane was introduced and the reaction was carried out for 1 hr at room temperature under stirring. After evaporating the pentane, the incubation occurred overnight at 150°C under nitrogen stream. The silanized slides were rinsed with pentane, THF and DI water in ultrasonic bath for 10 min, respectively. Figure 2- summarized the protocols of silanization with APDMES and GPDMES.

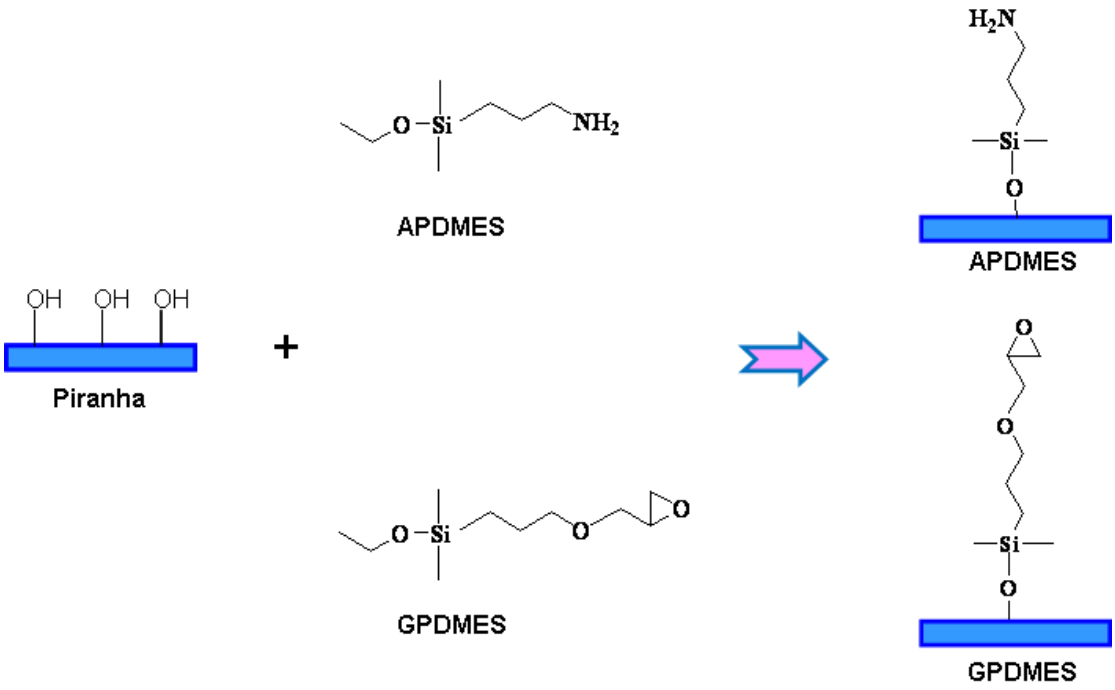

Figure 2-4 Schematic illustration of silanization with APDMES and GPDMES

2.2.4. Polymer grafting on silanized surfaces

Jeffamine, chitosan and MAMVE polymers were grafted as received without any chemical modification. CMD was synthesized according to our home-made protocols from two commercial dextrans (T10 and T40) at various substitution rates in carboxymethyl units.

2.2.4.1. Synthesis of carboxymethyl dextran (CMD)

Dextran with two different molecular weights (T40: M_w =40 000 g mol^{-1}; T10: M_w =100 000 – 200 000 g mol^{-1}) was exactly weighed and introduced under stirring into a conical beaker containing 85 ml iso-propanol until dissolving completely. 15 mL sodium hydroxide (NaOH, 3.8 M) solution was added slowly with stirring until the dextran was completely distributed into mixed solution, and the system was subjected to continuous stirring during 1 hr at room temperature. Then according to various molar ratio of BAA/Dextran, various weight of BAA (Bromo Acetic Acid) was added under stirring to complete homogeneity. The mixture was allowed to react at 60°C for 90 min, then cooled to room temperature and neutralized with glacial acetic acid. The reaction product was precipitated in methanol, and washed off with DI water and methanol for 3 times respectively, purified and dried at reduced pressure at 40°C for 2 hrs. The reaction scheme was illustrated in Figure 2-.

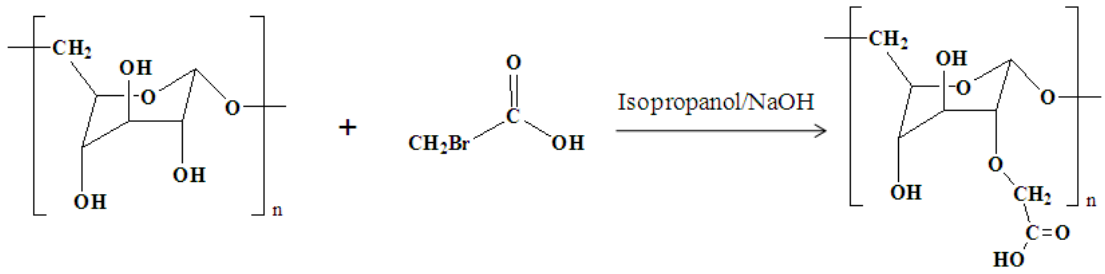

Figure 2-5 Scheme of the reaction between dextran and bromoacetic acid leading to carboxymethyl dextran

2.2.4.2. Grafting of Jeffamine on NHS activated surface

The NHS surface generated from TDSUM silanization was incubated in a 0.1 M solution of Jeffamine overnight at room temperature to generate aminated surface (Figure 2-). The slides were then washed for 30 min with 0.1 % SDS at 70 °C and rinsed with DI water.

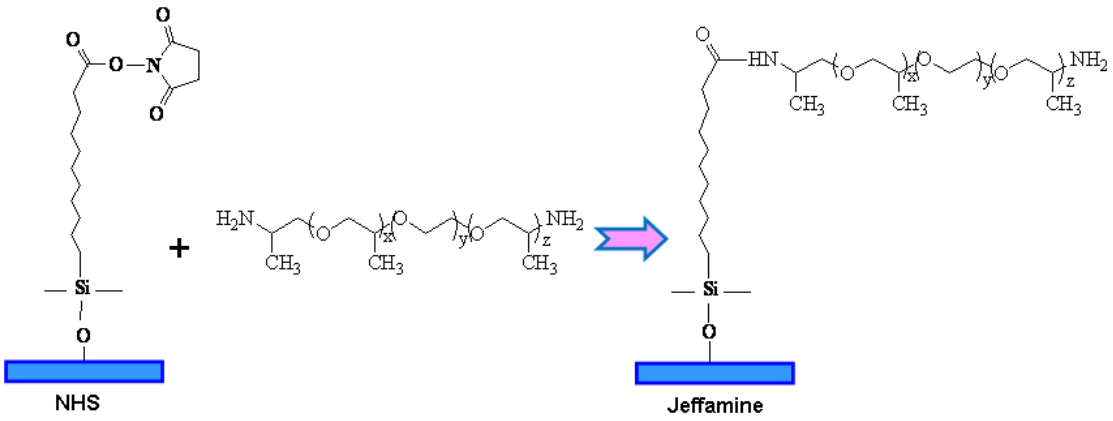

Figure 2-6 Schematic illustration of Jeffamine grafting on NHS surface

2.2.4.3. Grafting of chitosan on NHS-activated surface

Chitosan solution was prepared in acetic acid/DI-H_2O mixed solvents. The concentration of acetic acid was determined by the degree of deacetylation (DD) and expected concentration of chitosan. In this thesis, chitosan sample used (Mw = 416 000 g/mol) possesses DD=94%. At 1 mg/mL, chitosan was dissolved with 5.8 mM acetic acid in 100 mL DI water; and at 5 mg/mL, chitosan was dissolved with 29 mM acetic acid in DI water. These chitosan solutions were allowed to react with NHS surface for 4hr at room temperature (Figure 2-) and washed with DI water for 2x5 min.

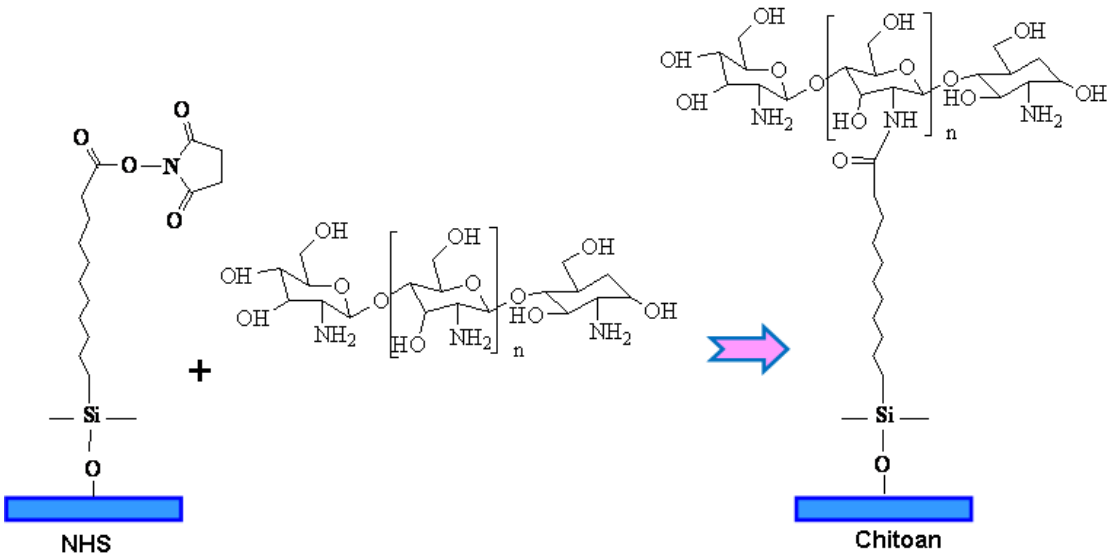

Figure 2-7 Schematic illustration of chitosan grafting on NHS surface

2.2.4.4. Grafting of CMD on aminated surfaces

Both Jeffamine and APDMES surfaces were used to graft CMD. First, they were incubated in 0.02 M sodium carbonate solution (pH 10.7) for 1 hr at room temperature in order to deprotonate amine groups. Concurrently, 1 mg/mL CMD (degree of substitution (DS) 63 %, unless specific statement) dissolved in MES buffer (pH =6.2) was allowed to react with EDC/NHS (CMD/EDC/NHS molar ration: 1/4/1) at room temperature for 30 min to activate carboxylic groups. Then NHS-activated CMD was incubated with aminated surfaces at room temperature for 4 hrs to generate CMD surfaces (Figure 2-). Prior to protein immobilization, carboxylic groups of CMD surface were re-activated with EDC/NHS (molar ratio 4/1 in MES pH = 6.2) for 30 min at room temperature. For preliminarily CMD grafting from Jeffamine, CMD concentration was set at 5 mg/ml.

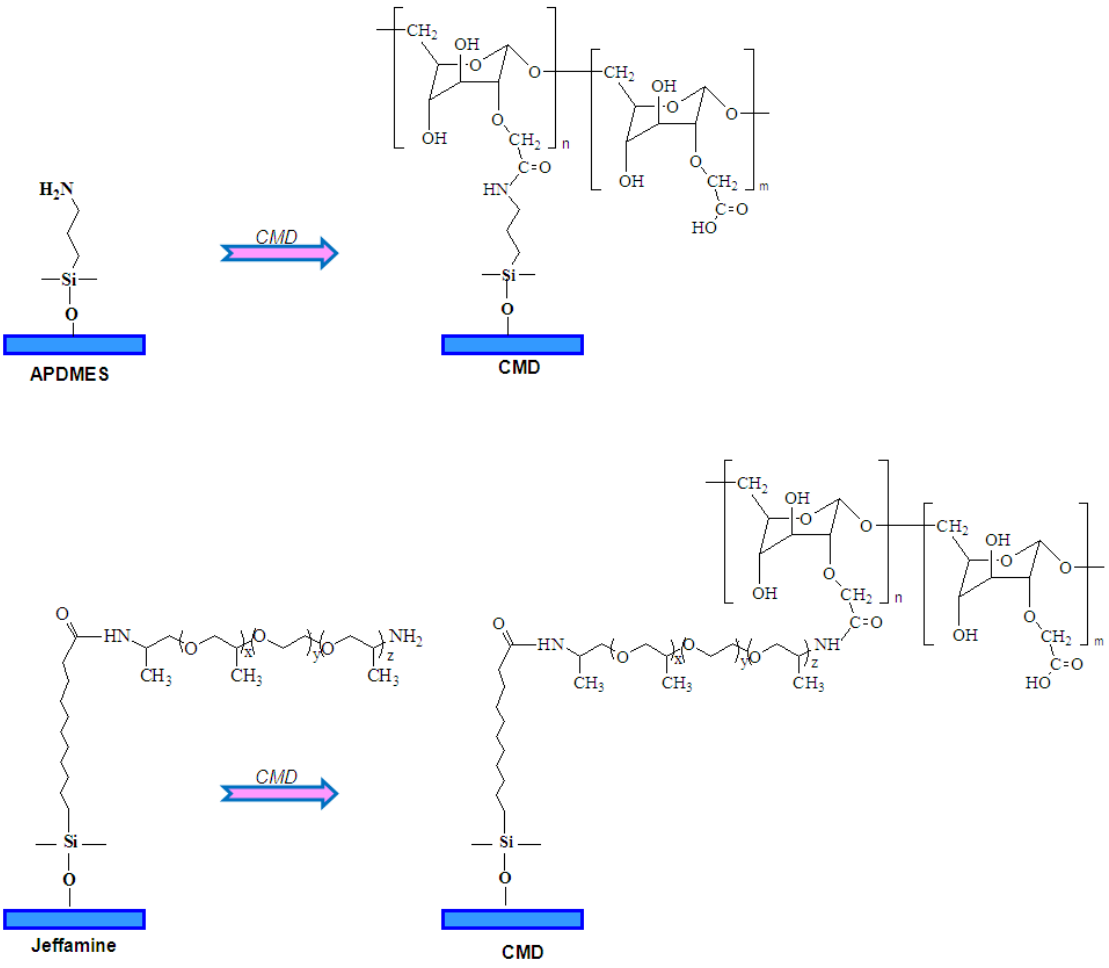

Figure 2-8 Schematic illustration of functionalization with CMD on two aminated surfaces (APDMES and Jeffamine)

2.2.4.5. Grafting of MAMVE copolymer on aminated surfaces

As previously described for CMD, the same deprotonated Jeffamine and APDMES surfaces were grafted with MAMVE copolymer. The incubation was allowed at room temperature for 4hrs with MAMVE (1 mg/ml, Mw=216 000 g/mol, unless specifically stated) solubilized in anhydrous DMSO to obtain MAMVE surface (Figure 2-). Slides were washed with THF and dichloromethane for 10 min each in ultrasonic bath. For preliminarily MAMVE grafting from Jeffamine, MAMVE concentration was set at 5 mg/ml.

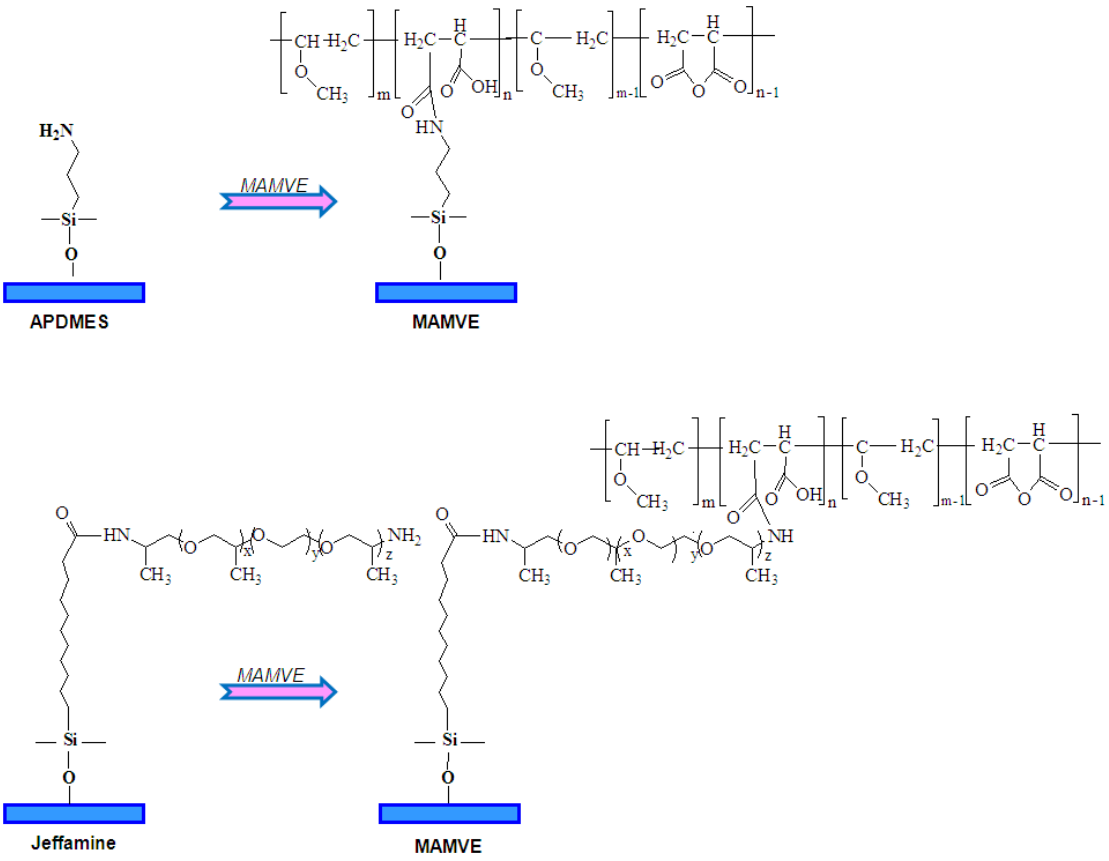

Figure 2-9 Schematic illustration of functionalization with MAMVE on two aminated surfaces (APDMES and Jeffamine)

It should be noticed that in the following text of the thesis, CMD and MAMVE surface were all grafted in 1 mg/ml solution from APDMES surface, unless specifically stated.

2.2.5. Characterization of CMD and functionalized surfaces

2.2.5.1. Nuclear magnetic resonance (NMR) of CMD

NMR analysis were performed at Institut de Chimie et Biochimie Moleculaire et Supramoleculaire (UMR-CNRS 5246, Université Lyon 1) with the kindly help of Dr. S. Vidal. The CMD samples were analyzed on a Bruker DRX 400 spectrometer equipped with a BBFO+ probe head. Chemical shifts are expressed in ppm with reference to water as an internal standard for proton spectra and to an integrated reference provided by Brucker software for carbon spectra. Non-exchangeable proton and carbon assignments of CMD were obtained from 1D (^{1}H, ^{13}C and DEPT) and 2D experiments (COSYDQF, 1H-13C HMQC) using the conventional pulse program provided by Bruker. ^{1}H NMR (300 MHz) and ^{13}C spectra (400 MHz) were recorded at 25 °C, and the parameters were as follows: pulse angle 30°; 1 s and 2s relaxation delay and 0.125898 Hz/ point and 0.366798 Hz/ point digital resolution for proton and carbon respectively. The degree of substitution (*DS*) of CMD can be determined with the following equation:

$$DS = \frac{I_2}{I_1 + I_2} \tag{2-1}$$

Where I_1 is the intensity of the peak at around 4.99 ppm, relative to the hydrogen of carbon in the dextran unit; I_2 is the intensity of the peak at around 5.19 ppm, relative to the chemical shift due to substitution with carboxymethyl group.

2.2.5.2. Acidimetric titration of CMD

The carboxylic acid content (*C*) of CMD was determined by acidimetric titration in a 1:1 water/acetone mixture as previously reported [14] and used in the following formula:

$$DS = 0.162\ C / (1 - 0.08\ C) \tag{2-2}$$

Where *DS* is the degree of substitution for CMD; *C* is carboxylic acid content; 0.162 (kg/mol) is the molecular mass of each unit of CMD; 0.08 (kg/mol) is the molecular mass difference between –CH_2COONa and -H.

In brief, about 0.05 g CMD was weighed and dissolve in 40ml DI- water/acetone mixture (1/1, v/v). 0.01M nitric acid solution (HNO_3) was added into the solution to reduce pH value up to 2. Then 0.1 M sodium hydroxide solution (NaOH) was added under stirring at room temperature until pH value of solution reached 13 (pH meter, Metrohm). Each sample

of CMD was titrated for three times to determine the mean value of DS and standard deviation (SD).

2.2.5.3. ATR-FTIR

The attenuated total reflectance Fourier transform infrared (ATR-FTIR) transmission spectra of CMD and dextran (grinded into powders) were recorded on ATR-FTIR spectrometers (Series 1600, Perkin-Elmer, 761 Main Ave., Norwalk, CT 06859) equipped with a SourceIR Technologies (15 Great Pasture Rd. Danbury, CT 06810) DuraScope single reflection diamond ATR. Results were obtained from averages of 64 scans at a resolution of 1 cm^{-1}.

Alternatively, silicon wafer functionalized with the various surface chemistries were analyzed under nitrogen purging using a Thermo Nicolet 6700 spectrometer with MCT detector (Electron Corporation, USA). All spectra were baseline corrected and area normalized. Results were obtained from averages of 256 scans at a resolution of 4 cm^{-1}.

2.2.5.4. X-ray Photoelectron Spectroscopy (XPS)

The XPS analysis was performed using an imaging Kratos Axis Ultra (UK) X-ray photoelectron spectrometer equipped with a conventional hemispherical analyser. A monochromatized Al Kα (1486.6 eV) operating at 150 W was employed at 150 W. Spectrum acquisition were performed under ultrahigh vacuum conditions (UHV, 10^{-9} Torr). Sample analysis area were 0.21 mm^2 and take off was 90° relative to the substrate surface. The pass energies were 80 and 20 eV for wide-scan and high-resolution elemental scans, respectively. Charge compensation was performed with low-energy electrons (0.1 eV). C main was adjusted to 285 eV. The data reduction (atomic concentration, shift, curve fitting, etc.) was performed with CasaXPS Version 2.3.14 software.

The operating software (Vision2) corrects for the transmission function. The relative sensitivity factors (RSF) were 0.278, 0.477, 0.780 and 0.339 for C 1s, N 1s, O 1s and Si 2p respectively.

Component peak positions were based on the results by Alexander et al. [15] who reported the binding energies of $Si(-O)_1$, $Si(-O)_2$, $Si(-O)_3$, and $Si(-O)_4$ to be around 101.5, 102.1, 102.8, and 103.4 eV, respectively. Full widths at half-maximum (FWHM) for each component peaks were constrained to be equal for all samples. The default relative sensitivity factor (RSF) values were used for determining the atomic concentrations (%AC) of the surface composition.

2.2.5.5. Evaluation of amine density

The grafting density of amino groups on the surface was determined using the Coomassie Blue method developed by Coussot et al. [16, 17].

Solution S1 was prepared by mixing 100 ml methanol (MeOH), 50 ml glacial acetic acid (CH_3COOH) and 850 ml DI water. CBB solution (S2) was prepared by dissolving 50 mg of CBB in 50 mL of MeOH and 25 mL of CH_3COOH under ultrasonic bath. Then, after complete dissolution, DI water was added to a final volume of 500 mL. The final composition was 0.05 mg/ml CBB in mixed solution of 10% (v/v) MeOH, 5% (v/v) CH_3COOH and 85% (v/v) H_2O. The detection solution (S3) was prepared by mixing 50 mL of 1 M ammonia buffer with 50 mL of MeOH.

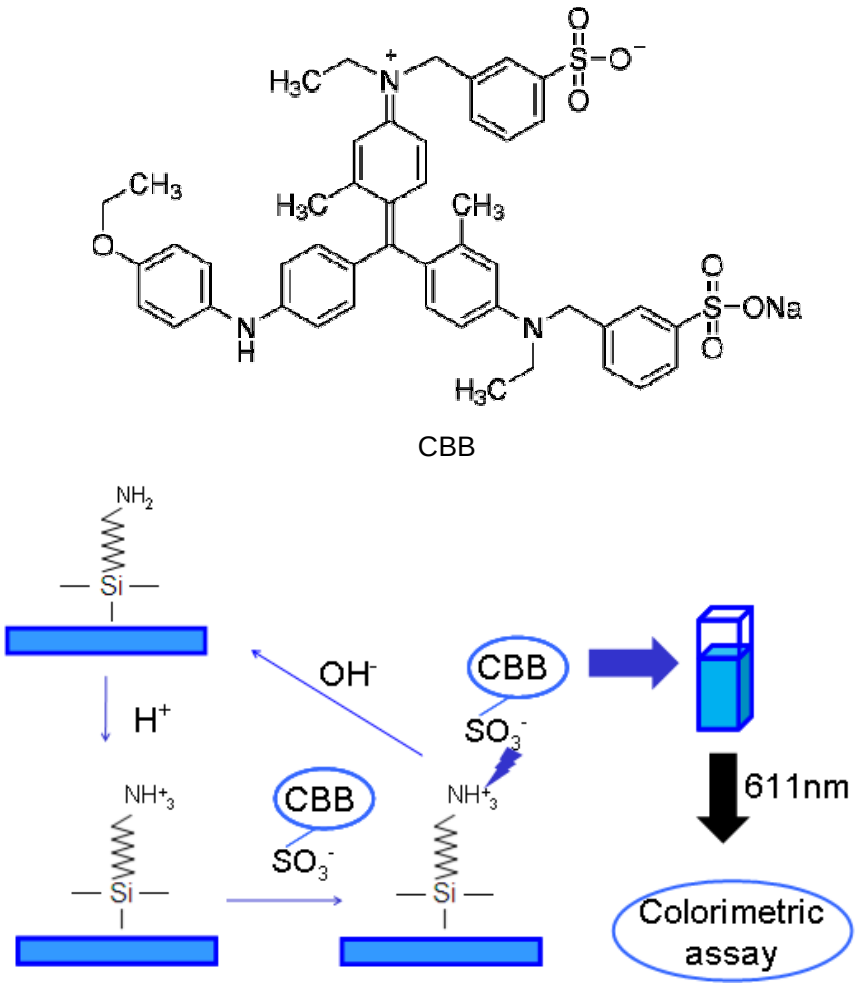

Figure 2-1 Structure of CBB and schematic illustration of the procedure for evaluation of amino density on aminated surface

Amino surfaces were protonated in solution S1 for 10 min, followed by immersion in solution S2 for 15 min for coloration of the surface, then washed with solution S1 for 3 x 10

min and DI water for 1 x 10 min under stirring. After drying by centrifugation, slides were transferred into solution S3 for 5 min under stirring for de-coloration, and this solution was collected for absorption measurement at 611 nm. The amine density of the sample was quantified by the amount of CBB released in solution S3. Each surface was tested at least for four times, and negative control was freshly piranhized glass slide. The concentration of CBB is given by the following equation:

$$A = \varepsilon c L \quad (2\text{-}3)$$

Where A: adsorption intensity; ε: 87893 L/mol cm at 611 nm; c: concentration of solution; L: width of the cuvette (1 cm). The illustration of the protocol was present in Figure 2-1.

2.2.5.6. Contact angle measurement

All chemically functionalized glass slides were characterized for surface energy by contact angle measurements (Digidrop Goniometer, GBX, France). De-ionized water, Ethylene-glycol and Diiodomethane were used in all measurements. To minimize the experimental error, the contact angle was measured at five random locations for each sample and the average value was reported. The surface tensions were determined according to Owens-Wendt model as mentioned in Chapter 1.

2.3. Results and discussion

2.3.1. Characterization of synthesized CMD

As reported in the literature [14], the degree of substitution (DS) in carboxymethyl groups of dextran is highly dependent on the concentration of each reactant, composition of reaction medium, time and temperature of reaction. Optimal conditions were obtained in 85% isopropanol / 15% water (v/v) mixture with 3.8 M NaOH, for 90 min at 60°C. Moreover, DS of CMD also depends on the molar ratio between hydroxide ions (OH^-) and hydroxyl group of dextran ($-OH_{dex}$), and on the molar ratio between bromoacetic acid (BAA) and $-OH_{dex}$. Taking into account these parameters, we synthesized four CMD from two different dextrans (T10 and T40) in optimal reaction conditions, by varying the different molar ratios described above. The conditions chosen are listed in Table 2-1. The molar ratio of $OH^-/-OH_{dex}$ was always set at 1.5 in order to activate enough hydroxyl groups of dextran to optimize substitution with carboxymethyl groups.

Table 2-1 Experimental conditions tested for the synthesis of various CMD (from dextran T10 and T40) at different DS determined from NMR (DS/N) and acidic titration (DS/T).

No.	Dex	W (g)	$-OH_{dex}$ (mmol)	NaOH (M)	OH^- (mmol)	$OH^-/-OH_{dex}$	BAA (g)	BAA (mmol)	BAA/$-OH_{dex}$	DS/T (%)	DS/N (%)
1	T40	2	37.5	3.8	57	1.5	2	14.4	0.4	28±4	28
2	T40	2	37.5	3.8	57	1.5	5	36	1.0	65±2	63
3	T10	2	37.5	3.8	57	1.5	2	14.4	0.4	32±1	30
4	T10	2	37.5	3.8	57	1.5	5	36	1.0	48±3	45

FTIR spectroscopy has been shown to be a useful tool in monitoring structural changes in dextran derivatives and the infrared characteristics of dextran and CMD are well reported [18, 19]. Carboxymethylation of dextran introduces into the polymer carboxylate anions which dominate the IR spectra at about 1600 and 1421 cm^{-1}. The peak at about 1600 cm^{-1} belongs to carboxylic carbonyl (C=O) stretching of CMD, and the peak at round 1421 cm^{-1} corresponds to vibration of stretching COO^- [19, 20]. Figure 2-2 presents ATR-FTIR spectra of dextran T10 and T40 as well as their carboxylmethylated derivatives. For all CMD spectra, stretching of carbonyl (C=O) is observed at around 1595-1597 cm^{-1} and vibration of COO^- is clearly present at 1421 cm^{-1}. These two specific bands are not observed on dextran T10 and T40 spectra. Thus, we can conclude that the substitution of dextran T10 and T40 with carboxymethyl groups was successful. Moreover, we can observed that the signal intensity of the band at 1600 cm^{-1} of CMD-T40 with DS=63% is higher than that of CMD-T40 with DS=27%. This data indicates that the degree of substitution in carboxymethyl groups can be reflected by infra-red spectroscopy. However, this characterization is not quantitative. Thus, we performed ^{1}H-NMR analysis to determine DS of synthesized CMD and ^{13}C-NMR analysis to determine the position of the substituted carboxymethyl group on the glucose residue.

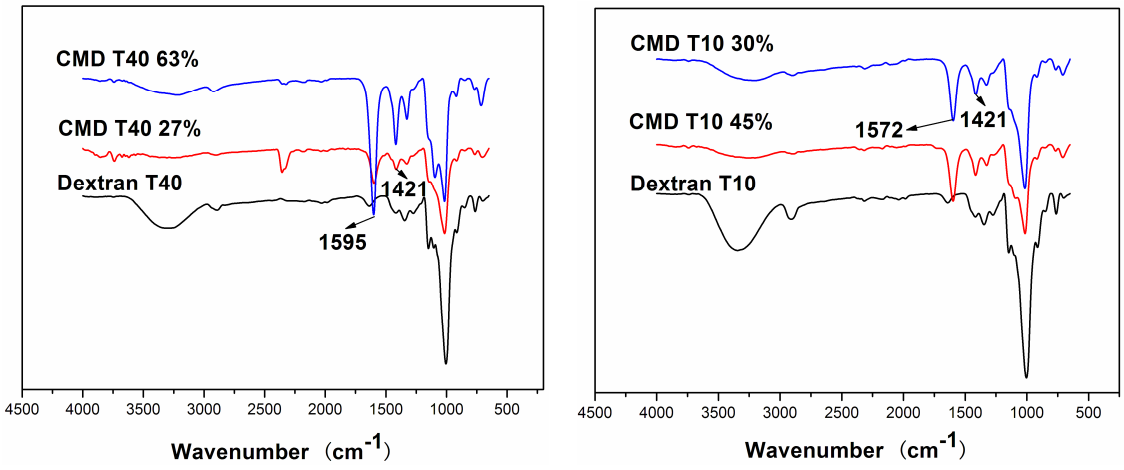

Figure 2-2 ATR-FTIR spectra of (a) dextran T40 and derived CMD at various DS; (b) dextran T10 and derived CMD at various DS.

As an example, the NMR spectrum (^{1}H and ^{13}C) of CMD-T40 with DS = 27% was presented in Figure 2-3. The ^{1}H NMR spectrum shows that the chemical shift observed at 5.19 ppm is associated to the anomeric carbon of the carboxymethylated glucose residue, the one at 4.99 ppm corresponding to the anomeric carbon of unsubstituted residues. The peak at (4.1– 4.3 ppm) results from the methylene of carboxymethyl in the CMD [20]. The peaks between 3.4 ppm and 4.1 ppm were assigned to proton on the polysaccharide backbone. As shown in the ^{13}C NMR spectrum (Figure 2-3 B), the chemical shift observed at 80.1 from 72.8 ppm, was assigned to the substitution of carboxymethyl on C2 on the polysaccharide backbone. It was noticed that the peaks observed at 3.35 ppm on ^{1}H curve and 49.3 ppm on ^{13}C spectrum, were relative to methanol introduced during the washing process of the products.

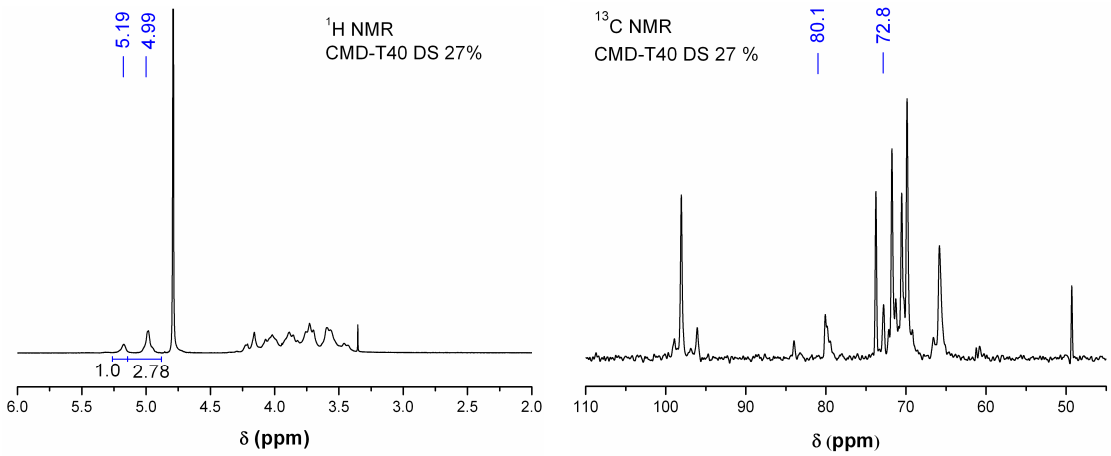

Figure 2-3 ^{1}H and ^{13}C NMR spectrum of CMD-T40 with DS= 27%.

^{1}H-NMR analysis allowed to quantify the substitution rate of the CMD by measuring the ratio of the area under the 5.19 ppm peak over the areas under both the 4.99 ppm peak and the 5.19 ppm peak (Eq.2-1), and the results are reported in Table 2-1. The molar ratio between BAA and $-OH_{dex}$ ($BAA/-OH_{dex}$) indicates the theoretical substitution rate of dextran considering the reaction is complete. For $BAA/-OH_{dex}$=0.4 (samples N°1 and 3), 28% and 30% of carboxymethyl groups were substituted on dextran T40 and T10, respectively, instead of 40%. For $BAA/-OH_{dex}$=1.0 (samples N°2 and 4), 63% and 45% substitution rate were obtained on dextran T40 and T10, respectively, instead of theoretically expected 100%. These results show that the yield of the dextran carboxymethylation reaction is not complete. Furthermore, the molecular weight of dextran seems to influence the efficiency of the reaction in defined range. Below 50% DS, there is no influence of dextran molecular weight on the

yield of the reaction. Indeed, both dextran (T10 and T40) display the same DS (about 30%) which is close to the theoretical one (40%). However, above 50% DS, the higher is the molecular weight of dextran, the lower is the reaction yield. For dextran T10 (100 000-200 000 g/mol) the reaction yield is about 45% whereas it turns to be about 63% for dextran T40 (40 000 g/mol). Therefore, different DS of carboxymethylation of dextran can be obtain by designing the parameters such as the molecular weight of the dextran, the molar ratios BAA/-OH_{dex} and OH^-/-OH_{dex}, under optimal reaction media. These results are in agreement with the report of Huynh and co-workers [14].

Additionally, the substitution rate of CMD was determined by acidimetric titration in order to quickly check the DS in hand after the sample was synthesized. Figure 2-4 presents a typical acidimetric titration curve from CMD sample. Volume V_1 is related to the excess of HNO_3 introduced in the solution.

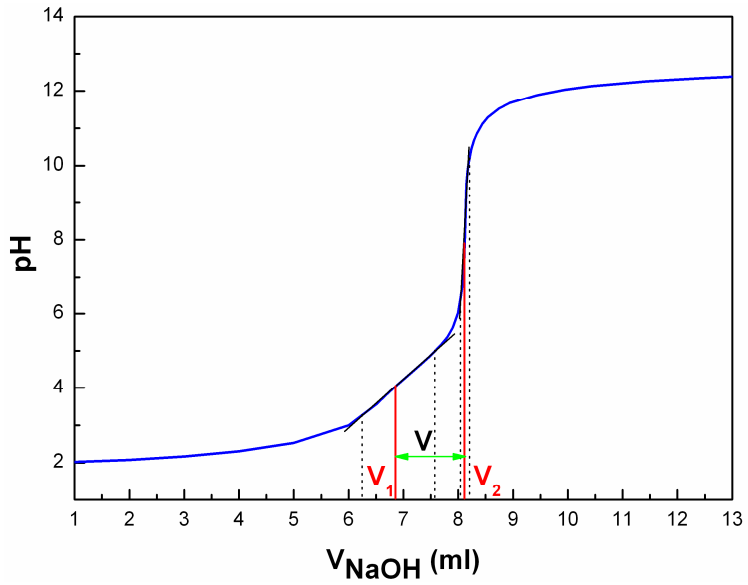

Figure 2-4 Acidimetric titration curve of CMD sample, V_1 is the volume of NaOH to neutralize excess of HNO_3, V_2 is the volume of NaOH to neutralize HNO_3 and CMD, V is the difference between V_2 and V_1 corresponding to the volume of NaOH to neutralize CMD.

The difference between V_2 and V_1 ($V=V_2-V_1$) corresponds to the titration of the carboxylic acid groups of CMD.

As shown in Table 2-1, the degree of substitution of CMD-T10 and CMD-T40 evaluated from acidimetric titration (DS/T) is similar to the one (DS/N) from NMR analysis. Thus, acidimetric titration can be used as a simple and convenient method to determine the degree of substitution for synthesized CMD.

2.3.2. Characterization of APDMES surface and its derivatives

Organosilanes are widely used and often serve as the foundation layer in the fields of biosensors and biochip technology. Our group possesses a well-known expertise in organosilane chemistry for the functionalization of silicon surface and glass slides [12, 13]. One of the basal silane layer developed in this thesis was made of the aminosilane APDMES which introduced $-NH_2$ groups on the functionalized surface.

Firstly, the effect of APDMES concentration introduced in the reaction medium on the grafting density was investigated. The quantitative detection for amine density was performed with the Coomassie Brillant Blue method as described in references [16, 17, 21]. This method has been proved to be a simple and powerful method for the exact estimation of available N^+ groups on surfaces of polymeric and silica-based materials.

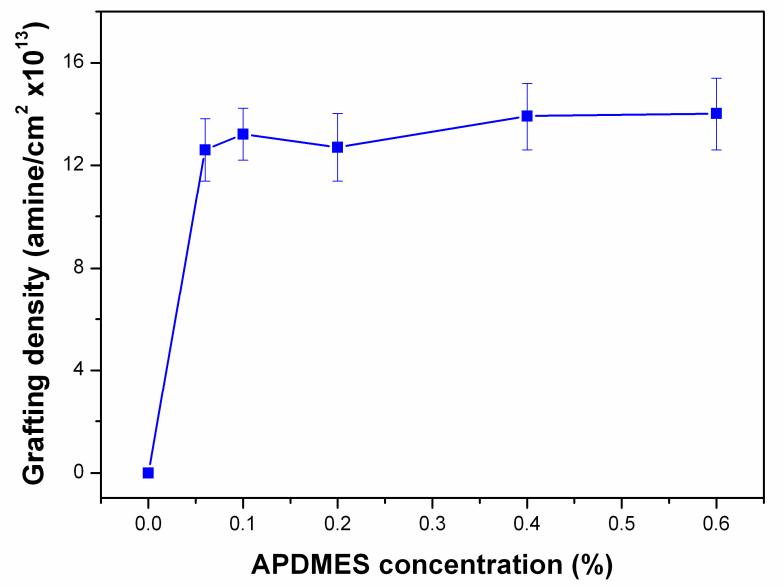

Figure 2-5 The effects of APDMES concentration (v/v, in pentane) on grafting density of glass slide.

As shown in Figure 2-5, the amino density on the glass slide surface remains around $1.3x10^{14}$ amino groups/cm^2 and does not depend on the concentration of APDMES introduced in the reaction mixture, in the tested range (APDMES from 0.05 to 0.6% v/v in pentane). This result is in agreement with the study of Oh et al. [22] where amine density was determined by a UV-vis spectrometry method described in [23] to be around 10^{14} amino groups/cm^2 for APDMES layer grafted on glass slides. In another study [24], covalently bonded monolayers of three aminosilanes were deposited on dehydrated silicon surface by chemical vapour deposition and the same films were obtained with either a large or a small volume of any of

the three aminosilanes. The constant amine density obtained on the surface of silicon or glass slides can be achieved due to the constant amount of active silanol groups. Indeed, in a previous work [8], it was demonstrated that substitution of silicon with monofunctional carboxysilane led to grafting density of about $8.4x10^{13}$ molecules/cm^2 (1.4 µM /m^2). It was suggested that the density of monofunctional silane grafting on silica/glass slide remains constantly at around $1.3x10^{14}$ amino groups/cm^2, which was independent on the silane concentration in the measured range. Complete reaction was achieved with 0.05% (v/v) APDMES in pentane. This result is important for the implementation of industrial production of APDMES functionalized surfaces. Indeed, the lack of dependence of surface grafting involves that a small change in organosilane volume (an important process variable) should have no effect on the amine density.

2.3.2.1. XPS characterization

The surface composition of APDMES layer coating polish silicon wafer was characterized by XPS analysis. Figure 2-6 shows the high-resolution XPS spectra of Si 2p and N 1s of piranha cleaned silica surface and monofunctional silane APDMES modified silica. The presence of nitrogen on silanized surface confirmed that APDMES was successfully introduced with our protocol. Besides, two fit peaks were present on the high-resolution N 1s spectra (Figure 2-6 B2) revealed two contributions, which were associated with to NH_2-C (around 400 eV) and NH^+_3-C (around 401.6 eV) [25], respectively. The presence of the mono-functional silane on APDMES surface is further sustained by the peak at 101.6 eV on the Si 2p peak corresponding to $Si(O-)_1$.

Alexander and co-workers [15] demonstrate that the Si 2p component peaks in Si $(-O)_x$ films can be resolved and quantitative peak fitting can be performed based on two assumptions: (1) each Si atom has a valence of four, resulting in four component peaks within the Si 2p envelope and (2) the shift of the Si binding energies depends primarily on the number of oxygen atoms attached to the Si. The four component peaks of the Si 2p envelope are referred to as $Si(-O)_1$, $Si(-O)_2$, $Si(-O)_3$, and $Si(-O)_4$, where the oxygen subscript indicates how many oxygen atoms are attached to the Si atom. This deconvolution is widely used to characterize Si(-O)x containing films on solid surfaces [26, 27].

The covalent attachment of monofunctional silane to SiO_2 resulted in the formation of a single siloxane bridge between the monovalent silane and the silanol groups of the surface. The silicon atom of the silane was then involved in only one bound with an oxygen atom and three bounds with carbon atoms. This silicon atom can be distinguished from the silicon atoms of the underlying silica involved in four bonds with oxygen atoms. As shown in Figure 2-6 A, for the piranha cleaned surface, only one component corresponding to $Si(-O)_4$ is

observed. In Figure 2-6 B1, C and D, however, curves fitting of APDMES grafted silica, CMD and MAMVE grafted amino surface, respectively, demonstrated the presence of the same contribution at 103.6 eV and an additional contribution at 101.6 eV. According to the method of Alexander et al. [15] , this new contribution was assigned to the Si $(-O)_1$ component peak, which was indicative of the $Si(-O)_1$ of APDMES bonded to the silica surface. This is further sustained by the fact that the ratio of the $Si(-O)_1$ over the area of the N 1s after correction by the RSF is close to 1 as expected from the molecule structure (one $Si(-O)_1$ for one N) (**Erreur ! Source du renvoi introuvable.**). Furthermore, this result indicates that the aminosilane layer is stable during the following polymer grafting.

Table 2-2 Atomic concentration obtained from XPS analysis of APDMES, CMD and MAMVE surfaces. Si $(-O)_1$: relative contribution in the Si 2p; N/Si $(-O)_1$: ratio between nitrogen and silicon atomic concentrations.

Surfaces	Atomic concentration (AC%)				Si $(-O)_1$ (%)	N/Si $(-O)_1$
	C	Si	N	O		
APDMES	14.6	27.7	1.24	56.4	4.9	1.0
CMD T40	24.6	24.5	1.22	49.7	2.9	1.1
MAMVE 216	25.2	22.9	0.88	51.0	6.3	1.4

The APDMES surface was cross-linked with CMD T40 (DS 63%) or MAMVE 216 polymers. The table 2 presents the respective atomic concentrations (AC %) of C, Si, N, O as well as the relative contribution of $Si(-O)_1$ in the Si 2p and the nitrogen to silicon ratio ($N/Si(-O)_1$) for APDMES, CMD and MAMVE modified surfaces. The relative contribution (%) of $Si(-O)_1$ was calculated as the contribution of the $Si(-O)_1$ determined by curve fitting over the total area of the Si 2p ($Si(-O)_1$ and $Si(-O)_4$). As mentioned above, $Si(-O)_1$ signal originated only from the silane molecule while the $Si(-O)_4$ originated from the underlying silica. Therefore, this ratio is independent on subsequent surface layers as far as they do not contain silicon. On the contrary, due to the mean inelastic free path of electrons (constant probing depth), increased surface coverage results in decreased signal originating from the substrate and therefore the decrease of Si 2p atomic percentage. A higher Si 2p atomic percentage was observed on APDMES surface (27.7 %) compared to CMD (24.5 %) and MAMVE (22.9%) surfaces. These results suggest that the thickness of MAMVE grafted on the APDMES surface is slightly higher than that of CMD. Moreover, upon reaction of APDMES surface with either CMD or MAMVE, the C 1s AC % increased from 14.6% to 24.6 % and 25.2 %, respectively, whereas the Si 2p AC % decreased as expected. Indeed, CMD and MAMVE polymers contain numerous carbons on their backbone and lateral functions. However, the atomic concentration of $Si(-O)_1$ from APDMES and its derived polymer surface stays at the same range (around 4.2 %).

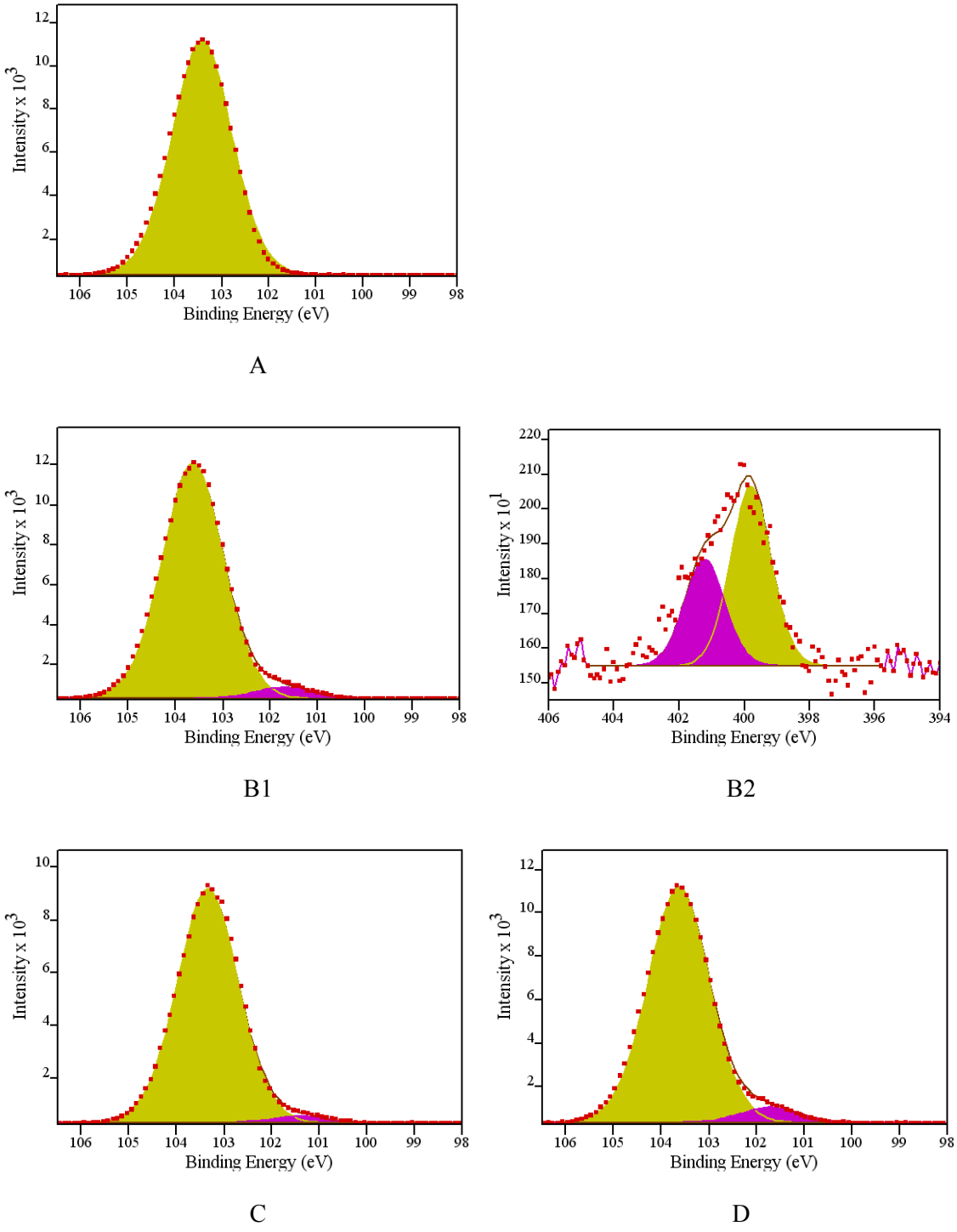

Figure 2-6 High-resolution XPS spectra of piranha cleaned silica surface (A: Si 2p spectrum), and APDMES silanized silica surface (B1: Si 2p spectrum; B2: N 1s spectrum), C: Si 2p spectrum of CMD, D: Si 2p spectrum of MAMVE

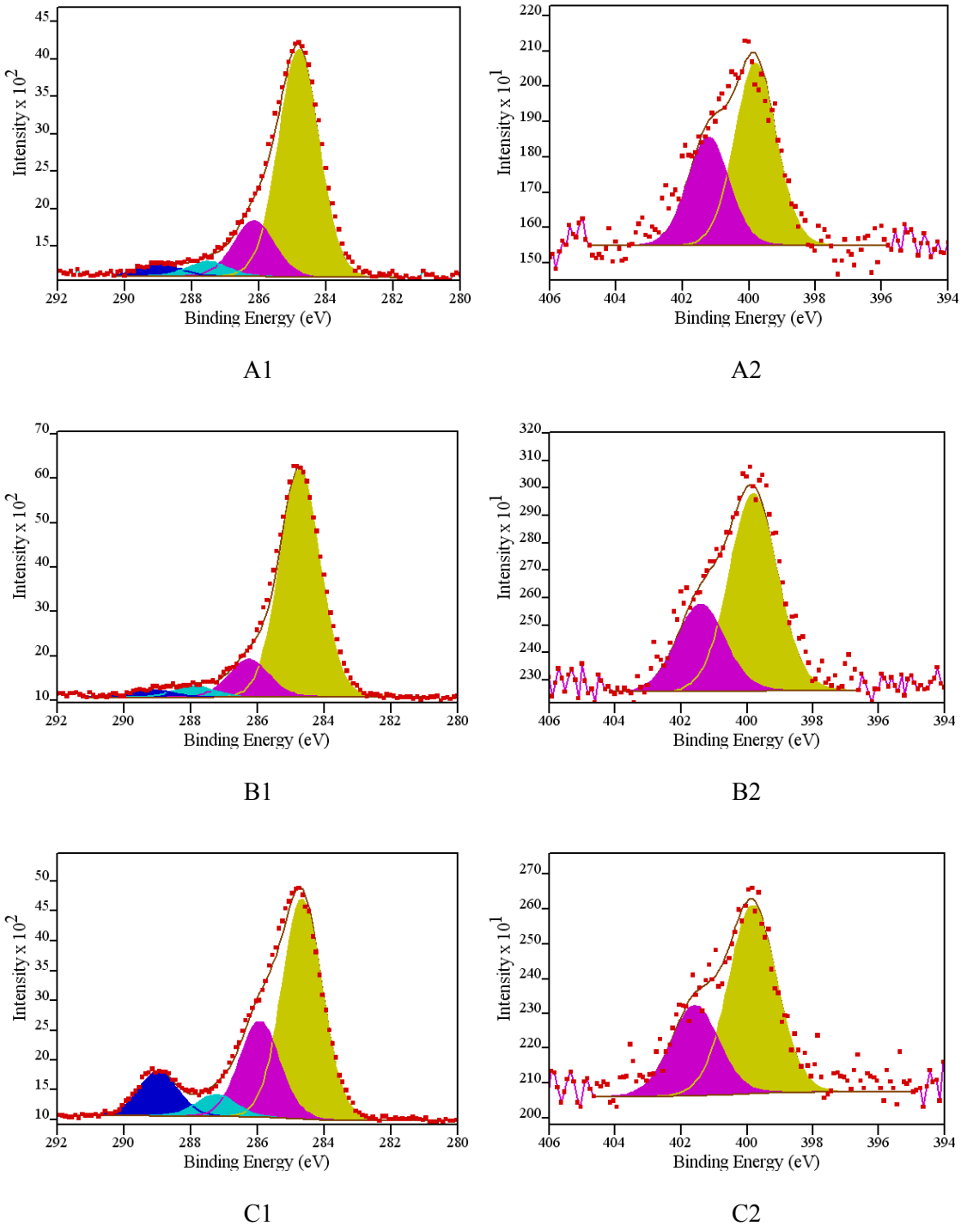

Figure 2-7 High-resolution XPS spectra of APDMES, CMD and MAMVE surfaces; A1, B1 and C1 are relative to C 1s spectra, respectively; A2, B2, C2 are relative to N 1s spectra, respectively.

Figure 2-7 presents the spectra of C 1s and N 1s from APDMES, CMD and MAMVE surfaces. The four peaks corresponded to C-C, C-H at around 284.7 eV, C-O, C-N at around 286.1 eV, C=O, O-C-O at around 287.5 eV and N-C=O, O-C=O at around 289 eV were observed on all surfaces [28, 29]. The atomic concentrations respective to each contribution

were presented in Table 2-3. The presence of the two peaks relative to C=O/O-C-O and N-C=O/O-C=O in APDMES spectra could be attributed to experimental contamination from air. The contribution at 286.1 eV was assigned to the amine group of APDMES. Because the contribution at around 289 eV in C 1s spectra of APMDES and CMD (Figure 2-7 A1 and B1) gave similar AC%, it was not possible to conclude about the covalent grafting of CMD on APDMES surface based on C 1s results. However, on N 1s spectra of CMD and MAMVE, two peaks are observed at 400 eV and around 401.6 eV (Figure 2-7 B2 and C2); these two contributions were probably assigned to either NH_2-C, N-C=O or NH_2-C, $^{+}H_3N$-C, respectively. Due to the reaction occurred in an aprotic tetrahydrofuran, solvent, the most probable contribution at 399.7 eV corresponds to NH_2-C and the contribution at 401.7 eV to a nitrogen involved in an amide bond. This result suggests that CMD and MAMVE are covalently linked to the aminosilane. Moreover, the atomic concentration of O-C=O at 288.9 eV was remarkably increased on MAMVE surface (11.6%) compared to APMDES (3.7%) indicating the presence of an amide bond. Indeed, MAMVE copolymer is composed of maleic anhydride moiety which is very reactive towards amine function leading to the formation of an amide bond.

Table 2-3 Atomic concentration (AC %) derived from XPS analysis for different C 1s and N 1s contribution appearing at each binding energy (BE) on APDMES, CMD and MAMVE surfaces

Surfaces	C-C C-H		C-O C-N		C=O O-C-O		N-C=O O-C=O		NH_2-C		N-C=O $^{+}H^3N$-C	
	BE (eV)	AC %	BE (eV)	AC %	BE (eV)	AC %	BE (eV)	AC %	BE (eV)	AC %	BE (eV)	AC %
APDMES	284.7	74.2	286.1	17.6	287.5	4.5	288.9	3.7	400	67.1	401.5	32.9
CMD	284.7	80.2	286.2	13.2	287.9	4.0	289.1	2.6	400	70.2	401.4	29.8
MAMVE	284.7	57.5	285.9	25.2	287.2	5.7	288.9	11.6	399.9	67.7	401.7	32.3

From the results of XPS analysis, it can be concluded that firstly the mono-functional aminosilane APDMES was successfully introduced onto silica and secondly CMD and MAMVE polymers were covalently grafted to the aminosilane. Thirdly, MAMVE layer is thicker than CMD layer. Our results are in agreement with an early study where water-soluble carbodiimide chemistry was used to covalently grafted CMD onto an aminated surface. XPS analysis indicated that CMD coating was much thinner than the analysis depth [30].

2.3.2.2. ATR-FTIR characterization

Surface analysis by ATR-FTIR was initially performed on functionalized silica substrate. However, this substrate contains a 90 nm depth layer of SiO_2 leading to very high signal in ATR-FTIR. It was impossible to significantly distinguish specific signals from the modified surface chemistry. Thus, we changed the substrate to silicon for IR analysis.

Silicon was functionalized with APDMES, CMD and MAMVE, in the same experimental conditions as silica. ATR-FTIR spectra of piranha cleaned silicon, APDMES, CMD and MAMVE surfaces were presented in Figure 2-8. The peak at around 1260 cm^{-1}, which was attributed to the Si-CH3 bend [31], found on all surfaces except piranha cleaned silicon, confirmed the effective silanization of silicon. Moreover there are some tiny peaks between 3300 cm^{-1} and 3500 cm^{-1}, corresponding to stretching of N-H on APMDES surface.

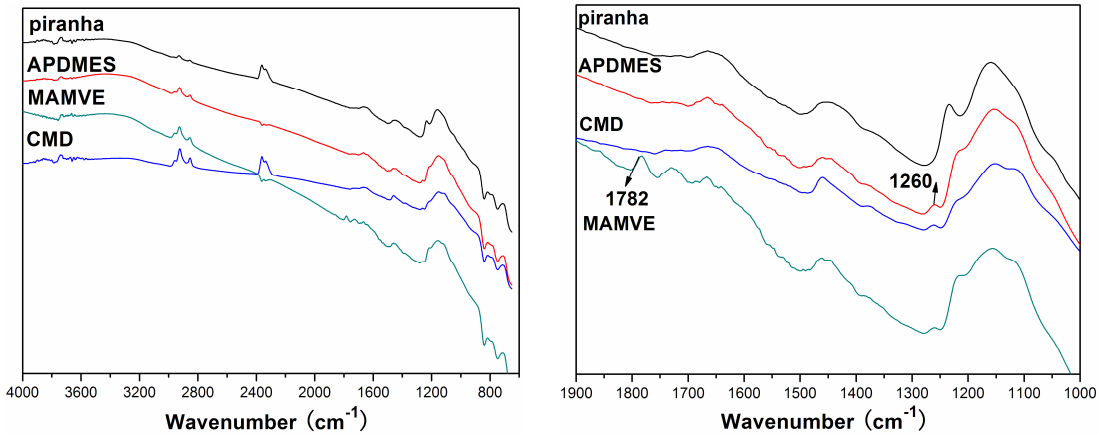

Figure 2-8 ATR-FIIR spectra of piranha cleaned silicon, APDMES, CMD and MAMVE modified silicon, (A) the full range of wavenumber and (B) zoom between 1900 and 1000 cm^{-1}.

On MAMVE surface, the peak at 1782 cm^{-1} was assigned to the anhydride group (O=C-O-C=O) or amide bond (N-C=O) [32]. The presence of this peak indicates that MAMVE copolymer was grafted on the APMDES surface. However, on CMD surface the expected bands at around 1600 cm^{-1} relative to stretching of carbonyl group (C=O) and at 1377 cm^{-1} assigned to the stretching of O-H on the polysaccharide [20] were not detected. As discussed in the XPS analysis, CMD layer is thinner than MAMVE layer. Thus, the presence of grafted CMD on APDMES surface can't be detected by ATR-FTIR analysis which is not sensitive enough.

To achieve further analysis of these polymer layers, CMD and MAMVE surface were also characterized by the previously proposed CBB method to evaluate the rest amino amount after grafting with polymer. The results show that the amino group density of CMD at 3.66 x

10^{13} amino group/cm^2 and MAMVE at 3.49 x 10^{13} amino group/cm^2 indicating that both of polymer layers were successfully introduced on APMDES surface leading to around a 75 % reduction of amino grafting density compared to APDMES surfaces.

2.3.2.3. Surface tension characterization

The piranha cleaned, APDMES, CMD and MAMVE surfaces were characterized by contact angle measurements to evaluate surface tension. The surface energies, viz., the total energy (E_T), the dispersive energy (E_D) and the polar energy (E_P) are calculated from the wetting angle (θ) accordingly to the Owens–Wendt equations.

Table 2-4 reports the wetting properties of APDMES surfaces obtained with various APDMES initial concentrations (volume %) as well as piranha cleaned glass slides. After APDMES silanization, both the polar and dispersive tension of the piranha cleaned surface decreased remarkably. However, the surface tension was constant whatever the APDMES concentration introduced in the reaction medium, which is in agreement with the amine surface density determined by the CBB method. This result demonstrated that APDMES functionalization of glass slide is reproducible and homogeneous.

Table 2-4 Wetting property of glass slides functionalized with different concentration of APDMES (V%) as well as piranha cleaned surface obtained from Owens-Wendt two parameter model treatments from contact angle measurement. E_T, E_P and E_D is relative to the total, polar and dispersive energy, respectively.

APDMES (V%)	E_T (mJ/m^2)	E_P (mJ/m^2)	E_D (mJ/m^2)	Contact angle (θ /°)		
				Water	Ethylene-Glycol	Diiodo-methane
0.6	33.1	7.1	26.0	79.5±0.3	64.7±0.5	58.0±0.6
0.4	32.2	5.9	26.3	78.8±0.1	65.5±0.3	62.9±0.3
0.2	31.3	6.1	25.2	80.0±0.1	63.3±0.4	61.7±0.3
0.1	31.6	6.2	25.4	79.5±0.2	64.6±0.4	59.6±0.5
0.06	32.4	6.0	26.2	79.7±0.3	62.8±0.6	59.9±0.5
0	67.4	35.5	31.9	0	0	37.7±0.7

The aminosilanized surface obtained with 0.1% APDMES was further grafted with CMD of various Mw and DS (T10: Mw=100 000 g/mol, DS= 45%; T40: Mw=40 000 g/mol, DS=63%), or MAMVE with different Mw (MAMVE 67: Mw=67 000 g/mol; MAMVE 216: Mw=216 000 g/mol). The wetting properties of the corresponding CMD and MAMVE

surfaces are reported in Table 2-5. Besides, The surface tension of CMD T40 DS =63 % and MAMVE 216 grafted from Jeffamine were also included for comparison.

Table 2-5 Wetting properties of CMD and MAMVE surfaces, T40 (Mw=40 000 g/mol, DS=63%) and CMD T10 (Mw=100 000 g/mol, DS=45 %) were activated with EDC/NHS before grafting on APDMES surface. CMD T40, CMD T10, MAMVE 67 (Mw=67 000 g/mol) and MAMVE 216 (216 000 g/mol) were grafted on APDMES surface at 1 mg/mL.

Surfaces	E_T (mJ/m^2)	E_P (mJ/m^2)	E_D (mJ/m^2)	Contact angle (θ /°)		
				Water	Ethylene-Glycol	Diiodo-methane
CMDT40	35.7	7.2	28.5	75.7±0.2	55.3±0.6	55.4±0.6
CMDT10	35.5	8.8	26.2	73.1±0.3	56.9±0.5	57.6±0.5
MAMVE67	45.8	17.2	28.6	36.5±0.9	39.8±0.9	51.5±0.6
MAMVE216	48.7	19.5	29.2	32.2±0.9	38.6±0.9	49.3±0.7
CMD T40*	36.8	8.1	28.7	74.2±0.3	50.8±0.6	56.4±0.6
MAMVE216*	42.0	12.0	30.0	65.3±0.4	42.7±0.5	52.5±0.5

***CMD and MAMVE were grafted from Jeffamine surface also used in the preliminary antibody microarray elaboration.**

Grafting of polymers onto APDMES surface led to increase polar surface energy from 6.2 mJ/m² of APDMES surface to 8.8 mJ/m² of CMD T10 and to 19.5 mJ/m^2 of MAMVE 216 surface. Indeed, CMD and MAMVE are hydrophilic polymers due to their polysaccharide backbone and anhydride moiety, respectively. Besides, either for CMD or MAMVE surface, polar surface tension slightly increased with increasing molecular weight of polymers. This could be attributed to the increase of the amount of hydrophilic monomer unit in the polymer layer (glucose unit for CMD and maleic anhydride unit for MAMVE). However, the influence of CMD molecular weight on the wetting properties was less significant than that of MAMVE. Hadjizadeh et al [30] examined the effect of CMD molecular weight (Mw, 70 and 500 kDa) and CMD solution concentration (1 and 2 mg/mL) during the immobilization procedure on the CMD coating onto amine surface and the results of contact angle measurement shows surface chemical compositions of the four CMD coatings were similar. It is well-known that the more hydrophilic surface is the less non specific protein adsorption occurs. As a result, CMD T40 (DS 63 %) and MAMVE 216 were selected for grafting at a concentration of 1 mg/mL onto APDMES surface. Additionally, surface tension of CMD grafted from Jeffamine was similar with that grafted from APDMES, but MAMVE surface grafted from APDMES was a little more hydrophilic than that from Jeffamine due to the higher polar tension. Thus,

CMD and MAMVE surfaces were both grafted from APDMES for surface characterization and microarray elaboration unless stated.

2.3.3. Characterization of TDSUM surface and its derivatives

Both silica and glass slide as substrates functionalized with TDSUM silane were extensively characterized and employed for the elaboration of biochips in our group [11-13, 33-40]. It was shown that reproducible and homogenous carboxysilane monolayer was achieved. Moreover, activation of carboxylic group with NHS led to efficient covalent immobilization of biomolecules (such as DNA, proteins) onto the substrate. Herein, Jeffamine (diamine) and chitosan (aminated polymer) were grafted onto NHS-activated TDSUM surface. Surface characterization of TDSUM, Jeffamine and chitosan surfaces was performed by XPS analysis and contact angle measurements. Moreover, the amine coverage on Jeffamine and chitosan surfaces was quantitatively evaluated with the CBB method.

2.3.3.1. Evaluation of amine density by CBB method

Jeffamine and chitosan were grafted by reaction with NHS activated carboxylic groups from TDSUM modified surfaces. The reaction leads to the formation of an amide bond. Jeffamine is a diamine, which can either react with only one NHS ester group leading to an aminated surface or react with two adjacent NHS ester groups leading to the formation of "bridge" with no available amine. Chitosan is a polyaminated polymer. As previously described for APDMES surface, amine density was determined with the CBB method (Figure 2-9).

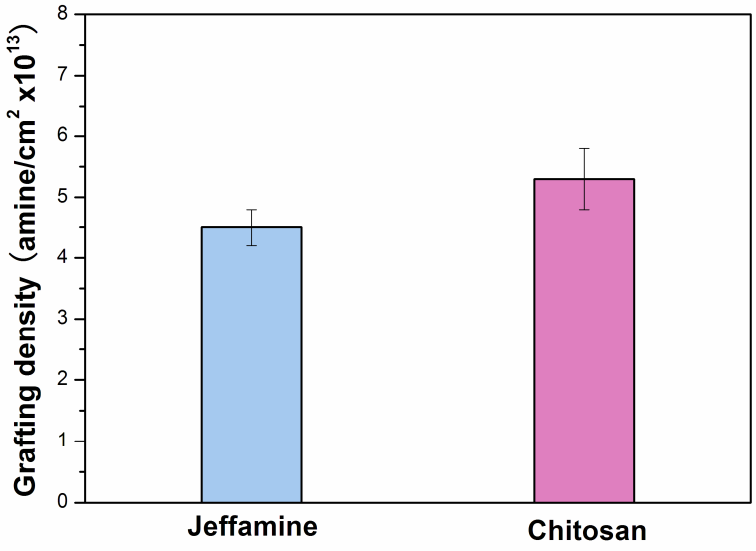

Figure 2-9 Amine density of functionalized glass slides with Jeffamine and chitosan

Results indicated that functionalization with these two polymers led to amine density about $4.5x10^{13}$ amino groups/cm^2. Surface density of NHS-activated carboxylic groups onto TDSUM surface was previously determined to be about $8.4x10^{13}$[8]. The chitosan used in this study was of high molecular weight (Mw = 470 000 g/mol) with high degree of deacetylation (94 %). These characteristics involved long-chain structure bearing large amount of amino groups. The low chitosan grafting observed suggests that low reaction yield, steric hindrance or electrostatic repulsion between chitosan molecules may occur leading to low amount of available amino groups on the surface. It is also possible that CBB could not reach all surface amino groups due to steric hindrance or diffusion limitations related to the long polymeric chains. Our results suggest that under our conditions, all amine groups of Jeffamine and chitosan have not reacted with NHS ester (and therefore remained available for proteins immobilization) and that most (probably not all) NHS ester reactive sites did react with amines. However, the amine density of chitosan modified surfaces was similar to the one observed on Jeffamine surfaces.

2.3.3.2. XPS analysis

Table 2-6 shows the respective atomic concentration (AC %) of C, Si, N, O as well as the relative contributions of $Si(-O)_1$ in the Si 2p for TDSUM, Jeffamine and chitosan modified surfaces. As mentioned above, the relative contribution (%) of $Si(-O)_1$ was calculated as the contribution of the $Si(-O)_1$ determined by curve fitting over the total area of the Si 2p ($Si(-O)_1$ and $Si(-O)_4$). Thus, $Si(-O)_1$ signal originated only from the silane molecule while the $Si(-O)_4$ originated from the underlying silica. Therefore, this ratio is independent on subsequent surface layers as far as they do not contain silicon.

Table 2-6 Atomic concentration calculated from XPS analysis, Si $(-O)_1$: relative contribution in the Si 2p.

Surfaces	Atomic concentration (AC%)				Si $(-O)_1$ (%)
	C	Si	N	O	
TDSUM	10.6	29.0	-	60.4	1.1
Jeffamine	22.1	25.0	0.56	52.4	1.4
Chitosan	14.0	27.6	0.42	58.0	2.8

On the contrary, due to the mean inelastic free path of electrons (constant probing depth), increased surface coverage results in decreased signal originating from the substrate and therefore the decrease of Si 2p atomic percentage. The percentages of $Si(-O)_1$ for TDSUM

was the mean of 1.1%, 1.4% and 2.8 % corresponding to TDSUM, Jeffamine and chitosan surfaces. Upon reaction of NHS-activated TSDUM surface with either Jeffamine or chitosan, the N 1s AC% increased from 0 to 0.56 and 0.42 % respectively, whereas the Si 2p AC% decreased as expected.

Figure 2-10 presents the spectra of Si 2p, C 1s and N 1s of Jeffamine and chitosan surfaces obtained after reaction with TDSUM modified surfaces (XPS spectra of Si 2p and C 1s only) leading to the formation of amide bonds. Unreacted amine groups are also present has demonstrated by CBB titration. The four peaks corresponded to C-C, C-H at around 284.7 eV, C-O, C-N at around 286.1 eV, C=O, O-C-O at around 288 eV and very weakly N-C=O, O-C=O at around 289 eV were observed on both surfaces. The contribution at 286.1 eV can be associated to the polyoxypropylene backbone of Jeffamine or to the polysaccharide backbone of chitosan. On N 1s spectra of Jeffamine, two peaks are observed at 399.7 eV and 401.7 eV; these contributions can be assigned to NH_2-C or N-C=O respectively. Alternatively, they can be attributed to N-C=O and $^{+}H_3N$-C or NH_2-C and $^{+}H_3N$-C (Figure 2-10 B3). The reaction proceeds in tetrahydrofuran, an aprotic solvent. Therefore, most probably the contribution at 399.7 eV corresponds to NH_2-C and the contribution at 401.7 eV to a nitrogen involved in an amide bond indicating that Jeffamine was covalently bound to the carboxysilane monolayer. In the case of chitosan, the contribution at 401.7 eV is not observed, indicating that reaction between the NHS ester and the amine of the chitosan did not proceed. It was probably suggested that chitosan is mostly physisorbed on the TDSUM surface.

2.3.3.3. Surface tension characterization

TDSUM surface as well as the deprotected one, i.e. COOH surface, the NHS-activated one, i.e. NHS surface, and the two aminated surfaces, i.e. Jeffamine and chitosan surfaces, were characterized by contact angle measurements to evaluate surface tension. As described above, the surface energies were calculated from the wetting angle (θ) accordingly to the Owens–Wendt equations and the results are reported in Table 2-7.

Surface tensions of TDSUM, COOH and NHS surfaces were similar, with lower dispersive energy for TDSUM surface, which was in agreement with Dugas et al. [40]. Grafting of Jeffamine onto NHS-activated surface led to a slight increase of surface tension, from 36.1 mJ/m^2 for NHS surface to 38.4 mJ/m^2 for Jeffamine surface, mainly due to increase in dispersive energy. This could be attributed to the long chain of polyoxypropylene backbone of Jeffamine. Chitosan surface was the most hydrophilic surface due to its high polar energy (12.4 mJ/m^2) which was about two times that of NHS and Jeffamine surfaces. Indeed, chitosan is a natural polysaccharide with hydrophilic characteristic due to numerous hydroxyl and amine groups.

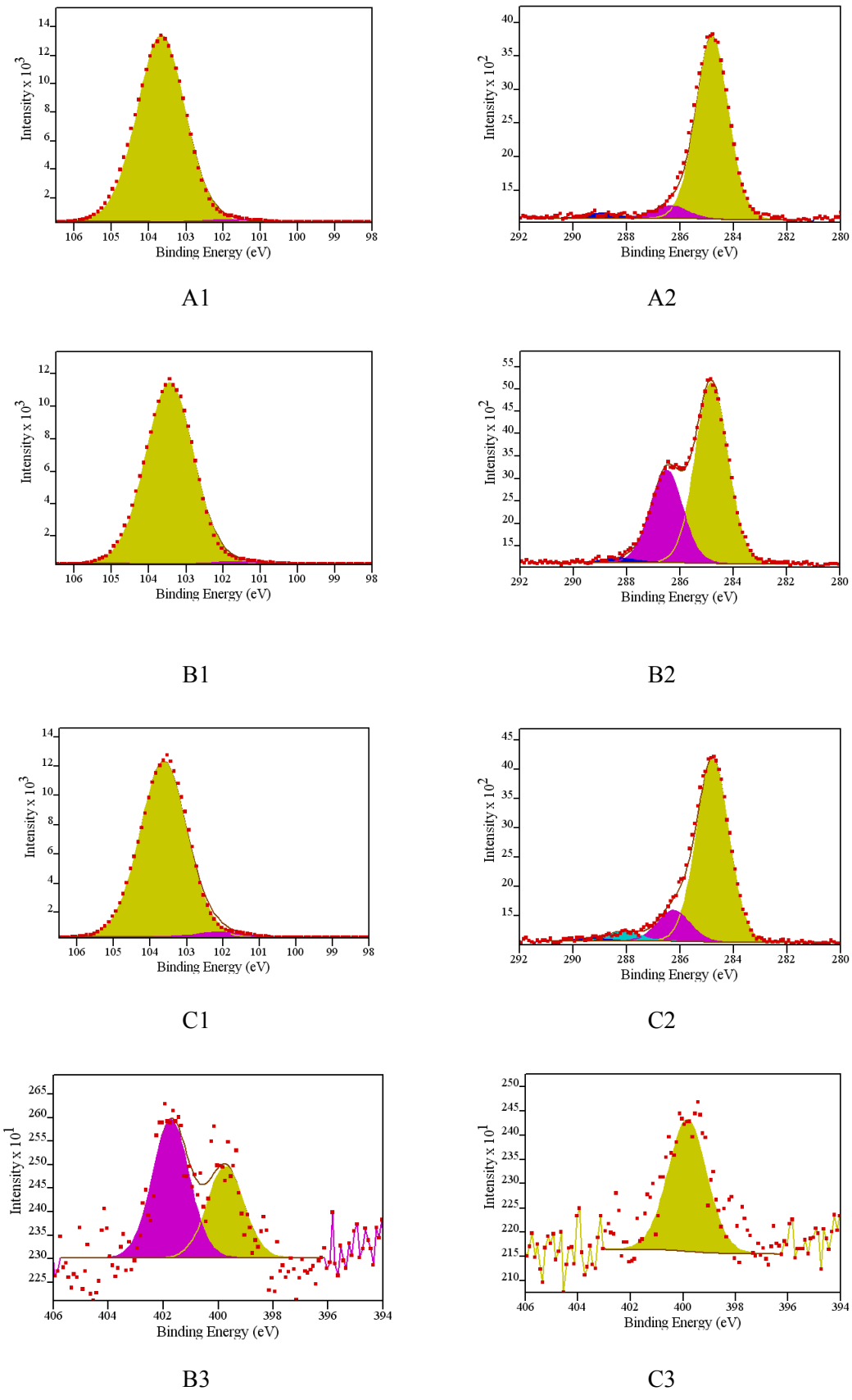

Figure 2-10 High-resolution XPS spectra for TDSUM, Jeffamine and chitosan surfaces, A1, B1 and C1 are relative to their Si 2p spectra; A2, B2, C2 are relative to their C 1s spectra; B3, C3 are relative to N 1s spectra of Jeffamine and chitosan.

Table 2-7 Wetting properties of TDSUM, deprotected COOH, NHS-activated, Chitosan and Jeffamine surfaces according to the Owens–Wendt equations.

Surfaces	E_T (mJ/m²)	E_P (mJ/m²)	E_D (mJ/m²)	Contact angle (θ /°)		
				water	Ethylene-Glycol	Diiodo-methane
TDSUM	34.3	6.8	27.5	78.3±0.2	54.2±0.6	59.3±0.5
COOH	37.6	6.7	30.9	74.6 ±0.3	55.2 ±0.6	49.7 ±0.6
NHS	36.1	6.9	29.2	75.8 ±0.2	55.5 ±0.6	53.9 ±0.6
Jeffamine	38.4	7.1	31.3	74.1±0.2	50.5±0.5	51±0.4
Chitosan	43.7	12.4	31.4	62.4±0.5	44.5±0.7	47.2±0.7

2.3.4. Characterization of GPDMES surface

Figure 2-11 shows the high-resolution XPS spectra of Si 2p, C 1s and O 1s of piranha cleaned silica and mono-functional silane GPDMES modified silica. The presence of the mono-functional silane on GPDMES surface is confirmed by the peak at 101.6 eV on the Si 2p spectra (Figure 2-11 A) corresponding to $Si(O-)_1$ according to Alexander et al [15]. The relative contribution of $Si(-O)_1$ was calculated to 6.3 %. Demirci et al [41] showed that the XPS spectrum of GPDMES consists of one sharp O 1s and two C 1s peaks. The first peak in the C 1s spectrum at 284.7 eV is due to C– H and C–C structural features. The second peak in the C 1s spectrum at 286.1 eV corresponds to C–O features of epoxy and ether groups of the GPDMES molecule (Figure 2-11 C, D).

The wetting properties of GPDMES surface are illustrated in Table 2-8. The surface tension of GPDMES (31.8 mJ/m^2) was found similar to APDMES (31.6 mJ/m^2) due to similar silane structure. However, the polar energy of GPDMES surface (7.1 mJ/m^2) is slightly higher than APDMES surface (6.2 mJ/m^2) but equal to the one of Jeffamine surface. Indeed, GPDMES possess epoxy and ether groups giving polar characteristics to the silane which are not present on APDMES. Jeffamine also possess ether functions on its polyoxypropylene backbone.

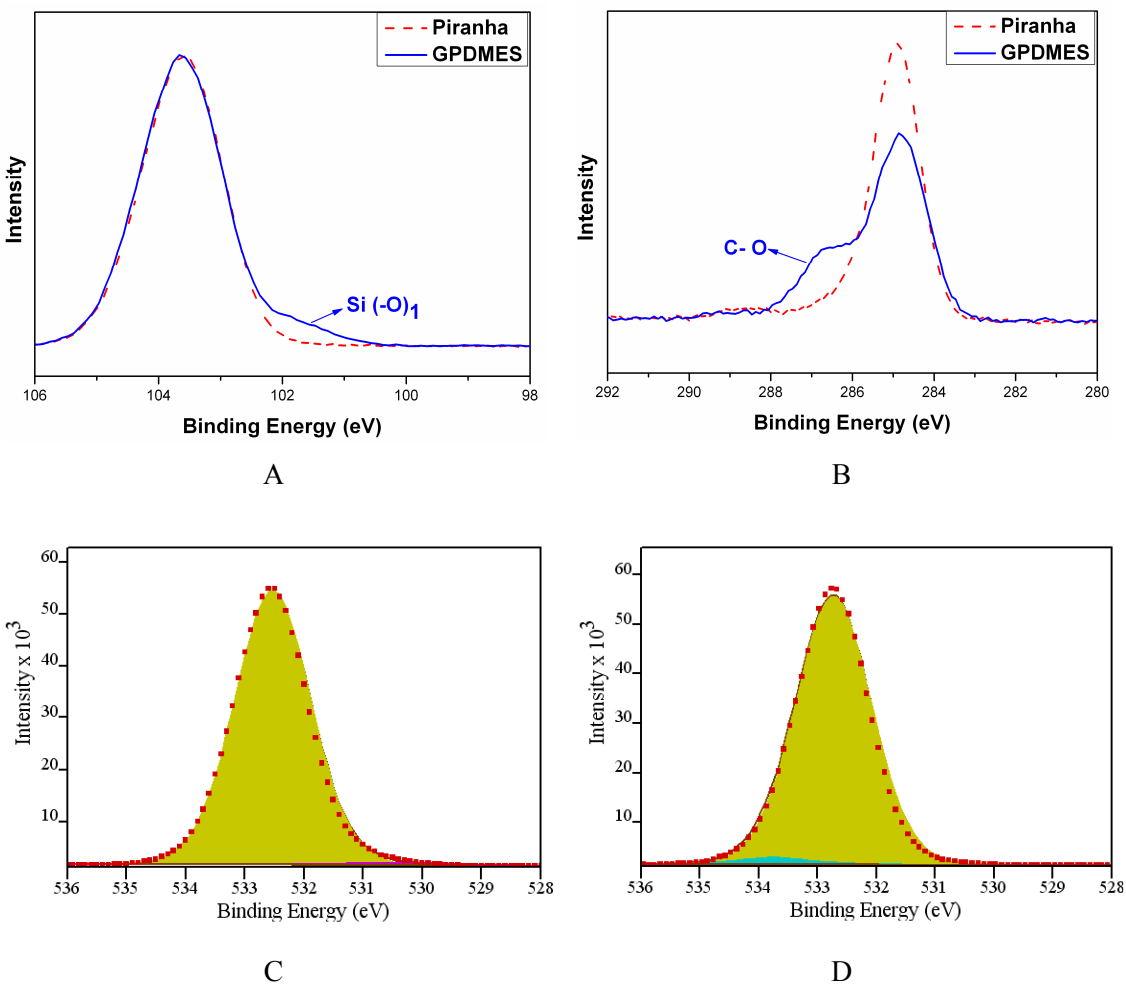

Figure 2-11 High-resolution XPS spectra in the (A) Si 2p and (B) C 1s of piranha cleaned silica and GPDMES modified silica, O 1s of piranha cleaned silica (C) and GPDMES modified silica (D)

Table 2-8 Wetting properties of GPDMES according to the Owens–Wendt equations.

Surface	E_T (mJ/m²)	E_P (mJ/m²)	E_D (mJ/m²)	Contact angle (θ /°)		
				water	Ethylene-Glycol	Diiodo-methane
GPDMES	31.8	7.1	24.7	78.5 ±0.2	61.6±0.5	62.2±0.5

2.4. Conclusions

In this chapter, various surface chemistries for the implementation of protein microarray were developed and characterized by ATR-FTIR, XPS, contact angle measurement and colorimetric assay.

Three mono-functional silanes bearing different functional groups, amino group for APDMES, carboxylic group for TDUSM and epoxy group for GPDMES, were successfully bound onto silica substrates. XPS analysis indicated that Si atomic percentage observed on APDMES surface (27.7 %), TDSUM surface (29.0 %) and GPDMES surface (26.0 %) were similar. These results suggest that surface coverage with the three mono-functional silanes was comparable indicating that our protocol of silanization is reproducible. Moreover, contact angle measurement showed that these three silanized surfaces displayed equivalent surface tension energies which are in agreement with their similar structure.

NHS-activated TDSUM surface was further functionalized with two aminated polymers, Jeffamine a diamine and Chitosan a polyaminated polysaccharide of high molecular weight, in order to generate aminated surfaces with different physico-chemical properties for physical adsorption of proteins. First, XPS analysis showed that Jeffamine was covalently bound to the silane monolayer whereas Chitosan was mostly physisorbed. Second, XPS analysis and CBB method suggested that part of Jeffamine molecules react with two adjacent NHS ester groups leading to the formation of "bridge" leading to no available amine group on the surface. Furthermore, the amine density of Jeffamine and Chitosan surfaces were similar, with about $4.5x10^{13}$ amino groups/cm^2 but half of the one obtained for APDMES surface ($1.3x10^{14}$ amino groups/cm^2). Although Chitosan used in this study is highly aminated polymer (DD=94%), the low amine density found on Chitosan surface could be attributed to low reaction yield, steric hindrance or electrostatic repulsion between chitosan molecules leading to low amount of available amino groups on the surface. It is also possible that CBB could not reach all surface amino groups due to steric hindrance or diffusion limitations related to the long polymeric chains.

APDMES surface was further functionalized with two amine-reactive polymers, CMD a carboxymethylated polysaccharide, and MAMVE bearing maleic anhydride moiety, in order to generate amine-reactive surfaces for covalent linking of proteins. XPS and ATR-FTIR analysis indicated that CMD and MAMVE polymers were covalently grafted to the aminosilane. However, MAMVE layer was found to be thicker than CMD layer.

Contact angle measurements allowed determining surface tension and wetting properties of polymer functionalized-silane monolayers. Interestingly, Jeffamine surface displayed slightly higher surface tension (38.4 mJ/m^2) than CMD surface (35.7 mJ/m^2). However, their polar energies stayed around 7.2 mJ/m^2. It was suggested that Jeffamine surface was more hydrophilic than CMD surface due to its higher dispersive energy, attributed to the polyoxyproplene backbone of Jeffamine. Chitosan and MAMVE surfaces were the most hydrophilic surfaces with surface tension about 43.7 mJ/m^2 and 45.8 mJ/m^2 respectively. This wetting property was mainly due to high polar energy (12.4 mJ/m^2 and 17.2 mJ/m^2, respectively). Actually, chitosan is a high molecular weight polysaccharide (Mw=470 000

g/mol) bearing numerous polar groups (amino groups (DD=94%) and hydroxyl groups) and MAMVE is a high molecular weight copolymer (Mw=216 000 g/mol) bearing anhydride moiety which leads to carboxylic groups following hydrolysis.

In the next chapter, all these well characterized surface chemistries were used to immobilize protein for the elaboration of efficient protein microarray.

References

[1] U. Sauer, Impact of substrates for probe immobilization, Methods Mol. Biol., 785 (2011) 363-378.

[2] B. Feng, S. Huang, F. Ge, Y. Luo, D. Jia, Y. Dai, 3D antibody immobilization on a planar matrix surface, Biosens. Bioelectron., 28 (2011) 91-96.

[3] H.Y. Lee, S.B. Park, Surface modification for small-molecule microarrays and its application to the discovery of a tyrosinase inhibitor, Mol. BioSyst., 7 (2011) 304-310.

[4] S.L. Seurynck-Servoss, A.M. White, C.L. Baird, K.D. Rodland, R.C. Zangar, Evaluation of surface chemistries for antibody microarrays, Anal. Biochem., 371 (2007) 105-115.

[5] W. Kusnezow, A. Jacob, A. Walijew, F. Diehl, J.D. Hoheisel, Antibody microarrays: An evaluation of production parameters, Proteomics, 3 (2003) 254-264.

[6] H. Zhu, M. Snyder, Protein chip technology, Curr. Opin. Chem. Biol., 7 (2003) 55-63.

[7] H. Zhu, M. Bilgin, R. Bangham, D. Hall, A. Casamayor, P. Bertone, N. Lan, R. Jansen, S. Bidlingmaier, T. Houfek, T. Mitchell, P. Miller, R.A. Dean, M. Gerstein, M. Snyder, Global analysis of protein activities using proteome chips, Science, 293 (2001) 2101-2105.

[8] V. Dugas, Y. Chevalier, Surface hydroxylation and silane grafting on fumed and thermal silica, J. Colloid Interface Sci., 264 (2003) 354-361.

[9] R. Mazurczyk, G. El Khoury, V. Dugas, B. Hannes, E. Laurenceau, M. Cabrera, S. Krawczyk, E. Souteyrand, J.P. Cloarec, Y. Chevolot, Low-cost, fast prototyping method of fabrication of the microreactor devices in soda-lime glass, Sens. Actuators B Chem, 128 (2008) 552-559.

[10] J. Zhang, Design and implementation of DNA-Directed Immobilization (DDI) glycoarrays for probing carbohydrate-protein interactions, in: Electronique, Electrotechnique et Automatique, Ecole Centrale de lyon, Lyon, 2010.

[11] J. Zhang, G. Pourceau, A. Meyer, S. Vidal, J.P. Praly, E. Souteyrand, J.J. Vasseur, F. Morvan, Y. Chevolot, Specific recognition of lectins by oligonucleotide glycoconjugates and sorting on a DNA microarray, Chem. Commun., (2009) 6795-6797.

[12] M. Phaner-Goutorbe, V. Dugas, Y. Chevolot, E. Souteyrand, Silanization of silica and glass slides for DNA microarrays by impregnation and gas phase protocols: A comparative study, Materials Science and Engineering: C, 31 (2011) 384-390.

[13] V. Dugas, G. Depret, B. Chevalier, X. Nesme, E. Souteyrand, Immobilization of single-stranded DNA fragments to solid surfaces and their repeatable specific hybridization: covalent binding or adsorption?, Sens. Actuators B, 101 (2004) 112-121.

[14] R. Huynh, F. Chaubet, J. Jozefonvicz, Carboxymethylation of dextran in aqueous alcohol as the first step of the preparation of derivatized dextrans, Angew. Makromol. Chem., 254 (1998) 61-65.

[15] M.R. Alexander, R.D. Short, F.R. Jones, W. Michaeli, C.J. Blomfield, A study of HMDSO/O2 plasma deposits using a high-sensitivity and -energy resolution XPS instrument: curve fitting of the Si 2p core level, Appl. Surf. Sci., 137 (1999) 179-183.

[16] G. Coussot, C. Faye, A. Ibrahim, M. Ramonda, M. Dobrijevic, A. Le Postollec, F. Granier, O. Vandenabeele-Trambouze, Aminated dendritic surfaces characterization: a rapid and versatile colorimetric assay for estimating the amine density and coating stability, Anal. Bioanal. Chem., 399 (2011) 2295-2302.

[17] G. Coussot, C. Perrin, T. Moreau, M. Dobrijevic, A. Le Postollec, O. Vandenabeele-Trambouze, A rapid and reversible colorimetric assay for the characterization of aminated solid surfaces, Anal. Bioanal. Chem., 399 (2011) 1061-1069.

[18] M. Mathlouthi, J.L. Koenig, Vibrational spectra of carbohydrates, Adv. Carbohydr. Chem. Biochem., 44 (1986) 7-89.

[19] J. Sandula, G. Kogan, M. Kacurakova, E. Machova, Microbial (1 -> 3)-beta-D-glucans, their preparation, physico-chemical characterization and immunomodulatory activity, Carbohydr. Polym., 38 (1999) 247-253.

[20] Y.X. Sun, X.Z. Zhang, H. Cheng, S.X. Cheng, R.X. Zhuo, A low-toxic and efficient gene vector: Carboxymethyl dextran-graft-polyethylenimine, Journal of Biomedical Materials Research Part A, 84A (2008) 1102-1110.

[21] G. Coussot, E. Nicol, A. Commeyras, I. Desvignes, R. Pascal, O. Vandenabeele-Trambouze, Colorimetric quantification of amino groups in linear and dendritic structures, Polym. Int., 58 (2009) 511-518.

[22] S.J. Oh, S.J. Cho, C.O. Kim, J.W. Park, Characteristics of DNA microarrays fabricated on various aminosilane layers, Langmuir, 18 (2002) 1764-1769.

[23] J.H. Moon, J.W. Shin, S.Y. Kim, J.W. Park, Formation of uniform aminosilane thin layers: An imine formation to measure relative surface density of the amine group, Langmuir, 12 (1996) 4621-4624.

[24] F. Zhang, K. Sautter, A.M. Larsen, D.A. Findley, R.C. Davis, H. Samha, M.R. Linford, Chemical Vapor Deposition of Three Aminosilancs on Silicon Dioxide: Surface Characterization, Stability, Effects of Silane Concentration, and Cyanine Dye Adsorption, Langmuir, 26 (2010) 14648-14654.

[25] S. Noel, B. Liberelle, L. Robitaille, G. De Crescenzo, Quantification of primary amine groups available for subsequent biofunctionalization of polymer surfaces, Bioconjug. Chem., 22 (2011) 1690-1699.

[26] R.A. Shircliff, I.T. Martin, J.W. Pankow, J. Fennell, P. Stradins, M.L. Ghirardi, S.W. Cowley, H.M. Branz, High-Resolution X-ray Photoelectron Spectroscopy of Mixed Silane Monolayers for DNA Attachment, ACS Appl. Mater. Interfaces, 3 (2011) 3285-3292.

[27] J.C. Shearer, M.J. Fisher, D. Hoogeland, E.R. Fisher, Composite SiO(2)/TiO(2) and amine polymer/TiO(2) nanoparticles produced using plasma-enhanced chemical vapor deposition, Appl. Surf. Sci., 256 (2010) 2081-2091.

[28] K.M. McLean, G. Johnson, R.C. Chatelier, G.J. Beumer, J.G. Steele, H.J. Griesser, Method of immobilization of carboxymethyl-dextran affects resistance to tissue and cell colonization, Colloids and Surfaces B-Biointerfaces, 18 (2000) 221-234.

[29] K.M.R. Kallury, P.M. Macdonald, M. Thompson, Effect of Surface-Water and Base Catalysis on the Silanization of Silica by (Aminopropyl)Alkoxysilanes Studied by X-Ray Photoelectron-Spectroscopy and C-13 Cross-Polarization Magic-Angle-Spinning Nuclear-Magnetic-Resonance, Langmuir, 10 (1994) 492-499.

[30] A. Hadjizadeh, C.J. Doillon, P. Vermette, Bioactive polymer fibers to direct endothelial cell growth in a three-dimensional environment, Biomacromolecules, 8 (2007) 864-873.

[31] L.D. White, C.P. Tripp, Reaction of (3-Aminopropyl)dimethylethoxysilane with Amine Catalysts on Silica Surfaces, J. Colloid Interface Sci., 232 (2000) 400-407.

[32] A.G. Filimoshkin, V.F. Kosolapova, E.B. Chernov, E.M. Berezina, T.V. Petrenko, Novel features of copoly(vinylacetate-maleic anhydride) microstructure, Eur. Polym. J., 39 (2003) 1461-1466.

[33] Z.G. Yang, Y. Chevolot, Y. Ataman, G. Choquet-Kastylevsky, E. Souteyrand, E. Laurenceau, Cancer Biomarkers Detection Using 3D Microstructured Protein Chip: Implementation of Customized Multiplex Immunoassay, Sens. Actuators B, in presss doi.org/10.1016/j.snb.2011.11.055 (2011).

[34] V. Dugas, Y. Chevalier, Chemical Reactions in Dense Monolayers: In Situ Thermal Cleavage of Grafted Esters for Preparation of Solid Surfaces Functionalized with Carboxylic Acids, Langmuir, 27 (2011) 14188-14200.

[35] Y. Chevolot, J. Zhang, A. Meyer, A. Goudot, S. Rouanet, S. Vidal, G. Pourceau, J.P. Cloarec, J.P. Praly, E. Souteyrand, J.J. Vasseur, F. Morvan, Multiplexed binding determination of seven glycoconjugates for Pseudomonas aeruginosa lectin I (PA-IL) using a DNA-based carbohydrate microarray, Chem. Commun., 47 (2011) 8826-8828.

[36] G. El Khoury, E. Laurenceau, Y. Chevolot, Y. Merieux, A. Desbos, N. Fabien, D. Rigal, E. Souteyrand, J.P. Cloarec, Development of miniaturized immunoassay: influence of surface chemistry and comparison with enzyme-linked immunosorbent assay and Western blot, Anal. Biochem., 400 (2010) 10-18.

[37] J. Zhang, G. Pourceau, A. Meyer, S. Vidal, J.P. Praly, E. Souteyrand, J.J. Vasseur, F. Morvan, Y. Chevolot, DNA-directed immobilisation of glycomimetics for glycoarrays

application: Comparison with covalent immobilisation, and development of an on-chip IC50 measurement assay, Biosens. Bioelectron., 24 (2009) 2515-2521.

[38] R. Mazurczyk, G. El Khoury, V. Dugas, B. Hannes, E. Laurenceau, M. Cabrera, S. Krawczyk, E. Souteyrand, J.P. Cloarec, Y. Chevolot, Low-cost, fast prototyping method of fabrication of the microreactor devices in soda-lime glass, Sens. Actuators B, 128 (2008) 552-559.

[39] Y. Chevolot, C. Bouillon, S. Vidal, F. Morvan, A. Meyer, J.-P. Cloarec, A. Jochum, J.-P. Praly, J.-J. Vasseur, E. Souteyrand, DNA-based carbohydrate biochips: A platform for surface glyco-engineering, Angewandte Chemie - International Edition, 46 (2007) 2398-2402.

[40] F. Bessueille, V. Dugas, V. Vikulov, J.P. Cloarec, E. Souteyrand, J.R. Martin, Assessment of porous silicon substrate for well-characterised sensitive DNA chip implement, Biosens. Bioelectron., 21 (2005) 908-916.

[41] S. Demirci, T. Caykara, Formation of dicarboxylic acid-terminated monolayers on silicon wafer surface, Surf. Sci., 604 (2010) 649-653.

Chapter 3 Elaboration of Protein Microarrays: Optimization of Protein Immobilization onto Functionalized Surfaces†

† This chapter is base on the following contributions:

- Z.G. Yang, Y. Chevolot, Y. Ataman, G. Choquet-Kastylevsky, E. Souteyrand, E. Laurenceau, Cancer Biomarkers Detection Using 3D Microstructured Protein Chip: Implementation of Customized Multiplex Immunoassay, Sens. Actuators B, in presss doi.org/10.1016/j.snb.2011.11.055 (2011)
- Z.G. Yang, Y. Chevolot, V. Dugas, N. Xanthopoulos, V. Laporte, T. Delair, Y. Ataman-Önal, G. Choquet-Kastylevsky, E. Souteyrand, E. Laurenceau. Antibody microarray based on different chain-length amino surfaces for the detection of tumor markers involved in colorectal cancer. Submitted to Biomaterials 2012

3.1. Introduction

The immobilization procedure of proteins is a crucial step in the elaboration of efficient protein microarrays. Many studies have reported that analytical performance of microarray mainly depends on surface chemistry and detection conditions to prevent loss of biological activity as well as achieving high signal-to-noise ratio [1-5]. Thus, in this chapter, the various surface chemistries presented previously were evaluated for protein immobilization under various conditions. Spotting buffers (component and pH), protein concentartion, blocking procedures were varied in order to define the best conditions on each surface and for each protein. Four proteins were chosen based on their different molecular weight and isoelectric point (pI). Characteristics of these proteins are reported in Table 3-1**.** They are fluorescently labeled with cyanine 3 (Cy3) or Alexa Fluor 647 (F647) for their detection on the surface and to evaluate their relative immobilization rate on the various surfaces. The choice for these proteins was driven by their similar properties with anti-tumor marker antibodies and tumor-associated antigens to be immobilized for cancer diagnosis. Indeed, IgG could preview the behaviour of anti-tumor markers antibodies immobilized for antibody microarray. Streptavidin, myoglobin and BSA are representatives of the protein diversity in Mw and pI, but with values closed to these of tumor antigens used for tumor-associated antigen microarray. Illustration of the proteins immobilized on the surface was shown in Figure 3-1.

Therefore, the aim of this study is to identify the main parameters influencing protein immobilization (by physical adsorption and by covalent linking) taking into account protein and surface properties. Results should allow fixing the best surface chemistry and the immobilization conditions for a given protein.

Table 3-1 Molecular weight, dyes/protein ratio and isoelectric point of fluorescent labeled proteins n.d.: not determined

Proteins	M_w (g/mol)	Dye/Protein ratio	Isoelectric point (pI)
IgG-Cy3	150000	2.6	n.d.
Streptavidin-Cy3	52800	3-9	6.1
Myoglobin-Cy3	17083	2.2	7.29
BSA-F647	66433	11	5.6

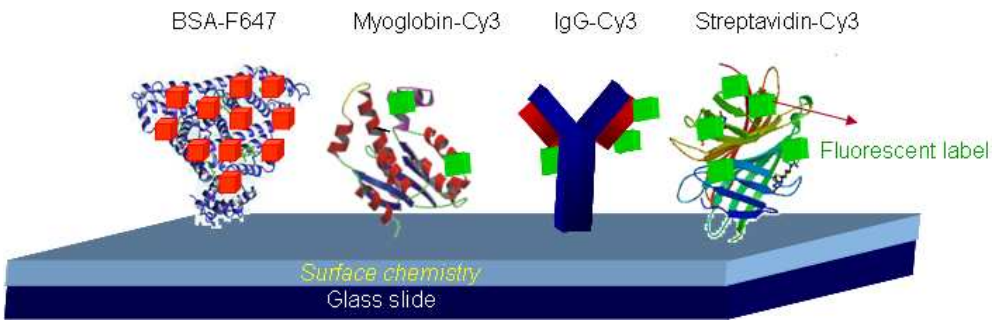

Figure 3-1 Schematic illustration of immobilized BSA-F647, myoglobin-Cy3, IgG-Cy3, and streptavidin-Cy3 onto glass slides functionalized with various surface chemistries

3.2. Experimental

3.2.1. Materials, chemical and biological products

Flat or microstructured borosilicate glass slides were functionalized with TDSUM (followed by deprotection: COOH; and NHS-activation), APDMES, GPDMES, Jeffamine, Chitosan (DD=94%), CMD T40 (DS=63%) or MAMVE 216 according to the protocols mentioned in Chapter 2. CMD and MAMVE surface were grafted from APDMES unless specifically stated.

Cy3-conjugated goat anti-mouse antibody (IgG-Cy3), streptavidin-Cy3, myoglobin, bovine serum albumin (BSA), glycerol, polyvinylalcohol (PVA), sodium acetate, tris-buffered saline (TBS), were purchased from Sigma-Aldrich (St. Quentin Fallavier, France). Tween 20 was purchased from Roth-Sochiel (Lauterbourg, France).

0.1 M sodium acetate was dissolved to obtain the sodium acetate buffer (pH 4.5). PBS 1X (pH 7.4) was prepared by dissolving the content of one pouch of dried powder in 1 L of ultrapure water. Carbonate buffer (pH 9.6) was prepared by dissolving one pouch of powder in 100 ml ultrapure water. MES buffer (pH 6.2) was prepared by 0.01 M 2-(N-morpholino) ethanesulfonic acid (MES) and pH was adjusted with 0.1 M hydrochloric acid (HCl). Tris-buffered saline (TBS, pH 7.4) were prepared by 50 mM Tris, 0.1 M sodium chloride (NaCl) and 0.002 M potassium chloride (KCl) and pH was adjusted with 0.1 M sodium hydroxyl (NaOH). Ultrapure water (18.2 MΩ) was delivered by an Elga water system. Washing buffer contained PBS 1X and 0.1 % Tween 20 (PBS-T) at pH 7.4. Blocking solution was prepared by dissolving 4 or 10 g of BSA in 100 ml of PBS 1X.

3.2.2. Fluorescent labeling of proteins

Myoglobin was Cy3-labelled using Cy3-NHS ester dye (Amersham) purchased from GE healthcare (USA) and according to manufacturer protocol. The dye/protein ratio was estimated to 2.2.

BSA was labelled according to Alexa Fluor 647 Microscale Protein labelling Kit (A30009) (Molecular Probes, Inc. USA). The dye/protein ratio was determined to 11.

3.2.3. Immobilization of fluorescent labeled proteins

IgG-Cy3, streptavidin-Cy3, myoglobin-Cy3 and BSA-F647 were spotted in several replicates (4 spots unless stated specifically) at various concentrations onto chemically functionalized glass slides (flat or microstructured). Contact spotter (Microgrid II, Biorobotics) or non-contact spotter (SciFlexarrayer S3, Scienon) were used for spotting. Spotting buffers were composed of sodium acetate (Ac, pH 4.5), PBS (1x, pH 7.4) and sodium carbonate (Car, pH 9.6), with additive (0.05 % PVA or 20 % glycerol, v/v).

Proteins were allowed to react with the surface under saturated water vapours overnight at 37°C, room temperature or 4 ^{o}C. Then slides were washed for 2 x 5 min with PBS and 1 x 5 min PBS-T, and dried by centrifugation for 3 min at 1300 rpm.

Then various blocking solutions were tested to reduce background and non specific adsorption of proteins: 4 % (m/v) BSA in PBS and 10 % (m/v) BSA in PBS-T 0.1%, respectively. Slides were immersed into blocking solutions for 2 h at room temperature, followed by washing with PBS-T for 3 x 5 min and drying by centrifugation.

3.2.4. Fluorescence scanning

Slides were scanned with the microarray scanner, GenePix 4100A software package (Axon Instruments) at wavelengths of 532 nm and 635 nm with the same photomultiplier tube (PMT) gain (PMT 400). The fluorescence signal of each protein was determined as the average of the median fluorescence signal of several replicates, and the value was divided by the signal background (median value) of the surface to get the signal-to-noise ratio (SNR) value.

3.3. Results and discussion

3.3.1. Protein-surface interactions

Depending on the surface chemistry, the immobilization process of proteins is different. Both surface reactivity and wetting properties (surface tension E_T) played significant roles in protein-surface interactions. Thus, preliminary experiments consisted to evaluate the immobilization of proteins towards various surfaces issued from TDSUM silanisation process. On COOH (E_T=37.6 mJ/m^2) and chitosan (E_T=43.7 mJ/m^2) surfaces, immobilization of proteins occur through physical adsorption, whereas covalent binding is achieved between activated carboxylic groups/anhydride moities of the surface and amine groups of proteins on NHS (E_T=36.1 mJ/m^2), CMD (E_T=35.7 mJ/m^2) and MAMVE (E_T=48.7 mJ/m^2) surfaces grafted from Jeffamine.

The spot morphology and protein surface density on these five surface chemistries were evaluated with three fluorescent labelled proteins: streptavidin-Cy3, BSA-F647 and IgG-Cy3. Proteins were spotted at 0.1 µM in PBS buffer (pH 7.4) with 20% (v/v) glycerol as additive to prevent protein drying. Measurements of fluorescence intensity were correlated to the yield of protein immobilization in the various conditions tested.

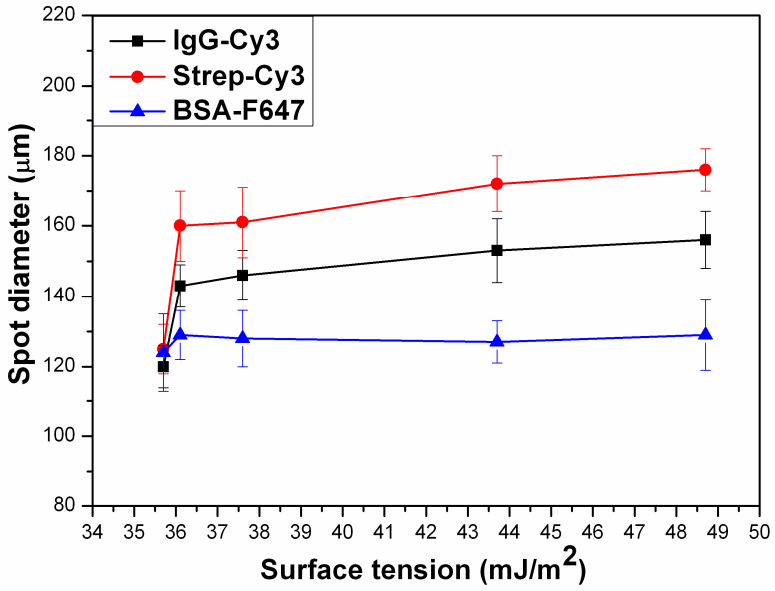

Figure 3-2 Spot diameters of fluorescent labeled proteins (IgG-Cy3, Strep-Cy3 and BSA-F647) immobilized on various surface chemistries leading to different wetting properties

Figure 3-2 shows the spot diameter of the three proteins measured by image analysis of scanning data versus total surface energy. Two different behaviors were observed: for IgG and streptavidin the spot diameter increased with total surface energy whereas for BSA the

spot diameter remained constant independently of the tested surface considering the standard deviation. It was suggested that under our spotting condition, IgG and streptavidin interact with hydrophilic surfaces via hydrophilic domains while some of these domains remain available to the surrounding buffer. Consequently, their hydrophobic domains should be unexposed to the buffer, indicating that the protein retains its folding. On hydrophobic surface, interaction between their hydrophobic domain and the surface may remain limited compared to the one observed on hydrophilic surface. On the contrary, BSA displays similar interactions towards all surfaces tested.

The relative immobilization rate of the 3 reference proteins was evaluated by measuring the signal to noise ratio (SNR) of immobilized fluorescent labeled proteins versus surface chemistry. As shown in Figure 3-3, the relative immobilization rate depended on the protein and on the surface chemistry. IgG was preferentially immobilized through covalent binding, the highest immobilization rate achieved on MAMVE surface. Alternatively, BSA mostly immobilized on surfaces by physical adsorption and the highest SNR was observed on chitosan surface. Furthermore, the fluorescence signal is not increased using NHS modified surfaces versus COOH surfaces. Covalent linking could be efficient on very reactive surfaces such as MAMVE surface. At least, the immobilization of streptavidin on surfaces was similarly efficient by covalent binding (highest SNR on NHS and MAMVE surfaces) and by physical adsorption on chitosan surface.

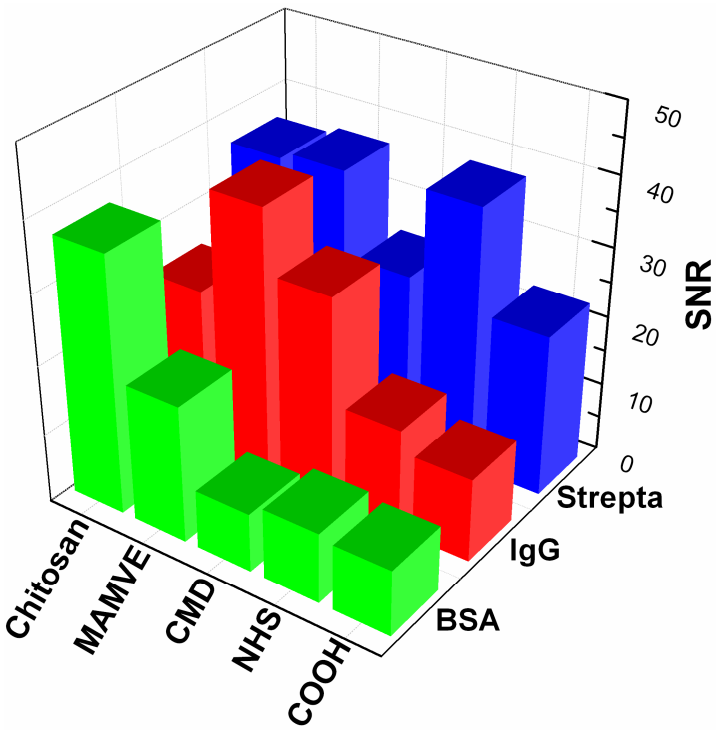

Figure 3-3 Signal to noise ratio of immobilized fluorescent labelled proteins versus surface chemistry; Standard deviation was in the range of 7% - 17 % of the mean value of SNR.

These results clearly demonstrate that many parameters are involved in protein immobilization on a solid support: surface properties (composition, number and kind of reactive functions, surface tension) and protein characteristics (M_w, pI, 3D structure, and hydropathicity) would determine the interactions and protein conformation at the solid-liquid interface. Therefore, it is essential to screen various immobilization conditions (surface chemistry, protein concentration, additives and pH of spotting buffer, blocking procedures etc) in order to define the best one for each protein.

3.3.2. Protein concentration

Among the various parameters that influence protein microarray performances, the spotting concentration of protein has to be initially optimized. Indeed, protein density on the surface should be optimal to reach maximal fluorescence signal.

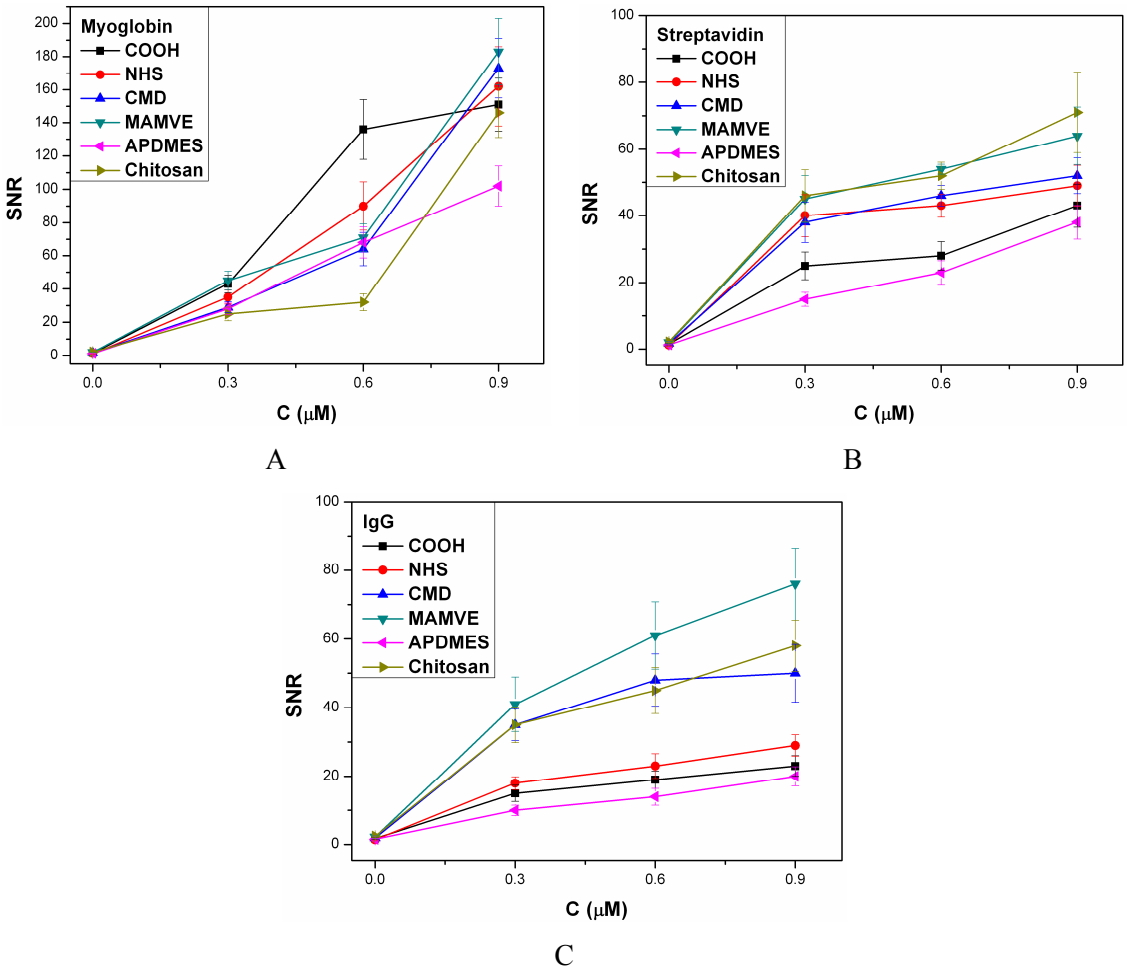

Figure 3-4 SNR of Cy3 labelled proteins immobilized with various concentration on each surface, spotted in PBS (pH=7.4) containing 20 % (v/v) glycerol (A) Myoglobin-Cy3, (B) streptavidin-Cy3, (C) IgG-Cy3.

Cy3-labelled myoglobin, streptavidin and IgG were immobilized at various concentrations in PBS buffer (pH 7.4) with 20 % glycerol, on COOH, NHS, CMD MAMVE, APDMES and chitosan surfaces and signal to noise ratio (SNR) was reported in Figure 3-4. As described above, SNR varied with surface chemistry and with the protein. As shown in Figure 3-4, SNR of all the three proteins increased with the increasing protein concentration but myoglobin displays the highest SNR compared to streptavidin and IgG. Variation of the immobilization level (SNR) of myolglobin on COOH surface displayed different behaviour than that on other surfaces. However, for streptavidin and IgG on all surfaces tested, the signal increased slightly with the increasing concentration, in particular for IgG on chitosan, CMD and MAMVE surfaces (Figure 3-4 C), the value of SNR almost reached a plateau at 0.3 μM. Typically, SNR of proteins immobilized on polymer layers (CMD, MAMVE, chitosan) for these two proteins are higher than those on silane layers (COOH, NHS, APDMES), indicating that polymer has more immobilization capacity than silane due to the hydrophilic surface and sufficient steric structures. It should be noted that not only the immobilization capacity of proteins on surface should be optimized, but their biological activity of these proteins once immobilized (and thus the signal related to the recognition properties) is an essential element of consideration. Therefore, the probe protein concentration (e.g. capture antibody) for elaboration of microarray will be discussed in the chapter 4.

3.3.3. Effects of the additive

Robotic spotter deposits nanoliter or even picoliter size droplets (400 pL/drop in our case) of protein solutions on the solid surface. As consequence, evaporation of the aqueous phase occurs in few seconds and could damage protein structure and its activity. In order to prevent such protein drying, humidity could be control during spotting or hydroxylated additives could be added to spotting buffer. Among the bulk protein cryo- and lyo-protectants, trehalose, sucrose, glucose, polyethylene glycol (PEG) and glycerol have all been used as additive for protein microarray [7].

The effect of two commonly used additives, glycerol (20% v/v) and PVA (0.05% w/v), was evaluated on spot morphology and SNR of myoglobin and IgG spotted at 0.3 μM in carbonate buffer (pH 9.6). As an example, Figure 3-5 illustrates the fluorescence scanning images of 4 replicates of myoglobin-Cy3 (first line) and IgG-Cy3 (second line) spotted on NHS surface with glycerol (Figure 3-5 A) or PVA (Figure 3-5 B) as additive in carbonate buffer (pH 9.6). It clearly appears that spot morphology with PVA produces the most homogeneous protein distribution with regular round-spot morphologies. This was mainly attributed to PVA surfactant properties that promote droplet-surface spreading, uniform wetting and preventing protein drying [7, 10]. Furthermore, SNR of both proteins spotted in

the presence of PVA was significant higher than that with glycerol (Figure 3-5 C), probably due to better wetting and spreading of proteins onto the surface.

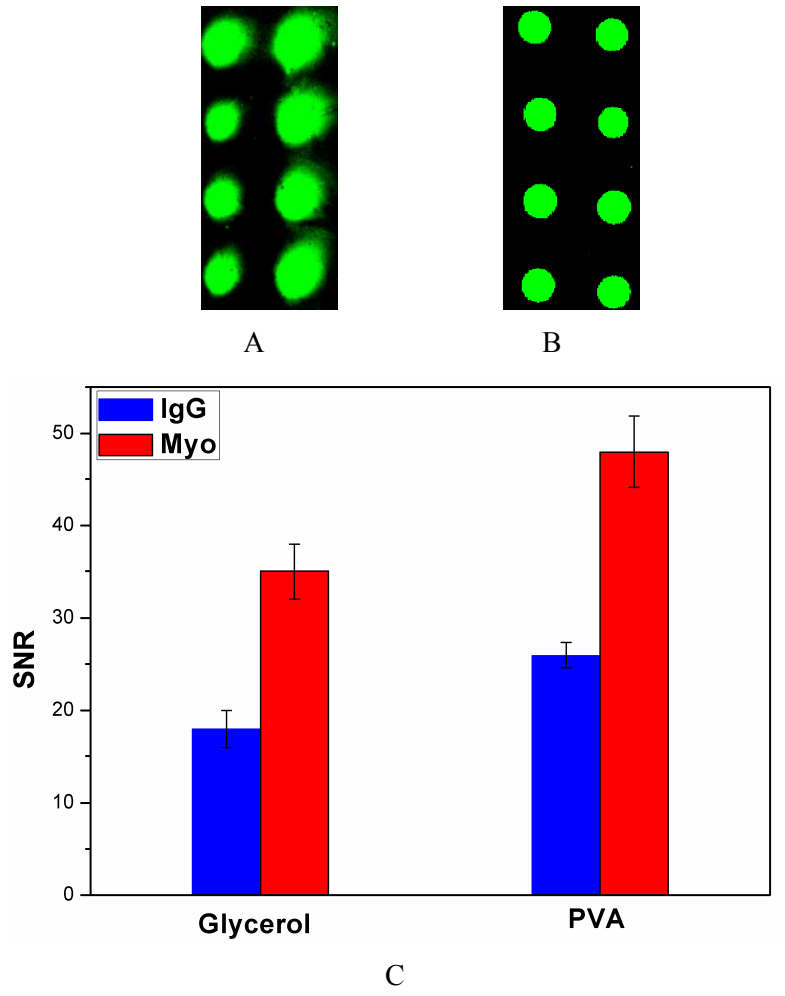

Figure 3-5 Spot morphology of Myoglobin-Cy3 (left column) and IgG-Cy3 (right column) spotted at 0.3 µM on NHS surface (4 replicates) in carbonate buffer (pH=9.6) containing 20 % glycerol (A) or 0.05 % PVA (B) or C: SNR of the two immobilized proteins spotted with glycerol or PVA as additives in carbonate buffer.

This result indicates better performance for PVA as spotting additive in agreement with Wu and co-workers [7]. They evaluated various hydroxylated additives at different concentrations in printing buffers to stabilize antibodies during normal array spot desiccation on commercial polymer-coated microarray slides. Results demonstrated that PVA displayed the best performance among several hydroxylated additives in terms of spotted antibody distribution homogeneity, uniform microspot morphology, immobilized antibody bioactivity, and spot-to-spot variance. PVA also maintained antibody capture activity reasonably well after one-month storage under dry conditions at 4 °C after blocking.

3.3.4. Effects of pH buffer

Interactions between proteins and the solid support are highly dependent on surface chemistry (reactive groups, wetting properties) and on physicochemical characteristics of proteins at defined pH. The global charge of a protein at a given pH is defined by its isoelectric point (pI), the pH value at which the global charge of the protein is neutral. For pH below the pI, the protein is positively charged, and negatively charged for pH above the pI. Surface chemistries developed in this thesis includes two groups according to the immobilization process: (1) physical adsorption via amine groups (APDMES, Jeffamine, chitosan) or carboxylic groups (COOH) on the surface; (2) covalent immobilization through amine-reactive surfaces (NHS, NHS-activated CMD, MAMVE and GPDMES).

In order to optimize protein-surface interactions, we evaluated pH effects on protein immobilization capacity on the various surface chemistries. Three fluorescent labeled proteins, streptavidin-Cy3, myoglobin-Cy3 and IgG-Cy3, were spotted at 0.6 µM in various spotting buffer containing 0.05% PVA according to previous results: sodium acetate (Ac) pH 4.5, PBS pH 7.4 and sodium carbonate (Car) pH 9.6. The relative immobilization capacity of proteins was evaluated by calculating the signal-to-noise ratio (SNR) of immobilized fluorescent labelled proteins versus surface chemistry (Figure 3-6).

SNR of myoglobin was overall higher than that of streptavidin and IgG. First, the molecular weight of myoglobin is 3 times and 9 times lower than that of streptavidin and IgG, respectively. Thus, more myoglobin than streptavidin and IgG could bind to surfaces leading to higher fluorescent signal. Secondly, the degree of labelling of myoglobin is about 2 times higher than that of streptavidin (see Table 3-1**)** giving a higher fluorescent signal whereas it is in the same range with IgG. Then regarding myoglobin and streptavidin, surfaces functionalized with carboxylic groups (COOH surface) or with amine reactive groups (NHS, CMD and MAMVE surfaces) displayed higher protein immobilization levels with acetate buffer (pH 4.5) than that with the other two buffers. By contrast, on chitosan surface, both proteins were more efficiently immobilized with carbonate buffer (pH 9.6). APDMES surface showed a middle behaviour, with best protein immobilization using PBS (pH 7.4). Regarding IgG, the highest immobilization level was always obtained with carbonate buffer (pH 9.6) whatever the surface chemistry except on MAMVE surface where acetate buffer (pH 4.5) gave the best results. These results pointed up the importance of electrostatic interactions between proteins and the surface chemistry.

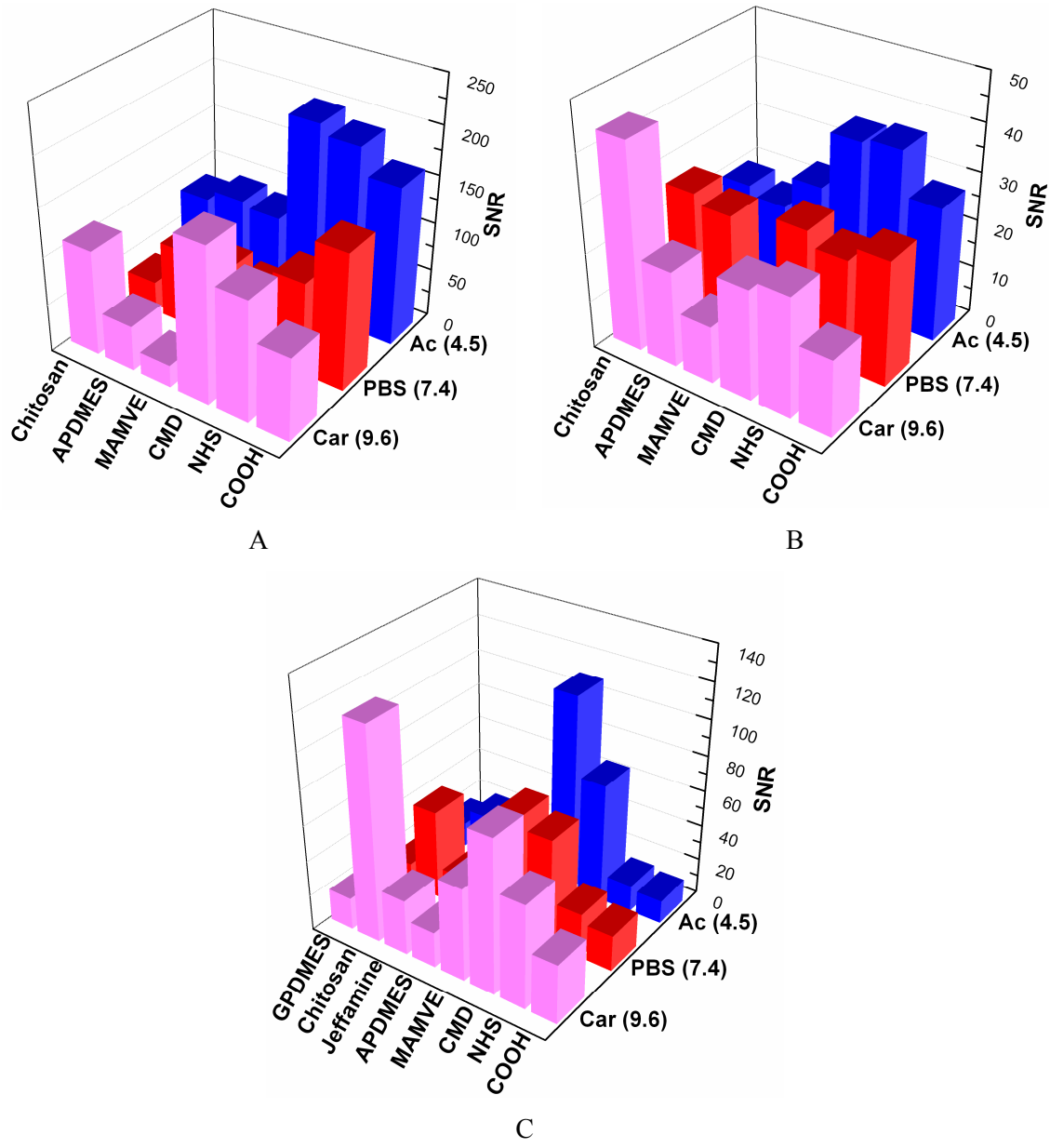

Figure 3-6 Signal-to-noise ratio (SNR) of fluorescent labeled protein myoglobin-Cy3 (A), streptavidin-Cy3 (B) and IgG-Cy3 (C) spotted at 0.6 µM in three different pH buffers on various surface chemistries; Standard deviation (SD) is in the range of 6%-18% of the mean value SNR.

Typically, in PBS (pH 7.4), myoglobin bears neutral global charge because pH is very close to its isoelectric point (pI=7.29) whereas in acetate buffer (pH 4.5) and in carbonate buffer (pH 9.6), myoglobin is positively and negatively charged, respectively. Concerning streptavidin (pI=6.1), in acetate buffer, the protein is positively charged whereas in PBS and carbonate buffer, it is negatively charged. For IgG, no precise pI was given by the company. At the same time, the net charge of the chemically functionalized surfaces was also affected by the pH of spotting buffers. COOH, NHS and CMD surfaces displayed similar pK_A values, around 6 for COOH and NHS surfaces and around 5 for CMD surface (experimental

determination by acidimetric titration), making them uncharged at pH 4.5 and negatively charged at pH 7.4 and 9.6. MAMVE surface bears two acidic functions with pK_A values 3.5 and 7.5 [11] . Thus it is highly negatively charged at pH 9.6. Whereas chitosan is highly aminated polysaccharide, its pK_A is 6.4, therefore it is protonated only at pH 4.5 and not charged at pH 7.4 and 9.6. Jeffamine was described with pK_A = 9.4 shifting to 7.1 when grafted on graphite surface [12]. We can suppose that Jeffamine surface is positively charged only in acetate buffer (pH 4.5). Finally, APDMES surface, with pK_A = 9.5 [13] , is deprotonated only in carbonate buffer (pH 9.6). Thus, when both surface and protein show the same charge, protein immobilization level is low (low SNR) due to repulsive forces. As it can be shown in Figure 3-6, this is the case with myoglobin (charge -) and streptavidin (charge -) on MAMVE surface (2 negative charges) in carbonate buffer (pH 9.6), and with myoglobin (charge +) and streptavidin (charge +) on APDMES (charge +) and chitosan (charge +) surfaces in acetate buffer (pH 4.5). On the contrary, the best conditions for high level of protein immobilization (high SNR) were obtained when the surface was not charged and the protein was positively or negatively charged. Thus, the highest level of immobilization was obtained for:

- myoglobin on CMD or NHS surface, *via* covalent binding, in acetate buffer;

- streptavidin on NHS surface, *via* covalent binding, in acetate buffer or on chitosan surface, *via* adsorption, in carbonate buffer;

- IgG on MAMVE surface, *via* covalent binding, in acetate buffer or on chitosan surface, *via* adsorption, in carbonate buffer.

According to these results, not only electrostatic interactions but also hydrogen bonds (related to polar energy higher on polymer surfaces), Van der Waals interactions (related to dispersive energy) and binding surface area (related to molecular weight, higher for polymer surfaces) are involved at the solid-liquid interface. Indeed, MAMVE and chitosan are high molecular weight polymers (216 000 g/mol and 470 000 g/mol, respectively) which were grafted on silanized surface displaying the highest polar energies (19.5 mJ/m^2 and 12.4 mJ/m^2, respectively). Furthermore, MAMVE is a highly amine reactive copolymer due to the maleic anhydride moieties. CMD and NHS surfaces displayed similar polar energy (about 7 mJ/m^2) and bear the same amine reactive group (NHS group) giving them the same reactivity towards protein immobilization. At least, for GPDMES surface, immobilization level of IgG was very low for all buffers and is the same range as NHS surface. We suggested that low amount of IgG was immobilized on these two surfaces due to its high molecular weight (150 000 g/mol) leading to steric hindrance of surface reactive groups. Hence, for each type of protein, it is essential to screen various immobilization conditions (surface chemistry, spotting buffer, concentration) in order to define the best one.

3.3.5. Effects of blocking procedure

From view-point of improving signal-to-noise ratio of protein microarray, it's essential to limit non specific adsorption of proteins for obtaining low background signal. Various protein solutions such as BSA, casein or milk, are usually used to block non specific site onto solid support.

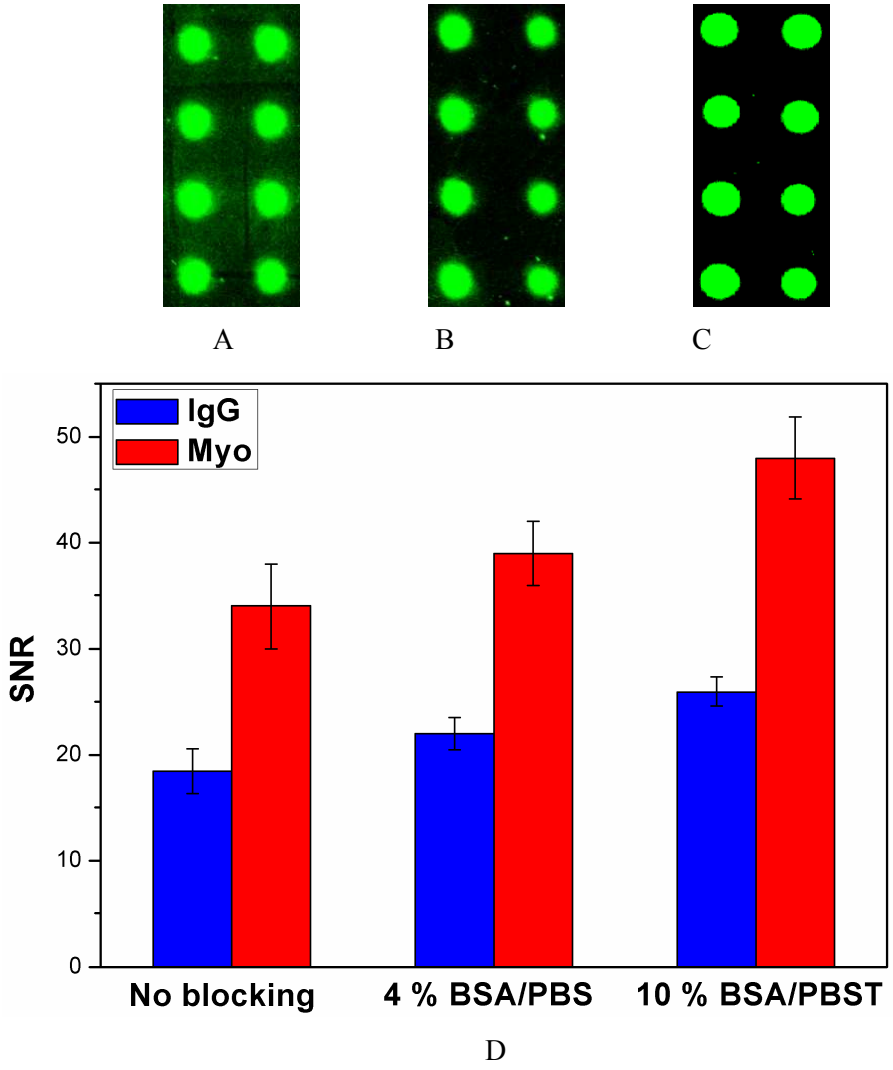

Figure 3-7 Spot morphology of Myoglobin-Cy3 (left column) and IgG-Cy3 (right column) spotted at 0.3 µM in carbonate buffer (pH=9.6) with 0.05 % PVA on NHS surface (4 replicates) A without blocking (A), blocked with 4 % BSA/PBS (B) and 10% BSA/PBS-T 0.1% (C); SNR of the two proteins versus blocking procedure.

Herein, two blocking solutions, 4% (w/v) BSA in PBS 1X (4% BSA-PBS) and 10% BSA in PBS 1X-0.1% Tween20 (10% BSA-PBS-T) were compared for reducing background after spotting of myoglobin-Cy3 and IgG-Cy3. Fluorescence scanning images presented in Figure 3-7 (A, B, C) confirm that blocking non specific sites reduced background signal on

the surface. Moreover, spot morphology of both fluorescent labeled proteins immobilized on the surface blocked with 10% BSA/PBS-T (Figure 3-7 C) are more regular than the ones without blocking (Figure 3-7 A) and blocked with 4% BSA/PBS (Figure 3-7 B). The fluorescence intensity of background from NHS surface (PMT 400 for scanning) shifted from 121 ± 11 without blocking to 98 ± 8 blocked with 4% BSA/PBS and 67 ± 6 blocked with 10 % BSA-PBS-T, respectively. Therefore, SNR of immobilized proteins blocked with 10% BSA-PBS-T were lower than values without blocking or with 4% BSA-PBS blocking solution (Figure 3-7 D), suggesting that optimal blocking procedures could led to increase of SNR values. Therefore, we choose 10% BSA/PBS-T as blocking solution for protein microarray assays.

3.4. Conclusions

In this chapter, we studied the effect of various parameters such as surface chemistry, protein concentration, pH of spotting buffers, additive and blocking procedures, on protein immobilization onto chemically functionalized glass slides. Four fluorescent labeled proteins, BSA, myoglobin, streptavidin and IgG, were immobilized in various conditions on 8 surface chemistries (COOH, NHS, CMD, MAMVE, APDMES, Jeffamine, Chitosan, GPDMES). The results showed that immobilization efficiency depends on surface properties (chemical groups, reactivity, wetting properties), protein characteristics (M_w, pI, 3D structure) and spotting conditions (pH, additive, concentration). However, some general behaviors could be defined. Large protein like IgG, were better immobilized on polymer surfaces than on silane monolayers either through covalent linking (MAMVE, CMD) or physical adsorption (chitosan). Small proteins like myoglobin, showed better immobilization by covalent linking than by physical adsorption either on silane monolayers (NHS-activated TDSUM) or on polymer surfaces (MAMVE, CMD). Medium protein like BSA and streptavidin, displayed an intermediate behavior. Furtheremore, protein-surface interactions are mainly driven by electrostatic interactions and hydrogen bonds. We found that best level of protein immobilization was obtained with non charged surface and charged protein.

At least, the quality of the spotting and image analysis could be improved by adding 0.05 % PVA in spotting buffer and using 10% BSA/PBS-T as blocking solution. The optimal concentration for fluorescent labelled protein immobilization was found to be 0.3 µM.

In conclusion, this study should allow defining the best immobilization conditions depending on the molecular weight and isoelectric point of the protein. However, following the immobilization process, the biological activity of immobilized protein should be verified. This major point is the aim of the two following chapters.

References

[1] C.M. Niemeyer, Semisynthetic DNA-protein conjugates for biosensing and nanofabrication, Angew. Chem. Int. Ed. Engl., 49 (2010) 1200-1216.

[2] S.L. Seurynck-Servoss, A.M. White, C.L. Baird, K.D. Rodland, R.C. Zangar, Evaluation of surface chemistries for antibody microarrays, Anal. Biochem., 371 (2007) 105-115.

[3] Q. Bi, X.D. Cen, W.J. Wang, X.S. Zhao, X. Wang, T. Shen, S.G. Zhu, A protein microarray prepared with phage-displayed antibody clones, Biosens. Bioelectron., 22 (2007) 3278-3282.

[4] W. Kusnezow, A. Jacob, A. Walijew, F. Diehl, J.D. Hoheisel, Antibody microarrays: An evaluation of production parameters, Proteomics, 3 (2003) 254-264.

[5] P. Angenendt, J. Glokler, D. Murphy, H. Lehrach, D.J. Cahill, Toward optimized antibody microarrays: a comparison of current microarray support materials, Anal. Biochem., 309 (2002) 253-260.

[6] P. Angenendt, J. Glokler, J. Sobek, H. Lehrach, D.J. Cahill, Next generation of protein microarray support materials: Evaluation for protein and antibody microarray applications, J. Chromatogr. A, 1009 (2003) 97-104.

[7] P. Wu, D.W. Grainger, Comparison of hydroxylated print additives on antibody microarray performance, J. Proteome Res., 5 (2006) 2956-2965.

[8] P. Peluso, D.S. Wilson, D. Do, H. Tran, M. Venkatasubbaiah, D. Quincy, B. Heidecker, K. Poindexter, N. Tolani, M. Phelan, K. Witte, L.S. Jung, P. Wagner, S. Nock, Optimizing antibody immobilization strategies for the construction of protein microarrays, Anal. Biochem., 312 (2003) 113-124.

[9] H. Zhu, M. Snyder, Protein chip technology, Curr. Opin. Chem. Biol., 7 (2003) 55-63.

[10] Y. Sakai, S.I. Yasueda, A. Ohtori, Stability of latanoprost in an ophthalmic lipid emulsion using polyvinyl alcohol, Int. J. Pharm., 305 (2005) 176-179.

[11] C. Ladaviere, T. Delair, A. Domard, C. Pichot, B. Mandrand, Covalent immobilization of biological molecules to maleic anhydride and methyl vinyl ether copolymers - A physico-chemical approach, J. Appl. Polym. Sci., 71 (1999) 927-936.

[12] P. Abiman, G.G. Wildgoose, A. Crossley, J.H. Jones, R.G. Compton, Contrasting pK(a) of protonated bis(3-aminopropyl)-terminated polyethylene glycol "Jeffamine" and the associated thermodynamic parameters in solution and covalently attached to graphite surfaces, Chemistry-a European Journal, 13 (2007) 9663-9667.

[13] R. Nidetz, J. Kim, Directed self-assembly of nanogold using a chemically modified nanopatterned surface, Nanotechnology, 23 (2012).

Chapter 4 Tumor Markers Detection from Colorectal Cancer Based on Antibody Microarrays‡

‡ This chapter is base on the following contributions:

- Z.G. Yang, Y. Chevolot, Y. Ataman, G. Choquet-Kastylevsky, E. Souteyrand, E. Laurenceau, Cancer Biomarkers Detection Using 3D Microstructured Protein Chip: Implementation of Customized Multiplex Immunoassay, Sens. Actuators B, in presss doi.org/10.1016/j.snb.2011.11.055 (2011)
- Z.G. Yang, Y. Chevolot, V. Dugas, N. Xanthopoulos, V. Laporte, T. Delair, Y. Ataman-Önal, G. Choquet-Kastylevsky, E. Souteyrand, E. Laurenceau. Antibody microarray based on different chain-length amino surfaces for the detection of tumor markers involved in colorectal cancer. Submitted to Biomaterials 2012

4.1. Introduction

Antibody microarray has played a significant role for detection and quantification of proteins in complex biological samples as a high throughput technique. The ability of antibodies to perform highly specific protein capture makes this approach particularly well suited for detecting rare analytes in highly heterogeneous mixtures, like cancer biomarkers in serum [1-3]. However, as presented in the previous chapter, many parameters such as surface chemistry, spotting buffer, blocking procedure, probe concentration, etc., influence protein immobilization and may significantly influence analytical performances (sensitivity, specificity, limit of detection) of antibody microarray [4, 5].

Thus, this chapter aims to achieve a first proof of concept of the validity of our customized microarrays applied for colorectal cancer (CRC) diagnosis. This study was conducted in collaboration with bioMérieux and CHU Saint-Etienne. Indeed, the choice of cancer biomarkers to target can be done only in close collaboration with clinicians and researchers in oncology. For the first validation, we are developing a sandwich immunoassay as pictured on Figure 4-1. Capture and detection antibodies were both monoclonal antibodies capable to specifically recognize different domains of targeted antigens. From Table 1-5 (Chapter 1), 3 tumor marker antigens have been selected (CEA, CA 19-9, Hsp 60) and their corresponding monoclonal antibodies was kindly provided by BioMérieux. Carcinoembryonic antigen (CEA) acts as one common oncofetal antigen belonging to the immunoglobulin superfamily. CEA has been used for many years as a biomarker of CRC as well as cancers developing in other tissues. High CEA levels are specifically relative to colorectal cancer (CRC) progression, and increased levels of the marker are expected to fall following colorectal cancer surgery [7]. Carbohydrate antigen (CA) 19-9 is the second most investigated gastrointestinal tumor marker [8]. Hsp 60, from the Heat Shock Protein family, is a marker of cell stress often found in cancer. In addition, PDI and DEFA6, two tumor markers recently identified by bioMérieux as involved in CRC, were also introduced in the study. At least, p53 often present but non-specifically in cancer sera, was added because it is considered as universal marker.

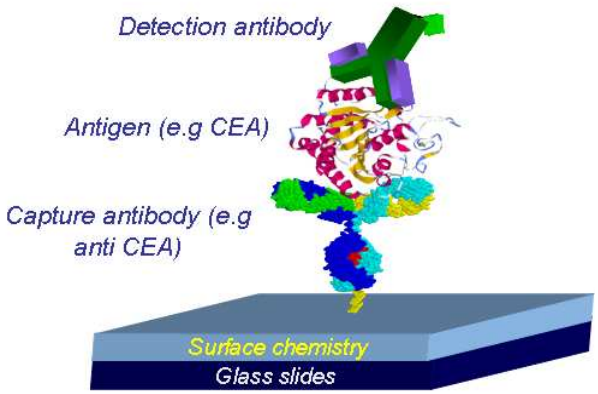

Figure 4-2 Schematic illustration of sandwich immunoassay on antibody microarray, capture antibody was immobilized on chemically functionalized surface, incubated with antigen/serum and detected with labelled detection secondary antibody.

Additionally, low concentration (nM range or even lower) of biomarkers should be detected in patients'sera. Thus high sensitivity assay is desirable and validation from clinical samples is essential. Herein, in this chapter, the selected anti-tumor marker antibodies (anti-CEA, anti-CA19-9, anti-Hsp60, anti-PDI, anti-DEFA6 and anti-p53 antibodies) were immobilized on as the various surface chemistries described in Chapter 2. Biological activity of the immobilized antibodies was evaluated by recognition of tumor markers detected using fluorescent labelled detection anti-tumor marker antibodies. The capture antibody and detection antibody concentration were optimized as well as the analytical performance according to various spotting conditions. Finally, under the optimal conditions, our antibody microarray was validated by evaluation of sera from colorectal cancer patients and healthy donors.

4.2. Experimental

4.2.1. Materials, chemical and biological products

Anti-CEA, anti-Hsp60, anti-PDI, anti-DEFA6 and anti-CA19-9 capture antibodies as well as biotinylated (anti-Hsp60-biot, anti-PDI-biot, anti-DEFA6-biot, anti-CA19-9-biot) or DyLight-labeled (anti-CEA-DL647) detection antibodies and tumor markers (Hsp60, PDI, DEFA6, CA19-9) were kindly supplied by Yasemin Ataman-Önal (Biomarkers Department, bioMérieux, France). p53 was obtained from Sigma-Aldrich. Capture anti-p53 antibody and biotinylated anti-p53 antibody (both monoclone) were supplied by Thermo Scientific (USA). All proteins were stored as aliquot at -20°C or -80°C following manufacturer specifications.

Cy3-conjugated goat anti-mouse antibody (IgG-Cy3), streptavidin-Cy3, myoglobin, bovine serum albumin (BSA), glycerol, polyvinylalcohol (PVA), sodium acetate, were purchased from Sigma-Aldrich (St. Quentin Fallavier, France). Tween 20 was purchased from Roth-Sochiel (Lauterbourg, France).

0.1 M sodium acetate was dissolved to obtain the sodium acetate buffer (pH 4.5). PBS 1X (pH 7.4) was prepared by dissolving the content of one pouch of dried powder in 1 L of ultrapure water. Carbonate buffer (pH 9.6) was prepared by dissolving one pouch of powder in 100 ml ultrapure water. Ultrapure water (18.2 MΩ) was delivered by an Elga water system. Washing buffer contained PBS 1X and 0.1 % Tween 20 (PBS-T) at pH 7.4. Blocking solution was prepared by dissolving 4 or 10 g of BSA in 100 ml of PBS 1X.

Four colorectal cancer sera and two healthy donor sera collected at Saint-Etienne Hospital (France) were kindly provided by Dr. Claude Lambert.

4.2.2. Surface modification of 3D-microstructured glass slides

The 3D-microstructured surfaces of glass sides were functionalized as described in Chapter 2 with COOH, NHS, Jeffamine, chitosan (these four surface derived from TDSUM silane), APDMES, CMD and MAMVE (CMD, MAVE grafted on APDMES or Jeffamine as specified in the text).

4.2.3. Multiplex immunoassays with purified tumor markers

Capture antibodies (anti-CA19-9, anti-CEA, anti-Hsp60, anti-PDI and anti-DEFA6) were spotted in triplicate (or more) at various concentrations onto chemically functionalized microstructured glass slides. Contact spotter (Microgrid II, Biorobotics) a non-contact spotter (SciFlexarrayer S3, Scienon, Germany) was used for spotting. Preliminary experiment was achieved by spotting proteins in PBS (pH 7.4)containing 20 % glycerol on TDSUM derived surfaces (COOH, NHS, chitosan, CMD and MAMVE) At the mean time, fluorescent labelled proteins, IgG-Cy3, streptavidin-Cy3 and BSA-F647, were spotted at 0.1 µM in the same experimental conditions in order to have quality control of protein immobilization. The design of the protein microarray in detail was illustrated in Figure 4-3.

Capture antibodies and fluorescent labelled proteins were allowed to react with the surface under saturated water vapours overnight at 37 ^{o}C. Then slides were washed for 2 x 5 min with PBS and 1 x 5 min PBS-T, and dried by centrifugation for 3 min at 1300 rpm.

Then slides were blocked with 4 % BSA/PBS solution to limit further non specific adsorption phenomena, and incubate for 2 hrs at room temperature, washed for 3 x 5 min with PBS-T and then dried.

Microwells were then incubated with antigens (CEA, CA19-9, Hsp60, PDI, DEFA6 in 1% BSA-PBS) at different concentrations (CEA, PDI and DEFA6: 0.01 nM, 0.1 nM, 1 nM, 10 nM, 50 nM, 100 nM and 500 nM; CA19-9: 10 U/ml, 30 U/ml, 50 U/ml, 100 U/ml, 250 U/ml, 500 U/ml, 1000 U/ml). The slides were left to react for 1 h at 37^{o}C in a water-saturated atmosphere, thoroughly rinsed for 3 x 5 min with PBS-T and then dried.

Microwells were then incubated with 5 μM labelled detection antibodies (anti-CEA-DL647, anti-CA19-9-biot, Hsp60-biot, PDI-biot, DEFA6-biot in 1% BSA-PBS-T 0.1%), for 1 h at 37 ^{o}C in a water-saturated atmosphere. After washing and drying, microwells were then incubated with streptavidin-Cy3 for 1 hr at 37^{o}C in a water-saturated atmosphere, except for the wells incubated with anti-CEA-DL647. The slides were washed for 3 x 5 min with PBS-T and for 1 min with water, followed by drying with centrifugation. The scheme of the sandwich assay on the glass slides was illustrated in Figure 4.2

On the basis of preliminary experiment, the protein microarray was spotted with several buffers such as: sodium acetate (Ac, pH 4.5), PBS (1x, pH 7.4) and sodium carbonate (Car, pH 9.6), with additive (0.05 % PVA). Besides, the CMD and MAMVE surfaces are both derived from APMDES. The blocking procedure was optimized using 10% BSA-PBS-T at room temperature. The design of other protein microarray design will be illustrated in detail Figure 4-6.

4.2.4. Multiplex immunoassays with colorectal cancer sera

Sodium acetic (pH=4.5), and carbonate (pH=9.6) were used as the buffer with additive of 0.05 v % PVA. 10 μM capture antibody (anti-CEA, anti-Hsp60, anti-PDI, anti-DEFA6 and anti-p53) and 0.6 μM for goat anti rabbit IgG-Cy3 as control proteins. The proteins were spotted on glass slides functionalized with three optimized surfaces (NHS, MAMVE 216 grafted with APDMES, and chitosan). The detail of the immobilization maps was presented in Figure 4-11.

After incubation and blocking with the same protocol of purified tumor markers assay, slides were incubated with 10 nM antigens (CEA, Hsp60, PDI, DEFA6 and p53 in 4% BSA/PBS) as positive control and sera (2 normal and 4 colorectal cancer sera in 4% BSA/PBS_T 0.1%) as well as buffer (4% BSA/PBS) for negative control. The slides were left to react for 1 h at room temperature in a water-saturated atmosphere, thoroughly washing and drying. Then the slides were allowed to incubated with 0.5 μM (4% BSA/PBS_T 0.1%) respective biotinylated antibody and streptavidin-Cy3 at 0.05 mg/ml (1% BSA/ PBS), followed by washing and drying, which was performed with the same with above mentioned protocol.

4.2.5. Fluorescence scanning

Slides were scanned with the microarray scanner, GenePix 4100A software package (Axon Instruments) at wavelengths of 532 nm or 635 nm with the same photomultiplier tube (PMT) gain. The fluorescence signal of each protein was determined as the average of the median fluorescence signal of several replicates, and the value was divided by the signal background (median fluorescence) from surface to get the signal-to-noise ratio (SNR) value.

The threshold value (cut-off) for the determination of LOD (Limit of Detection) of antigen was calculated as followed:

Cut off =Mean of median blank + 3 SD (3-1)

where SD represents standard deviation. The dynamic range corresponded to the ratio of high detection limit over low detection limit of each immunoassay.

For the sera assay, the cut-off was determined from the mean of all the replicates of the healthy donors plus 3 times of standard deviation (SD).

4.3. Results and discussion

4.3.1. Optimization of antibody microarray with purified tumor markers

To maintain optimal biological activity of immobilized antibodies, parameters such as capture and detection antibody concentration, spotting buffer, and surface chemistry, have to be optimized for implementation of multiplex sandwich immunoassays for the detection of tumor markers involved in colorectal cancer (CEA, Hsp60, PDI, DEFA6 and CA19-9).

Capture anti-tumor marker monoclonal antibodies were immobilized on chemically functionalized microstructured glass slides at various concentrations in different spotting buffers. They were allowed to interact with their respective tumor markers at various concentrations, and then biological recognition was detected using secondary labelled anti-tumor marker monolonal antibodies (biotinylated or fluorescent label). Finally, incubation with Cy3-labeled streptavidin allowed revelation of the formed sandwich.

4.3.1.1. Influence of capture antibody concentration

Capture anti-CA19-9, anti-CEA, anti-Hsp60, anti-PDI and anti-DEFA6 antibodies were spotted in triplicates, at various concentrations (0.1 µM, 1 µM, 5 µM and 10 µM) in PBS 1X (pH 7.4) with 20% glycerol as additive, on chemically functionalized microstructured glass slides (COOH, NHS, CMD, MAMVE, chitosan). The spotting design is presented in Figure

4-3. Fluorescent labelled proteins (IgG-Cy3, streptavidin-Cy3, BSA-F647) were also spotted for control quality of protein immobilization and surface chemistry.

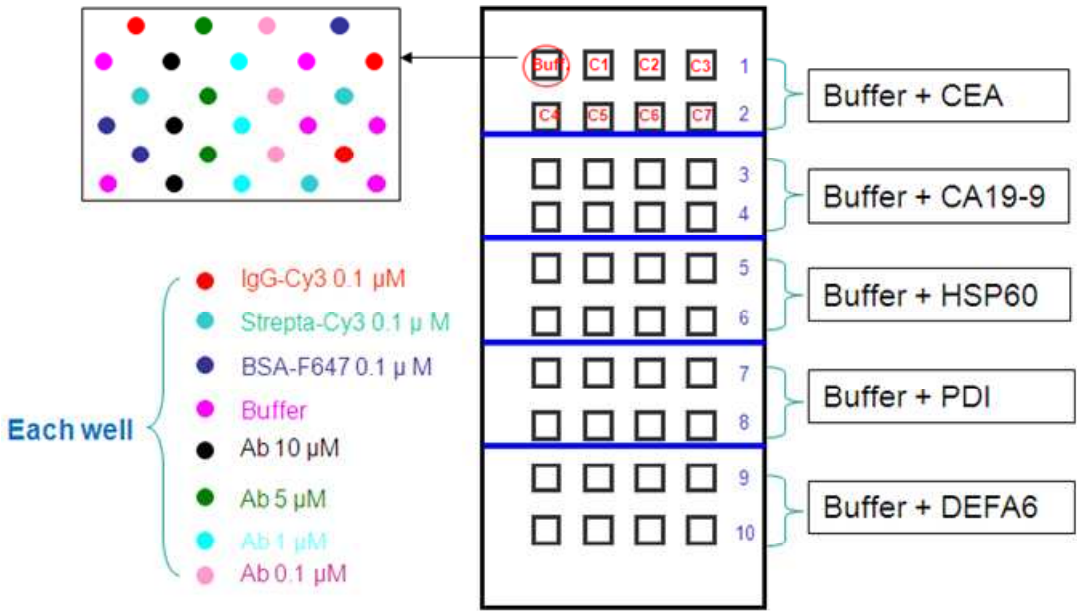

Figure 4-3 Scheme of microarray design: For lines 1 and 2, capture anti-CEA antibody was spotted at 0.1, 1, 5 and 10 µM according to the map. Similarly, capture anti-CA19-9 antibody, anti-HSP 60 antibody, anti-PDI antibody and anti-DEFA6 antibody were spotted in lines 3-4, 5-6, 7-8, and 9-10, respectively. The corresponding tumor markers were then incubated at concentrations ranking from C1 to C7 (C1=0.01 nM, C2=0.1 nM, C3=1 nM, C4=10 nM, C5=50 nM, C6=100 nM, C7=500 nM for CEA, Hsp60, PDI and DEFA6; C1=10 U/ml, C2=30 U/ml, C3=50 U/ml, C4=100 U/ml, C5=250 U/ml, C6=500 U/ml, C7=1000 U/ml for CA19-9). Buff. stands for buffer (1% BSA-PBS).

Figure 4-4 illustrates the influence of capture anti-Hsp60 antibody concentration immobilized on NHS surface for the detection of Hsp60. All anti-tumor marker antibody/tumor marker systems studied displayed the same behaviour on all tested surfaces. Low capture antibody concentrations, typically 0.1 µM to 1 µM, were not sufficient to detect significant amount of tumor marker in our miniaturized immunoassay (slope = 0). Fluorescence scanning image showed the low fluorescence signal of the corresponding spots. From 5 to 10 µM, SNR increased with tumor marker concentration, and the best dynamic range was obtained with 10 µM (slope = 38.1, R^2 = 0.98). Therefore, capture anti-tumor marker antibody concentration in printing buffer was set at 10 µM in the following.

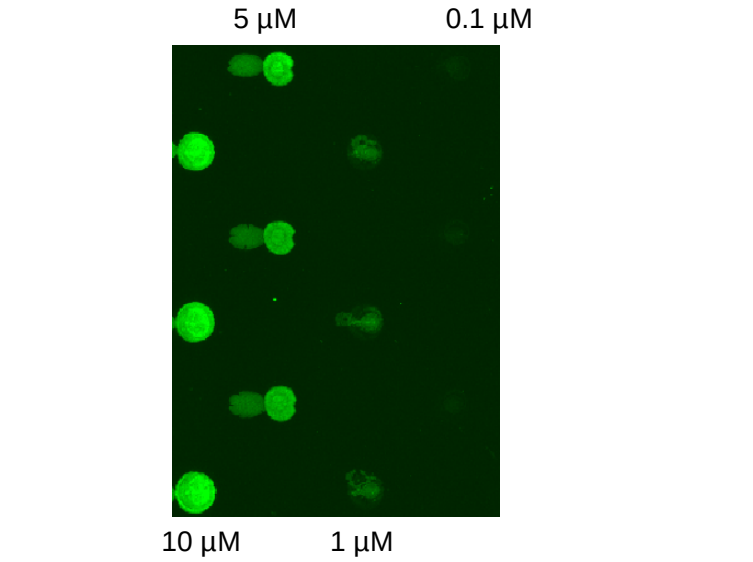

Figure 4-4 Effects of various concentrations of capture anti-Hsp60 antibody on the detection of Hsp60 tumor antigen. Fluorescence scanning images of the spots at different capture antibody concentrations were shown in upper; from left to right columns: 10, 5, 1 and 0.1 µ M of capture anti-Hsp60 antibody (triplicates) incubated with Hsp60 at 10 nM, according to the spotting map of Figure 4-3. For 5 µ M of capture anti Hsp60 antibody, the slope of the curve determined as 15.2 with R^2 = 0.94; for 10 µ M of capture anti Hsp60 antibody, the slope of the curve determined as 38.1 with R^2 = 0.96.

Additionally, two concentrations of biotinylated anti-Hsp60 detection antibody (0.5 µM and 5 µM) were tested to improve detection of Hsp60 in our miniaturized sandwich immunoassay on NHS surface. As shown in Figure 4-5, SNR value from the two concentrations have no obvious differences, indicating that the detection antibody

concentration has tiny effects on the fluorescence signal. Therefore, detection antibody concentration was set at 0.5 μM from the economic viewpoint in the following experiments.

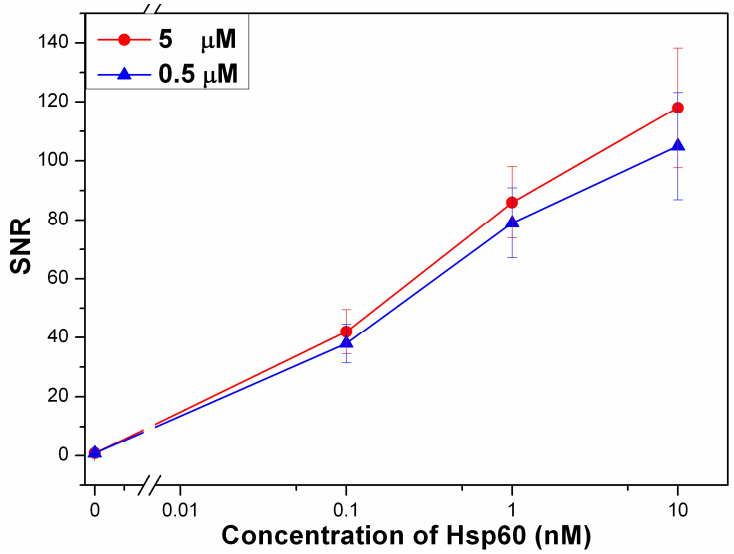

Figure 4-5 Effects of the biotinylated antibody concentration (detection anti-Hsp60 antibody at 5 and 0.5 μM) on the detection of Hsp60 tumor antigen (0.1 nM, 1nM and 10 nM), the capture anti-Hsp60 antibody was spotted at 10 μ M in 20 % glycerol /PBS on NHS surface.

4.3.1.2. Influence of spotting buffer pH

As discussed in Chapter 3, pH of spotting buffer has great effect on the immobilization efficiency of proteins and depends on surface chemistry. Moreover, PVA as the additive instead of glycerol was shown to give more regular spot morphology and slightly improve protein immobilization. In order to obtain regular and homogeneous spots, 0.05% PVA was added in each spotting solution.

Four capture anti-tumor antibodies (anti-CEA, anti-Hsp60, anti-PDI, anti-DEFA6) were spotted at 10 μM in different pH buffers (sodium acetate pH 4.5, PBS pH 7.4 and sodium carbonate pH 9.6) on aminated surfaces (APDMES, Jeffamine, chitosan) and on amine reactive surfaces (NHS, CMD and MAMVE grafted on APMDES). The detail of the microarray design was illustrated in Figure 4-6.

Then capture antibodies were allowed to interact with their tumor markers at various concentrations. Detection of the biological recognition was performed using biotinylated monoclonal antibodies directed against another epitope of the corresponding tumor marker, followed by incubation with Cy3 labelled streptavidin

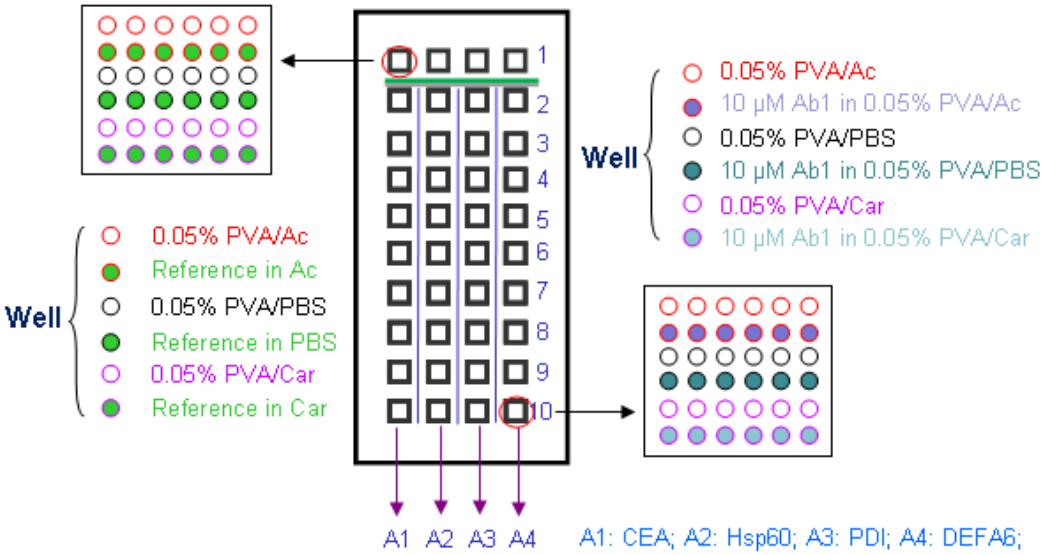

Figure 4-6 Scheme of antibody microarray design. Line 1: each well contains one fluorescent labelled protein (reference) at 0.6 µ M (Column A1: IgG-Cy3; Column A2: myoglobin-Cy3; Column A3: streptavidin-Cy3; Column A4: replicate of Column A1) spotted in the different spotting buffers. Lines 2 to 10: 10µM of capture anti-tumor marker antibody (Column A1: anti-CEA; Column A2: anti-Hsp60; Column A3: anti-PDI; Column A4: anti-DEFA6) were spotted in the different spotting buffers. The corresponding tumor markers were then incubated at various concentrations from Line 2 to 10 (Line 2: 0; Line 3: 0; Line 4: 50 nM; Line 5: 0.001 nM; Line 6: 0.01 nM; Line 7: 0.1 nM; Line 8: 1 nM; Line 9: 10 nM; Line 10: 50 nM, for CEA and Hsp 60) (Line 2: 0; Line 3: 0; Line 4: 500 nM; Line 5: 0.1 nM; Line 6: 1 nM; Line 7: 10 nM; Line 8: 50 nM; Line 9: 100 nM; Line 10: 500 nM, for PDI and DEFA6). Line 3 and Line 5 were replicated for incubation with/without detection antibody and streptavidin, respectively, in order to observe their non-specific adsorption.

Figure 4-7 presents the effects of pH buffer on the biological activity of anti-CEA antibody immobilized on APDMES, Jeffamine and chitosan surfaces for the detection of CEA. The other three anti-tumor marker antibody/tumor marker systems (anti-Hsp60/Hsp60, anti-PDI/PDI and anti-DEFA6/DEFA6) displayed the same behaviour on each aminated surface (See Annex 1). Typically, SNR increased with the increasing tumor marker concentration. The best immunoassay response was obtained with carbonate buffer (pH 9.6) in agreement with data obtained for IgG-Cy3 immobilized on the different amino-functionalized surfaces (Figure 3-6 A). This result demonstrated that carbonate buffer (pH 9.6) as spotting buffer not only facilitated the immobilization of antibodies on aminated surfaces but also allowed to maintain their biological activity. Therefore, carbonate buffer at pH 9.6 with 0.05% PVA was chosen as spotting buffer on amino-functionalized surfaces.

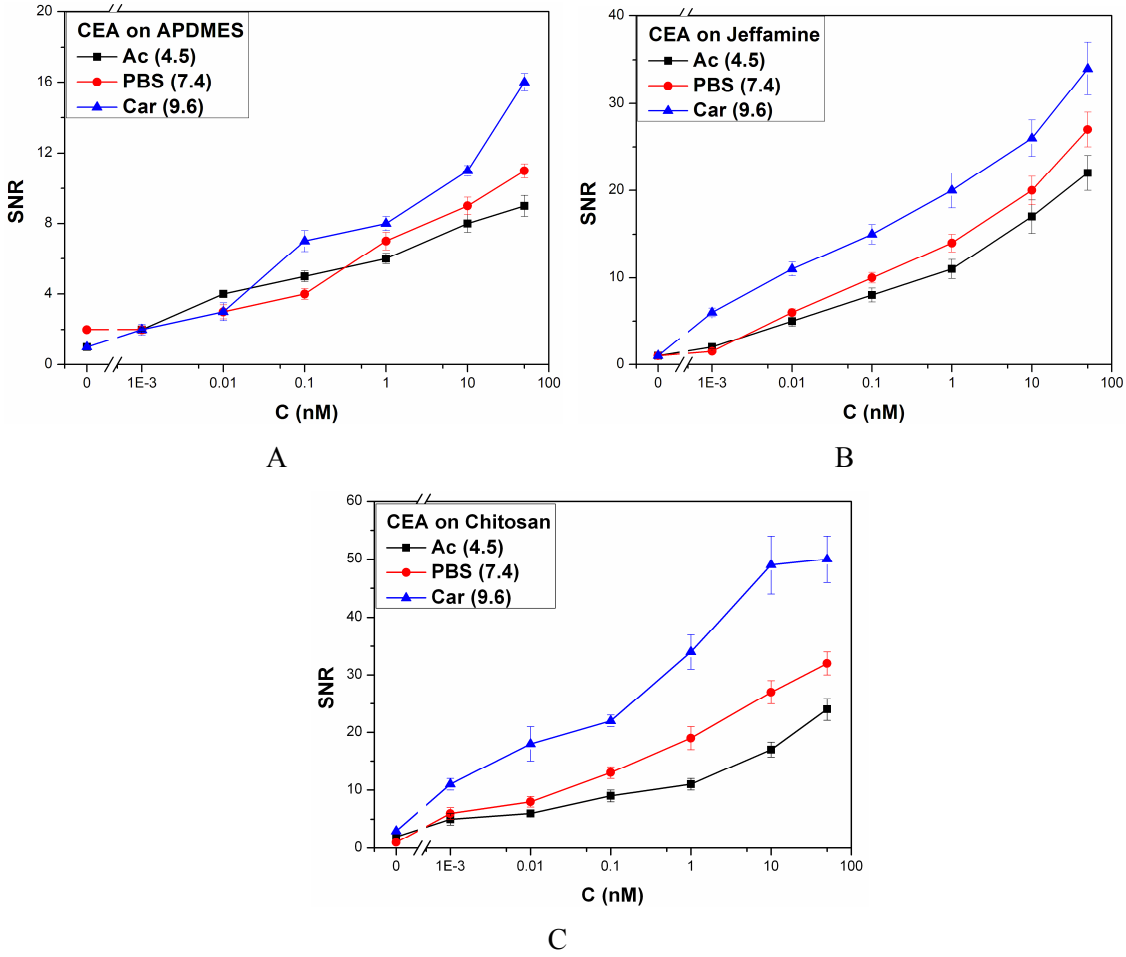

Figure 4-7 Signal to noise ratio (SNR) relative to biological recognition of anti-CEA antibody spotted in different pH buffers on APDMES (A), Jeffamine (B) and chitosan (C) surfaces, versus CEA concentrations.

Figure 4-8 presents the effects of pH buffer on the biological activity of the four anti-tumor marker antibodies immobilized on NHS, CMD and MAMVE surfaces for the detection of 50 nM of their respective tumor markers. On NHS and CMD surfaces, the best spotting buffer was found to be sodium carbonate (pH 9.6) for all anti-tumor marker antibody/tumor marker systems tested. On MAMVE surface, the best buffer for all the four systems was sodium acetate (pH 4.5). These results are in agreement with those obtained for the immobilization of IgG-Cy3 (Section 3.3.4).

From both results we can conclude that conditions (surface chemistry with spotting buffer and concentration) for optimal antibody immobilization onto chemically functionalized surface led to optimal biological recognition of the immobilized antibody for its specific antigen. Furthermore, in optimal spotting conditions, the highest biological activity (highest SNR) for immobilized anti-CEA, anti-Hsp60 and anti-PDI was obtained on NHS surface with sodium carbonate buffer, whereas it was obtained on MAMVE or NHS surfaces for anti-PDI

with sodium acetate or sodium carbonate buffers. These results demonstrated that it is essential to determine the best conditions for each protein.

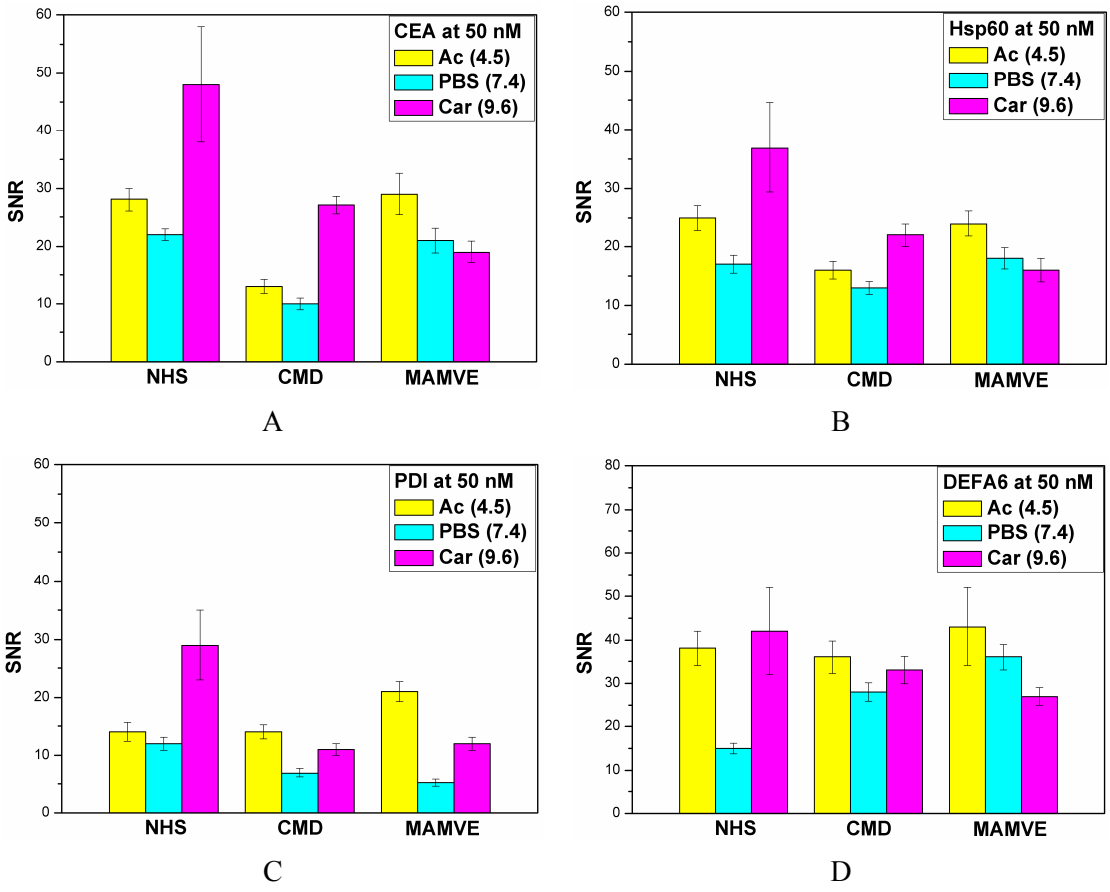

Figure 4-8 Signal noise ratio (SNR) relative to biological recognition of anti-CEA (A), anti-Hsp60 (B), anti-PDI (C) and anti-DEFA6 (D) spotted in different pH buffers on NHS, CMD and MAMVE surface, for 50 nM of their respective tumor marker.

4.3.1.3. Detection of tumor markers on amino functionalized surfaces

Taking into account the results presented above, the four capture antibodies (anti-CEA, anti-Hsp60, anti-PDI and anti-DEFA6) were spotted at 10 µM in carbonate buffer (pH 9.6) with 0.05% PVA on the three aminated surfaces, and evaluated for the detection of various concentrations of their respective tumor markers. Previous study showed that CEA and Hsp60 had more sensitive responses than PDI and DEFA6 on various surfaces including chitosan surface. As a consequence, we have adapted the concentration. CEA and HSP60 were set from 0.001 nM to 50 nM while PDI and DEFA6 were set from 0.1 nM to 500 nM. Figure 4-9 illustrates the results of multiplex immunoassays. Comparison of the graphs demonstrated that, on the three amino-functionalized surfaces, SNR increased with increasing the tumor

marker concentration. SNR was proportional to the biological recognition between the anti-tumor marker antibody and its tumor marker.

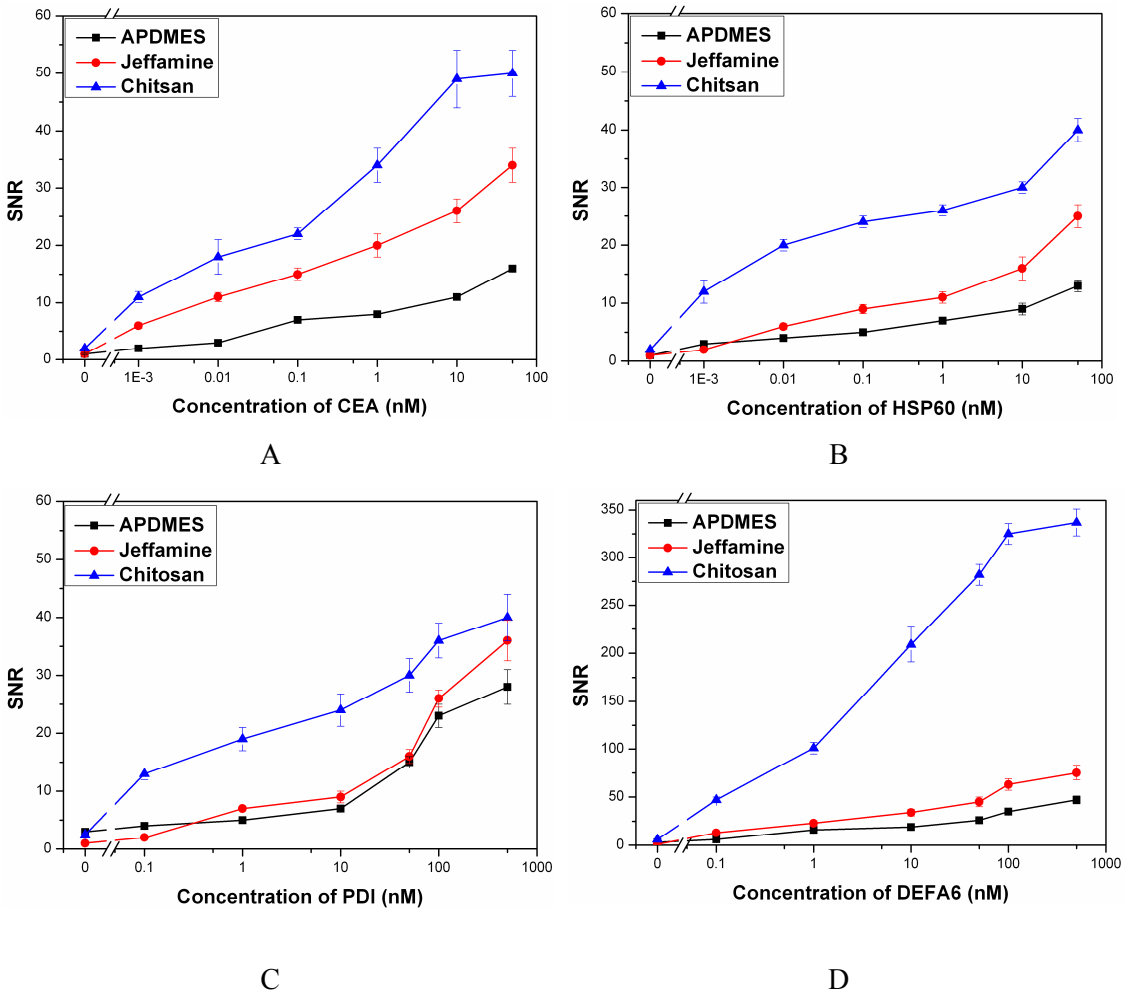

Figure 4-9 Detection of tumor markers in multiplex immunoassays on aminated surfaces; A: CEA, B: Hsp60, C: PDI and D: DEFA6; capture anti-tumor marker antibody concentration was 10 µM spotted in carbonate buffer pH=9.6 with 0.05% PVA as additive.

Moreover, the range of SNR values depended both on the tumor marker and on the kind of aminated surface. All antibody/antigen systems displayed the lowest SNR on APDMES surface and the highest one on chitosan surface, Jeffamine surface showing an intermediate behaviour. However, the most significant variations were obtained for the detection of DEFA6 with up to 7 times SNR on chitosan surface than on Jeffamine or APDMES surfaces (Figure 4-9 D). For the other tumor markers, a maximum of 5 times SNR was obtained on chitosan surface compared to APDMES surface. These results confirmed that the binding capacity of chitosan surface for the immobilisation of antibodies is higher than that of Jeffamine and APDMES surfaces (see Chapter 3). Moreover, chitosan surface allowed

maintaining the biological activity of the immobilized anti-tumor marker antibodies in order to efficiently detect tumor markers.

Additionally, SNR curves obtained for CEA and DEFA6 on chitosan surface showed saturation plateau from 10 nM and 100 nM of tumor marker, respectively. This result suggested that maximum binding capacity of biologically active immobilized antibodies was reached. For Hsp60 and PDI, the saturation plateau was not reached in the tested range indicating that the detection of these two tumor markers was less efficient than the detection of CEA and DEFA6. In the case of PDI, the signal remains to background level until 10 nM. Thus, chitosan surface will be selected for the implementation of antibody microarray to detect tumor markers in colorectal cancer sera.

4.3.1.4. Analytical performances of antibody microarray

The evaluation of the analytical performances of our antibody microarray was performed with the five capture antibodies (anti-CEA, anti-Hsp60, anti-PDI, anti-DEFA6 and anti-CA19-9) immobilized at 10 µM in PBS (pH 7.4) with 20% glycerol as spotting buffer, on COOH, NHS, CMD, MAMVE and chitosan surfaces. Spotting buffer used was not the optimal one because this study was done before optimization of experimental conditions. However, we could suppose that results would be better with the optimal buffer. The biological activity of immobilized antibodies was followed as SNR versus tumor marker concentrations.

Figure 4-10 shows results of multiplex immunoassays of the five tumor antigens tested on the various surface chemistries developed for protein microarray implementation. Comparison of the graphs indicates that signal to noise ratio (SNR), which is proportional to the biological interaction between the anti-tumor marker antibody and its tumor marker, increases with increasing tumor marker concentration and depends not only on the tumor marker but also on the surface chemistry. Indeed, SNR obtained for CEA and Hsp60 are around 10 times more than those for PDI and DEFA6. All five antibody/antigen systems display lower fluorescence signal on COOH surface than on the other surfaces. This result suggests that the immobilization of antibodies by physical adsorption on COOH surface leads to low immobilization rate according to results of Section 3.3.1 (Figure 3-3 with PBS), and/or to partial loss of biological activity. Although on chitosan surface, antibodies were also immobilized by physical adsorption with relatively lower immobilization capacity than covalent binding on CMD and MAMVE surfaces (Figure 3-3 with PBS). SNR obtained from sandwich assay on chitosan surface is significantly stronger than that on COOH surface.

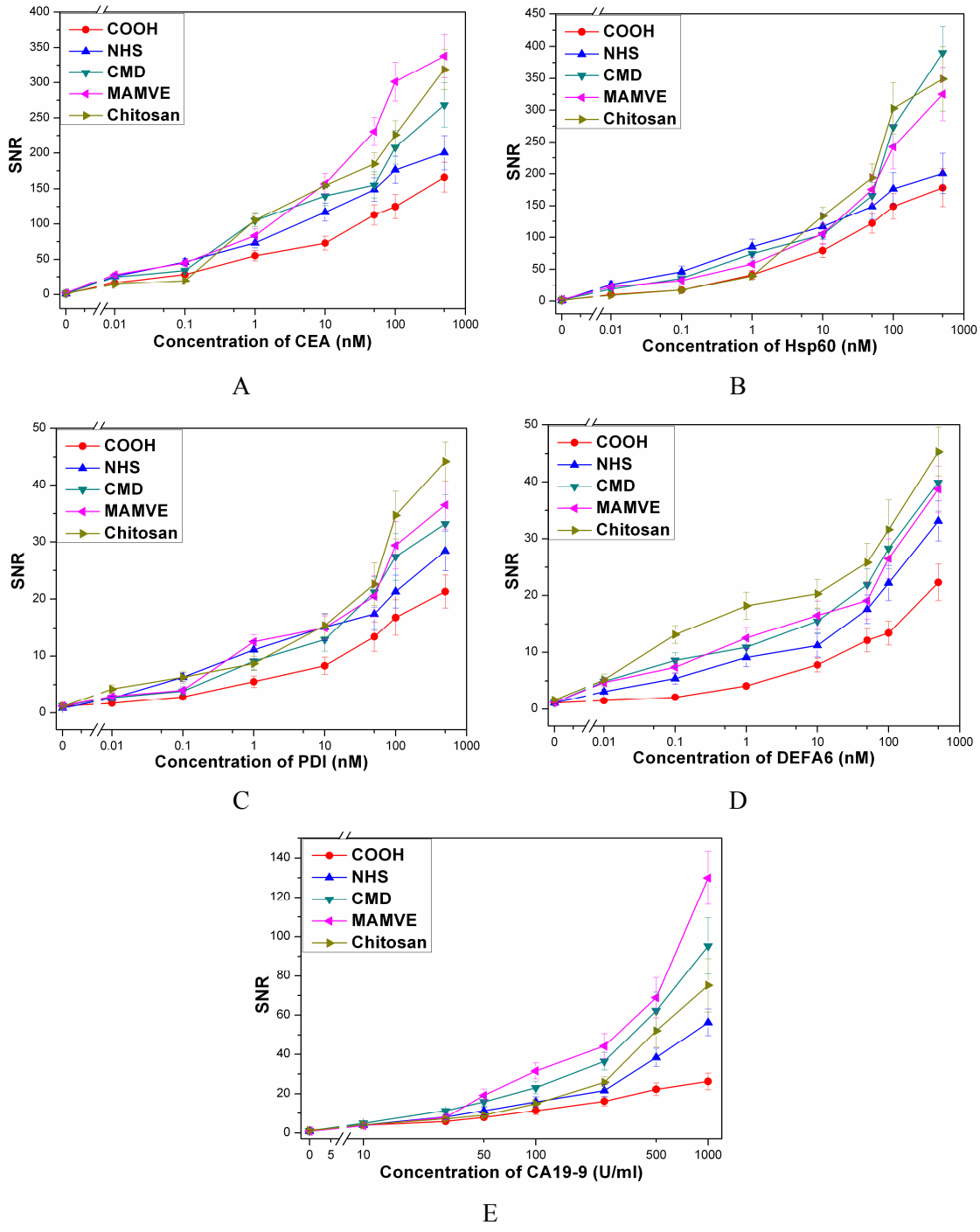

Figure 4-10 Multiplex immunoassays of tumor markers on functionalized protein chip surfaces; A: CEA, B: Hsp60, C: PDI, D: DEFA6 and E: CA19-9. Capture anti-tumor marker antibody concentration is 10 µM.

Moreover SNR obtained on chitosan surface were in the same range for CEA, Hsp60, CA19-9 and PDI antigens or even stronger for DEFA6 antigen than on covalent coupling surfaces (NHS, CMD and MAMVE). Because of its high molecular weight and its hydrophilic character, functionalization of glass slide with chitosan polymer increases the specific surface available for antibody immobilization. This enables to maintain immobilized

proteins away from the surface, in the aqueous solution, allowing a better preservation of biological activity. According to IgG results presented in Figure 3-3, covalent immobilization of anti-tumor marker antibodies is more efficient than physical adsorption in most cases (CEA, Hsp60, CA19-9, and PDI) to keep biological activity of immobilized proteins. Furthermore, surfaces functionalized with hydrophilic reactive polymers such as CMD or MAMVE, exhibit better tumor marker detection probably because they display larger specific area for antibody immobilization.

Table 4-1 Optimal analytical performances of tumor markers immunoassays on functionalized antibody microarray

Tumor antigens	Optimal surfaces	LOD	Dynamic range
CEA	MAMVE/CMD	10 pM	4.7 log/4.0 log
Hsp60	NHS/Chitosan/MAMVE	10 pM	4.7 log/4.0 log/ 4.7 log
PDI	NHS	10 pM	4.7 log
DEFA6	Chitosan	10 pM	4.7 log
CA19-9	NHS/CMD	10 U/mL	3.0 log/3.0 log

The limit of detection (LOD) and the dynamic range were determined to evaluate analytical performances of our multiplex immunoassays (Table 4-1). The results clearly demonstrate that performances of the immunoassays depend on both the antibody to be immobilized and on the surface characteristics. Limit of detection as low as 10 pM (10 U/ml for CA19-9) and dynamic range as wide as 4.7 log (3.0 log for CA19-9) were obtained for tumor markers on the optimal surfaces. In classical immunoassays such as ELISA, the limit of detection for CEA is about 1 ng/ml (5.5 nM) and that of CA19-9 is about 25 U/ml with a dynamic range around 2.0 log (CEA ELISA Catalog # EA-0104, CA 19-9 ELISA Catalog #EA-0102, Signosis Inc. CA, USA). Other research groups working on the development of a highly sensitive electrochemical immunosensor to quantify CEA reported a limit of detection at 0.01 ng/ml (55 pM) [9]. Table 4-1 presents optimal antibody microarray surfaces for the optimal detection of the five tumor markers tested. Detection of Hsp60, PDI and CA19-9 could be performed on NHS surface, whereas detection of CEA should be performed on MAMVE surface and detection of DEFA6 on chitosan surface.

These results demonstrate that it is important to adapt surface chemistry to the immobilized protein and to detection criteria. A similar approach was reported in the work of Angenendt et al [10] where they screened 11 different array surfaces of both types and compared them with respect to their detection limit, inter- and intra-chip variation, and storage characteristics. There is not a unique surface which suits all antibodies; surface

modifications should be chosen according preliminary experimental data and may depend on the species of antibody to be immobilized. Although it is difficult to predict the suitability of microarray coatings for protein and antibody microarray technology using one protein and one antibody, we can point towards surface modifications that offer outstanding qualities for detection of serum tumor markers involved in colorectal cancer.

In conclusion, according to the analytical performances of each anti-tumor marker antibody/tumor marker system, NHS, MAMVE and chitosan surfaces were selected for the elaboration of antibody microarray to detect tumor markers in colorectal cancer sera.

4.3.2. Antibody microarray validation with colorectal cancer sera

Antibody microarray was elaborated to detect tumor markers in colorectal cancer (CRC) sera. According to optimization results, capture antibodies (anti-CEA, anti-Hsp60, anti PDI and anti-DEFA6) were spotted at 10 µ M in acetate buffer (pH 4.5) and in carbonate buffer (pH 9.6), both with 0.05% PVA, on NHS, MAMVE and chitosan surfaces. Anti-CA19-9/CA19-9 system was removed due to its low sensitivity and dynamic range (Table 4-1). Detection of p53 was introduced in the test. Capture anti-p53 antibody was spotted at 5 µ M in PBS (pH 7.4) with 0.05% PVA instead of optimal conditions due to sample constraint. IgG-Cy3 was also spotted as quality control for antibody immobilization and surface chemistry. The blocking procedure was performed with 10% BSA/PBS-T.

The presence of the 5 tumor markers was examined from 6 serum samples: 2 healthy donor sera and 4 cancer patient sera with histopathologic diagnosis of colorectal cancer (CRC). All human samples were prospectively collected at the CHU Saint-Etienne. Detail of the microarray design was presented in Figure 4-11.

An example of fluorescence scanning images for the recognition of anti-PDI antibody towards PDI tumor marker on MAMVE surface is shown in Figure 4-11. As expected, IgG-Cy3 spotted in acetate buffer (pH 4.5) gave better fluorescence signal than in carbonate buffer (pH 9.6). Moreover, reproducibility and quality of spot morphology of replicates were very clear.

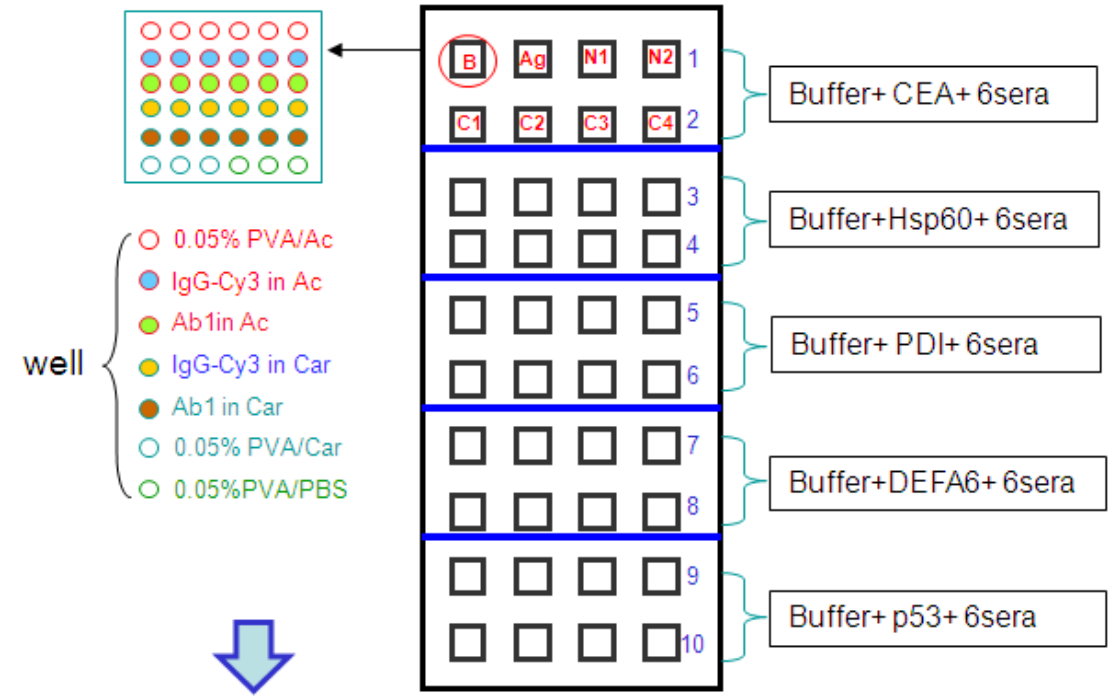

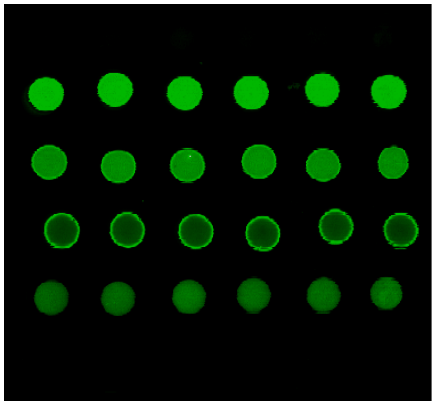

Buffer: PVA/Ac (pH 4.5)

IgG-Cy3 in PVA/Ac (pH 4.5)

PDI in PVA/Ac (pH 4.5)

IgG-Cy3 in PVA/Car (pH 9.6)

PDI in PVA/Car (pH 9.6)

Buffer: first 3 spots PVA/Car, last 3 PVA/PBS

Figure 4-11 Scheme of antibody microarray design and fluorescence scanning images of anti-PDI/PDI recognition on MAMVE surface. Lines 1 and 2 of microarray, anti-CEA antibody was spotted at 10 μM in 0.05 % PVA/Acetate buffer and 0.05 % PVA/Carbonate buffer. Similarly, anti-Hsp60 antibody, anti-PDI antibody, anti-DEFA6 antibody and anti-p53 antibody, were spotted lines 3 - 4, 5 - 6, 7 - 8, and 9 - 10, respectively. The corresponding antigen (Ag at 10 nM) as well as normal (N1 and N2) and colorectal cancer (C1 to C4) sera diluted at 1/250 were then incubated in separate microwells. B stands for buffer. No serum was added in B microwells. IgG-Cy3 was also spotted as quality control.

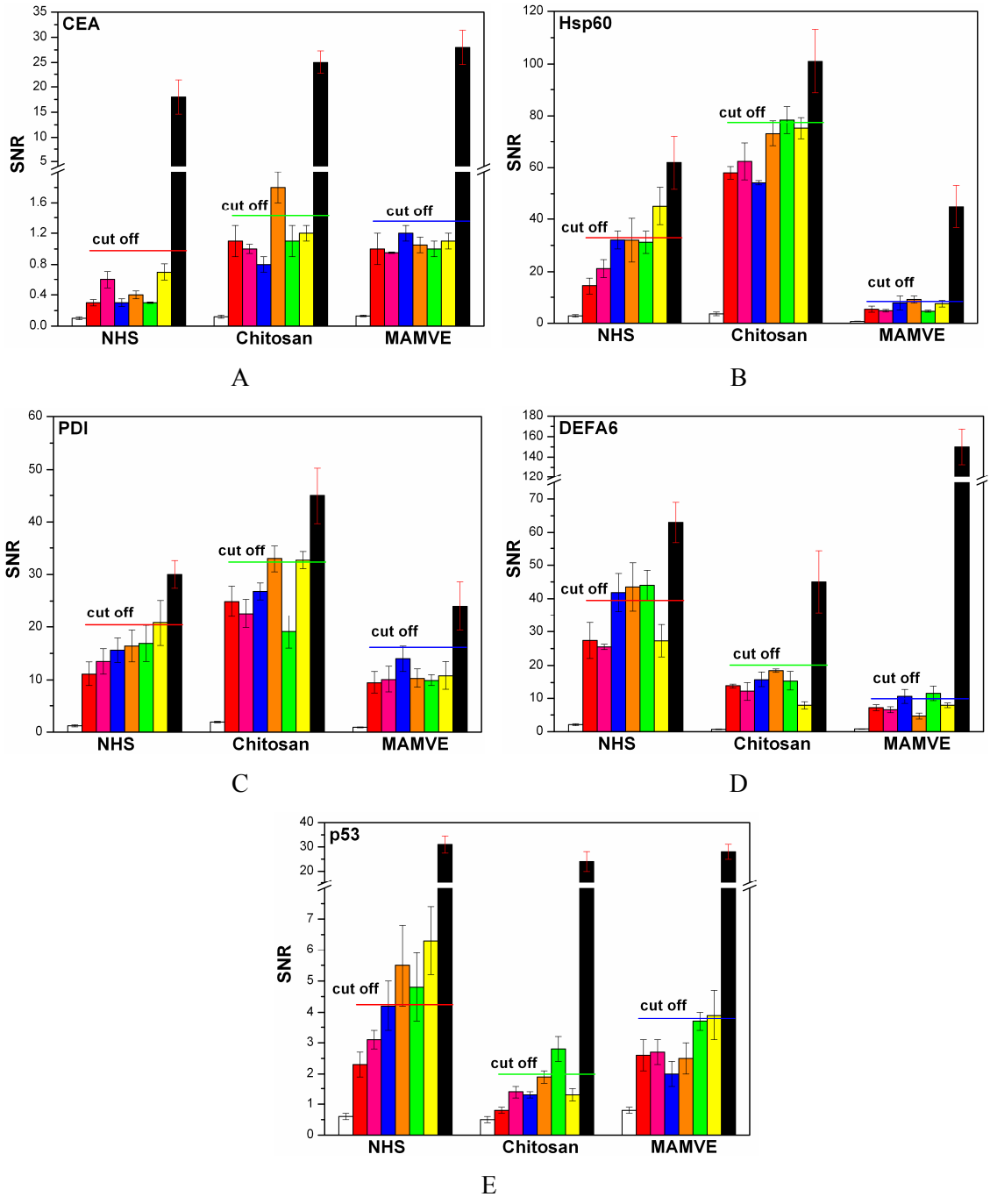

Figure 4-12 Detection of tumor markers (A: CEA, B: Hsp60, C: PDI, D: DEFA6, E: p53) present in colorectal cancer sera using antibody microarray. Anti-tumor marker antibodies were spotted on optimal surface chemistries (NHS, Chitosan and MAMVE). 2 healthy donor sera (red and pink bars) and 4 colorectal cancer sera (blue, orange, green and yellow bars) were tested in our multiplex immunoassay; white bar: buffer signal; black bar: purified tumor marker signal incubated at 10 nM; for each tumor marker, the cut-off value was calculated as the mean SNR + 3 SD of healthy donor sera.

For each anti-tumor marker antibody immobilized on each surface, a cut-off value for the detection of the corresponding tumor marker was calculated from healthy donor sera as

the mean of SNR + 3 SD (Standard Deviation). A serum was considered as positive toward a given tumor marker if the corresponding SNR value was higher than the cut-off. Figure 4-12 presents SNR value of healthy donor sera and colorectal cancer sera compared to this cut-off value.

Table 4-2 Detection of CEA, Hsp60, PDI, DEFA6 and p53 in 4 colorectal cancer sera. anti-tumor marker antibodies were spotted with 0.05 % PVA/Acetate buffer (pH 4.5) or 0.05 % PVA/Carbonate buffer (pH 9.6) onto NHS, chitosan and MAMVE surfaces; for each TAA, the cut-off value was calculated as the mean SNR + 3 SD of healthy donor sera.

TAA/surface	CRC1		CRC2		CRC3		CRC4	
	Ac	Car	Ac	Car	Ac	Car	Ac	Car
CEA/NHS	-	-	-	-	-	-	-	-
CEA/chitosan	-	-	-	+	-	-	-	-
CEA/MAMVE	-	-	-	-	-	-	-	-
Hsp60/NHS	-	-	-	-	-	-	+	-
Hsp60/chitosan	-	-	-	-	+	+	+	-
Hsp60/MAMVE	-	-	+	+	-	-	-	-
PDI/NHS	+	-	-	-	-	-	-	+
PDI/chitosan	-	-	-	+	-	-	-	+
PDI/MAMVE	-	+	-	-	-	-	-	-
DEFA6/NHS	+	+	+	+	+	-	-	-
DEFA6/chitosan	-	-	-	-	+	-	-	-
DEFA6/MAMVE	+	-	-	-	+	-	-	-
p53/NHS*	-		+		+		+	
p53/chitosan*	-		-		+		+	
p53/MAMVE*	-		-		-		+	

* p53 was spotted only in 0.05 % PVA/PBS (pH 7.4) on the three surfaces.

On NHS and chitosan surfaces, only results from antibodies spotted in carbonate buffer (pH 9.6) are given, whereas on MAMVE surface they were from antibodies spotted in acetate buffer (pH 4.5), according to optimization study. Detection of Hsp60, PDI and DEFA6 display higher SNR than detection of CEA and p53. Their amount in cancer sera was lower than 10 nM corresponding to the concentration introduced for the purified tumor marker assay (black bars). Then, for a given tumor marker, the detection of cancer sera according to the cut off value depends on the surface chemistry. One or more tumor markers could be specifically

detected in each cancer serum tested. For example, the "green" cancer serum in Figure 4-12, was positive for Hsp60, DEFA6 and p53 using NHS and chitosan surfaces. Moreover, immobilization of anti-DEFA6 on NHS surface led to the detection of 3 cancer sera on a total of 4 (75%). Combination with anti-Hsp60 or p53 on the same surface led to positive detection of all cancer sera (100%). Of course, other combinations could be proposed to improve the specificity. As previously noted by many researchers, the detection of any individual tumor marker is not able to reach the level of sensitivity which would be useful as diagnostic biomarkers. Not only the combination of several tumor markers on the same surface but also the combination of tumor markers on various surfaces can remarkably increase the positive responses of tested cancer sera.

At last, as can be seen in Table 4-2, the spotting buffer of immobilized anti-tumor marker antibodies could influence the sensitivity of the detection of tumor markers. For example, anti-CEA spotted in carbonate buffer (pH 9.6) on chitosan surface could positively detect CEA in cancer serum CRC2 whereas not if spotted in acetate buffer (pH 4.5). Thus, as we discussed above, the optimization of spotting buffer, surface chemistry, was urgently required for the implementation of efficient immunoassay. This can be well performed on the basis of microarray technology, due to the high throughput and multiplex detection on one assay.

4.4. Conclusions

In this study, we developed antibody microarray for the specific and sensitive detection of tumor markers involved in colorectal cancer: CEA, Hsp60, PDI, DEFA6 and p53. Fast screening and identification of optimal conditions for anti-tumor marker antibody/tumor marker recognition were performed on microstructured glass slides functionalized with various surface chemistries: aminated surfaces (APDMES, Jeffamine, chitosan) and amine reactive surfaces (NHS, CMD, MAMVE).

For the aminated surfaces, influences of amino chain length and physico-chemical characteristics were studied on the binding capacity of antibodies and on the ability to maintain biological activity of the immobilized proteins. For all tested antibody/antigen systems, significant enhanced signal-to-noise ratio was obtained on chitosan surface. Furthermore, carbonate buffer (pH 9.6) was found to be the optimal spotting buffer on the three amino-functionalized surfaces. Immobilization of antibodies on these surfaces occurred *via* physical adsorption. Although APDMES surface displayed more amine density than Jeffamine and chitosan surfaces (see chapter 2), it showed the worse binding capacity and biological activity of immobilized antibodies. This was attributed to its low surface energy leading to poor wettability properties and to the shortness of the amino chains reducing

binding surface capacity. On the contrary, chitosan surface was demonstrated to be the most hydrophilic surface leading to numerous and stronger interactions with immobilized antibodies. Indeed, it has been reported [11, 12] that the most hydrophilic and biocompatible surfaces were favourable for the immobilization of proteins limiting non-specific adsorption. Moreover, the high binding capacity of chitosan surface could be attributed to its long amino chains increasing specific area. At least, chitosan is a hydrosoluble biopolymer giving good properties to preserve biological activity of adsorbed proteins.

For amine reactive surfaces (NHS, CMD, MAMVE), results indicated that surfaces functionalized with high molecular weight hydrophilic polymers such as MAMVE exhibited excellent performances for the immobilization of anti-tumor marker antibodies and preservation of the biological activity. However, since proteins display great variability it is essential to adjust the surface chemistry in each case.

Analysis of performances indicated the limit of detection and the wide dynamic range obtained for each tumor marker tested on optimal surfaces.Under purified conditions, MAMVE surface displayed the best analytical performance for CEA and Hsp60, NHS surface for PDI and CA19-9, and chitosan surface for DEFA6. Limit of detection as low as 10 pM was reached for all tested tumor markers.

Under optimal conditions, the detection of tumor markers on our 3D-microstructured antibody microarray was validated in a proof-of-concept with few samples of colorectal cancer sera. NHS, chitosan and MAMVE surfaces were selected for this validation according to optimization results. The results demonstrated single tumor marker detected on one surface always displays low sensitivity. However, both the combination of several tumor markers detected on the same surface and the combination of tumor markers detected on their specific surface could increase the positive responses of tested cancer sera.

Perspectives will focus on the detection of larger panel of cancer biomarkers in serum from colorectal patients on the basis of the optimal surfaces and detection conditions. Large number of cancer and healthy donor sera would be involved for such assay in order to improve the robustness of our customized antibody microarray.

References

[1] G. Kijanka, D. Murphy, Protein arrays as tools for serum autoantibody marker discovery in cancer, Journal of Proteomics, 72 (2009) 936-944.

[2] D. Boehm, K. Keller, N. Boehm, A. Lebrecht, M. Schmidt, H. Koelbl, F.-H. Grus, Antibody microarray analysis of the serum proteome in primary breast cancer patients, Cancer Biol. Ther., 12 (2011) 772-779.

[3] S. Matarraz, M. Gonzalez-Gonzalez, M. Jara, A. Orfao, M. Fuentes, New technologies in cancer. Protein microarrays for biomarker discovery, Clin. Transl. Oncol., 13 (2011) 156-161.

[4] P. Angenendt, Progress in protein and antibody microarray technology, Drug Discov. Today, 10 (2005) 503-511.

[5] P. Peluso, D.S. Wilson, D. Do, H. Tran, M. Venkatasubbaiah, D. Quincy, B. Heidecker, K. Poindexter, N. Tolani, M. Phelan, K. Witte, L.S. Jung, P. Wagner, S. Nock, Optimizing antibody immobilization strategies for the construction of protein microarrays, Anal. Biochem., 312 (2003) 113-124.

[6] T. Tanaka, M. Tanaka, T. Tanaka, R. Ishigamori, Biomarkers for Colorectal Cancer, Int. J. Mol. Sci., 11 (2010) 3209-3225.

[7] M.J. Duffy, Carcinoembryonic antigen as a marker for colorectal cancer: Is it clinically useful?, Clin. Chem., 47 (2001) 624-630.

[8] H. Koprowski, M. Herlyn, Z. Steplewski, H.F. Sears, Specific antigen in serum of patients with colon carcinoma, Science, 212 (1981) 53-55.

[9] Z. Zhong, W. Wu, D. Wang, J. Shan, Y. Qing, Z. Zhang, Nanogold-enwrapped graphene nanocomposites as trace labels for sensitivity enhancement of electrochemical immunosensors in clinical immunoassays: Carcinoembryonic antigen as a model, Biosens. Bioelectron., 25 (2010) 2379-2383.

[10] P. Angenendt, J. Glokler, D. Murphy, H. Lehrach, D.J. Cahill, Toward optimized antibody microarrays: a comparison of current microarray support materials, Anal. Biochem., 309 (2002) 253-260.

[11] E. Ruckenstein, Z.F. Li, Surface modification and functionalization through the self-assembled monolayer and graft polymerization, Adv. Colloid Interface Sci., 113 (2005) 43-63.

[12] W. Kusnezow, J.D. Hoheisel, Solid supports for microarray immunoassays, J. Mol. Recognit., 16 (2003) 165-176.

Chapter 5 Evaluation of the Humoral Immune Response in Breast Cancer Based on Tumor Antigen Microarrays[§]

[§] This chapter was on the basis of manuscript submitted to:

- Yang ZG, Chevolot Y, Gehin T, Solassol J, Mange A, Souteyrand E, Laurenceau E. Improvement of protein immobilization for the elaboration of tumor- associated antigen microarrays: Application to the sensitive and specific detection of tumor markers from breast cancer sera. Biosens Bioelectron 2012. (in press)

5.1. Introduction

In the past decades, with the recent development of proteomic technologies, varieties of tumor markers were identified and employed for cancer detection with immunoassay methods [1, 2]. However, the lack of sensitivity and specificity of these biomarkers tested individually and their low frequency and heterogeneity in patient sera are a challenge to testing techniques for cancer diagnosis. Multiplex detection of a set of tumor-associated antigens (TAAs) was shown to be more sensitive and specific than the detection of a single tumor marker [5-7]. Unlike traditional tumor markers, auto-antobodies against tumor-associated antigens are found in serum from patients with different cancers, and may represent early indicators of tumor development [6, 8].

This study aims to develop TAA microarrays based on different surface chemistries to detect autoantibodies in breast cancer sera. However, in the literature, a tremendous number of tumor markers are relative to breast cancer: Mucins (CA15-3, CA27-29), oncofoetal proteins (CEA), oncoproteins (Her2, c-myc, p53), cytokeratins (TPA, ESR), mammaglobin, survivin, livin, NY-ESO-1, Annexin XI-A, Endostatin, Hsp60 and p62 [3, 4]. Thus, the choice of TAAs tested in the present work was driven in collaboration with clinician in oncology at CHU Montpellier. 10 tumor-associated antigens (TAAs) were selected, such as carcinoembryonic antigen (CEA), heat shock proteins (Hsp60, Hsp70), p53, Her2-Fc (extracellular domain), NY-ESO-1, MYCL1, CHEK2, HNRNPK, NME1, according to the literature and the results of Montpellier resaerch group. These TAAs were immobilized onto 3D-microstructured glass slides functionalized with the various surface chemistries presented in Chapter 2. The presence of auto-antibodies directed against these TAAs was evaluated in 29 sera from breast cancer patients and 28 healthy donors.

5.2. Experimental

5.2.1. Materials, chemical and biological products

All chemicals were of reagent grade or highest available commercial-grade quality and used as received unless otherwise stated. 0.01 M phosphate-buffer saline (PBS, pH 7.4) at 25 ^{o}C (0.0027 M potassium chloride and 0.138 M sodium chloride), sodium bicarbonate $NaHCO_3$ (M_r = 84.01 g/mol), sodium carbonate Na_2CO_3 (M_r = 105.99 g/mol), poly vinylalcohol (PVA), were obtained from Sigma-Aldrich (St. Quentin Fallavier, France). Tween 20 was purchased from Roth-Sochiel (Lauterbourg, France).

Anti-tumor antibodies (anti-CEA, anti-Hsp60) and tumor antigens (CEA, Hsp60) were provided by bioMérieux. Other tumor markers and recombinant proteins are commercial products. Myoglobin and p53 were obtained from Sigma-Aldrich. MYCL1, CHEK2, HNRNPK, NME1, glutathione S-transferase P1 (GSTP1), Transglutaminase 1(TMG1), Ebstein Bar Virus Nuclear Antigen 1 (EBV-NA) were supplied by Abnova Corporation (Taiwan). Hsp70 and Measle Hemagglutinin Protein (MHP) were provided by Abcam (UK). All the proteins were stored as aliquot at -20°C or -80°C following manufacturer specifications. Her2-Fc antigen was purchased from R&D system (Minneapolis, USA). NY-ESO-1 antigen and anti-Her2-Fc antibody was supplied by Thermo Scientific (USA). Cy3-labeled goat anti-human antibody (IgG + IgA + IgM) and Cy3-labeled streptavidin were purchased from Jackson ImmunoResearch and Sigma, respectively. Characteristics of each TAA are reported in Table 5-1.

0.01 M PBS or PBS 1X (pH 7.4) was prepared by dissolving the content of one pouch of dried powder in 1 L of ultrapure water. 0.1 M sodium acetate powder was dissolved to obtain the sodium acetate buffer, and pH was adjusted to 4.5. Washing buffer contained PBS 1X (pH 7.4) and 0.1 % Tween 20 (PBS-T). Blocking solution was prepared by dissolving 10 g of BSA in 100 ml of PBS–T (10% BSA/PBS-T).

Table 5-1 Parameters of recombinant proteins such as molecular weight, isoelectric point (pI) and Tag for each TAAs

TAAs	Molecular weight (g/mol)	pI	Tag	Notes
CEA	180 000	5.44	His6	Full length
Hsp60	60 000	5.24	His6	Full length
Hsp70	69 921	5.48	His6	Full length
p53	53 000	6.1	His6	Full length
Her2-Fc	135 662	5.58	His6	Homodimer
NY-ESO-1	17 992	8.79	His6	Full-length
MYCL1	48 730	5.47	GST	Full-length
CHEK2	60 914	5.7	GST	Full-length
HNRNPK	77 000	5.4	GST	Full-length
NME1	42 460	5.8	GST	Full-length
TGM1	115 870	5.7	GST	Full-length
EBV-NA	44 000	9.55	His6	1-90, 408-498
MHP	4 604	5.4	His6	106-114, 519-550
GSTP1	23 224	5.44	GST	Full-length

5.2.2. Serum samples

All human samples were prospectively collected between 2005 and 2007 at the CRLC Val d'Aurelle Cancer Institute, Montpellier, France, at the time of cancer diagnosis after obtaining written informed consent. Blood samples were centrifuged at 1250 × *g* for 5 min, and the serum was stored at -80°C. For the multiplex immunoassay, 57 serum samples were examined: 28 healthy controls with negative mammograms, negative physical breast exams for at least 4 years, and no history of prior malignancy, and 29 patients who underwent surgery and had a histopathologic diagnosis of early-stage breast cancer (Among the cancer sera: 11 of stage I, 9 of stage II and 9 of stage III). This study was approved by the Montpellier University Hospital human research committee and the INSERM review board (RBM-03-63).

5.2.3. Surface modification of 3D-microstructured glass slides

The microstructured surfaces of glass slides were functionalized as mentioned in Chapter 2 with COOH, NHS, chitosan, APDMES, CMD and MAMVE (both grafted from APDMES surface).

5.2.4. Effects of spotting concentration of tumor antigen

Proteins including Her2, Myoglobin-Cy3, IgG-Cy3 as well as the buffer were spotted at designed concentration (from 0.1 mg/ml to 0.0005 mg/ml) onto NHS functionalized glass slide. Each spot corresponded to a dispense volume of 400 pL and the distance of each spot is 200 μm. Spotting buffers were composed of sodium acetate PBS (1x, pH 7.4) with 0.05 % PVA as additive. Buffers, IgG-Cy3 at 0.9 μM and myoglobin-Cy3 at 0.6 μM, were spotted for negative and reference protein for quality control, respectively. The covalent grafting between chemistries and proteins was allowed to react under water-saturated atmosphere overnight at 4^{o}C, follwed by washing thoroughly and blocked with 10% BSA/PBS-T solution for 2 hr at room.

Slides were then incubated with anti-Her2 antibody at 1 μM, 0.5 μM and 0.1 μM in 4% BSA/PBS_T 0.1%, respectively. The incubation was allowed to react for 1 h at room temperature in a water-saturated atmosphere, thoroughly rinsed dried. The Her2 spots were then incubated with 0.1 mg/ml goat anti mouse IgG-Cy3 (1% BSA/ PBS) for 1 h at room temperature in a water-saturated atmosphere, followed by washing for 3 x 5 min with PBS-T 0.1 %, 1 min with DI water and dried by centrifugation.

5.2.5. Antigen microarray design

CEA, Hsp60, Hsp70, p53, Her2-Fc, NY-ESO-1, MYCL1, CHEK2, HNRNPK, NME1 were spotted at 0.1 mg/mL with sciFLEXARRAYER S3 (Scienion, Germany) into microwells as described in Figure 5-1. Each spot corresponded to a dispense volume of 400 pL. Spotting buffers were composed of sodium acetate (pH 4.5), PBS (1x, pH 7.4) and sodium carbonate (pH 9.6) with 0.05 % PVA as additive. Buffers, EBV-NA and MHP at 0.1 mg/mL, myoglobin-Cy3 at 0.6 μM, were spotted for negative, positive controls and quality controls, respectively. Proteins were allowed to react with functionalized surfaces under water-saturated atmosphere overnight at 4°C. Slides were then washed for 2 x 5 min with PBS and for 5 min with PBS-T, and then dried by centrifugation for 3 min at 1300 rpm. To limit further non specific adsorption, slides were blocked with 10% BSA/PBS-T solution for 2 hr at room temperature, then washed for 3 x 5 min with PBS-T and dried.

Microwells were then incubated with biotinylated antibodies (anti-CEA, anti-Hsp60, anti-p53, anti-Her2) and sera from breast cancer patients and healthy donors diluted at 1/250 in 4% BSA/PBS-T. Each microwell was incubated with one sample (biotinylated antibody or serum) and left to react for 1 hr at room temperature in a water-saturated atmosphere, thoroughly rinsed for 3 x 5 min with PBS-T and then dried. Microwells tested with sera were then incubated with Cy3-conjugated goat anti-human Ig(A+M+G) (0.015 mg/ml diluted in 1% BSA/PBS-T), and microwells tested with purified biotinylated antibodies were incubated with streptavidin-Cy3 (0.1 mg/ml in 1% BSA/PBS) for 1 hr at room temperature in a water-saturated atmosphere, followed by washing for 3 x 5 min with PBS-T 0.1 %, 1 min with DI water and dried by centrifugation.

5.2.6. Fluorescence scanning

The slides were scanned after drying with the Microarray scanner, GenePix 4100A software package (Axon Instruments) at 532 nm with photomultiplier tube (PMT) 400. The fluorescence signal of each antibody was determined as the average of the median fluorescence signal of six spots, and the value was divided by the signal of surface background to get the signal-to-noise ratio (SNR).

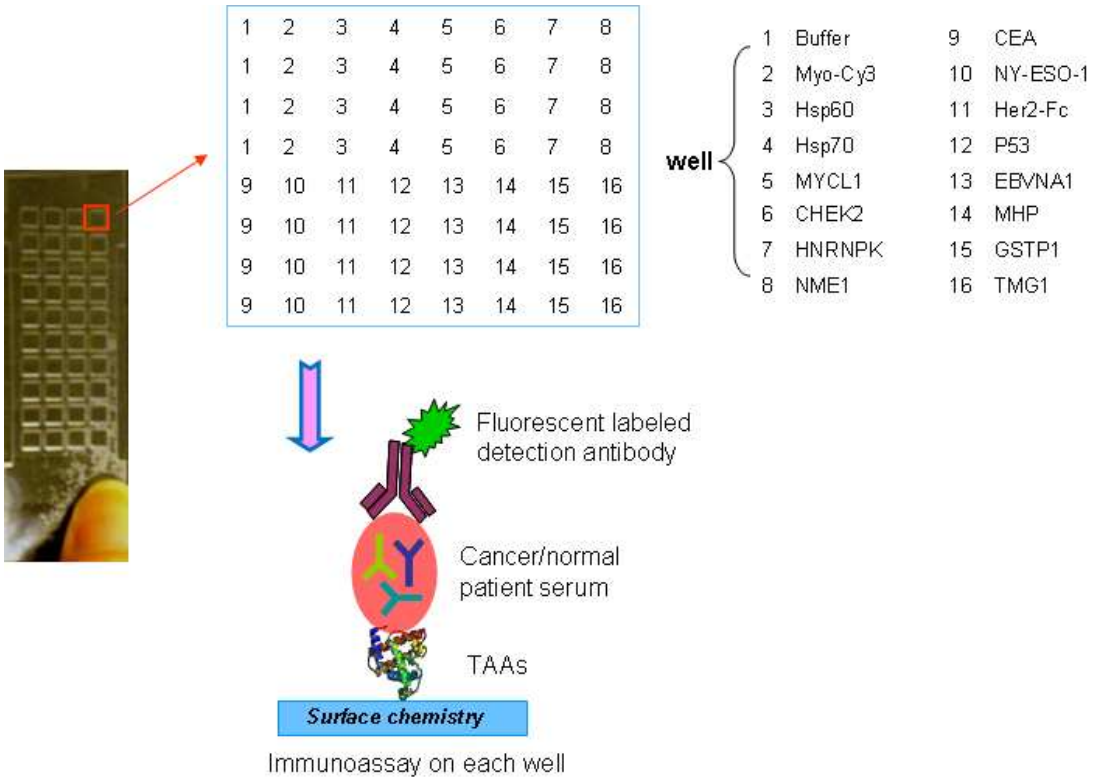

Figure 5-1 Design of tumor antigens microarray on 3D-microstructured glass slides and immunoassay on the miniaturized system. A panel of TAAs were immobilized on various surface chemistries, incubated with respective biotinylated antibody or sera from breast cancer patients/healthy donors, detected with Cy3-conjugated detection antibody.

5.3. Results and discussion

5.3.1. Effects of antigen concentration

As mentioned in Section 3.3.2 and 4.3.1.1, the probe protein concentration has great effects on immobilization/recognition level on the surface. Hererin, various concentrations of Her2-Fc (from 0.1 mg/mL to 0.0005 mg/mL) were spotted onto NHS surface to investigate the influence on biologlical recognition. The image was scanned with PMT 500 in order to get the signals at lower spotting concentration.

As shown in Figure 5-2, the antigen probe concentration has significant effects on the signal-to-noise ration (SNR) of Her2-Fc/anti-Her2-Fc antibody system. Typically, SNR increased with the increasing concentration of Her2-Fc in spotting buffer and SNR of Her2-Fc at 0.1 mg/ml was about 100 times more than that at 0.0005 mg/mL. However, the target antibody concentration (0.1 μM, 0.5 μM and 1 μM) slightly influenced SNR in our tested range, probably due to the lowest antibody concentration (at 0.1 μM) is sufficient to be captured by the active immobilized Her2-Fc. Consequently, the probe concentration of antigen was selected to 0.1 mg/mL as the following microarray assay.

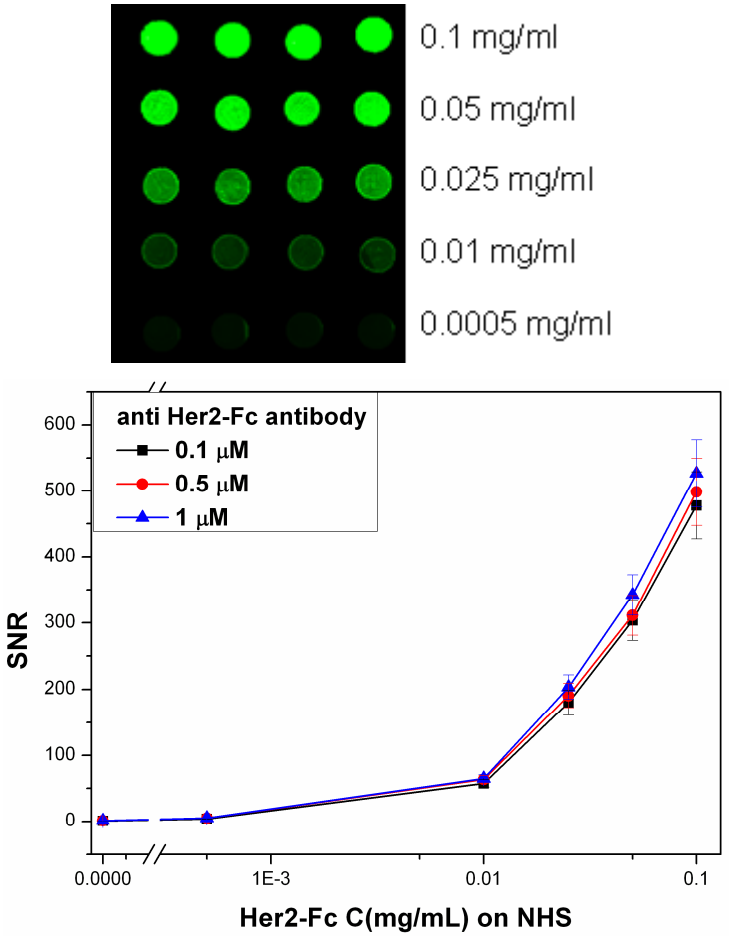

Figure 5-2 Fluorescence intensity related to Her2-Fc/anti-Her2-Fc antibody recognition on NHS surface, different Her2-Fc concentrations were spotted with BSA in print buffer. For a constant concentration of protein at 0.1 mg/mL, incubated with different concentrations of anti Her2-Fc antibody, the upper is its fluorescence scanning image incubated with 0.1 μM anti-Her2-Fc antibody.

5.3.2. Validation of TAAs immobilization and biological activity in purified conditions

The availability and reactivity of the immobilized antigens towards their human antibodies, and the spotting reproducibility are crucial parameters in the implementation of TAA microarray to achieve the best analytical performances. Four TAAs (CEA, Hsp60, Her2-Fc, p53) were spotted at 0.1 mg/mL (according to the results of Section 5.3.1) in acetate buffer (pH 4.5) on the six surface chemistries and tested for their biological recognition properties towards commercial biotinylated antibodies (anti-CEA, anti-Hsp60, anti-Her2-Fc and anti-p53). As shown in Figure 5-3, the range of SNR values depended on the TAA/anti-TAA system. CEA/anti-CEA recognition displayed very low SNR on all tested surfaces,

compared to the other TAA/anti-TAA system, while Hsp60/anti-Hsp60 exhibiting the highest ones. Thus the detection of anti-CEA autoantibody in patients' sera should not be sensitive enough and will required further implementation. However, the recognition of other three pairs of antigens-antibodies can be well detected but SNR was dependent of surface chemistry. Hsp60/anti-Hsp60 exhibited the most remarkable signals, with about 2 to 4 times more than p53/anti-p53 and Her2-Fc/anti-Her2-Fc on COOH, NHS, MAMVE and APDMES surfaces.

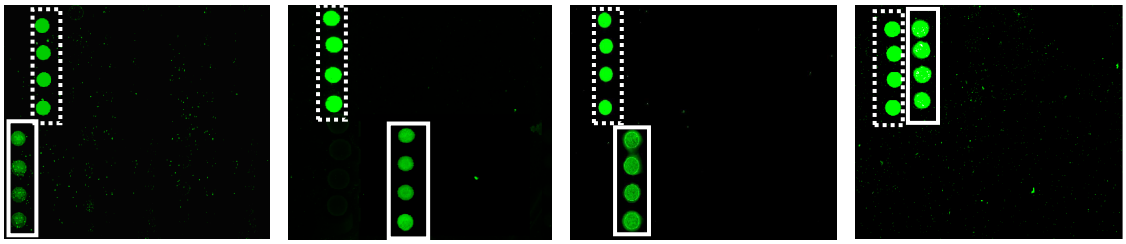

CEA on MAMVE p53 on APDMES Her2-Fc on CMD Hsp60 on COOH

A

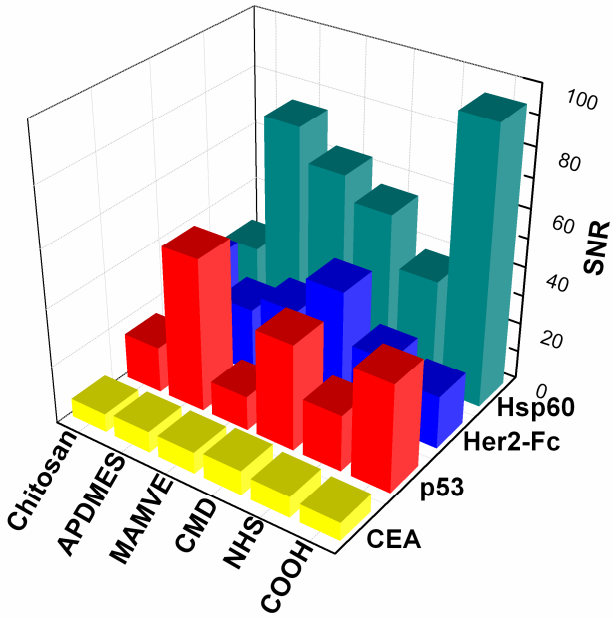

B

Figure 5-3 Fluorescence scanning images (A) and signal analysis (B) of the specific recognition of immobilized TAAs (CEA, p53, Her2-Fc and Hsp60) with biotinylated anti-TAAs antibodies on the different surface chemistries; all SD were in the range of 9% - 20 % of the mean value SNR. A: Spots of myoglobin-Cy3 are framed by dash line; spots of TAA/anti-TAA recognition are framed by solid line.

Physical adsorption of Hsp60 on the silanized surfaces (COOH, APMDES) led to better immobilization and/or allowed better recognition of anti-Hsp60 antibody than covalent

linking on amino-reactive surfaces (NHS, CMD, MAMVE). However, covalent coupling on polymer surfaces (CMD, MAMVE) displayed higher efficiency than on NHS surface, which is a monolayer reactive surface. p53 exhibited the same behaviour with higher immobilization/recognition activities *via* physical adsorption on APDMES and COOH surfaces, and on amino-reactive polymer surface such as CMD. Hsp60 and p53 displayed similar molecular weight, 60 000 g/mol and 53 000 g/mol respectively, and similar isoelectric point (pI), 5.24 and 6.3 respectively. Therefore it is likely that these two TAAs behave the same types of interactions towards our surfaces. Concerning the biological activity of Her2-Fc immobilized on the various surfaces, best results were obtained on polysaccharide functionalized surfaces, both through physical adsorption on chitosan surface and through covalent linking on CMD surface. It was previously suggested that immobilization of proteins by physical adsorption could be more efficient than covalent coupling but depends on probe proteins and surface chemistry [10, 12, 13].

Consequently, there is not a unique surface which suits all proteins. Thus, surface modifications should be chosen after optimization of immobilization parameters. Here, we have demonstrated that all developed surface chemistries were suitable for the immobilization of tumor-associated antigens with respect to their biological activity. In most cases, optimal immobilization of TAAs occurred by physical adsorption or covalent linking through amino-reactive polymer surfaces could increase binding capacity of the surface. Thus, for a given TAA, two or three surface chemistries could be chosen and tested for the detection of autoantibodies against TAAs in breast cancer patient sera.

5.3.3. Detection of anti-TAA autoantibodies in breast cancer sera

Herein, 3D-microstructured glass slides functionalized with the six above described surface chemistries, were spotted with 15 protein probes for the multiplex immunoassay approach. These probes included 5 well-known TAAs involved in breast and other cancers (CEA, Her2-Fc, Hsp60, NY-ESO-1, p53), 5 potential new biomarkers of breast cancer (Hsp70, MYCL1, CHEK2, HNRNPK, NME1), 3 positive controls (GSTP1, MHP, EBV-NA), 1 negative control (TMG1) and Cy3-labelled myoglobin as quality control of protein immobilization (Figure 5-1). The presence of anti-TAAs autoantibodies was evaluated from 29 breast cancer sera and 28 healthy donor sera collected by CHU Montpellier (France). According to preliminary results, the best serum dilution avoiding saturation and allowing the detection of low TAA concentration was 1/250 (data not shown). The response of some probes toward both normal and cancer sera were insufficient to be detected or distinguished from buffer spot, such as CEA, MYCL1, CHEK2, HNRNPK, NME1, GSTP1 and TMG1.

These probe proteins displayed very low or even no signals probably due to weak immobilization/recognition on our microarray platform, and/or loss of biological activity after receipts of commercial products. In previous experiments, these probes were tested with 5 breast cancer sera and 2 healthy donor sera included in this study. Low or no responses were obtained (data not shown). Future work will focus on the purchase of these antigens in other commercial agent to repeat the experiments, as well as the incubation with available purified antibodies, in order to check the reasons of no responses and implement our detection system for such probes. Consequently, CEA, MYCL1, CHEK2, HNRNPK, NME1, GSTP1 and TMG1 were removed in the following discussion. Positive controls EBV-NA and MHP displayed significant signal (1.5<mean SNR<13) with all sera. As expected, no significant differences were obtained between breast cancer sera and healthy donor sera. From these data, we can conclude that all tested sera were suitable for the immunoassay.

For each TAA immobilized on each surface, a cut-off value for the detection of the corresponding autoantibody was calculated from healthy donor sera as the mean of SNR + 3 SD (Standard Deviation). A serum was considered as positive toward a given TAA if the corresponding SNR value was higher than the cut-off. According to this criterion, the occurrence of positive sera from healthy donors and breast cancer patients were reported in Table 5-2.

Table 5-2 Occurrence (%) of positive sera from breast cancer patients and healthy donors (value in the brackets) for each TAA immobilized on the various surface chemistries

Surfaces/TAAs	p53	Hsp60	Hsp70	NY-ESO-1	Her2-Fc
COOH	6.9 (0)	6.9 (***3.6***)	*0* (0)	*0* (0)	3.4 (0)
NHS	3.4 (0)	**41.4** (0)	**13.8** (0)	**20.7** (0)	**31.0** (0)
CMD	**10.3** (0)	*0* (***3.6***)	*0* (0)	**13.8** (0)	3.4 (0)
MAMVE	3.4 (0)	*0* (0)	*0* (***4.8***)	6.9 (0)	*0* (***7.1***)
APDMES	**31.0** (0)	**20.7** (0)	*0* (0)	*0* (0)	6.9 (***7.1***)
Chitosan	**17.2** (0)	6.9 (0)	*0* (0)	*0* (0)	**13.8** (0)

Hsp60 on COOH and CMD surfaces, Hsp70 and Her2-Fc on MAMVE surface, and Her2-Fc on APDMES surface displayed false positive from the healthy donor samples. Moreover, depending on the surface chemistry, Hsp60, Hsp70, NY-ESO-1 and Her2-Fc didn't show any positive response from breast cancer samples. However, each TAA were able to detect more than 10% of breast cancer patients when immobilized on optimal surface chemistry: p53 on CMD, APDMES and chitosan surfaces; Hsp60 on NHS and APDMES surfaces; Hsp70 on NHS surface; NY-ESO-1 on NHS and CMD surfaces; Her2-Fc on NHS and chitosan surfaces. For p53, these results are in agreement with data obtained from

purified monoclonal antibodies. For Hsp60 and Her2-Fc, the best surfaces with monoclonal antibodies were COOH and CMD, respectively, NHS surface giving very low signal. However, APDMES surface for Hsp60 and chitosan surface for Her2-Fc were also identified as good surface with monoclonal antibodies. These differences could be due to variation in antibodies specificities. In serum samples, antibodies against TAAs are polyclonal recognizing various epitopes of the antigen, whereas monoclonal antibodies recognizing a single epitope were used in the first part of the study.

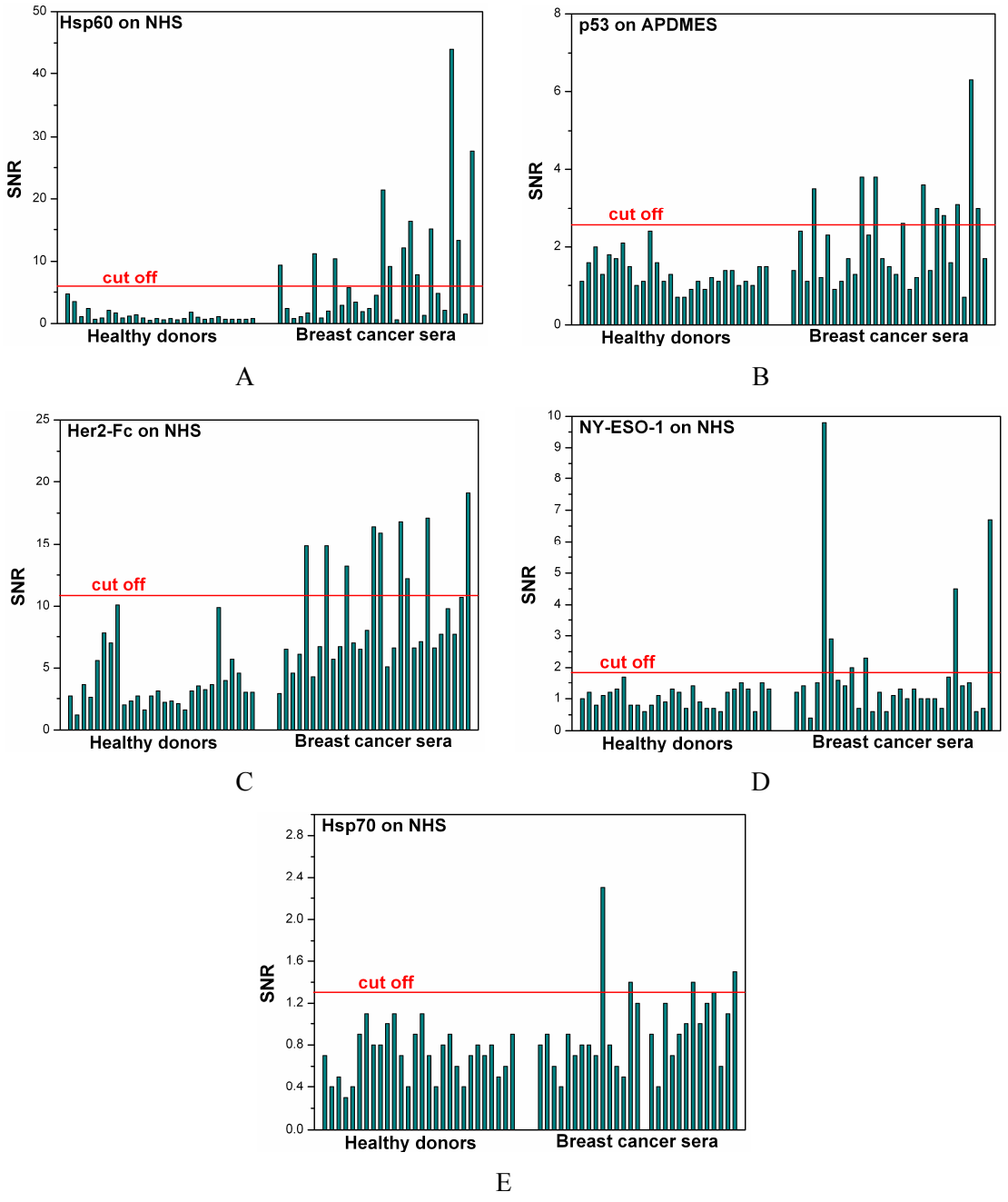

Figure 5-4 Detection of autoantibodies directed against the five selected TAAs immobilized on the best surface chemistry, in healthy donor and breast cancer patient sera using multiplex immunoassay; For each TAA, the cut-off value was calculated as the mean SNR + 3 SD of healthy donor sera.

These results clearly demonstrated that the surface chemistry used to immobilize TAAs in particular, and proteins in general, were a key parameter for efficient immunoassay. On the basis of these results, we selected surfaces and TAAs which compiled the best predicting parameters to discriminate the healthy donor and breast cancer groups. Figure 5-4 presented SNR values of healthy donor and breast cancer sera related to this selection: Hsp60, Her2-Fc, NY-ESO-1, Hsp70 immobilized on NHS surface, and p53 immobilized on APDMES surface.

Table 5-3 Dependency of tumor-associated antigen autoantibodies occurrence in breast cancer patient sera (%) with combination of TAAs

Selected TAAs (surface chemistry)	Occurrence (%)
Hsp60 (NHS)	41.4
Hsp60 (NHS) + p53 (APDMES)	62
Hsp60 (NHS) + p53 (APDMES) + He2-Fc (NHS)	68.9
Hsp60 (NHS) + p53 (APDMES) + He2-Fc (NHS) + NY-ESO-1 (NHS)	75.8
Hsp60 (NHS) + p53 (APDMES) + He2-Fc (NHS) + NY-ESO-1 (NHS) + Hsp 70 (NHS)	82.7

We can observe that the combination of several TAAs led to increase TAA autoantibodies occurrence in breast cancer sera (Table 5-3). Indeed, combining Hsp60 (on NHS) and p53 (on APDMES) increased the predicting percentage of positive patients from 41.4% to 62%. Adding Her2-Fc (on NHS), NY-ESO-1 (on NHS) and Hsp70 (on NHS) allowed increasing more this predicting percentage to 68.9%, 75.8% and 82.7%, respectively. Thus, using a panel of only five TAAs, each of them immobilized on the best surface chemistry, 82.7% of breast cancer patients could be detected in one immunoassay thanks to our customized 3D-microstructured microarray. Additionally, among the sera with positive response, the frequency depends on the stage of cancer (including 11 of stage I, 9 of stage II and 9 of stage III). For example, Hsp60 on NHS can detect 12 positve sera (4 of Stage I, 3 of Stage II and 5 of Stage III), increasing to 18 sera (5 of Stage I, 7 of Stage II and 6 of Stage III) with combination of p53 on APDMES, and 24 (7 of Stage I, 9 of Stage II and 8 of Stage III) by cominbation of 5 TAAs mentioned above on theirs specific surfaces. Moreover, notice that in addition to NHS and APDMES surfaces selected above, immobilization of p53 and Her2-Fc on chitosan surface, and of NY-ESO-1 on CMD surface could confirm the positivity of 37.9% of breast cancer sera.

5.4. Conclusions

In this chapter, a panel of 10 tumor-associated antigens (TAAs) was immobilized onto 3D-microstructured glass slides functionalized with 6 different surface chemistries in order to detect autoantibodies in breast cancer patient sera. Surface chemistries included covalent binding through protein amino groups or physical adsorption.

Firstly, to validate our customized microarray, four well-known TAAs (CEA, p53, Hsp60, Her2) were immobilized on each surface chemistry and tested with purified monoclonal antibodie,. We have demonstrated the dependence of the detection signal of anti-TAA autoantibodies (SNR) on surface chemistry. It relates to the immobilization yield of TAA and to their remaining biological activity.

Additionally, 29 breast cancer patient and 28 healthy donor sera were tested on our tumor antigen microarrays. At least 10% of breast cancer sera could be detected with one TAA in optimal conditions. Thanks to a combination of five TAAs (Hsp60, p53, Her2, NY-ESO-1 and Hsp70) immobilized on the optimized surface chemistry, over 82% of breast cancer patients have been specifically detected. Our results are comparable with other studies concerning anti-TAA autoantibodies detection for cancer diagnosis [14, 15]. Further works will focus on increasing the number of tested TAAs in order to identify other relevant TAAs for breast cancer. Moreover, the accuracy will be probably improved by increasing the number of immobilized TAAs on the microarray. Finally, larger cohort of healthy donors and cancer patients will be used to validate the diagnosis test. Thanks to the microstructuration, all optimal surface chemistries would be integrated on the same support leading to improve the accuracy of a cost-effective test.

References

[1] J.A. Ludwig, J.N. Weinstein, Biomarkers in cancer staging, prognosis and treatment selection, Nat. Rev. Cancer, 5 (2005) 845-856.

[2] D. Sidransky, Emerging molecular markers of cancer, Nat. Rev. Cancer, 2 (2002) 210-219.

[3] M.J. Duffy, Serum tumor markers in breast cancer: Are they of clinical value?, Clin. Chem., 52 (2006) 345-351.

[4] R. Molina, V. Barak, A. van Dalen, M.J. Duffy, R. Einarsson, M. Gion, H. Goike, R. Lamerz, M. Nap, G. Soletormos, P. Stieber, Tumor markers in breast cancer - European Group on Tumor Markers recommendations, Tumor Biol., 26 (2005) 281-293.

[5] K.L. Cheung, C.R.L. Graves, J.F.R. Robertson, Tumour marker measurements in the diagnosis and monitoring of breast cancer, Cancer Treat. Rev., 26 (2000) 91-102.

[6] C. Desmetz, C. Cortijo, A. Mange, J. Solassol, Humoral response to cancer as a tool for biomarker discovery, Journal of Proteomics, 72 (2009) 982-988.

[7] J. Madoz-Gurpide, R. Kuick, H. Wang, D.E. Misek, S.M. Hanash, Integral protein microarrays for the identification of lung cancer antigens in sera that induce a humoral immune response, Mol. Cell. Proteomics, 7 (2008) 268-281.

[8] W.H. Liu, B. Peng, Y.M. Lu, W.J. Xu, W. Qian, J.Y. Zhang, Autoantibodies to tumor-associated antigens as biomarkers in cancer immunodiagnosis, Autoimmun. Rev., 10 (2011) 331-335.

[9] C. Desmet, G.C. Le Goff, J.C. Bres, D. Rigal, L.J. Blum, C.A. Marquette, Multiplexed immunoassay for the rapid detection of anti-tumor-associated antigens antibodies, Analyst, 136 (2011) 2918-2924.

[10] Z.G. Yang, Y. Chevolot, Y. Ataman, G. Choquet-Kastylevsky, E. Souteyrand, E. Laurenceau, Cancer Biomarkers Detection Using 3D Microstructured Protein Chip: Implementation of Customized Multiplex Immunoassay, Sens. Actuators B, in presss doi.org/10.1016/j.snb.2011.11.055 (2011).

[11] E. Laurenceau, Z.G. Yang, Y. Chevolot, Y. Attaman, G. Choquet-Kastylevsky, E. Souteyrand, Tumor antigens titration on novel miniaturized immunoassay: 3D-Protein chip performance evaluation, Bull. Cancer (Paris), 98 (2011) S70-S70.

[12] P. Angenendt, J. Glokler, J. Sobek, H. Lehrach, D.J. Cahill, Next generation of protein microarray support materials: Evaluation for protein and antibody microarray applications, J. Chromatogr. A, 1009 (2003) 97-104.

[13] W. Kusnezow, A. Jacob, A. Walijew, F. Diehl, J.D. Hoheisel, Antibody microarrays: An evaluation of production parameters, Proteomics, 3 (2003) 254-264.

[14] C. Chapman, A. Murray, J. Chakrabarti, A. Thorpe, C. Woolston, U. Sahin, A. Barnes, J. Robertson, Autoantibodies in breast cancer: their use as an aid to early diagnosis, Ann. Oncol., 18 (2007) 868-873.

[15] C.J. Chapman, G.F. Healey, A. Murray, P. Boyle, C. Robertson, L.J. Peek, J. Allen, A.J. Thorpe, G. Hamilton-Fairley, C.B. Parsy-Kowalska, I.K. Macdonald, W. Jewell, P. Maddison, J.F. Robertson, EarlyCDT(R)-Lung test: improved clinical utility through additional autoantibody assays, Tumour Biol., in press (2012).

Conclusions

The main goal of this thesis focused on implementation of protein microarrays to improve the sensitive and specific detection of tumor biomarkers for cancer diagnosis and prognosis.

To this purpose, various surface chemistries were developed to functionalize 3D-microstructured glass slides, for protein immobilization by adsorption or covalent linking. Three monofunctional silane bearing different functional groups, amino group for APDMES, carboxylic group for TDUSM and epoxy group for GPDMES, were successfully introduced onto glass slides. Surface characterization indicated comparable surface coverage (about 10^{14} silane/cm^2) and surface tension (31-34 mJ/m^2). TDSUM monolayer was further grafted with aminated polymers (chitosan and jeffamine) and APDMES monolayer was grafted with, amine reactive polymers (CMD and MAMVE). Surface characterization of these polymer layers showed that chitosan was mostly physisorbed on the silane monolayer whereas CMD and MAMVE were covalently grafted. MAMVE and chitosan surfaces were found to be the most hydrophilic surfaces probably due to their high molecular weight and highly polar structure.

Then, these well characterized surface chemistries were employed to immobilize proteins, through physical adsorption or covalent linking. Protein-surface interactions were studied in various conditions (additive and pH of spotting buffers, blocking procedures, protein concentration) in order to optimize protein microarray efficiency. The results showed that immobilization efficiency depends on surface properties (chemical groups, reactivity, wetting properties), protein characteristics (M_w, pI, 3D structure) and spotting conditions (pH, additive, concentration). Thus, it is essential to screen various immobilization conditions for each protein in order to determine the best one. We found that protein-surface interactions are mainly driven by electrostatic interactions and hydrogen bonds. Furthermore, the quality of the spotting and image analysis was improved by adding 0.05 % PVA in spotting buffer and using 10% BSA/PBS-T as blocking solution.

Taking into account these results, we developed antibody microarray for the specific and sensitive detection of tumor biomarkers involved in colorectal cancer: CEA, Hsp60, PDI, DEFA6 and p53. Fast screening and identification of optimal conditions for antigen/antibody recognition were performed on microstructured glass slides functionalized with aminated surfaces (APDMES, Jeffamine, chitosan) and amine reactive surfaces (NHS, CMD, MAMVE). Influences of surface reactivity and physico-chemical characteristics were studied on the binding capacity of antibodies and on the ability to maintain biological activity of the

immobilized proteins. For aminated surfaces, all tested antibody/antigen systems displayed significant enhanced signal-to-noise ratio on chitosan surface. Furthermore, carbonate buffer (pH 9.6) was found to be the optimal spotting buffer on the three amino-functionalized surfaces. Immobilization of antibodies on these surfaces occurred *via* physical adsorption. The high binding capacity of chitosan surface could be attributed to its long amino chains increasing specific area. At least, chitosan is a hydrosoluble biopolymer giving good properties to preserve biological activity of adsorbed proteins. For amine reactive surfaces (NHS, CMD, MAMVE), experimental results indicated that surfaces functionalized with high molecular weight hydrophilic polymers such as MAMVE, exhibited excellent performances for the immobilization of antibodies and preservation of the biological activity. Then, analysis of performances indicated the limit of detection and the wide dynamic range obtained for each tumor biomarker tested on optimal surfaces. Under purified conditions, MAMVE surface displayed the best analytical performances for CEA and Hsp60, NHS surface for PDI and CA19-9, and chitosan surface for DEFA6. Limit of detection as low as 10 pM was reached for all tested tumor biomarkers. Under optimal conditions, the detection of tumor biomarkers on our microstructured antibody microarray was validated in a proof-of-concept with a few samples of colorectal cancer (CRC) sera. NHS, chitosan and MAMVE surfaces were selected for this validation according to optimization results. Positive CRC patients were well detected on the platform of our implemented microarray. Single tumor marker on one surface usually displays low sensitivity. However, both the combination of several tumor markers on the same surface and the combination of tumor markers on their specific surface could increase the positive responses of tested cancer sera.

Finally, antigen microarrays were developed to identify autoimmune profile in breast cancer. First, four well-known TAAs (CEA, p53, Hsp60, Her2) were immobilized on our chemically functionalized customized microarray and tested with purified monoclonal antibodies. We demonstrated the dependence of the immobilization yield of TAA and their remaining biological activity on surface chemistry. Then, a panel of 10 tumor-associated antigens (TAAs) was immobilized onto microstructured glass slides functionalized with 6 different surface chemistries, including covalent binding (NHS, CMD, MAMVE) through protein amino groups or physical adsorption (COOH, APDMES and chitosan). 29 breast cancer patient and 28 healthy donor sera were evaluated on our tumor antigen microarrays. At least 10% of breast cancer sera could be positively detected with one TAA in optimal conditions. Thanks to a combination of five TAAs (Hsp60, p53, Her2, NY-ESO-1 and Hsp70) immobilized on their optimal surface chemistry, over 82% of breast cancer patients have been specifically detected.

Consequently, this work demonstrated the potentialities of the 3D-microstructured microarray as powerful screening platform. Then, we proved the necessity to adapt surface

chemistry to each protein in order to improve performances of protein microarrays. Thanks to the microstructuration, all optimal surface chemistries could be integrated on the same support leading to improve the accuracy of a cost-effective test. At last, our customized antigen microarray was successfully applied for the identification of autoimmune profile in the diagnosis of breast cancer.

Perspectives will focus on the integration of the various surface chemistries on the same support (one chemistry per microwell). One can also immobilize antibody (*e.g.* anti-CEA antibody) to capture autoantigen (*e.g.* CEA) in serum, meanwhile immobilize antigen (*e.g.* CEA) to capture autoantiboy (*e.g.* anti-CEA antibody) but for the same serum assay. Then, in order to give a simple and powerfull tool to end-user such as physician, storage and stability of immobilized proteins will be studied. Indeed for medical application, the storage and stability of protein chips are essential parameters for commercial development. Future work will also focus on increasing the number of tested tumor biomarkers in order to identify other relevant biomarkers for colorectal, breast cancer and others. Moreover, the accuracy will be probably improved by increasing the number of immobilized probes on the microarray. Finally, larger cohort of healthy donors and cancer patients will be used to validate the diagnosis test. Increasing the number of biomarkers and the size of cohort will require developing special software for quickly analysing the multitude of data.

Annexes

Annex 1

The effects of pH buffer on the biological activity of anti-Hsp60, anti-PDI and anti-DEFA6 antibody immobilized on APDMES, Jeffamine and chitosan surfaces for the detection of Hsp60, PDI and DEFA6 (Figure A-1). The three anti-tumor marker antibody/tumor marker systems displayed the same behaviour on each aminated surface. Typically, SNR increased with the increasing tumor marker concentration. The best immunoassay response was obtained with carbonate buffer (pH 9.6)

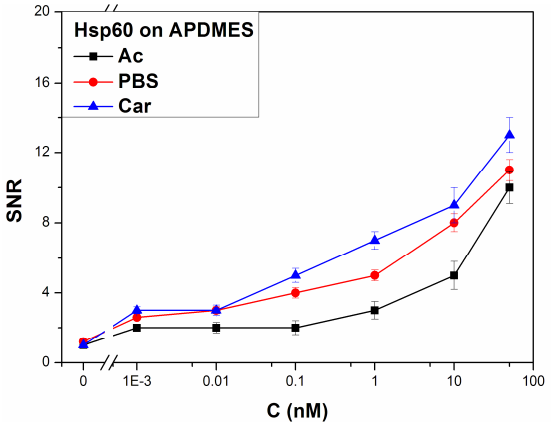

A1

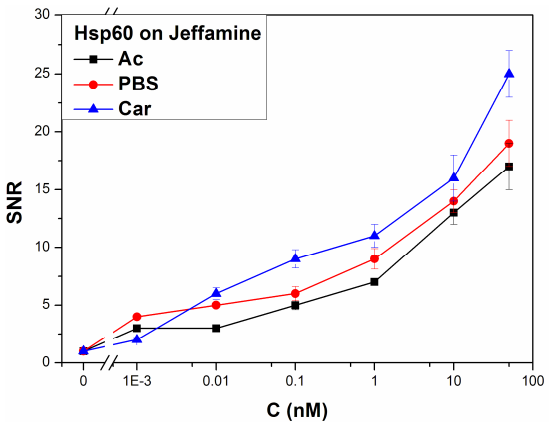

A2

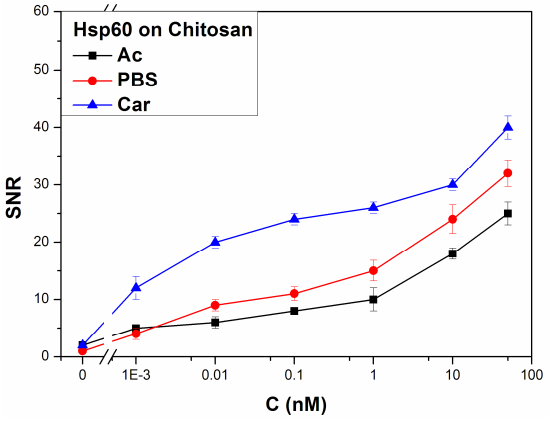

A3

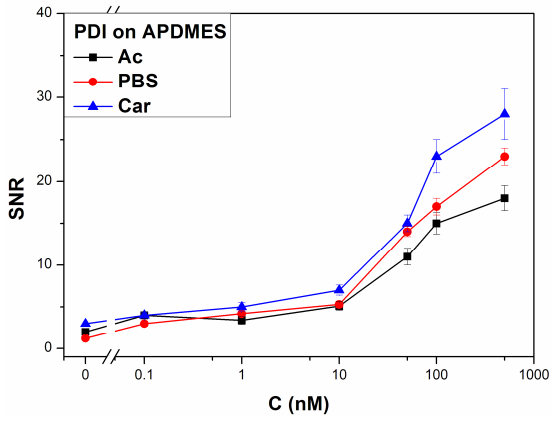

B1

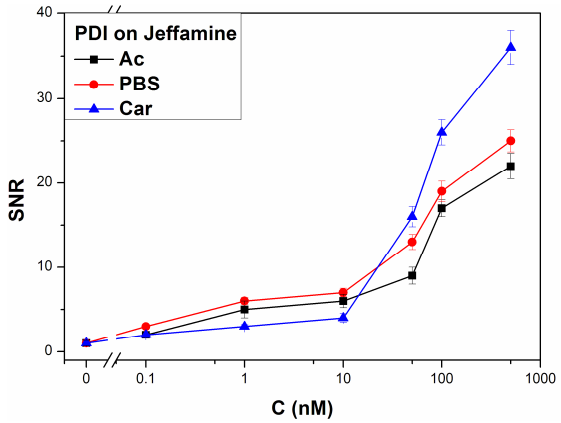

B2

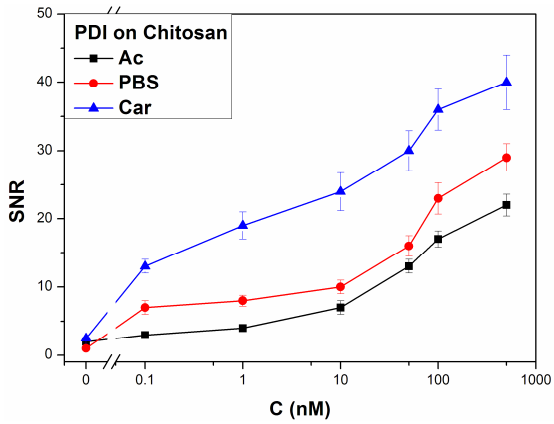

B3

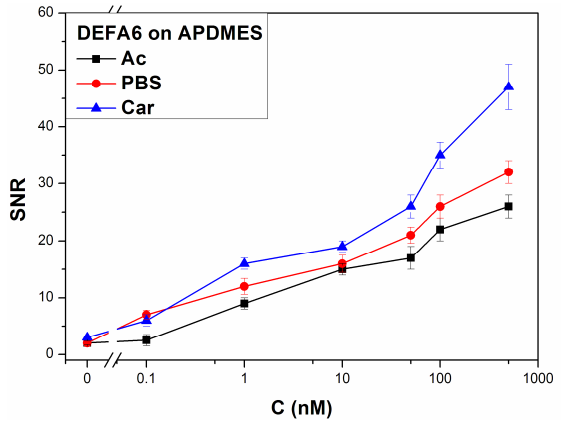

C1

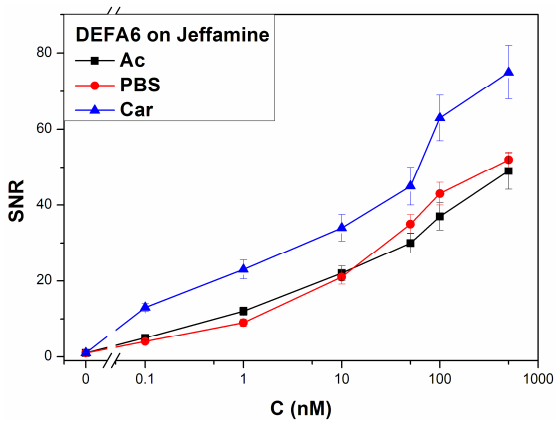

C2

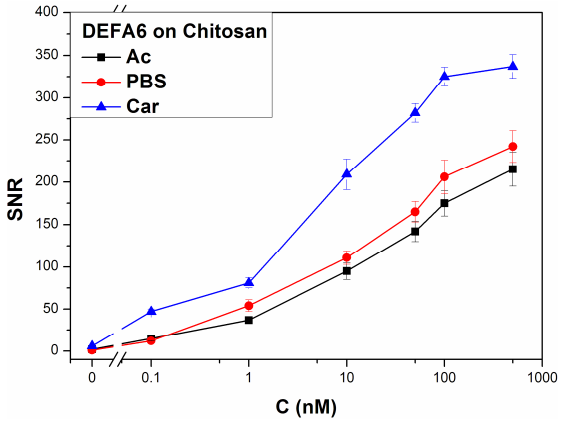

C3

Figure A-1 Signal to noise ratio (SNR) relative to biological recognition of anti-Hsp60, anti-PDI, anti-DEFA6 antibody spotted in different pH buffers on APDMES (A1, B1, C1), Jeffamine (B1, B2, B3) and chitosan (C1, C2, C3) surfaces, versus Hsp60, PDI, DEFA6 concentrations, respecitively.

Curriculum vitae

EDUCATION

09.2009 – 07.2012 **PhD** of *Micro and Nanotechnology,* University of Lyon, site *Ecole Centrale de Lyon*, Lyon, France;

09.2006 – 07.2009 **Master** of Polymer Chemistry & Physics, national key discipline *Sun Yat-sen University (SYSU)*, Guangzhou (Canton), P.R. China.

09. 2002 – 07.2006 **Bachelor** of *Polymer Materials & Engineering,* Harbin, P.R. China *Harbin Institute of Technology (HIT)*, Harbin, P.R. China

RESEARCH EXPERIENCE

09.2009 – present **PhD fellow**, Lyon Institute of Nanotechnology (INL), CNRS UMR 5270; subject "***3D-Microstructured protein chip for early cancer diagnosis***", supervised by Dr. Eliane Souteyrand (HDR) and Dr. Emmanuelle Laurenceau, in collaboration with Department of Biomarkers of bioMérieux company and two French hospitals (CHU Montpellier, CHU Saint-Etienne).

09.2006 – 07.2009 **Master Thesis** at Key Laboratory of Polymeric Composites and Functional Materials of the Ministry of Education; subject "***Structures and properties of β-nucleated polypropylene /polyamide 6 alloys***", supervised by Prof. Kancheng Mai; sponsored by National Natural Science Foundation (Grant No. 50873115) and Project of Science Technology, Guangdong Province (Grant No. 0711020600002).

01.2006 – 07.2006 **Training period/thesis of bachelor**; subject "***Surface modification of carbon fiber with super critical ammonia and grafting with acrylic acid***", supervised by Prof. Linghui Meng.

SUMMARY OF SCIENTIFIC OUTPUT

Sum of times cited: **136**; H-index **6** (June 2012).

PUBLICATIONS

Published papers:

1. ***Yang ZG***, Chevolot Y, Attaman Y, Choquet-Kastylevsky G, Souteyrand E, Laurenceau E. Cancer Biomarkers Detection Using 3D Microstructured Protein Chip: Implementation of Customized Multiplex Immunoassay. ***Sens Actuators B: Chem*** 2012; in press.

2. ***Yang ZG***, Chevolot Y, Gehin T, Solassol J, Mange A, Souteyrand E, Laurenceau E. Improvement of protein immobilization for the elaboration of tumor- associated antigen microarrays: Application to the sensitive and specific detection of tumor markers from breast cancer sera. ***Biosens Bioelectron*** 2012. (in press)
3. ***Yang ZG***, Laurenceau E, Chevolot Y, Attaman Y, Choquet-Kastylevsky G, SouteyrandE. Cancer Biomarkers Detection Using 3D Microstructured Protein Chip: Implementation of Customized Multiplex Immunoassay. ***Procedia Engineering*** 2011; 25: 952 – 955.
4. Laurenceau E, ***Yang ZG***, Chevolot Y, Attaman Y, Choquet-Kastylevsky G, Souteyrand E. Tumor antigens titration on novel miniaturized immunoassay: 3D-Protein chip performance evaluation. ***Bull Cancer*** 2011; 98: S70-S70.
5. Sui N, Monnier V, ***Yang ZG***, Dugas V, Chevolot Y, Laurenceau E, Souteyrand E. Preparation of Ag@SiO_2 and its application for enhancement of Cy3 fluorescence. ***Int J Nanosci*** 2011. (Accepted)
6. ***Yang ZG***, Mai KC. Nonisothermal crystallization and melting behavior of β-nucleated isotactic polypropylene and polyamide 66 blends. ***J Appl Polym Sci*** 2011; 119(6): 3566-3573.
7. ***Yang ZG***, Mai KC. Crystallization and melting behavior of beta-nucleated isotactic polypropylene/polyamide 6 blends with maleic anhydride grafted polyethylene-vinyl acetate as a compatibilizer. ***Thermochim Acta*** 2010; 511(1-2): 152-158.
8. ***Yang ZG***, Chen CY, Liang DW, Zhang ZS, Mai KC. Melting characteristic and β-crystal content of β-nucleated polypropylene/polyamide 6 alloys prepared by different compounding methods. ***Polym Int*** 2009; 58(12): 1366-1372.
9. ***Yang ZG***, Zhang ZS, Tao YJ, Mai KC. Preparation, Crystallization Behavior and Melting Characteristic of β-Nucleated Isotactic Polypropylene Blends with Polyamide 6. ***J Appl Polym Sci*** 2009; 112(1): 1-8.
10. ***Yang ZG***, Zhang ZS, Tao YJ, Mai KC. Effects of polyamide 6 on the crystallization and melting behavior of β-nulceated polypropylene. ***Eur Polym J*** 2008; 44(11): 3754-3763.
11. Zhang ZS, Tao YJ, ***Yang ZG***, Mai KC. Preparation and characteristics of nano-$CaCO_3$ supported β-nucleating agent of polypropylene. ***Eur Polym J*** 2008; 44(7):1955-1961.
12. Zhang ZS, Wang CG, ***Yang ZG,*** Chen CY, Mai KC. Crystallization behavior and melting characteristics of PP nucleated by a novel supported β-nucleating agent. ***Polymer*** 2008; 49(23): 5137-5145.

Submitted manuscripts:

1. ***Yang ZG***, Chevolot Y, Dugas V, Xanthopoulos N, Laporte V, Delair T, Attaman Y, Choquet-Kastylevsky G, Souteyrand E, Laurenceau E. Characterization of three amino-functionalized surfaces and evaluation of antibody immobilization for the multiplex detection of tumor markers involved in colorectal cancer. Submitted to ***Biomaterials*** 2012.

Manuscripts in preparation:

1. ***Yang ZG***, Chevolot Y, Attaman Y, Choquet-Kastylevsky G, Souteyrand E, Laurenceau

E. Implementation of protein microarray based on 3D-microstructured glass slides modified with carboxylic chemistry to directly detect colorectal cancer biomarkers in sera. (in preparation)

2. ***Yang ZG***, Laurenceau E, Chevolot Y, Souteyrand E, Cloarec JP. Multiplex detection of breast cancer biomarkers with implemented anti-tumor-associated antigen microarray. (in preparation)

PATENT

1. Mai KC, ***Yang ZG***, Zhang ZS. Preparation method for beta-crystal polypropylene/nylon alloy. *China Patent* Publication No. CN 101538388 published on 23-Sep-2009, Application No. CN 200910038697.0 filed on April 17, 2009.

SCIENTIFIC MEETING COMMUNICATIONS (6 x oral and 8 x poster)

1. ***Yang ZG***, Laurenceau E, Chevolot Y, Attaman Y, Choquet-Kastylevsky G, Souteyrand E. Multiplex and Sensitive Cancer Biomarkers Detection Based on 3D-Microstructured Protein Chip. 1st Workshop of Cancer Cells on-Chips, Lyon, France, June 11, 2012. ***(Poster)***

2. ***Yang ZG***, Chevolot Y, Solassol J, Souteyrand E, Laurenceau E. Customized tumor-associated antigen microarrays for the sensitive and specific detection of tumor markers from breast cancer sera. *The World Congress on Biosensors- Biosensors 2012*, Cancun, Mexico, May 15-18, 2012. (***Oral***)

3. ***Yang ZG***, Laurenceau E, Chevolot Y, Attaman Y, Choquet-Kastylevsky G, Souteyrand E. Early diagnosis of cancer based on protein chip. *Journées des doctorants de l'INL*, Lyon, France, October 13-14, 2011. (***Oral***)

4. ***Yang ZG***, Laurenceau E, Chevolot Y, Attaman Y, Choquet-Kastylevsky G, Souteyrand E. Implementation of protein chip for cancer diagnosis. (*Seminar*) Nano-organic Chemistry group (Prof. *E.J.R. Sudhölter*), Department of Chemical Engineering, Faculty of Applied Sciences, *Delft University of Technology*, Deflt, The Netherland, October 10, 2011. (***Oral***)

5. ***Yang ZG***, Laurenceau E, Chevolot Y, Attaman Y, Choquet-Kastylevsky G, Souteyrand E. Cancer Biomarkers Detection Using Microstructured Protein Chip: Implementation of Customized Multiplex Immunoassay. *2nd International Conference on Bio-Sensing Technology*, Amsterdam, The Netherlands, October 10-12, 2011. ***(Poster)***

6. ***Yang ZG***, Laurenceau E, Chevolot Y, Attaman Y, Choquet-Kastylevsky G, Souteyrand E. Cancer Biomarkers Detection Using 3D Microstructured Protein Chip: Implementation of Customized Multiplex Immunoassay. *25th Anniversary EUROSENSORS XXV*, Athens, Greece, September 4-7, 2011. ***(Poster)***

7. ***Yang ZG***, Laurenceau E, Chevolot Y, Attaman Y, Choquet-Kastylevsky G, Souteyrand E. A novel 3D protein chip to detect tumor associated antigen for cancer diagnosis. *17th Colloque de Recherche Inter Ecoles Centrales*, Paris, France, Juin 14-17, 2011. ***(Oral)***

8. ***Yang ZG***, Chevolot Y, Attaman Y, Choquet-Kastylevsky G, Souteyrand E, Laurenceau E. Novel miniaturized immunoassay for cancer diagnosis: Implementation of 3D-protein

chip with different surface chemistries for tumor antigens detection. *Journée Rhône-Alpes des Biomolécules (JRAB) 2011*, Lyon, France, May 27, 2011. ***(Poster)***

9. ***Yang ZG***, Chevolot Y, Attaman Y, Choquet-Kastylevsky G, Souteyrand E, Laurenceau E. Tumor antigens titration on novel miniaturized immunoassay: 3D-protein chip performance evaluation. *6th Scientific Forum of CLARA and the BioVision Forum*, Lyon, France, March 28-29, 2011. ***(Poster)***
10. ***Yang ZG***, Chevolot Y, Souteyrand E, Laurenceau E. Characterization of various surface chemistries for antibody microarrays: detection of carcino embryonic antigen (CEA). *12th International Meeting and Workshop of the Society for Biochromatography and Nanoseparations*, Lyon, France, October 19-22, 2010. ***(Poster)***
11. ***Yang ZG***, Chevolot Y, Souteyrand E, Laurenceau E. Functionalization of 3D-biochip for cancer diagnosis. *3ème colloque du Laboratoire International Associé « Nanotechnologies & Nanosystèmes » (LIA-LN2)*, Sherbrooke, Canada, July 12-16, 2010. (***Poster)***
12. ***Yang ZG***, Chevolot Y, Souteyrand E, Laurenceau E. Implementation of Protein Chips for Cancer Diagnosis. *16th Colloque de Recherche Inter Ecoles Centrales*, Lille, France, Juin 14-17, 2010. ***(Oral)***
13. ***Yang ZG***, Vernier A, Chevolot Y, Souteyrand E, Laurenceau E. Evaluation de diverses chimies de surface pour l'immobilisation de protéines: Application au développement de puces à protéines 3D. *Journée Rhône-Alpes des Biomolécules (JRAB) 2010*, Grenoble, France. Juin 3, 2010. ***(Oral)***
14. ***Yang ZG***, Chevolot Y, Souteyrand E, Laurenceau E. Implementation of protein chips: Application to the diagnosis of cancer. *4th Centrale-Beihang Research Workshop*, Lyon, France, May 26-28, 2010. ***(Poster)***

Thesis summary in french
Résumé étendu en français

Le cancer est en passe de devenir la première cause de décès dans le monde avec un nombre de cas de cancer qui a pratiquement doublé sur les trente dernières années. Le diagnostic du cancer est d'autant plus important qu'il est maintenant reconnu que, plus la prise en charge du patient est rapide, plus les traitements thérapeutiques sont efficaces. Ce diagnostic doit être précis, fiable, et établi dans les premiers stades de la maladie afin d'augmenter significativement les chances de succès du/des traitements. Les techniques conventionnelles pour le diagnostic du cancer sont essentiellement basées sur des techniques d'imagerie (radiographies, IRM…) associés à des tests cytologiques et biochimiques. Avec le développement récent des technologies de biologie moléculaire (et notamment en protéomique), de nombreux marqueurs tumoraux ont été identifiés et sont utilisés dans des tests d'immunoassay pour le diagnostic voire pronostic du cancer en oncologie clinique. Cependant, le faible taux de marqueurs tumoraux dans le sérum de patient, ainsi que leur grande diversité, sont un challenge important pour l'établissement d'un diagnostic d'autant plus que les techniques de détection souffrent souvent d'un manque de sensibilité et de sélectivité. De plus, du fait de la diversité et de la variabilité des cancers, aucun marqueur tumoral n'est suffisamment spécifique pour permettre un diagnostic précis. Aussi, afin d'augmenter la fiabilité et la précision du diagnostic, il est nécessaire d'utiliser plusieurs marqueurs tumoraux.

Dans ce contexte, grâce à leur capacité d'analyse haut débit en parallèle et le faible volume d'échantillon nécessaire, les technologies de puces à protéines (protein microarray) présentent de nombreux avantages pour l'identification de marqueurs tumoraux associés à la réponse humorale. Comme les marqueurs tumoraux sont souvent présents dans les échantillons en très faible quantité (à l'échelle sub micro-molaire), il y a un besoin urgent de développer des puces à protéines avec une détection ultrasensible de marqueurs tumoraux. La spécificité du diagnostic sera fortement liée au choix des protéines que l'on veut détecter (notées protéines cibles) et par conséquent au choix des protéines sondes que l'on va immobiliser sur le support. Un des paramètres critiques dans le développement de puces à protéines sensibles est la chimie de surface qui détermine le mode d'immobilisation de la protéine sonde sur le support et influence son activité biologique et donc sa capacité à reconnaitre et interagir avec la protéine cible que l'on cherche à détecter. Comme de nombreuses études suggèrent qu'un seul biomarqueur n'est pas suffisamment spécifique et

sensible, la recherche d'une combinaison pertinente de biomarqueurs est un axe important pour l'amélioration d'un tel diagnostic.

L'objectif de ce travail de thèse est donc le développement d'un outil original basé sur la technologie de puces à protéines fonctionnalisées avec différentes chimies de surface pour la détection sensible et spécifique de biomarqueurs tumoraux afin d'améliorer le diagnostic du cancer. Deux types de puces à protéines seront développés pour des applications différentes. Une première puce, avec comme protéines sondes des anticorps, sera développée pour la détection de biomarqueurs tumoraux impliqués dans le cancer colorectal. Une deuxième puce, où les protéines sondes seront des antigènes, sera étudiée en vue de l'identification de réponses autoimmunes de patientes atteintes d'un cancer du sein.

Le chapitre 1 intitulé « Etat de l'art » donne quelques chiffres clés sur le cancer pour rappeler l'importance de cette maladie et les enjeux en termes de diagnostic : l'établissement d'un diagnostic précis, fiable et le plus en amont possible devra permettre une prise en charge adaptée et un traitement thérapeutique personnalisé augmentant ainsi les chances de succès du traitement. Les différentes techniques conventionnelles actuellement employées pour le diagnostic et le suivi du cancer sont décrites ainsi que les techniques en cours de développement. En particulier, le test de biologie moléculaire ELISA (Enzyme Linked Immunosorbent Assay) est décrit plus en détail et à partir d'une recherche bibliographique, une liste (non exhaustive) des marqueurs tumoraux actuellement les plus utilisés pour la détection de cancer est établie. Des données bibliographiques (reportées en table I.2) montrent que selon la méthode de détection utilisée, les limites de détection d'un même marqueur tumoral comme par exemple le CEA varient fortement (de 1ng/ml pour une détection colorimétrique à 0.012ng/ml pour une détection colorimétrique à l'aide de nanoparticules d'or). Deux sous chapitres sont plus particulièrement consacrés aux techniques de détection du cancer colorectal et du cancer du sein. Une large partie de ce chapitre est ensuite dédié à l'élaboration des puces à protéines. Chaque étape d'élaboration de tels systèmes est décrite depuis le choix du matériau support, la chimie de surface et éventuellement les agents de couplage utilisés, le choix des protéines sondes (en fonction des protéines cibles visées) et les différentes techniques de détection. Soulignons que le choix du matériau support peut être imposé par le mode de détection utilisé: par exemple avec une détection par imagerie de résonance de plasmon de surface, il faut une interface diélectrique de fort indice tel que l'or ou l'argent, pour une détection électrique, il est nécessaire que le support soit conducteur tandis que pour des détections plus classiques par marqueurs fluorescents, les lames de verres sont largement utilisés. De plus, la chimie de surface utilisée conditionne le mode d'immobilisation des protéines (simple adsorption, liaison électrostatique, liaison covalente)

et par conséquence l'activité biologique de la protéine sonde. Sachant que chacune des étapes à une incidence sur les performances in fine de la biopuce, et compte tenu du large éventail de choix possibles, on mesure à travers cette courte revue des systèmes rapportés dans la littérature, toute la complexité du problème.

Le choix des protéines à immobiliser dépend des marqueurs tumoraux que l'on cherche à détecter. On peut distinguer deux grandes classes : **les TAAs et les AAbs**.

Au cours du processus de tumorigénèse, la dégradation des cellules saines entrainent la production d'antigènes tumoraux et la prolifération excessive de cellules malignes. Ces antigènes tumoraux (notés **TAA, Tumor Associated Antigens**) présents dans le sérum de patients peuvent être considérés comme des biomarqueurs de cancer et être détectés avant l'apparition des signes cliniques. Pour cela, il faut développer une **puce 'anticorps'** sur laquelle sont immobilisés un panel d'anticorps suceptibles de reconnaitre les antigènes tumoraux. L'identification de biomarqueurs pertinents et donc le choix des anticorps à immobiliser sur la puce font l'objet de nombreux travaux depuis 2005. En effet, il faut souligner que la variabilité de ces biomarqueurs et leur manque de spécificité restent sont des verrous importants pour une analyse correcte. Ainsi, dans le cadre de cancer du pancréas, Orchekowski et al [171] ont pu distinguer les donneurs sains et les malades et donner une classification des tumeurs (malignes ou bénignes) avec une sensibilité supérieure à 92% et une spécificité de l'ordre de 80%.

En parallèle, la présence de cellules tumorales entraine une réponse du système immunitaire qui produit des autoanticorps spécifiques **(notés AAb, autoantibodies).** On peut donc considérer ces autoanticorps associés au cancer (notés AAb) comme une autre catégorie de marqueurs tumoraux que l'on peut cibler pour établir un diagnostic. On développera donc également **une puce 'antigènes'** qui devra détecter les autoanticorps associés au développement d'une tumeur. Notons que les AAbs ont une meilleure stabilité dans le temps que les TAAs ce qui peut améliorer la fiabilité de l'analyse.

Ce chapitre se termine en dressant les objectifs de la thèse et indique les principales étapes du travail.

En vue de pouvoir détecter de manière précoce et précise les cancers, nous développons des puces protéines de haute sensibilité que nous testons sur différents sérums de patients. Afin d'optimiser chacune des étapes de l'élaboration de ces puces, nous avons d'abord fabriqué des puces 3D microstructurées en gravant des microcuvettes sur une lame de verre standard. A l'intérieur de chaque microcuvette, on peut déposer un ensemble de biomarqueurs. Ainsi, chaque microcuvette représente une mini puce. Chaque cuvette étant un réacteur indépendant, on peut ainsi tester simultanément et en parallèle, un très grand nombre de conditions expérimentales permettant de sélectionner pour chaque protéine les meilleurs protocoles expérimentaux afin d'augmenter la sensibilité des puces.

Une des étapes clés du procédé d'élaboration de biopuces fiables et reproductibles est l'immobilisation efficace des protéines sur une surface sans qu'elles perdent leur activité biologique. Aussi, plusieurs chimies de surface sur lames de verre seront testées soit à partir des seules monocouches de silane ayant différentes terminaisons réactives (amino, époxy ou carboxy), soit en ajoutant un polymère biocompatible tel que la Jeffamine, le chitosan, le carboxymethyl dextran (CMD) ou un copolymère MAMVE (Maleic Anhydride-alt-Méthyl Vinyl Ether). Ces surfaces et leur capacité d'immobilisation de protéines seront caractérisées à l'aide de différents outils d'analyse tels que l'InfraRouge (en mode ATR-FTIR), l'XPS, les mesures d'angles de contact et des tests colorimétriques permettant de valider l'immobilisation effective des protéines sur les différentes surfaces fonctionnalisées.

Ensuite, l'influence de différents paramètres expérimentaux (concentrations des protéines sondes, composition du tampon de dépôt des sondes, conditions d'incubation, et concentrations de protéines cibles) sera étudiée afin de valider les puces à l'aide de protéines purifiées. Enfin, deux types de puces seront développés et testés sur des sérums de patients.

- une puce 'anticorps' dédiée à la détection de cancer colorectal
- une puce 'antigènes' ciblant les auto-anticorps, dédiée à la détection du cancer du sein.

Le chapitre 2 rapporte les différentes fonctionnalisations de surface testées sur des supports lames de verre. Il est bien connu que l'activité biologique d'une protéine est très influencée par son environnement et peut être fortement perturbée lorsqu'elle est immobilisée sur une surface. En effet, les fonctions de reconnaissance de la protéine peuvent être utilisées pour coupler la protéine à la surface ou devenir moins disponibles à la reconnaissance du fait d'une gêne stérique importante liée à la proximité de la surface. De plus, le mode d'immobilisation de la protéine sur une surface (simple adsorption physique, liaison covalente, piégeage…) dépend essentiellement de l'étape préalable de fonctionnalisation de surface.

Aussi, dans ce chapitre, différents protocoles de fonctionnalisation de surface sont décrits. Trois types de silane formant une monocouche ont été utilisés:

- TDSUM tert-butyl-11-(diméthylamine)silylundecanoate,

- **GPDMES** (3-GlycidoxyPropyl) DiMéthylEthoxySilane,

- **APDMES** (3- AminoPropyl) DiMéthylEthoxySilane.

Les analyses XPS montrent que ces 3 silanes monofonctionnels sont bien liés à la surface de silice avec un pourcentage de Si atomique respectivement de 29% sur les surfaces TDSUM, de 26% pour le GPDMES et de 27,7% sur les surfaces APDMES.

Les lames TDSUM sont ensuite hydrolysées avec de l'acide formique durant 7 heures à température ambiante pour obtenir des fonctions carboxyliques terminales. L'utilisation d'une

solution N- Hydrosuccinimide NHS/DIC permet d'activer les fonctions ester qui pourront se coupler avec une fonction amine.

En vue de générer une surface aminée sur les lames TDSUM activées, deux types de polymères (la **Jeffamine** qui est une diamine et le **chitosan** qui est un polysaccharide polyaminée de haut poids moléculaire) ont été greffées. Les analyses XPS indiquent que la Jeffamine est greffée de manière covalente sur la couche de silane sous-jacente, tandis que le chitosan était principalement physisorbé sur le silane. Pour ces deux polymères, la densité surfacique d'amine est similaire (de l'ordre de 4,5 10^{13} par cm^2) mais de manière surprenante plus faible que celle obtenue sur des surfaces fonctionnalisées à l'APDMES (de l'ordre de 1,3 10^{14} par cm^2). Une hypothèse est la formation de ponts entre les groupements « amine » des polymères ce qui diminuerait la densité de groupements « amine » terminaux disponibles pour le greffage des protéines.

Toujours dans l'objectif d'augmenter la densité de groupements amine en surface, nous avons aussi testé deux autres polymères, le **CMD** et le **MAMVE**, portant un grand nombre de fonctions amines. Le carboxymethly dextran (CMD) est un polymère biocompatible, largement utilisé dans le domaine des capteurs et de la délivrance de médicaments. Le CMD a été synthétisé au Laboratoire sous différentes conditions réactionnelles. On peut obtenir différents degrés de substitution en changeant le rapport du mélange d'acide acétique de brome et du dextran à différents poids moléculaires. Ainsi, les meilleurs résultats ont été obtenus pour un CMD de poids moléculaire Mw = 40 000 $g.mol^{-1}$, un degré de substitution DS de 63% et une concentration de 1 mg/ml dans du MES (2-(N-morpholino)ethane sulfonic acid). Pour le MAMVE, 2 poids moléculaires ont été testés (Mw = 216 kDa et Mw = 67 kDa). Les meilleurs résultats sont obtenus pour le MAMVE 216 à 1mg/ml. La couche de MAMVE greffée est plus épaisse que celle de CMD.

L'étude comparative de l'ensemble des surfaces testées par mesure d'angle de contact indique que le caractère plus hydrophile des polymères dans l'ordre suivant :

MAMVE > Chitosan > Jeffamine, CMD, NHS, COOH, APDMES.

Le chapitre 3 est consacré à l'étude de l'immobilisation des protéines sur les différentes surfaces précédemment fonctionnalisées et à l'influence des paramètres de dépôts sur la qualité d'immobilisation. De nombreuses études montrent que les performances analytiques d'une biopuce dépendent en partie de la chimie de surface et des conditions de détection. Il est donc important de limiter la possible perte d'activité biologique des molécules immobilisées et d'améliorer le rapport signal sur bruit afin d'augmenter la spécificité et la sensibilité des puces. Aussi, l'influence des tampons de dépôt des protéines (composition, pH), de la concentration des protéines, des protocoles de blocage des sites non actifs de

surface est étudié afin de déterminer les meilleures conditions expérimentales sur chaque surface et pour chaque protéine.

Pour mener à bien cette étude, quatre protéines de poids moléculaire et de point isoélectrique différents ont été choisies. Pour permettre le contrôle d'immobilisation sur les différentes surfaces, ces molécules sont marquées par un groupement fluorescent (Cy3 ou F647). Les protéines utilisées dans cette étude ont été sélectionnées pour leurs propriétés similaires avec les marqueurs anticorps anti-tumoraux et les antigènes associés aux tumeurs qui seront immobilisés pour les tests diagnostiques de cancer. Ainsi, IgG a été choisi pour illustrer le comportement des anticorps que nous utiliserons dans la suite de l'étude sur la puce 'anticorps'. Streptavidine, Myoglobin et BSA sont représentatives de la diversité en poids moléculaires (Mw) et en point isoélectrique (pI) avec des valeurs proches de celles des antigènes tumoraux que l'on utilisera dans la puce 'antigènes associés aux tumeurs'.

Les quatres protéines marquées à l'aide d'un groupement fluorescent sont immobilisées sur 8 surfaces chimiques différentes (COOH, NHS, CMD, MAMVE, APDMES, Jeffamine, Chitosan, GPDMES).

Il résulte que l'efficacité de l'immobilisation dépend des propriétés de la surface (groupement chimique réactif en surface, propriété de mouillage), des caractéristiques de la protéine (Mw, pI, 3D structure) et des conditions de dépôts (pH, composition du tampon, concentration). Malgré le nombre important de paramètres, nous avons pu déterminer des comportements généraux :

- les grosses protéines telles que l'IgG sont mieux immobilisées sur des surfaces de polymeres que sur des monocouches de silane que ce soit par liaison covalente (sur MAMVE et CMD) ou par adsorption physique (chitosan).
- Les petites protéines telles que la myoglobin montre une meilleure immobilisation par liaison covalente que par adsorption physique que ce soit sur les monocouches de silane (TDSUM activé au NHS) ou sur les polymères (MAMVE, CMD).
- Les protéines de taille moyenne telles que la BSA et la streptavidine ont un comportement intermédiaire.

De plus, les interactions sont principalement guidées par des interactions électrostatiques et des liaisons hydrogène. Nous avons trouvé que le plus haut taux d'immobilisation de protéines est obtenu sur des surfaces non chargées avec des protéines chargées.

Enfin, la qualité des spots et donc l'analyse d'images est améliorée en ajoutant 0.05 % PVA (Poly vinyl alcool) dans le tampon de dépôt et en utilisant une solution de blocage de 10% BSA/PBS-T. La concentration optimale de protéines pour l'immobilisation est de 0.3 μM.

Cette étude nous a permis de déterminer pour chaque type de protéine la meilleure chimie de surface et les meilleures conditions pour obtenir le meilleur taux d'immobilisation des protéines. Cependant, il reste à vérifier l'activité biologique des protéines immobilisées. Ce sera le point majeur des deux chapitres suivants.

Le chapitre 4 vise à donner une première preuve de concept de l'utilisation d'une puce à façon pour le diagnostic médical. Pour valider notre approche, nous avons développé une puce dédiée au diagnostic du cancer colorectal (CRC). Le choix des biomarqueurs à détecter ne peut se faire qu'en étroite collaboration avec des cliniciens et des chercheurs en oncologie. Cette étude a été menée en collaboration avec bioMérieux (qui nous a fourni gracieusement les anticorps monoclonaux) et le CHU de Saint-Etienne. D'autre part, dans le cas d'un diagnostic, il est nécessaire de pouvoir détecter à des niveaux de concentration très faibles les biomarqueurs (dans la gamme des nM, voir plus bas) dans des sérums de patient, c'est-à-dire dans des milieux biologiques complexes. Pour cette première validation, nous avons développé en format puce, un test immunologique sandwich. Les anticorps de capture (fixés sur la surface) et de détection (deuxième partie du sandwich) sont des anticorps monoclonaux capables de reconnaitre de manière spécifique différents domaines de l'antigène cible que l'on veut détecter.

A partir de la bibliographie faite au chapitre 1, nous avons sélectionné un certain nombre de marqueurs tumoraux que nous cherchons à détecter. Les 3 marqueurs antigènes tumoraux les plus connus (CEA, CA 19-9, Hsp 60). L'antigène carcino-embrionnaire (CEA) est un antigène oncofétal courant appartenant à la superfamille des immunoglobulines. CEA a été utilisé depuis plusieurs années comme biomarqueur de cancer colorectal mais également de cancer se développant sur d'autres tissus. Des niveaux élevés de CEA sont relatifs à une progression de cancer colorectal. Ce marqueur est également utilisé pour suivre le bénéfice d'un traitement thérapeutique. L'antigène carbohydrate (CA) 19-9 est un marqueur de tumeur gastrointestinal. Nous avons également sélectionné la protéine Hsp 60, de la famille des Heat Shock Protein qui est un marqueur de stress cellulaire souvent trouvé dans les cancers. Enfin, PDI et DEFA6, sont deux marqueurs tumoraux récemment identifiés par bioMérieux et impliqués dans les CRC. La protéine p53, souvent présente dans les sérums de patients atteints de cancer mais n'est pas un marqueur spécifique, mais elle est considérée comme marqueur universel, c'est pourquoi, nous l'avons ajoutée à notre étude.

Nous avons fabriqué des puces à micropuits présentant des chimies de surfaces différentes (APDMES, Jeffamine, chitosan,NHS, CMD, MAMVE) sur lesquelles ont été immobilisés les différents anticorps (anti-CEA, anti-CA19-9, anti-Hsp60, anti-PDI, anti-DEFA6 et anti-p53) correspondant aux marqueurs ciblés que l'on veut détecter.

Dans un premier temps, nous avons validé le bon fonctionnement des puces et optimisé les conditions expérimentales à l'aide d'antigènes tumoraux purifiés. De cette étude, il ressort que les protéines immobilisées perdent une partie de leur activité biologique et que les meilleures performances de captures sont obtenues lorsque l'on utilise des concentrations à 10 µM d'anticorps à déposer. Pour chaque marqueur tumoral, le signal de détection (SNR= rapport signal sur bruit) est fortement dépendant de la chimie de surface. Par exemple, le signal de détection de HSP60 est beaucoup plus important sur les couches polymères (CMD, MAMVE, chitosan) que sur des monocouches de silane. Nous avons déterminé pour chaque marqueur tumoral et sur chacune des chimies de surface, la gamme dynamique et la limite de détection (LOD) du signal. De manière générale, les limites de détection atteintes sur nos puces sont plus basses que celles trouvées dans la bibliographie. A titre d'exemple la LOD pour le CEA sur MAMVE est de l'ordre de 10pM ce qui est inférieur aux données reportées dans la littérature (2.5 nM).

En accord avec les performances analytiques, les surfaces NHS, MAMVE and chitosan ont été choisies pour les tests sur les sérums de patients. (4 sérums de patients et 4 sérums sains). Nous montrons que la détection d'un seul marqueur ne permet pas de déterminer l'ensemble des patients malades. Il faut la combinaison de 3 marqueurs tumoraux (Hsp60/chitosan, PDI/chitosan, DEFA6/MAMVE) sur leurs surfaces optimisées respectives pour atteindre les 100% de réponses positives sur le panel de patients.

Dans le chapitre 5, une démarche identique a été suivie pour réaliser une puce dédiée à la détection de marqueurs de cancer du sein. Outre les marqueurs tumoraux classiques, des auto-anticorps dirigés contre des antigènes tumoraux et produits en réaction défensive du système immunitaire sont trouvés dans les sérums de patients et peuvent donc être des indicateurs précoces d'un développement tumoral. Le but de cette étude est donc de réaliser une puce 'TAA' (portant des sondes antigènes associées aux tumeurs) et capables de détecter les auto-anticorps dans des sérums de patientes atteintes d'un cancer du sein. A partir d'une recherche bibliographique et en collaboration avec les cliniciens en oncologie du CHU Montpellier, un set de 10 TAAs (tumor-associated antigens) a été sélectionné, comprenant l'antigène carcino-embryonaire (CEA), les heat shock proteins (Hsp60, Hsp70), p53, Her2-Fc (domaine extracellulaire), NY-ESO-1, MYCL1, CHEK2, HNRNPK, NME1. Ces TAAs ont été immobilisés sur des lames de verres structurées en micro-cuvettes et fonctionnalisées avec les différentes chimies de surface étudiées précédemment. La présence d'auto-anticorps dirigés contre ces TAAs a été évalué sur un panel de 29 sera de patientes ayant un cancer du sein et de 28 donneurs sains.

D'abord, ces nouvelles puces à façon ont été validées à l'aide de 4 TAAs bien connus (CEA, p53, Hsp60, Her2) et testées avec des solutions d'anticorps monoclonaux purifiés. Là

encore, on démontre que le signal de détection (SNR) des auto-anticorps anti TAA dépend de la chimie de surface et des conditions expérimentales de mise en œuvre de la puce.

Au moins 10 % des cancers du sein sont détectés si l'on utilise un seul marqueur TAA dans les conditions optimales. Avec une combinaison de 5 marqueurs TAAs sur la chimie la mieux adaptées (Hsp60 (NHS)+ p53 (APDMES)+ He2-Fc (NHS)+ NY-ESO-1 (NHS)+ Hsp 70 (NHS), 82% des patients sont détecté. Ce résultat est comparable aux autres travaux concernant la détection des autoanticorps TAAs pour le diagnostic du cancer. Ces résultats sont encourageants, car ils valident la technologie mise en œuvre et l'intérêt d'utiliser des puces 3D qui permet grace à la microstructuration d'utiliser sur une même puce la meilleure chimie de surface pour chacune des sondes. De plus, la précision du test pourra être améliorée en augmentant le nombre de TAAs sur la puce. Enfin, une cohorte beaucoup plus importante sera nécessaire pour valider correctement un test diagnostic. Soulignons également que cette approche multi-test sur puce devrait permettre d'abaisser fortement les coûts du diagnostic.